Deletion of *F4L* (ribonucleotide reductase) in Vaccinia Virus Produces a Selective Oncolytic Virus and Promotes Anti-tumor Immunity with Superior Safety in Bladder Cancer

by

Kyle Gordon Potts

A thesis submitted in partial fulfillment of the requirements for the degree of

Doctor of Philosophy

in

Experimental Oncology

Department of Oncology
University of Alberta

ABSTRACT

Overall recurrence of non-muscle-invasive bladder cancer (NMIBC) can be as high as 80% within 5 years of initial treatment. High-grade NMIBC has the greatest risk of recurrence and treatment for these patients includes surgery followed by intravesical therapy with the immunotherapeutic agent Bacillus Calmette-Guérin (BCG). BCG however, can be particularly dangerous for immunocompromised patients. Additionally, up to 40% of patients fail BCG therapy and cystectomy remains the standard treatment in these cases. This project examines whether vaccinia virus (VACV) can be used to treat preclinical models of NMIBC and in particular, bladder cancer that is refractory to BCG therapy. Here we have generated a novel oncolytic VACV by mutating the *F4L* gene that encodes the viral homolog of the stringently cell-cycle-regulated small subunit (RRM2) of ribonucleotide reductase. The *F4L*-deleted VACVs are highly attenuated in normal tissue and have a tropism that favors cancer cells commonly elevated in RRM2 levels, resulting in selective replication and tumor cell killing. VACVs efficiently replicate in BCG-resistant and BCG-susceptible AY-27 cells. *F4L*-deleted VACVs selectively replicate in both the orthotopic AY-27 immunocompetent rat model and RT112-luc xenograft models, causing significant tumor regression or complete tumor ablation with no toxicity, while the commonly used ΔJ2R VACV causes significant toxicity in immunocompromised mice. Furthermore, rats cured of AY-27 tumors by VACV-treatment develop a protective anti-tumor immunity that is evident by tumor rejection upon challenge, as well as by *ex vivo* cytotoxic T-lymphocyte assays. Finally, the mutant VACVs replicate in both primary human bladder cancer cultures and tumor explants. Our findings demonstrate the enhanced safety and selectivity of our modified oncolytic VACV, making the *F4L*-deleted VACV a promising therapy for patients with BCG-refractory cancers and immune dysregulation.

ACKNOWLEDGMENTS

I would like to thank my supervisor, Dr. Mary Hitt for her continued guidance and support during graduate school. Dr. Hitt always made herself available to review data, answer question or trouble shoot a problem. She instilled sound scientific methodology and always encouraged me to think independent and explore new ideas. I would also like to thank my co-supervisor, Dr. David Evans for his leadership and encouragement. Dr. Evans pushed me to challenge the status quo while providing a critical eye and technical assistance. I am truly grateful to both Drs. Hitt and Evans, they have made my studies an extremely rewarding experience. I would also like to thank my committee member, Dr. Ronald Moore for his continued advice, guidance, mentorship, and encouragment throughout my studies. Dr. Moore was instrumental in providing me with the clinical insight related to my project.

I would like to thank Nicole Favis and Megan Desaulniers for their assistance in all the animal studies conducted during my degree. This work would not have been possible without their help and dedication. I also want to thank Dr. David Sharon for training me when I joined the lab and always posing thought provoking questions. I am grateful to Dr. Chad Irwin who has played a key role in the development of this project. He helped teach me many of the virological techniques and was always available to help troubleshoot an experiment. I thank Powel Crosley keeping me company on the many weekends in the lab and for becoming a truly great friend.

I thank Shyambabu Chaurasiya, Kate Agopsowicz, and Ryan Noyce for helpful discussions and technical assistance. I am truly grateful to my family and all the friends I have made during graduate school. Flow cytometry was performed at the University of Alberta, Faculty of Medicine and Dentistry Flow Cytometry Facility, with assistance from Aja Rieger. I would also like to recognize the selfless act and generosity of the patients for providing tissue used in these studies.

Finally, I thank my partner, Nubia for her continued love, encouragement, and support throughout my degree. You made the difficult times easier and the good times unforgettable.

This work was supported by an Alberta Cancer Foundation/Canadian Institutes for Health Research (CIHR) Bridge, Alberta Innovates Health Solutions (AIHS)/Alberta Cancer Foundation "High Risk for High Return" award, a Li Ka Shing Institute of Virology "Translational Research" grant, and a CIHR grant. Funding from the AIHS in support of the Li Ka Shing Institute of Virology and Applied Virology is also acknowledged. K.G.P. stipend was in part funded by the Antoine Noujaim Graduate Entrance Scholarship, Queen Elizabeth II Graduate Scholarship, and the University of Alberta Faculty of Medicine and Dentistry 75th Anniversary Graduate Student Award.

TABLE OF CONTENTS

LIST OF FIGURES

LIST OF ABBREVIATIONS

AKT	Protein kinase B
ANOVA	Analysis of variance
APC	Antigen presenting cell
ATP	Adenosine triphosphate
BCA	Bicinchoninic acid
BCG	Bacillus Calmette–Guérin
BiTEs	Bispecific T-cell engagers
BMDC	Bone marrow derived dendritic cells
BSA	Bovine serum albumin
CD40L	Cluster of differentiation 40 ligand
CDK	Cyclin-dependent kinase
CDKN2A	Cyclin-dependent kinase Inhibitor 2A
CEA	Carcinoembryonic antigen
CIS	Carcinoma *in situ*
CFU	Colony forming units
CPA	Cyclophosphamide
CT	Computed tomography
CTL	Cytotoxic T-lymphocyte
CTLA-4	Cytotoxic T-Lymphocyte Associated Protein 4
DAMPs	Damage-associated molecular patterns
DC	Dendritic cell
dGMP	Deoxyguanosine monophosphate
DMEM	Dulbecco's Modified Eagle Medium
DNA	Deoxyribonucleic acid
dNDP	Deoxyribonucleoside diphosphate
dNTP	Deoxynucleotide triphosphate
dTh	Deoxythymidine
dTMP	Deoxythymidine monophosphate
dTTP	Deoxythymidine triphosphate
dUMP	Deoxyuridine monophosphate
EDTA	Ethylenediaminetetraacetic acid
EGF	Epidermal growth factor
eIF2	Eukaryotic initiation factor 2
EV	Enveloped virion
FAP	Fibronectin attachment protein
FBS	Fetal bovine serum
FGFR3	Fibroblast growth factor receptor 3
FITC	Fluorescein isothiocyanate
FMO	Fluorescence-minus-one
FSC-A	Forward-scattered light-area
FSC-H	Forward-scattered light-height
GALV	Gibbon ape leukemia virus envelope
GM-CSF	Granulocyte-macrophage colony-stimulating factor
HBSS	Hanks' Balanced Salt Solution

HER2 (ERBB2)	Human epidermal growth factor receptor 2
HMGB1	High mobility group box 1
HPGD	Hydroxyprostaglandin Dehydrogenase 15-(NAD)
HSD	Honest significant difference
HSV	Herpes simplex virus
hTERT	Human telomerase reverse transcriptase
ICAM-1	Intracellular adhesion molecule-1
IFN	Interferon
IL	Interleukin
ITR	Inverted terminal repeat
IV	Intravenous
kbp	Kilobase pair
kDa	Kilodalton
LDH	Lactate dehydrogenase
LFA-3	Leukocyte function-associated antigen-3
MAPK	Mitogen-activated protein kinase
MDM2	Mouse double minute 2 homolog
MDSC	Myeloid-derived suppressor cell
MHC	Major histocompatibility complex
MIBC	Muscle-invasive bladder cancer
MOI	Multiplicity of infection
MRI	Magnetic resonance imaging
mRNA	Messenger ribonucleic acid
mTOR	Mechanistic target of rapamycin
MUC1	Epithelial mucin 1
MV	Mature virion
NAT	N-Acetyltransferase
NK	Natural killer cell
NMIBC	Non-muscle-invasive bladder cancer
NSG	NOD SCID gamma (NOD.Cg-Prkdc^{scid} Il2rg^{tm1Wjl}/SzJ)
NYCBH	New York City Board of Health
OV	Oncolytic virus
p53	Tumor protein p53
Pak1	p21-activated kinase 1
PAMPs	Pathogen-associated molecular patterns
PBS	Phosphate-buffered saline
PCR	Polymerase chain reaction
PD-1	Programmed cell death protein 1
PD-L1	Programmed death-ligand 1
PDX	Patient-derived xenograft
PE	Phycoerythrin
PFU	Plaque forming unit
PI	Propidium iodide
PI3K	Phosphatidylinositol-4,5-bisphosphate 3-kinase
PKR	Protein kinase R
PSA	Prostate-specific antigen

PTEN	Phosphatase and tensin homolog
PVDF	Polyvinylidene fluoride
RRM1	Ribonucleotide Reductase Catalytic Subunit M1 (Large subunit)
RRM2	Ribonucleotide Reductase Catalytic Subunit M2 (Small subunit)
Rac1	Ras-related C3 botulinum toxin substrate 1
Rb	Retinoblastoma protein
RNA	Ribonucleic acid
rNDP	Ribonucleoside diphosphate
RNR	Ribonucleotide reductase
RPMI	Roswell Park Memorial Institute medium
SDS	Sodium dodecyl sulfate
SDS-PAGE	Sodium dodecyl sulfate polyacrylamide gel electrophoresis
shRNA	Short hairpin ribonucleic acid
siRNA	Short interfering ribonucleic acid
SSC-A	Side-scattered light-area
TB	Tuberculosis
TCGA	The Cancer Genome Atlas
TCR	T-cell receptor
TK	Thymidine kinase
TLR	Toll-like receptor
TMK	Thymidylate kinase
TNF	Tumor necrosis factor
TRAIL	Tumor necrosis factor-related apoptosis-inducing ligand
TRIF	TIR-domain-containing adapter-inducing interferon-β
TURBT	Transurethral resection of bladder tumor
UCC	Urothelial cell carcinoma
UV	Ultraviolet
VACV	Vaccinia virus
VGF	Vaccinia virus growth factor
VSV	Vesicular stomatitis virus
WR	Western reserve
WT	Wild-type
ΔF4L	Vaccinia virus lacking *F4L* gene
ΔF4LΔJ2R	Vaccinia virus lacking *F4L* and *J2R* genes
ΔJ2R	Vaccinia virus lacking *J2R* gene

CHAPTER 1 – GENERAL INTRODUCTION

PREFACE

A portion of this chapter has been published in the manuscript: **Potts, K.G.,** Hitt, M.M., Moore, R.B. Oncolytic Viruses in the Treatment of Bladder Cancer. *Adv Urol.* 2012 Jul; 2012(1):404581. Advances in Urology states: "This is an open access article distributed under the Creative Commons Attribution License, which permits unrestricted use, distribution, and reproduction in any medium, provided the original work is properly cited."

1.1 Bladder cancer

In Canada, it is estimated that 8,700 men and women will be diagnosed with and 2,300 will die of cancer of the urinary bladder in 2016, making it the fourth and twelfth most common cancers among men and women, respectively. With a recurrence rate of up to 80%, many patients require lifelong surveillance and multiple treatment strategies [1]. However, if resistance to current therapies develops, removal of the bladder is often the only remaining option. In Canada, the 5-year relative survival for bladder cancer varies with stage and grade and can range from upwards of 98% in patients with low-grade Ta tumors to as low as 16% for stage IV (metastatic) bladder cancer [2]. The most common cause for bladder cancer is smoking and other toxin exposure (*e.g.*, petrochemical industry products), where the carcinogen is removed from the body by the kidney and stored for long periods of time in the bladder [3]. This results in destabilization of the urothelium resulting in a field effect which is characterized by cellular and molecular changes that prompt the development of cancer within a region [4,5]. Urothelial cell carcinoma (UCC) of the bladder can be divided into two broad categories – non-muscle-invasive bladder cancer (NMIBC) and muscle-invasive bladder cancer (MIBC) (reviewed in [6]). Upwards of 80% of bladder cancer are diagnosed as NMIBC and approximately 20% as MIBC. The majority of NMIBC are low grade whereas MIBC are typically high grade and often metastatic. NMIBCs is treated with surgery and intravesical therapies. In the case of MIBC, the gold standard is radical cystectomy with neoadjuvant systemic chemotherapy.

1.1.1 Epidemiology of bladder cancer

More than 90% of cancers in the bladder are UCCs, which were previously termed transitional cell carcinomas [7]. In bladder cancer, the tumor stage describes how far the tumor has penetrated into the bladder and whether the cancer has metastasized (**Figure 1.1**). In contrast,

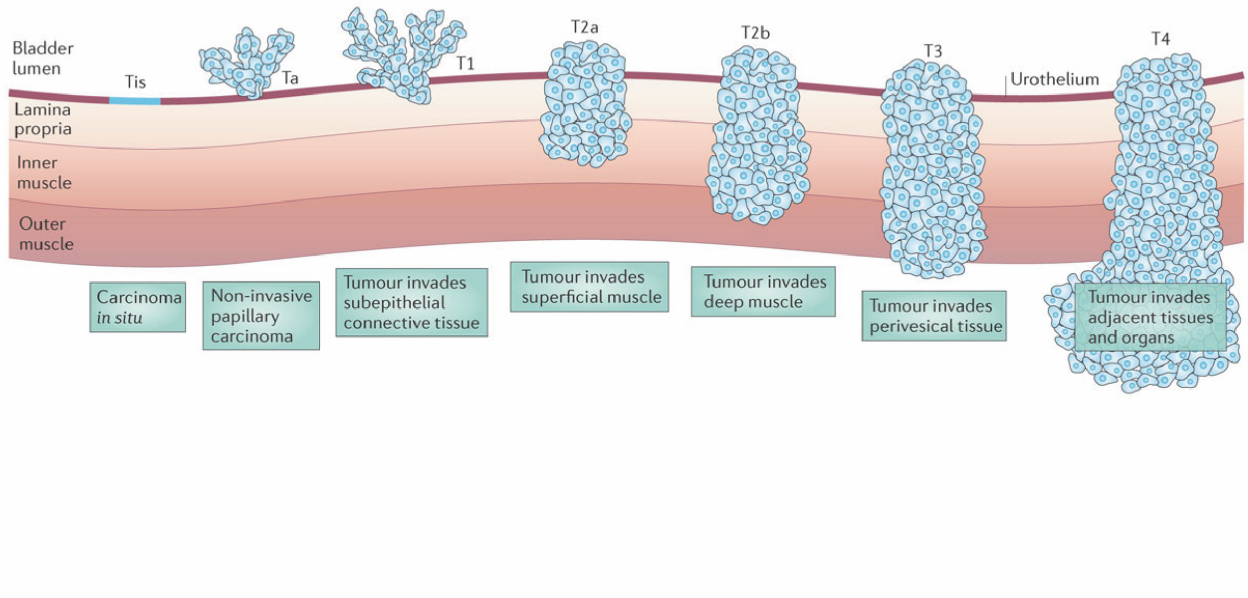

Figure 1.1: Bladder cancer grading and staging. Staging of bladder cancer according to the Tumor–Node–Metastasis (TNM) system. Figure and text adapted from [8] with permission.

grading is a way of categorizing cancer cells based on cell morphology. The grade of a tumor increases with the loss of cellular differentiation compared to adjacent normal cells. Bladder tumors are usually described as high grade or low grade however, in some cases they are denoted grade 1-4. Low grade tumors are well differentiated and look similar to normal cells. Lower grade cancers are typically slower growing and are less likely to metastasize. High grade tumors are poorly differentiated, often grow more quickly and have a higher metastatic potential. The combined stage and grade help a physician determine the appropriate treatment plan for a patient.

Approximately 80% of patients with bladder cancer have tumors that are non-muscle-invasive, meaning the tumor is limited to the mucosa of the bladder (stage Ta and carcinoma *in situ* (CIS)) or penetrates into the submucosa (stage T1) [9]. These NMIBC have also been termed superficial bladder cancers, however this description is now less commonly used (reviewed in [10]). With NMIBC, approximately 70–80% are stage Ta, 20% are T1, and 10% are CIS [11]. Stage Ta tumors are generally low grade, with only about 7% diagnosed as high grade [12]. Stage Ta tumors have a papillary appearance (with increased surface area) and are limited to the urothelium, with no infiltration of the deeper lamina propria or underlying muscle. Early, low-grade lesions carry a 50–70% recurrence rate and a 5–20% risk of progression to muscle-invasive disease over a 5-year period [13]. Stage T1 tumors show early invasiveness, crossing the basement membrane into the lamina propria, although not yet invading the deeper muscle layers. There is significant risk of under-staging patients with these T1 NMIBCs, especially high-grade tumors [14]. High-grade T1 tumors have a 70% to 80% recurrence rate and a 30-50% chance of progression to muscle-invasive disease [15,16]. CIS (also known as Tis) is restricted to the urothelial layer, but its anaplastic morphology indicates that it is likely a precursor to the development of invasive high-grade bladder cancer. 90% of cases of CIS are found in association

with papillary or nodular bladder tumors [17]. Between 40% and 85% of patients with CIS will develop muscle invasion if left untreated [18,19]. About 25% of patients with high-grade UCC have muscle-invasive cancer at initial diagnosis, half of whom will go on to have distant metastasis within 2 years, and 60% of whom will not survive 5 years, despite aggressive treatment [20,21].

1.1.2 Risk Factors

Cigarette smoking is the most significant risk factor for developing bladder cancer. Freedman *et al.* have reported that smoking contributes to upwards of 50% of bladder cancer in both men and women [22]. It can take 20-30 years for bladder cancer to develop in smokers and rates of bladder cancer are highly linked with smoking rates from around the world [23]. Another significant contributor to bladder cancer, that often receives much less attention, is air pollution [24,25], particularly that generated from combustions engines and coal-fired power plants. Studies have found both engine exhaust [26] and polycyclic aromatic hydrocarbons [27] generated from burning coal to be carcinogenic and associated with increased risk of developing bladder cancer. Occupational exposure to other cancer-causing compounds is highly connected with an increased risk of developing bladder cancer. The most noteworthy compounds that increase the risk of bladder cancer are aromatic amines (e.g. 2-naphthylamine, 4-aminobiphenyl and benzidine) and 4,4'-methylenebis(2-chloroaniline) [28,29]. These compounds are found at high levels in the dye, rubber, and plastic industries [30]. Some limited data have also shown that there may be a genetic predisposition for the development of bladder cancer. One example is related to the development of bladder cancer from exposure to aromatic amines. These aromatic amines are metabolized and intermediate products can be carcinogenic. N-acetyl transferase 1 and 2 (NAT1 and NAT2) are critical enzymes in the metabolism of these compounds. Numerous studies have found

polymorphisms of the NAT2 enzyme that produce a 'slow acetylator' phenotype are associated with a strong increase in bladder cancer incidence [31,32].

1.1.3 Genetics of bladder cancer

1.1.3.1 NMIBC. Deletion of all or part of chromosome 9 is found in up to 50% of NMIBCs [33,34]. This deletion almost always includes the cyclin-dependent kinase inhibitor 2A (CDKN2A) locus which encodes p16 and $p14^{ARF}$. These two proteins both act as tumor suppressors through negative regulation of the cell cycle (reviewed in [35]). p16 prevents cell cycle progression from G1 to S phase by inhibiting cyclin-dependent kinases such as cyclin-dependent kinase 4 (CDK4) and CDK6 [36]. This prevents the phosphorylation of retinoblastoma protein (Rb) and thus halts the cell cycle. $p14^{ARF}$ is an alternate reading frame protein product of the CDKN2A locus [37,38]. $p14^{ARF}$ inhibits mouse double minute 2 homolog (MDM2), blocking MDM2-induced degradation of p53 and enhancing p53-signalling and ultimately cell cycle arrest. Deletion of $p14^{ARF}$ removes this inhibition of MDM2 resulting in cell cycle progression and resistance to cell death.

Activating mutations in fibroblast growth factor receptor 3 (FGFR3) are found in upwards of 80% of low grade Ta tumors [39,40]. FGFR3 mutation frequency decreases in NMIBC as the grade increase, with only 5-20% of MIBC harboring the mutation [41]. FGFR3 leads to activation of Ras and mitogen-activated protein kinase (MAPK) pathways resulting in cell proliferation and survival. FGFR3 and Ras activating mutations seem to be mutually exclusive genetic events [42], with Ras mutations found in only ~15% (HRas and KRas combined) of NMIBC. Interestingly, FGFR3 activating mutations are associated with favorable outcomes and with a lower chance of progression to muscle-invasive disease [40]. FGFR3 mutation are strongly linked with low grade

tumors and therefore has been proposed as a marker in urine analysis to reduce overtreatment since it is only the high-grade Ta and T1 tumors that are at an increased risk of progression [43].

1.1.3.2 MIBC. While NMIBC have few chromosomal rearrangements and are generally genomically stable, MIBC typically have many genomic alterations. Nearly all MIBC have some form of cell cycle checkpoint dysregulation which comes from loss-of-function mutations in the tumor suppressor genes encoding p53 and Rb [44]. One study based in Poland found that as tumor grade increased, so did the frequency of mutation of p53 (from 3.3% in low grade to 39% in high grade) [45]. Additionally, amplification of MDM2 frequently occurs and when combined with p53 mutation, p53 function is compromised in upwards of 76% of MIBCs [44]. Mutations found in Rb are almost always inactivating. Dysregulation of cell cycle checkpoints can also occur by inactivation of the CDKN2A locus (p16 and $p14^{ARF)}$ much like in NMIBC. Interestingly, Rb mutations and loss of the CDKN2A locus were found to be mutually exclusive events [44]. Deletion of phosphatase and tensin homolog (PTEN) is also associated with stage and grade of bladder cancer and can be found in over a third of MIBC [46,47]. Mutations in FGFR3 are also seen in MIBC but at a much lower frequency (10-20% in T2 or greater) than in NMIBC [48].

1.1.4 Presentation and diagnosis

Most bladder cancer patients present initially in the clinic with hematuria, *i.e.*, blood in the urine. Macroscopic hematuria, meaning blood is visible in the urine, has been shown to be highly predictive for bladder cancer, especially in older patients [49]. Microscopic hematuria, where blood is not visible in the urine by eye, is most often detected as part of a routine urine analysis. However, there are many possible reasons for microscopic hematuria and further diagnostic tests are required to determine if the patient has bladder cancer [50]. The diagnosis of bladder cancer in patients that present with macroscopic hematuria is 20%, whereas it is only 2% in patients with

microscopic hematuria [51]. Non-specific urinary tract issues such as pain while voiding urine, frequency of urination, or abdominal pain, may warrant further testing [52]. In patients suspected of bladder cancer, further diagnosis is done through cystoscopy. Any suspicious findings require further evaluation and histology is performed following surgery (see below). Cytology, where a sample of urine is examined to see if it has any cancerous cells, is often performed alongside cystoscopy to improve cancer detection. Cytology can be particularly useful for patients with high-grade disease such as CIS, which can be difficult to diagnose through cystoscopy alone [53]. More recently, new imaging techniques such as blue light cystoscopy and narrow band imaging have improved tumor detection and some studies have shown the superior diagnosis to result in increased recurrence-free survival [54]. In cases where upper urinary tract tumors are suspected, patients will undergo an ultrasound or computed tomography (CT) scan or magnetic resonance imaging (MRI). Proper diagnosis and evaluation of the tumor histology is critical for deciding an appropriate management strategy for each patient.

1.2 Management of bladder cancer

1.2.1 TURBT

Standard first line therapy for NMIBC is transurethral resection of bladder tumor (TURBT). A schematic for management of bladder cancer is shown in **figure 1.2**. TURBT is an endoscopic surgical procedure to completely resect any tumor tissue or suspicious areas from the bladder. Resection of the tumor should include muscularis propria to allow for appropriate histological evaluation (staging) of the disease. There is a 50% chance that the first TURBT incompletely removes the tumor, necessitating a second surgery [55,56]. A restaging TURBT should be performed if the initial surgery is thought to be incomplete or a T1 tumor is identified in the absence of muscularis propria [57]. A second surgery can often provide additional tissue for

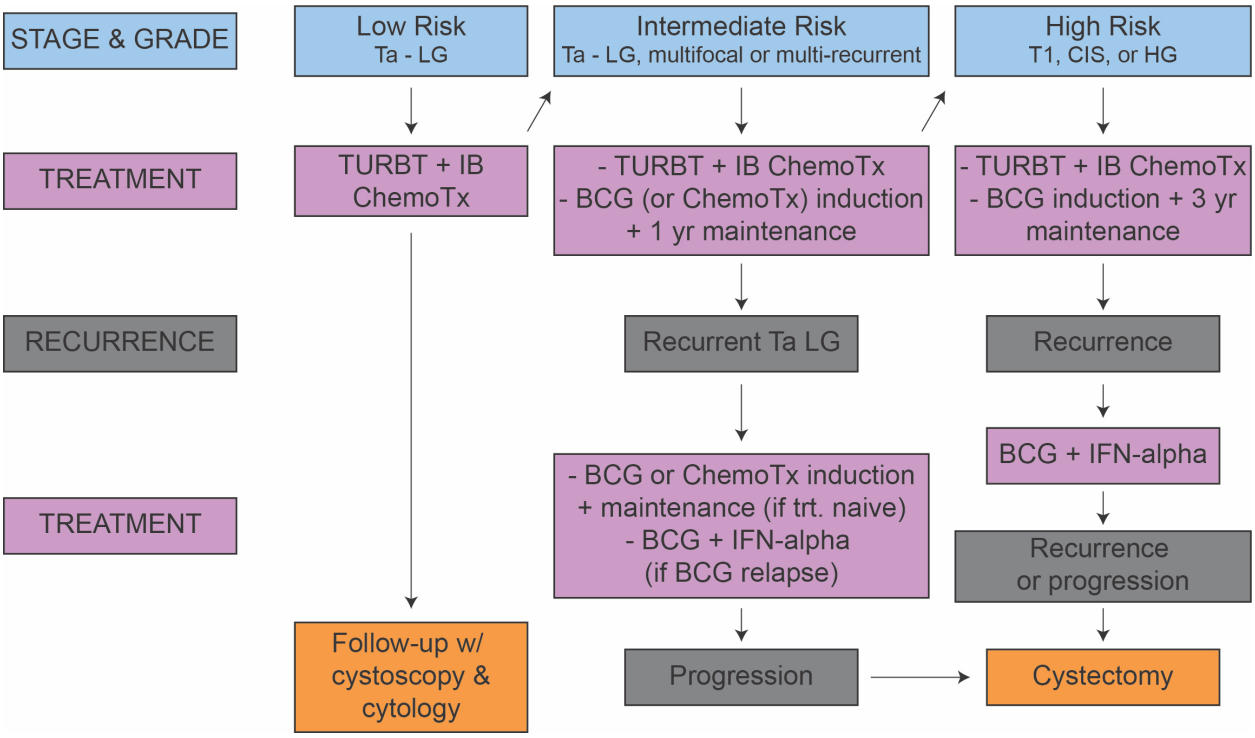

Figure 1.2: Management of non-muscle invasive bladder cancer. Treatment algorithm for non-muscle-invasive bladder cancer based on risk stratification. IB ChemoTx: intrabladder intravesical chemotherapy; Ta LG: Ta low-grade disease; TURBT: transurethral resection of bladder tumor; BCG: Bacillus Calmette-Guerin. Figure adapted from [57].

histological examination allowing for more accurate staging. It has been reported that under staging can occur in up to 50% of patients with high-grade T1 tumors if there is insufficient muscularis propria in the first surgical sample. Even with excellent initial tissues samples, upstaging occurs in 14% of patients after receiving a second TURBT [56]. Herr has reported that 76% of patients had residual disease detected in their second TURBT resulting in a change in the treatment course for a third of the patients [58]. This initial surgery plays a critical role in the diagnosis and management of bladder cancer.

1.2.2 Intravesical therapy

For patients with NMIBC at low risk of tumor recurrence (and without a bladder wall puncture), early instillation of a chemotherapeutic agent following TURBT is now the standard treatment recommendation [57]. Intravesical chemotherapy, however, is not without risk given that the urothelium is already potentially destabilized by the field effect of carcinogen exposure [59]. Immediate post-operative instillations of mitomycin C, epirubicin, or doxorubicin are all valuable options for reducing disease recurrence [60]. A number of clinical studies have also shown gemcitabine to give good outcomes when used as an intravesical therapy [61,62]. In Canada, the most commonly used intravesical chemotherapy is mitomycin C. In one study, a single post-operative instillation of chemotherapy resulted in a recurrence rate of 37% compared with 48% for patients who only received a TURBT [60]. Interestingly, Onishi *et al.* showed that simply irrigating the bladder with saline after TURBT reduces recurrence in low risk NMIBC. Additionally, the recurrence-free survival was not significantly different between saline irrigation and a single instillation of mitomycin C [63,64]. This study indicates that recurrences are partly due to tumor cell seeding after surgery.

For patients with intermediate-risk NMIBC, intravesical chemotherapy in combination with TURBT is the current recommendation for preventing disease recurrence [57]. One study found no significant differences between time to recurrence and progression, as well as overall survival when comparing standard Bacillus Calmette-Guerin (BCG) induction to mitomycin C induction followed by instillations every month for 5 months [65]. However, further randomized clinical studies need to be performed to fully evaluate maintenance chemotherapy compared to induction therapy in preventing recurrence. High-grade Ta, T1, or CIS tumors put patients at an increased risk for recurrence and, more significantly, progression. Recommended treatment for patients with these high-grade tumors is TURBT followed by intravesical treatment with the immunotherapeutic agent BCG and maintenance immunotherapy for at least 1 year [57,66,67].

1.2.3 Bacillus Calmette-Guerin (BCG)

1.2.3.1 History. BCG is a live, attenuated, but genetically stable *Mycobacterium bovis* that was initially isolated from the udder of an infected cow in 1921 (reviewed in [68]). The principal use of BCG was as a vaccine for tuberculosis (TB). The first link between TB and cancer was reported by Pearl in 1929 [69]. Here he showed that patients who survived cancer had higher rates of previous or ongoing TB infections than those succumbing to cancer. However, due to contaminations of BCG vaccines with a virulent strain of *M. tuberculosis,* the excitement of using BCG as a cancer therapy faded [68]. Interest in BCG as a cancer therapy regained traction again in the 1950's when Lloyd Old showed that mice infected with BCG rejected tumors at higher rates when challenged than did uninfected mice [70]. It was later found that the anti-tumor activity of BCG was not due to direct cytotoxic effects but was a result of delayed hypersensitivity type immunological responses [71]. Burton Zbar conducted a number of experiments to determine the requirements for successful BCG therapy. These requirements include contact between BCG and

the tumor cells, an immune competent host that can generate an immune response against BCG, and finally, a relatively small tumor [71]. In 1976, Alvaro Morales was the first to publish the results of intravesical BCG therapy for NMIBC [72]. Morales' original protocol for BCG instillation consisted of 120 mg instilled into the bladder in 50 ml of saline. This treatment was performed weekly for six weeks. Amazingly, this is the exact same induction protocol used today. Initially ten patients with recurrent bladder cancer were treated and in seven cases there was no sign of visible tumor [72]. Based on these early results two additional trials were performed and it was concluded that BCG dramatically reduced tumor recurrence [73,74]. Many subsequent trials demonstrated efficacy of BCG immunotherapy in reducing recurrence and progression of bladder cancer which led to FDA approval in 1990. BCG remains the standard of care for high-grade non-muscle-invasive Ta, T1, or CIS tumors [57].

1.2.3.2 Mechanism of action. Amazingly, despite ~40 years of use the exact anti-tumor mechanism of BCG is still not completely understood (reviewed in [75]). Current evidence indicates that the initial attachment and internalization of BCG to bladder cancer cells are critical first steps. Here BCG binds to fibronectin attachment protein (FAP) [76] then this FAP/BCG complex binds to cell surfaces through integrin $\alpha5\beta1$ [77,78]. Internalization of BCG *in vitro* can vary widely between bladder cancer cell lines [79,80]. It has also been show that BCG can be internalized in *in vivo* bladder cancer models [81]. Recently, is was found that BCG is internalized through macropinocytosis as a result of oncogenic activation of the Rac1-Cdc42-Pak1 signaling pathway [80,82] downstream of Ras which is commonly activated in bladder cancer. However, *in vivo* evidence for the importance of internalization is lacking and further work is required. After BCG attachment and internalization, bladder cancer cells secrete numerous cytokines resulting in immune cell recruitment. One of the primary cytokines that is released after BCG internalization

is interleukin (IL)-6 [83]. IL-6 has been show to increase integrin α5β1 on bladder cancer cells [84] to recruit neutrophils [85], and to induce secretion of IL-8, granulocyte-macrophage colony-stimulating factor (GM-CSF), tumor necrosis factor (TNF)-α, and TNF-related apoptosis-inducing ligand (TRAIL) [86]. In addition, expression of major histocompatibility complex (MHC) class II on the surface of bladder cancer cells is increased, which contributes to the development of an anti-BCG immune response [87]. This upregulation of MHC II may be a direct result of BCG internalization [87]. There is some evidence that shows BCG can be directly cytotoxic to bladder cancer cells *in vitro* [88]. However, this generally requires 50-100 bacteria per cell and these levels are unlikely to be achieved *in vivo* [75]. $CD4^+$ cell recruitment to the bladder after BCG therapy results in a shift in the urinary cytokine environment from Th2-like to Th1 [89,90]. Efficacy of BCG has been shown to be dependent on the generation of this Th1-like immune response [91]. The Th1 cytokines secreted by monocytes and $CD4^+$ cells work to activate cytotoxic lymphocytes. The presence of both $CD4^+$ and $CD8^+$ T-cells is required for tumor cell killing [92]. Natural killer (NK)-cells mediated lysis has also been shown to be critical for an anti-tumor response [93]. Macrophages have been found in the bladder wall of patients treated with BCG [94] and can be cytotoxic *in vitro* against bladder cancer cells but there is no *in vivo* evidence of tumor killing by macrophages [95]. Despite decades of research, there are still many aspects of BCG therapy that are not fully understood.

1.2.3.3 Bladder cancer treatment with BCG. The use of BCG in the treatment of bladder cancer was first described by Morales *et al.* [72] in 1976. Since then, BCG has become the standard of care for high-grade NMIBC. A number of clinical trials have shown BCG after TURBT decreases recurrence rates [96,97]. Additionally, several meta-analyses have shown BCG to be superior to intravesical chemotherapy for preventing recurrence of high-grade disease [98-100].

BCG is administered to patients 2-4 weeks after they undergo a TURBT to limit the possibility of systemic side effects. For patients with high-risk NMIBC the Canadian Urological Association recommends an induction course of BCG that consists of 6 weekly intrabladder instillations followed by maintenance therapy (3 weekly cycles at 3 months and 6 months, then every 6 months up to 36 months) [57]. Intravesical chemotherapy is the first treatment choice for patients with intermediate-risk NMIBC. However, patients with intermediate-risk NMIBC who fail intravesical chemotherapy may be treated with induction and maintenance courses of BCG.

1.2.3.4 Recurrence and BCG failure. Approximately 50% to 70% of NMIBC patients will have a recurrence within 5 years, and up to 20% will progress to muscle-invasive disease [101]. The greatest risk is with high grade T1 tumors which have a 70% to 80% recurrence rate. If BCG therapy is unsuccessful in high-grade T1 disease and/or CIS, the risk of progression to muscle-invasive disease may reach 50% [15,16]. Additionally, 30 to 40% of patients treated with BCG do not respond to this therapy (reviewed in [102-104]). There has been very little improvement in the treatment of high-grade NMIBC in the last 20 years and recurrence after BCG therapy is still one of the most significant problems in the management of bladder cancer [102]. This highlights the urgent need for safer and more reliable bladder-sparing approaches.

There are numerous disease categories for patients who do not respond to BCG therapy [105]. BCG refractory is defined as persistent high-grade disease at 6 months despite BCG therapy, or progression in stage, grade, or disease extent by 3 months after the induction cycle of BCG. BCG resistant means there is recurrence or persistence of disease (of lesser stage or grade) at 3 months after the induction cycle, which subsequently resolves by 6 months. BCG relapse occurs when there is recurrence of disease after tumor clearance for at least 6 months. Finally, BCG intolerance occurs when therapy must be stopped because of side effects.

In patients whose cancer fails to respond to any of the above bladder-sparing treatments and who refuse surgery or are not suitable patients for surgery, the treatment choices become limited. Patients with NMIBC recurrence after intravesical chemotherapy can benefit from BCG instillations [98]. However, if this treatment fails, the treatment options are restricted and comprise a modified immunotherapy treatment (low-dose BCG plus interferon-alpha [106]), chemotherapy with intravesical gemcitabine [107-109] or docetaxel [110]. Cystectomy, however, remains the standard treatment for high-risk patients whose cancers have been unsuccessfully treated with BCG therapy and/or chemotherapy [103,111]. Patients who receive a cystectomy before their bladder cancer progresses to a muscle-invasive disease have shown an excellent disease-free survival [112]. However, cystectomy is not without the possibility of significant morbidity and the possibility of mortality, especially in the older patient with associated comorbidities [113]. Patients with NMIBC that fail BCG need other bladder-sparing treatment options.

1.2.4 Bladder preservation

Even though radical cystectomies are the gold standard for patients diagnosed with MIBC or who progress to muscle-invasive disease, there are circumstances where other bladder-sparing treatment options are desired. In eligible patients, bladder preservation can maximize a patient's survival while at the same time decreasing toxicity and improve a patient's quality of life [114].

Radical TURBT may be a viable option for patients with solitary tumors that are accessible to the surgeon. In appropriately selected patients treated this way, survival can be equal to that of radical cystectomies [115]. Partial cystectomy is another bladder-preserving treatment that involves surgical removal of the bladder tumor and adjacent bladder wall [116]. To be a candidate, the tumor should be primary, isolated, easy to access and <3 cm in size. Multiple studies have shown that partial cystectomy offer sufficient control of MIBC in select patients [116,117].

However, recurrence is not uncommon and patients require regular monitoring with cystoscopy. If there is a recurrence, a radical cystectomy is the preferred treatment.

Trimodal therapy comprises a radical TURBT followed by concurrent chemotherapy and radiation therapy and is currently the best treatment option for bladder preservation (reviewed in [118]). The time course and doses of chemotherapy and radiotherapy can vary between centers, and is an area of active evaluation. In a phase III study, concurrent chemotherapy with fluorouracil and mitomycin C combined with radiotherapy was compared to radiotherapy alone. Here they found disease-free survival was significantly improved in the chemoradiotherapy group compared to the radiotherapy alone group [119]. Ploussard *et al.* have performed an extensive systematic review of trimodal therapy and the data they collected indicate that trimodal therapy leads to satisfactory outcomes and may be considered a suitable treatment option in appropriate patients [120]. They also concluded that any patient that does not respond to trimodal therapy or that does have recurrence should undergo a cystectomy. Even though trimodal therapy has shown promising outcomes, there is still a need for larger randomized clinical trials, as well as novel treatment options.

1.2.5 Emerging bladder cancer therapies

Although bladder cancer is the 5th most common cancer in Canada, it only ranks 20th in research funding according to Bladder Cancer Canada. There have been very few advances in the management of bladder cancer in the past two decades [121]. Recently there has been an increased interest in developing therapies for both NMIBC as well as MIBC [122]. It is clear from the clinical outcomes and cost of managing bladder cancer that there is a significant need for effective therapies not only to prolong patient survival but to improve their quality of life as well. The next

few sections will give an overview of some of the new therapies that have moved into clinical trials.

1.2.5.1 Fibroblast growth factor signaling. Bladder cancer has a high rate of FGFR overexpression or activating mutations and this has generated significant interest in targeting this pathway as a treatment option. Multiple *in vitro* and *in vivo* studies have shown promising results with a variety of FGFR inhibitors. Ponatinib (AP24534) is a pan-FGFR inhibitor that has been shown to strongly inhibit the activity of all 4 FGFRs *in vitro* [123]. Another pan-FGFR inhibitor AZ12908010 (or AZD4547), showed significant anti-proliferative activity that was associated with unregulated FGFR signaling in cell culture models [124]. A phase I dose-escalation study of JNJ-42756493, an oral pan–FGFR inhibitor, showed a good toxicity profile with some signs of tumor control [125]. A confirmed response was seen in one patient with bladder cancer. Based on these promising results, a phase II study in metastatic or unresectable bladder cancer harboring FGFR gene alterations is underway (NCT02365597). Although there have been encouraging results with FGFR inhibitors, pre-clinical and clinical data are limited and more studies will need to be conducted to determine their true efficacy.

1.2.5.2 PI3K/AKT/mTOR inhibitor. The PI3K/AKT/mTOR signaling pathway is involved in cell cycle regulation, survival, proliferation, and motility. Forty percent of bladder cancers can have genetic alterations in this pathway. These include both activating mutations as well as deletion of the tumor suppressor PTEN [126]. Another pan-PI3K inhibitor LY294002 showed pre-clinical efficacy in bladder cancer [127] and this has resulted in a clinical trial for patients with metastatic bladder cancer (NCT01551030). Dual PI3K/mTOR inhibitors have also been investigated in bladder cancer. NVP-BEZ235 was shown to have a synergistic interaction

with cisplatin and was effective in cisplatin-resistant cell lines. However, it was found to cause MEK/ERK pathway activation [128], therefore its clinical development will likely be limited.

1.2.5.3 Epidermal growth factor receptor 2 (HER2)/ERBB2. HER2 is a receptor tyrosine kinase that activates a variety of signaling pathways resulting in cell proliferation, survival, and differentiation [129]. One study found HER2 overexpression in 41 of 80 patients with bladder cancer. Expression correlated with tumor stage and grade as well as overall survival [130]. However, analysis of the The Cancer Genome Atlas (TCGA) data set showed HER2 amplification or mutations in only 9% of bladder cancer [44]. A phase II study examined patients with metastatic bladder cancer and confirmed over-expression or amplification of HER2. Patients were treated with a combination of trastuzumab (HER2 monoclonal antibody), paclitaxel, carboplatin, and gemcitabine. Thirty-one of 44 patients showed a response to the treatment, and survival for HER2 negative vs. HER2 positive patients was 9.3 and 14.1 months, respectively [131].

Although it is encouraging to see new drugs being investigated in bladder cancer there has been a lack of overly promising results and further investigation is required.

1.3 Overview of oncolytic viruses

1.3.1 History of oncolytic viruses

Oncolytic viruses (OVs) are a form of cancer immunotherapy where a natural or genetically engineered virus selectively replicates in cancer cells while leaving normal cells unharmed (**Figure 1.3** and reviewed in [132-134]). Replication of the OV within cancer cells results in cell death and spread of the virus while at the same time stimulating an anti-tumor immune response. Although only recently have OVs really started to gain traction in the clinic, the history of virus infections and anti-tumor responses have a much longer history. As far back as the mid-1800s there have

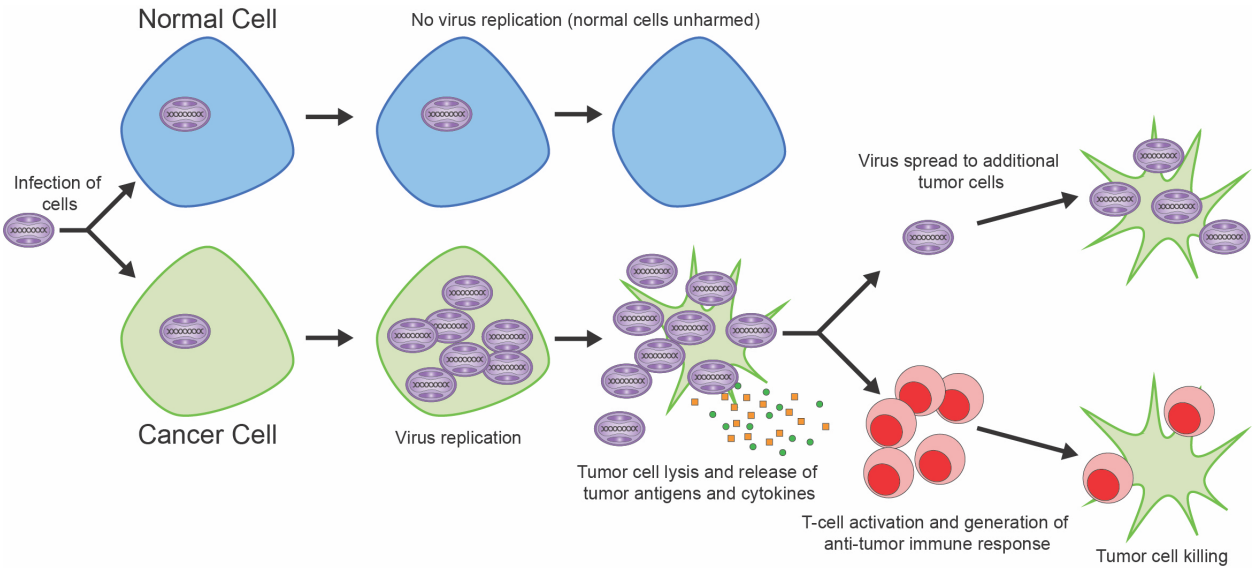

Figure 1.3: Oncolytic virus mechanism of action. Oncolytic viruses replicate in cancer cells but leave normal cells unharmed. The efficiency of oncolytic viruses is achieved through direct lysis of cancer cells and activation of anti-tumor immune responses. Figure from [135].

been reports on dramatic tumor regression in patients that had ongoing viral infections at the same time [136]. One of the first reported cases was a leukaemia patient that acquired influenza in 1896 [137]. Another well know case occurred in 1912: a patient with cervical cancer was vaccinated for rabies then experienced a reduction in disease [138]. These early observations paved the way for further investigation into viruses as possible cancer therapies.

One of the first documented clinical studies of viruses in cancer therapy was in 1949 [139], after two patients with Hodgkin's lymphoma were seen to have a partial anti-tumor response after contracting hepatitis. Based on these observations a clinical study with 22 Hodgkin's lymphoma patients was conducted. Here patients were administered serum from known hepatitis patients. In this study, 7 of 22 treated patients had signs of disease improvement, 4 of 22 showed a reduction in tumor size, 14 of 22 developed hepatitis and one patient death was reported. Over the next couple decades several other viruses were analyzed in clinical studies.

In 1952, Egypt 101 virus (early passage West Nile virus) was administered by intravenous (IV) injection to patients with various different cancers [140]. Only 4 of 34 patients had a transient anti-tumor response while five patients suffered severe encephalitis. In 1956, adenovirus was tested as treatment for cervical cancer [141]. Interestingly, nearly two-thirds of patients had signs of necrosis within the tumor, and the necrosis seemed to be confined to the tumor tissues. However, the virus was rapidly cleared and there was little to no improvement in survival. Then in 1974, wild-type (WT) mumps virus was tested in a variety of cancers including gastric, pulmonary, and uterine [142]. Amazingly, 37 of 90 patients treated had tumors that shrank to half of their original size or smaller. However, numerous studies carried out around the same time showed no dramatic improvement in clinical outcomes [143,144]. Due to lack of efficacy paired with increasing

regulatory and ethical guidelines, the use of viruses as cancer therapies significantly decreased through the 1970' and 80's.

The introduction of recombinant deoxyribonucleic acid (DNA) technologies in the 1990's meant that viruses could now be engineered to enhance their tumor selectivity and ultimately their safety. Interestingly, this was 30 years after Southam suggested that altering the virus genome could improve viral therapies [145]. The ability to genetically modify viruses brought a new wave of excitement in using viruses as not only cancer therapies but as gene therapies for a variety of diseases. One of the first reported OVs in the new era of recombinant DNA was by Martuza *et al*. where they described a thymidine kinase (TK)-deleted herpes simplex virus type 1 (HSV-1) in a preclinical model of glioma [146]. This virus could replicate in dividing cancer cells but had limited replication capacity in non-dividing cells resulting in significant tumor control with little toxicity in nude mice. From there, numerous viruses were engineered and tested for their oncolytic capabilities and the new wave of OVs emerged.

1.3.2 Mechanism of oncolytic virus immunotherapy

OV induced cell death following infection of a cancer cell is a complicated and multifactorial process that varies widely between viruses and cell type. The anti-tumor actions of OVs fall under two general categories: direct cell lysis and generation of an anti-tumor immune response (**Figure 1.3** and reviewed in [132,133]). Direct killing of tumor cells occurs through virus replication within the cancer cells and then subsequent lysis and destruction. Cell death has been reported to occur through a variety of mechanisms such as apoptosis, necrosis, and autophagy [147]. Different viruses utilize a variety of mechanisms to lyse cells. Cell lysis not only results in death of the infect cells but allows the virus progeny to spread to adjacent cells, continuing the cycle of cell killing. This 'self-amplifying' feature of OVs is one of their unique properties. While

the initial thought was that more virus replication would result in more cell killing and thus better clinical outcomes, more recently it has been show that the development of anti-tumor immunity is critical for complete and long term tumor control [148]. Much of the recent work in the OV field has been focused on enhancing the anti-tumor immune response after virus delivery.

During lysis, tumor cells release tumor-associated antigens that can be recognized by the immune system. Virus replication and cell lysis also result in an inflammatory environment and the release of numerous compounds that help initiate immune cell recruitment. Some of these include pathogen-associated molecular patterns (PAMPs), danger-associated molecular patterns (DAMPs) (such as high mobility group box 1 (HMGB1) and ATP), as well as cytokines (TNF-α and interferon (IFN)-γ) [149,150]. Ultimately, activation of anti-viral signaling, cytokine production and an 'immunogenic' type of cell death promotes the stimulation of immune responses (reviewed in [151]). Immune activation within the tumor site results in the infiltration of antigen-presenting cells (APC) such as dendritic cells (DCs) that can process the tumor-associated antigens to activate $CD4^+$ and $CD8^+$ T-cells. Activated and expanded anti-tumor cytotoxic $CD8^+$ T-cells are key mediators of tumor clearance and long term control. Activated $CD8^+$ T-cells not only help to destroy the primary tumor but they are also capable of circulating throughout the body destroying distant tumor cells.

Although $CD8^+$ T-cells are often the primary focus of anti-tumor immune responses, several other cell types have been shown to contribute. NK cells can be activated by the release of type I interferons and DAMPs from the lysis of tumor cells [152]. NK cells are particularly efficient at killing cells that have lowered expression of MHC class I receptors at the cell surface [153]. Decreased MHC expression has been shown to be a common way for cancer cells to evade cytotoxic T-cell recognition [154]. Neutrophils are also critically important for initiating the anti-

tumor immune response after OV therapy [155]. Neutrophils are one of the first immune cells recruited to the site of viral infections. Here they are able to kill tumor cells as well as release TRAIL and TNF-α, enhancing cell death and increasing additional immune cell infiltration [156]. Although direct tumor cell lysis is essential for the anti-tumor activity of OVs, it has also been show that viruses such as vaccinia virus (VACV) [157,158], vesicular stomatitis virus (VSV) [159], and HSV [160] can infect and replicate in the tumor vasculature where they can destroy the blood vessels thus starving the tumor of required nutrients.

1.3.3 Development of tumor selective viruses

The most important safety consideration when developing and testing a OV is tumor selectivity. Ideally, a virus will have robust replication and killing within tumor cells but will be unable to infect and/or replicate in normal tissues. Numerous strategies have been used to restrict virus replication to tumor sites and some of them will be highlighted in this section.

Several viruses have a natural selectivity for cancer cells. Tumors have numerous aberrant signaling pathways that result in sustained growth, evasion of cell death, immune suppression, and increased angiogenesis (reviewed in [161]). Viruses such as reovirus [162], myxoma virus [163], VSV [164], and Coxsackievirus [165] can take advantage of these altered signaling pathways to replicate preferentially in cancer cells while leaving normal cells unharmed.

Although some native viruses have selectivity for cancer cells, many viruses are able to infect normal cells and replicate in them. Because of this, most viruses are genetically engineered to restrict their replication to cancer cells (reviewed in [166]). Numerous engineering strategies have been developed and some common strategies will be briefly highlighted below. Transductional targeting involves genetically modifying a virus in order to alter the ligands expressed on the virion surface (reviewed in [167]). This results in a virus that is restricted to

entering only tumor cells that express the corresponding receptor. Transcriptional targeting is achieved by placing essential viral genes under the regulation of a tumor-specific promoter. The virus is then able to replicate only in cells that activate the expression of this essential viral gene. This technique is limited to DNA viruses that replicate in the nucleus. For example, tumor-specific promoters from genes such as telomerase reverse transcriptase (hTERT) [168] or survivin [169] are highly active in many different tumor types. Additionally, there are tissue-specific promoters such as prostate-specific antigen (PSA) that are overexpressed in prostate cancer [170]. Finally, complementation-based targeting involves removing viral genes that are redundant in cancer cells with aberrant signaling pathways.

The tumor targeting strategies above are used to improve the tumor selectivity of viruses and thus improve their safety. However, many of these viruses show minimal anti-tumor activity, and consequently significant research has gone into enhancing the anti-tumor response. One of the main strategies applied has been to engineer the viruses to express immune-stimulating molecules such as cytokines and chemokines which are intended to improve the anti-tumor immune response. The most commonly used immune-stimulating cytokine is GM-CSF. Other cytokine genes such as IL-2, IL-12, IL-15, and IFN-ß have been engineered into OVs. OVs have also been generated to express cytotoxic proteins like TRAIL. In order to further enhance immune activation, viruses have been generated to express the T-cell costimulatory molecule CD40 ligand (CD40L) [171]. Even more recently, viruses have been engineered to express tumor antigens and bispecific antibodies [172]. There is a constant evolution to try to engineer safer and more effective OVs.

1.4 Bladder cancer as a target for oncolytic viruses

Recently developments in cancer immunotherapies, which include OVs, have shown dramatic efficacy in patients and can often eliminate tumors. OVs could potentially be used in the

many patients that fail conventional bladder cancer treatments. The urinary bladder is an excellent organ to evaluate local OV therapy for a number of reasons. The urethra permits easy intravesical instillation of this isolated organ, allowing the tumor to be exposed to large titers of vector [173], while the trilaminar (asymmetric) unit membrane limits systemic exposure [174,175]. Furthermore, the papillary configuration of NMIBC exposes a large surface area ideal for topical virus application. The success of BCG therapy highlights the immunosensitivity of bladder cancer, providing a basis for examination of other immunomodulatory agents as therapies [75]. OVs could potentially be administered earlier during therapy (immediately after TURBT) without the significant risk of severe systemic illness, unlike BCG [176,177]. Direct oncolysis by selective replication in transformed NMIBC cells could potentially avoid a high degree of inflammation and the profound symptoms of cystitis while also promoting the development of an anti-tumor immune response. Since OVs often take advantage of multiple dysregulated pathways there is less chance to develop resistance. Finally, there is an urgent need for more bladder-sparing therapies for patients failing conventional therapies.

1.5 Oncolytic activity of specific viruses (excluding vaccinia virus)

Many different OVs have been developed and evaluated in preclinical models with a number of them having moved on to clinical trials (reviewed in [132-134,178]). A complete review of all OVs is beyond the scope of this thesis, so the discussion of specific OVs is limited here to those that have been tested for activity against bladder cancer.

1.5.1 HSV

HSV is a large (150–200 nm diameter) enveloped virus [179] with a double-stranded DNA genome of approximately 150 kbp [180]. HSV commonly causes infections in the orofacial region (HSV-1) and in the genital region (HSV-2) (reviewed in [181]). Multiple genetic manipulations to

HSV have been implemented in the development of viruses that selectively replicate in cancer cells. One mutation that has been examined is the inactivation of the viral *UL39* gene, which codes for the large (RRM1) subunit of ribonucleotide reductase (RNR) [182,183]. RNR plays a key role in making the deoxyribonucleotide triphosphates (dNTPs) that are needed for DNA synthesis [184]. RNR levels are elevated in dividing tumor cells but low in normal cells. This mutation therefore renders the virus dependent on the cellular enzyme, resulting in tumor selectivity. A second modification that has been investigated is the inactivation of the γ_1-34.5 gene that encodes the ICP34.5 protein which is important for viral replication [185], viral exit from cells [186], prevention of the early shut-off of protein synthesis [187], and neurovirulence [188]. In normal cells, the double-stranded- ribonucleic acid (dsRNA-) dependent protein kinase (PKR) shuts off protein synthesis and prevents viral replication [189]. Tumor cells often have defects in this signaling pathway and thus allow viral replication. Mutation of the viral *UL23* (TK) gene also renders the virus dependent on host cell TK1 expression [190].

Oncolytic HSV armed with immunomodulating transgenes such as GM-CSF [191], IL-2 [192], IL-12 [193], and B7-1 [194] have also been developed. In addition, conditionally replicating HSV has been used to deliver gene products that convert pro-drugs into cytotoxic agents. One example of this is rRp450, a replication-selective HSV that has a deletion in the viral *UL39* (RRM1) gene and codes for the rat cytochrome P450. Cytochrome P450 activates prodrugs such as cyclophosphamide (CPA) to generate highly toxic metabolites. It has been shown *in vitro* that rRp450 oncolytic cell killing was improved by administration of CPA [195]. Another enzyme/prodrug system used is HSV-1-encoded thymidine kinase (HSV-TK) that phosphorylates the prodrug ganciclovir. The resulting activated metabolite induces increased cell death compared to virus oncolysis alone. HSV-TK activation of ganciclovir in infected cells also stops viral

replication [196]. HSV-TK and ganciclovir could therefore be used as a safety mechanism to prevent virus spread if serious virus toxicity were to develop.

Cozzi *et al*. reported on two attenuated, replication-competent HSVs, G207 and NV1020, for treatment of bladder cancer in a mouse model [197]. G207 is modified by deletions of both copies of γ_1-34.5 and interruption of the *UL39* gene (RRM1) [198]. NV1020 has a deletion in the *UL23* (TK) region of the genome and a 15 kb deletion across the junction of the long and short segments of the HSV-1 genome that disrupts one copy of several diploid genes [199]. Both G207 and NV1020 were compared to BCG treatment and proved very successful when delivered by intravesical instillation weekly for 3 weeks (10^7 plaque forming units (PFU)) in the immune competent MBT-2 orthotopic bladder cancer model [197]. Ten of 11 animals in the control group had bladder tumors at autopsy. A significant increase in tumor clearance was shown in the treated groups, with tumors observed in only six of 12 animals in the BCG group, 5 of 13 animals in the G207 group, and only 2 of 12 animals in the NV1020 group. These encouraging pre-clinical results suggest that there should be further evaluation of intravesical oncolytic HSV therapies for bladder cancer in clinical trials.

Simpson *et al*. have reported results with OncoVEX$^{GALV/CD}$ as an intravesical therapy for bladder cancer [200]. OncoVEX$^{GALV/CD}$ is an oncolytic HSV-1 that expresses a potent prodrug activating gene Fcy::Fur which combines the activity of the yeast cytosine deaminase and uracil phosphoribosyltransferase to sensitize cells to 5-fluorocytosine [200]. It also encodes the fusogenic gibbon ape leukemia virus envelope (GALV) glycoprotein that enhances tumor cell killing [201]. Deletion of the viral γ_1-34.5 genes in OncoVEX$^{GALV/CD}$ results in tumor-selective viral replication. An 85% decrease in tumor size in the presence of both OncoVEX$^{GALV/CD}$ and 5-fluorocytosine

when compared with control was observed in the rat AY-27 orthotopic bladder tumor model (model described in detail within results section of this thesis).

Talimogene laherparepvec or T-Vec (previously named OncoVEX^{GM-CSF} [202]) is similar in structure to OncoVEX$^{GALV/CD}$ and has shown promising results in phase I, II, and III clinical trials for a variety of cancers; including breast, head and neck, and malignant melanoma [202-205]. T-Vec has recently received US clinical approval and is the first and only oncolytic virus to do so thus far [205]. It has been modified by deletion of γ_1-34.5 and replacement of *US12* (encodes ICP47) with the coding sequence for human GM-CSF under the control of the human cytomegalovirus immediate early promoter [206]. ICP47 blocks the MHC class I antigen presentation pathway by binding to the transporter associated with antigen presentation protein [207]. As a safety mechanism, the TK gene remains intact, maintaining sensitivity to ganciclovir or related antiviral agents. A phase II study of T-Vec in metastatic melanoma demonstrated a 26% objective response rate after direct injection into accessible melanoma lesions. Patients that showed a response had regression of both injected and noninjected lesions [204]. The safety profile of oncolytic HSVs in both the phase I and II studies has been encouraging, and further evaluation was conducted with a phase III trial for unresectable stage III or IV melanoma to determine significance [202,205,208]. Multiple oncolytic HSV mutants have shown promise in both preclinical bladder cancer models and in clinical trials for other cancers. Thus, there is a huge untapped potential for oncolytic HSV to be used in the treatment of bladder cancer patients.

1.5.2 Adenovirus

Adenovirus (Ad) is a nonenveloped, linear, double-stranded DNA virus with a genome of approximately 36 kbp. The human Ad subgroup C, which contains 2 of the most studied serotypes (types 2 and 5), is widespread in the population and associated with a mild upper respiratory tract

infection [209]. Ads have been genetically modified to take advantage of the altered tumor environment to allow selective replication. Two general approaches have been used to generate this tumor selectivity. The first is to delete gene functions that are critical for efficient viral replication in normal cells but are expendable in tumor cells [210,211]. For example, ONYX-015 (dl1520 or CI-1042) was the first conditionally replication-competent engineered Ad to enter a clinical trial. In 2006 a similar adenovirus (H101) became the first oncolytic viral therapy to be approved in China [212]. ONYX-015 and H101 contain a deletion of the E1B-55 kDa coding sequence and demonstrate oncolytic activity in cancer cells with mutant p53, but only limited cytotoxicity in normal human cells with WT p53 function [213,214] (however, it has become clear that this is not the reason for selective replication) [215]. A second general approach is to limit the expression of the E1A gene product using tumor- and/or tissue-specific promoters [216]. E1A functions to stimulate S-phase and transcriptional activation of both cellular and viral genes, allowing virus replication to proceed. An example is the CN706 virus in which the E1A gene is transcriptionally controlled by the PSA promoter, resulting in a virus that selectively replicates in tissue with high PSA levels [217]. Another Ad has a 24-base pair deletion in the Rb-binding domain of the E1A protein (Ad5-Δ24) and is unable to inhibit RB1. Van Beusechem *et al.* reported on an Ad5-Δ24 transductionally modified by producing bispecific antibody directed towards the Ad fiber knob and the epidermal growth factor receptor (EGFR) [218]. This virus had increased infectivity and replication in cells (including T24 bladder cancer cells) resistant to a non-modified oncolytic adenovirus. Onco^{Ad}.RGD-hTERT-TRAIL is a multiply-modified adenovirus with Δ24-E1A and E1B-55K deletions, TRAIL transgene under control of the tumor-specific hTERT promoter, and with an RGD motif genetically incorporated into the fiber protein on the viral capsid to target integrins on the cell surface. This virus showed promising results in both *in vitro* and

xenograft models of bladder cancer [219]. There are many other examples of selectively replicating oncolytic Ads that have been reviewed elsewhere [220].

Ramesh *et al*. have reported both preclinical and clinical results of their oncolytic adenovirus, CG0070 for the treatment of bladder cancer [221,222]. CG0070 is a selectively replicating Ad in which the human E2F-1 promoter drives expression of the viral E1A gene. E2F-1 is regulated by Rb, which is commonly mutated in many bladder cancers [223,224]. Loss of RB binding to E2F-1 results in a transcriptionally active E2F. In addition, CG0070 encodes human GM-CSF [225], a cytokine that stimulates the maturation and recruitment of macrophages and dendritic cells and is known to be a potent inducer of local anti-tumor immunity. CG0070 preferentially replicates in Rb protein-defective bladder cancer cells resulting in increased production of GM-CSF that activates the host immune response. The tumor selectivity of CG0070 was indicated by the 100-fold higher replication and 1000-fold greater cytotoxicity in bladder UCC cells compared to normal fibroblast cells. Expression of GM-CSF in MRC-5 (normal lung fibroblast) cells was up to 45-fold lower than in the UCC cell lines used in these experiments. CG0070 showed tumor killing in orthotopic and subcutaneous human xenograft bladder tumor models. A significant anti-tumor effect was seen after five intratumoral injections of CG0070 at concentrations up to 3×10^{10} viral particles per dose. Half of the mice (5 of 10) treated with the highest dose showed complete tumor regression compared with no regression in mice treated with PBS.

These promising preclinical data led to a phase I clinical trial of CG0070 that focused on NMIBC (CIS, Ta, and T1 groups) in patients with recurrent bladder cancer after BCG treatment [221]. Results with CG0070 delivered intravesically at doses up to $3x10^{13}$ virus particles showed response rates of 23% (3/13) in single dose and 64% (14/22) in multi-dose (weekly 6x or monthly

3x) groups as assessed by cystoscopy and urine cytology or biopsy [226]. Local toxicities (dysuria, bladder pain, and frequency) and flu-like symptoms were the most common adverse events observed. To our knowledge, this is the first report of a clinical trial using an oncolytic Ad in bladder cancer. The encouraging results have led to CG0070 currently being evaluated in a phase II study (BOND2) that is designed to determine the safety and efficacy in high-grade NMIBC that has failed BCG therapy (NCT02365818). There are also plans for CG0070 to be studied in a phase I/II study (NAOMI), to assess the safety and efficacy of neo-adjuvant combination of CG0070 plus anti-cytotoxic T-lymphocyte associated protein 4 (CTLA-4) in patients with MIBC who are ineligible for platinum-based chemotherapy.

1.5.3 Reovirus

Reoviridae are a family of viruses that includes viruses that infect the gastrointestinal tract and respiratory system. Human reoviruses contain 10 segments of double-stranded RNA and a double shell of proteins that compose the inner capsid or core and the outer capsid (reviewed in [227]).

The first report of the oncolytic properties of these viruses came following the realization that the virus replicated in transformed cell lines but not in normal cells [228]. In normal cells, infection is attenuated because reovirus activates PKR that inhibit eukaryotic initiation factor 2α (eIF2α) blocking viral protein synthesis. In cancer cells with activated Ras, activation of PKR is inhibited, allowing viral protein synthesis and an oncolytic infection to occur. Around 30% of all cancers have mutations in the Ras proteins [229]. The majority of the remaining cancers rely on mutations in members of the epidermal growth factor (EGF) pathway that initiates Ras function. Up to 90% of bladder cancers have an overactive EGF pathway [230].

Reovirus has been extensively studied as an oncolytic virus in a variety of cancers (reviewed in [231]). Hanel *et al*. demonstrated oncolytic activity of reovirus *in vitro* and in the AY-27 orthotopic rat bladder tumor model [232]. Rats were treated twice a week for 3 weeks with low, medium, and high doses (2.5×10^5, 2.5×10^6, 2.5×10^7 PFU) of intravesical reovirus or BCG as control. Complete tumor response was observed in 90% of animals by 100 days after tumor implantation in medium- and high-dose reovirus-instilled animals, while the highest survival in the BCG-treated groups was 50%. Despite these encouraging results, little research has gone into further use of reovirus for bladder cancer.

Multiple phase I, II, and III studies have been completed with over 1,000 patients being treated (reviewed in [233]). Only one clinical study has reported on activity of oncolytic reovirus in bladder cancer patients [234]. Two out of 33 patients in the phase I trial presented with UCC, however, as it was a phase I trial no significant data on clinical repose was obtained. These clinical results, as well as the relatively low risk due to reovirus' limited pathogenicity in humans, highlight the promising potential for this oncolytic agent to expand its clinical potential to include bladder cancer.

1.6 Poxvirus biology

1.6.1 History

The most notable member of the poxvirus family is variola virus, the causative agent of smallpox which is one of the most devastating diseases in human history [235]. The last naturally occurring case of smallpox was diagnosed in October 1977 after an extensive eradication program using VACV as a vaccine. By 1980 the World Health Organization had declared smallpox eradicated, the only disease eradicated so far that specifically affects humans. Because of its use as a vaccine, VACV is the most extensively studied poxvirus, however the origin and natural host

are not fully understood. Some evidence indicates that it may be a derivative of horsepox virus [236,237]. There are many different strains of VACV (reviewed in [238,239]) that have been used and studied. Here we will highlight some of the strains that have been used in the development of oncolytic VACVs.

The New York City Board of Health (NYCBH) is a first-generation smallpox vaccine that was the most widely used vaccine strain in North America during the smallpox eradication campaign. Western Reserve (WR) is a highly neuropathogenic laboratory strain that originated from passaging the NYCBH vaccine strain in mice. Dryvax is a non-clonal vaccine that was derived by passaging the NYCBH strain in the skin of calves. Genetic analysis has shown that Dryvax is composed of various different VACV strains [240]. Dryvax strains are often also termed Wyeth, the manufacturer of the vaccine. The Lister strain was developed at the Lister Institute and was used in Europe during the smallpox eradication campaign.

1.6.2 Entry and early gene expression

VACV has a linear double-stranded DNA genome that replicates exclusively in the cytoplasm (reviewed in [241]). The general life cycle for VACV is shown in **Figure 1.4**. VACV encodes many of the proteins required for transcription and replication of the viral genome as well as many virulence factors that modulate the immune response upon infection, allowing robust virus replication in a wide range of hosts and cell types [242,243]. There are two main infectious forms of VACV particles: the mature virion (MV) and the enveloped virion (EV) [244,245]. MVs are comprised of a single lipid bilayer membrane containing over 20 viral proteins. MVs account for over 99% of virions released upon cell lysis [246]. EVs are formed when MVs gain a second lipid bilayer during exit of the cell through the plasma membrane.

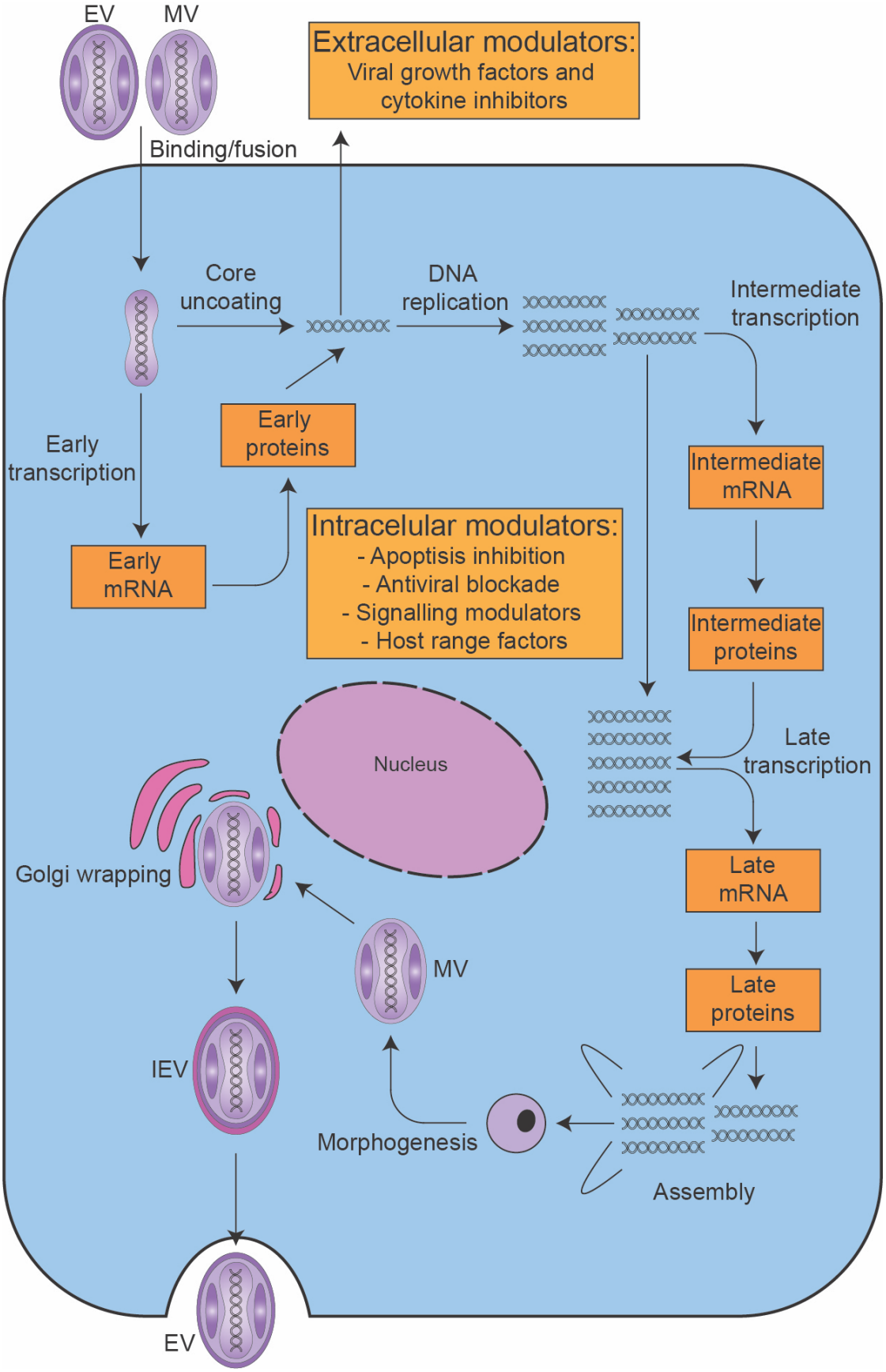
EV
MV
Extracellular modulators:
Viral growth factors and
cytokine inhibitors
Binding/fusion
Core
uncoating
DNA
replication
Intermediate
transcription
Early
transcription
Early
proteins
Intermediate
mRNA
Early
mRNA
Intracelular modulators:
- Apoptisis inhibition
- Antiviral blockade
- Signalling modulators
- Host range factors
Intermediate
proteins
Nucleus
Late
transcription
Golgi wrapping
Late
mRNA
MV
Late
proteins
IEV
Morphogenesis
Assembly
EV

Figure 1.4: Poxvirus replication cycle. There are two distinct infectious virus particles, the mature virus (MV) and the enveloped virus (EV), that can initiate infection. The MV and EV virions differ in their surface glycoproteins and in the number of wrapping membranes. The binding of the virion is determined by several virion proteins and by glycosaminoglycans (GAGs) on the surface of the target cell or by components of the extracellular matrix. Poxviruses utilize two primary modes of infection: uptake via macropinocytosis or fusion with the cellular membrane. Fully permissive viral replication is characterized by three waves of viral mRNA and protein synthesis (known as early, intermediate and late), which are followed by morphogenesis of infectious particles. The initial mature virus (MV) is transported via microtubules and is wrapped with Golgi-derived membrane, after which it is referred to as an intracellular enveloped virus (IEV). The IEV fuses to the cell surface membrane, which is either extruded away from the cell by actin-tail polymerization (not shown) or is released to form free EV. The majority of MVs are released upon cell lysis. Poxviruses also express a range of extracellular and intracellular modulators to facilitate virus infection and spread. Figure and text adapted from [241] with permission.

Although there are slight variations between virus strains [247], in general MV can utilize multiple modes of entry into a cell, including fusion with the cellular plasma membrane during low-pH-dependent endosomal uptake [248,249] or through macropinocytosis [250]. EV first loses its outer lipid membrane upon binding to the cell surface, then the inner membrane can enter through the same mechanism as MVs. Once the virion has crossed the plasma membrane, the viral core is released into the cytoplasm. Early transcription takes place within the viral core by a virally-encoded RNA polymerase [251]. mRNAs produced within the core are extruded and translated by host cell ribosomes. The viral early gene products are host cell modulators (intra- and extracellular), proteins for DNA replication, and initiators of intermediate gene transcription. The viral core is uncoated and the viral genomes are released to serve as templates for DNA replication [252].

1.6.3 Genome replication and virion assembly

Once the viral core has been uncoated and the viral genome is released into the cytoplasm, genome replication begins and 'viral factories' are formed [253]. The VACV genome is structured so that conserved genes are located in the central region of the genome. These genes are primarily involved in essential functions like transcription, DNA replication, and virion assembly. The outer ends of the genome are more variable between poxviruses and encode genes primarily involved in immune manipulation and evasion of host defenses [241]. There are also inverted terminal repeats that are identical telomeric sequences located on both ends of the genome. The onset of viral DNA replication signals intermediate and late gene transcription that begin 1.5 and 2-4 hrs post-infection, respectively [254,255]. Intermediate genes code for transcription factors that initiate late gene expression. Late gene products are primarily structural components of the virion or enzymes packaged within the virion that are required for virion entry or initial transcription upon infection

[252]. Virion assembly begins with a crescent-shaped structure containing lipids and protein that grows to eventually enclose the viral genome and core proteins [256]. As virion assembly progresses, these crescent shaped immature virions are proteolytically processed into MV. Most of these MV particles are contained within the cell until lysis, at which point they are released [252]. A proportion of the MVs are shuttled along microtubules towards the plasma membrane and along the way they pick up an additional membrane derived from the trans-Golgi network [252]. Once these intracellular wrapped virions arrive at the plasma membrane the outer viral membrane fuses with the plasma membrane. Actin projections can drive the newly formed EV particles to infect neighboring cells which allows for virus spread before cell lysis occurs.

1.6.4 Nucleotide metabolism

VACV encodes many of the proteins required for robust replication in normal and/or non-dividing cells (**Figure 1.5**) [241]. The rate of VACV DNA replication is extremely high and this requires an abundant supply of dNTPs [257]. VACV has evolved to accommodate the restriction in two main ways. Firstly, VACV encodes many proteins that are responsible for shutting down host cells protein synthesis and DNA replication thus limiting the host's use of dNTPs [258]. Secondly, VACV encodes its own proteins involved in dNTP synthesis allowing it to replicate its DNA independent of many of the host proteins. dNTPs are synthesized through two parallel pathways referred to as '*de novo*' and 'salvage' pathways [259]. In *de novo* synthesis of dNTPs, several enzymes and enzyme complexes catalyze reactions that generate phosphorylated purine and pyrimidine nucleosides from precursor molecules such as carbon, amino acids, and sugars. On the other hand, the salvage pathway recycles purine and pyrimidine nucleosides to generate dNTPs.

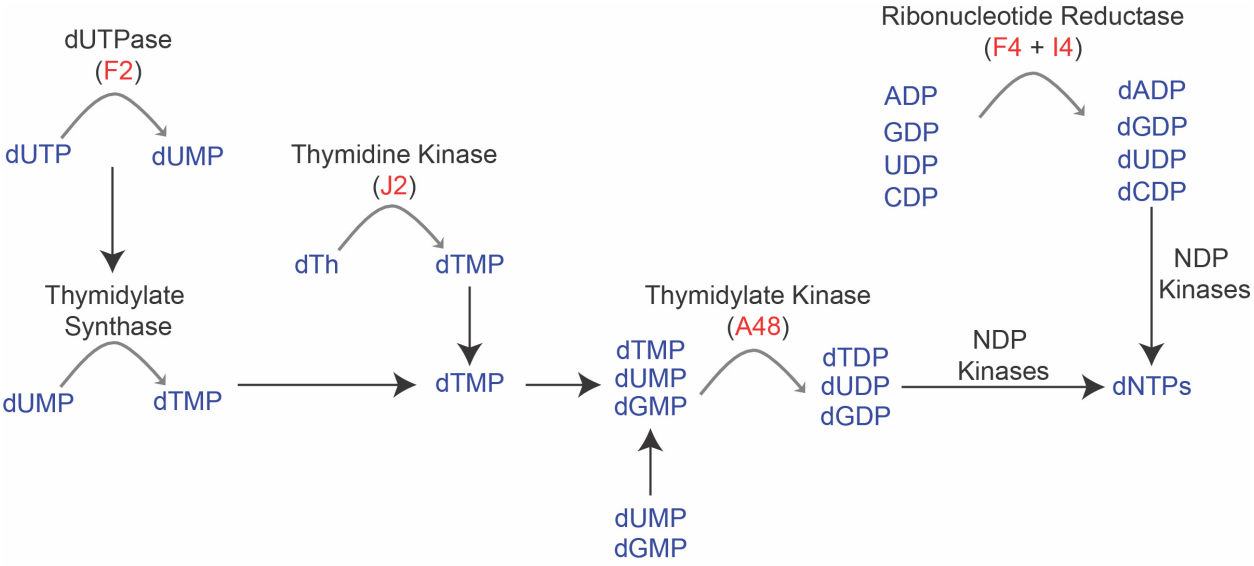

Figure 1.5: Nucleotide biosynthetic pathway. Cellular enzymes involved in dNTP metabolism are shown in black, the VACV-encoded homologs are shown in red, and metabolites are shown in blue. Figure modified from David Evans.

Cellular dNTP levels are a key determinant of DNA replication and ultimately cell proliferation [260]. The rate-limiting step in the generation of dNTPs for DNA replication is the *de novo* reduction of ribonucleoside diphosphates (rNDPs) to deoxyribonucleoside diphosphates (dNDPs) by the enzyme RNR (reviewed in [184] and **Figure 1.6**). The mammalian RNR complex is composed of the large (RRM1) and small (RRM2) subunits that form the heterotetrameric enzyme. The RRM1 subunit carries the active site and the RRM2 subunit contains a diferric iron center, producing a tyrosyl free radical required for catalysis of the reaction [261]. Both the RRM1 and RRM2 proteins are transcribed during S/G2-phase but because of the long half-life (15 hr) of the RRM1 protein, it remains relatively constant throughout the cell cycle [262]. In contrast, the RRM2 protein is rapidly degraded in the G2/M-phase making it the rate-limiting factor in the RNR reaction [263]. The RRM2 protein contains a "KEN box" sequence that is identified by the anaphase-promoting complex-Cdh1 ubiquitin ligase. The anaphase-promoting complex cause polyubiquitination, which leads to degradation of RRM2 [264]. Mammals also encode an additional RNR protein, p53R2. Like the RRM2 protein, p53R2 contains a tyrosyl free radical and can form an active RNR complex with the RRM1 protein [265,266]. Although p53R2 is almost identical (~80%) to the rapidly degraded RRM2 protein, it lacks the 33 N-terminal amino acid residues found in RRM2 that contain the KEN box and is therefore not targeted by the anaphase-promoting complex [263]. This allows p53-dependent induction of p53R2 in response to DNA damage and stabilization of the protein outside of S-phase [267]. VACV expresses both the large (RRM1; *I4L* gene product) and small (RRM2; *F4L* gene product) subunits of the heterodimeric RNR complex, which are critical for dNTP biosynthesis [268]. These proteins interact to form active complexes with each other and with their cellular homologs allowing for dNTP production outside of S-phase [269].

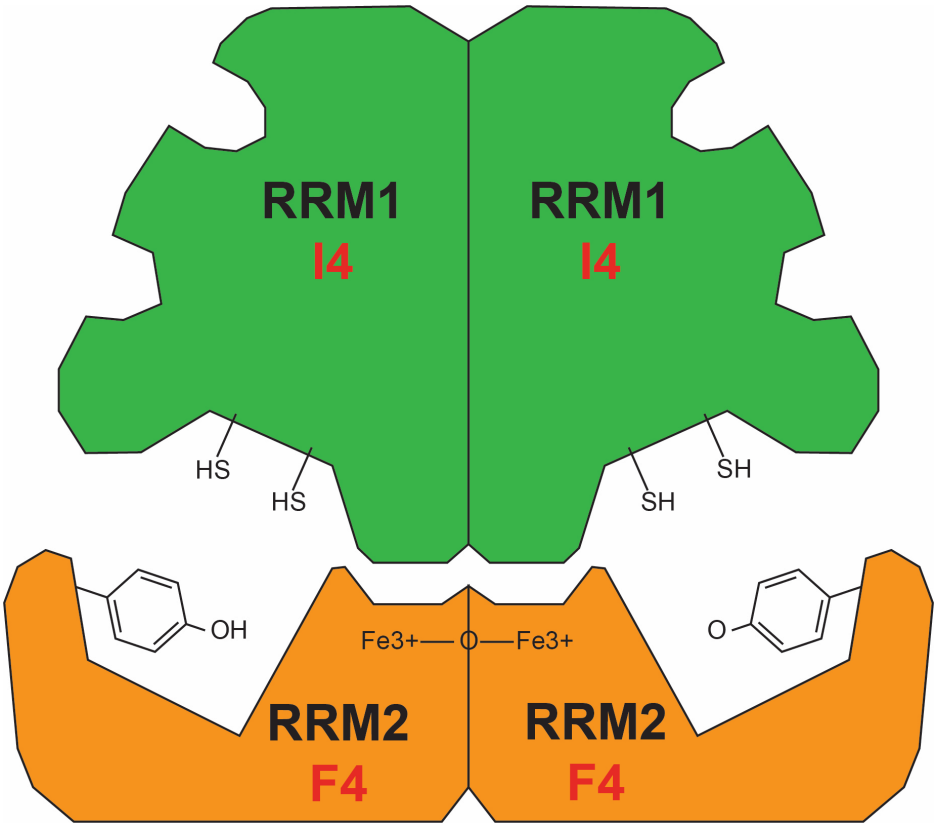

Figure 1.6: Ribonucleotide reductase (RNR) structure. The mammalian RNR complex is composed of the large (RRM1) and small (RRM2) subunits that form the heterotetrameric enzyme. VACV encodes homologs of the large (I4) and small (F4) subunits. The RRM1/I4 subunit carries the active site and the RRM2/F4 subunit contains a diferric iron center, producing a tyrosyl free radical required for catalysis of the reaction. Figure and text adapted from [270] with permission.

De novo dNTP synthesis provides the majority of nucleotides required for DNA replication. However, the salvage pathway also plays an important role in the recycling of dNTPs independently of RNR. Two enzymes critical in the salvage pathway (and of most importance to this thesis) are TK1 [271] and thymidylate kinase (TMK) [272]. VACV homologs of the cellular proteins are encoded by *J2R* and *A48R* genes, respectively. Viral TK plays a role in the salvage pathway through the phosphorylation of deoxythymidine (dTh) to deoxythymidine monophosphate (dTMP) [273]. TMK is responsible for dTMP phosphorylation in the salvage pathway but it is also able to phosphorylate deoxyguanosine monophosphate (dGMP) and deoxyuridine monophosphate (dUMP) [272]. TK1 and TMK are critical in the generation of deoxythymidine triphosphate (dTTP) whereas RNR is required to produce all four nucleotides.

1.7 Development of oncolytic vaccinia virus

Over the past two decades there has been extensive research into VACV as a cancer therapy. Genetic mutations that occur in cancer can generate an environment that is optimal for VACV replication; thus, some of the viral genes involved in replication become expendable. Therefore, deletion of these genes from the viral genome greatly reduces the ability of the virus to replicate productively in most normal cells, while allowing them to retain their replication ability in cancer cells. A range of VACV gene deletions with such properties have been engineered to increase tumor selectivity of the virus. Oncolytic VACVs reported to date are most commonly generated by mutations that inactivate *J2R* (thymidine kinase, TK) and *C11L/R* (vaccinia growth factor, VGF), which reduce virulence in the host (animals) and favors virus growth in rapidly dividing cells [274,275]. Cellular TK1 is briefly expressed during S-phase in normal cells but is expressed at high levels in many cancers throughout the cell cycle [276]. VGF is an epidermal growth factor (EGF) homolog that can bind to cellular EGF receptor [277,278]. VGF is released

from infected cells to induce proliferation, and VACV strains with VGF deletions preferentially replicate in cancers with an activated EGFR. The VGF deletion can be combined with the TK deletion to generate a further attenuated virus [279]. Our group has also shown that, by deleting the gene encoding the small subunit of VACV RNR (*F4L*), one can render the virus highly dependent upon the cellular homolog to provide the complementing activity that is needed for virus replication [269]. The *F4L*-deleted viruses are thus quite highly attenuated in infected animals and show a tropism that greatly favors cells containing high levels of RNR.

Oncolytic VACVs armed with a variety of transgenes have also generated much attention recently. Viruses have been developed that encode cytokines such as GM-CSF [280], IFN-β [281], and IL-2 [282]. Interestingly, VACV naturally encodes an inhibitor of type-I IFNs, the *B18R* gene product. An oncolytic VACV has been constructed with deletion of the *B18R* gene and insertion of the IFN-β gene. Replication of this VACV should be highly restricted in normal cells, but permissive in IFN-resistant cancer cells. Furthermore, IFN-β is predicted to elicit an increased anti-cancer response [283]. Anti-angiogenic agents have been expressed to help complement the oncolytic effects of the virus [284]. Finally, prodrug-converting enzymes have been introduced into VACVs to convert nontoxic prodrugs into toxic products within the tumor [279].

There has been limited investigation of oncolytic VACVs in bladder cancer. One study reports on a Lister strain VACV that expresses p53 and has an inactivating mutation in *J2R* (rVV-TK-53) that was evaluated in the murine MB-49 bladder cancer model [285]. Instillation of a single dose ($1x10^6$ PFU) of rVV-TK-53 increased animal survival over PBS treatment and 2 of 10 mice were tumor free at endpoint. Although the luciferase expressing control virus (rVV-L15) increased survival over PBS, none of the rVV-L15 treated animal were cleared of their tumors.

To date we are only aware of one clinical study of VACV in bladder cancer. Gomella *et al*. reported a phase I study in 2001 where increasing doses of WT VACV (Dryvax) were administered intravesically to patients with MIBC for whom radical cystectomy was planned as final treatment [286]. The study examined 4 patients that were treated 3 times over 2 weeks with a maximum dose of 10^8 PFU per instillation prior to cystectomy. It demonstrated that even WT VACV can be administered safely into the bladder and cause the recruitment of lymphocytes and induction of a local inflammatory response. Besides mild local toxicity, no serious treatment-related side effects were reported. The excellent patient tolerance of intravesical VACV and the significant immune infiltrates seen after instillation support the potential use of VACV as an oncolytic agent for intravesical bladder cancer therapy.

Several clinical studies have now been published for the first targeted and armed oncolytic poxvirus to be used in the clinic, Pexastimogene devacirepvec (Pexa-Vec) [previously called JX-594]. It is a Wyeth strain VACV with inactivation of *J2R* (viral TK) and insertion of the GM-CSF gene [280]. Phase I reports describe on the intratumoral injection of seven patients with surgically incurable cutaneous melanoma [287]. Multiple injections with Pexa-Vec at doses up to 2×10^7 PFU/lesion/injection were given over 6 weeks. Overall the treatment had limited side effects that included transient flu-like symptoms and local inflammation, with the occasional pustule formation at the site of injection. Five of seven patients had some response to the treatment with one patient having a complete remission.

In another phase I trial, direct injection of Pexa-Vec into refractory primary or metastatic liver tumors was well tolerated, with virus replication, expression of active GM-CSF, and tumor killing observed [288]. In this dose escalation study, patients who had previously received multiple therapies were injected with up to 3×10^9 PFU every 3 weeks with an average of 3.4 treatments. Of

the ten patients assessed, three showed partial responses, six had stable disease, and one showed progression. Pexa-Vec was generally well tolerated up to a dose of 10^9 PFU. The dose-limiting toxicity, hyperbilirubinemia, seen at 3×10^9 PFU, was due to tumor swelling causing a bile-duct obstruction.

Results of a phase II trial examining intratumoral administration of either low-dose (10^8 PFU) or with a high-dose (10^9 PFU) Pexa-Vec to patients with hepatocellular carcinoma have been reported [289]. It was found that the overall survival was significantly longer for patients receiving the high dose treatment.

Pexa-Vec has also been administered intravenously (IV) in a phase I dose-escalation trial with a cohort of 23 cancer patients with advanced solid tumors that had developed resistance to multiple other treatments. This study established a maximum feasible dose of 3×10^7 PFU/kg (equivalent to a total dose of about 2×10^9 PFU) [290]. This is the first report demonstrating replication and transgene expression in metastatic tumors after IV administration of an oncolytic virus.

Because of the anatomical isolation of the bladder, it may be possible to administer higher doses of virus locally without systemic side effects. Encouraging clinical results for the treatment of other cancers with oncolytic VACV further suggest that the investigation of oncolytic VACV as a bladder cancer therapy should be a priority.

1.8 Project summary and rationale

Up to 80% of NMIBC can recur within 5 years of initial treatment, with high-grade NMIBC posing the greatest risk of recurrence and progression to muscle-invasive disease. Treatment for these patients includes transurethral resection followed by intravesical therapy with the immunotherapeutic agent BCG. BCG, however, carries the risk of systemic infection and can be

particularly dangerous for immunocompromised patients. Additionally, up to 40% of patients do not respond to or go on to fail BCG therapy, requiring cystectomy. There is an urgent need for more bladder-sparing therapies for patients failing conventional therapies. We hypothesize that a *F4L*-deleted VACV will show superior safety and efficacy in models of bladder cancer.

Here, we report the generation and testing of a novel oncolytic VACV that is lacking the viral *F4L* and *J2R* genes, homologs of cellular genes *RRM2* and *TK1*, respectively, that normally promote nucleotide biosynthesis in infected cells. This oncolytic virus, ΔF4LΔJ2R VACV, was highly attenuated in non-cancerous cells and replicated selectively in both an orthotopic AY-27 immunocompetent rat tumor model and an RT112-luc xenografted human tumor model, causing significant tumor regression or complete tumor ablation with no toxicity. In contrast, a VACV with a more commonly employed deletion, ΔJ2R, spread to normal organs and caused significant toxicity in immunocompromised mice. Furthermore, rats cured of AY-27 tumors by VACV treatment developed a protective anti-tumor immunity that was evidenced by tumor rejection upon challenge, as well as by *ex vivo* cytotoxic T-lymphocyte assays. Finally, ΔF4LΔJ2R VACV replicated in BCG-resistant human bladder cancer cell line and in cultures of primary human bladder tumors.

This thesis demonstrates the high degree of safety and anti-tumor activity of a novel oncolytic virus in pre-clinical bladder cancer models. Given the high rate of recurrence and the lack of treatment options for BCG-resistant bladder cancer, our oncolytic VACV could provide a safe and urgently needed therapy for BCG failure. More significantly, based on its tropism for replicating cells it could target early cellular transformation; clearing the bladder of neoplastic cells and decreasing the rate of recurrence.

CHAPTER 2 - DELETION OF *F4L* (RIBONUCLEOTIDE REDUCTASE) IN VACCINIA VIRUS PRODUCES SAFE AND SELECTIVE ONCOLYSIS *IN VITRO* AND IN XENOGRAFT MODELS BASED ON ESTABLISHED BLADDER CANCER CELL LINES

PREFACE

A portion of this chapter has been published in the manuscript: **Potts, K. G**., Irwin, C. R., Favis, N. A., Pink, D. B., Vincent, K. M., Lewis, J. D., Moore, R. B., Hitt, M. M.* and Evans, D. H.* (2017), Deletion of *F4L* (ribonucleotide reductase) in vaccinia virus produces a selective oncolytic virus and promotes anti-tumor immunity with superior safety in bladder cancer models. EMBO Mol Med, e201607296. (* These authors contributed equally). EMBO Molecular Medicine states: "This is an open access article under the terms of the Creative Commons Attribution 4.0 License, which permits use, distribution and reproduction in any medium, provided the original work is properly cited."

Contributions:

I designed and performed experiments (except where noted), analyzed the data, and prepared the manuscript. Dr. Chad Irwin designed and constructed the viruses used in these studies and performed the siRNA silencing experiment. Nicole Favis assisted in all RT112-luc xenograft animal experiments. Megan Desaulniers assisted in patient-derived xenograft model experiments. Dr. Krista Vincent performed microarray data analysis. Dr. David Evans, Dr. Mary Hitt, and Dr. Ronald Moore provided guidance in experimental design, data interpretation, and manuscript preparation.

2.1 INTRODUCTION

OVs are intended to replicate selectively in, and kill, cancer cells while sparing normal tissues (reviewed in [132,133,178]). Some of the many cell pathways that affect virus replication are those that regulate cell proliferation and DNA replication, processes that are critically dependent upon dNTP production [291]. The rate-limiting step in dNTP biosynthesis is the *de novo* reduction of rNDPs to dNDPs by the RNR [184]. Since DNA virus replication requires dNTPs, this requirement for RNR activity provides an important biological feature that can be exploited to target DNA viruses to cancer cells.

Most oncolytic VACVs reported to date encode mutations in *J2R* (viral TK). Little research has been conducted to determine whether mutating the viral RNR genes [292] might also produce advantageous oncolytic properties. The *F4L* gene (encoding the viral homolog of the small subunit of RNR, RRM2) is an important determinant of VACV virulence and viruses lacking *F4L* (ΔF4L) are attenuated *in vivo* whereas ΔI4L mutants (deleted in the viral homolog of the large subunit of RNR, RRM1) are not [269]. The fact that cellular RRM2 is cell-cycle-regulated whereas RRM1 is constitutively expressed can perhaps explain this observation [293] and leads to the prediction that a ΔF4L virus should replicate selectively in dividing cancer cells. This complementation-based strategy might be especially useful for treating more aggressive bladder cancers since increased levels of cellular RRM2 predict a poorer prognosis for this disease [294].

Here we describe pre-clinical studies showing that VACV can be used safely as a treatment for NMIBC. We find that *F4L*-deleted VACVs retain much of their cytotoxicity and replication proficiency in bladder cancer cells. *F4L*-deleted VACVs also safely and effectively clear bladder tumors in a xenograft model as well as in model. These findings highlight the safety and selectivity of a *F4L*-deleted VACV in treating bladder cancer.

2.2 MATERIALS AND METHODS

2.2.1 Cell lines. Human (253J, RT4-luc, HTB-3, HTB-9, MGH-U3, RT112-luc, T24) and rat (AY-27) bladder cancer cell lines were maintained in RPMI 1640 medium supplemented with 10% fetal bovine serum (FBS), 2 mM L-glutamine, 100 U/mL penicillin, 100 U/mL streptomycin, and 0.25 μg/mL Fungizone® (Gibco). Human bladder cancer cell lines HT-1376 (CRL-1472), UM-UC3-luc, UM-UC6, UM-UC9, and UM-UC14-luc were maintained in Dulbecco's Modified Eagle's Medium (DMEM)/F12 medium with the same supplements as above. MB49-luc (murine urothelial cell carcinoma), N60 (early passage human skin fibroblast), NKC (normal human kidney epithelial), HeLa (CCL-2), and RK3E (E1A immortalized rat kidney) cells were cultured in DMEM, also with the same supplements. BSC-40 cells (CRL-2761) were grown in minimal essential medium (MEM) supplemented as above, but using 5% FBS. Cells were cultured at 37^{o}C in 5% CO_2. RT4-luc, RT112-luc, and UM-UC3-luc cell lines were provided by D. McConkey (MD Anderson), 253J and T24 cells were provided by M. Gleave (University of British Columbia), MGH-U3 cells were provided by Y. Fradet (University of Laval), UM-UC6 and UM-UC9 were provided by H.B. Grossman (MD Anderson), HTB-3 were provided by C. Cass (University of Alberta), MB49 cells were provided by J. Greiner (National Cancer Institute), and early passage N60 human skin fibroblast cells were kindly by T. Tredget (University of Alberta). All lines were routinely tested for and found free of mycoplasma either by Hoechst 33342 staining (Thermo Fisher Scientific) and fluorescence imaging, or using the LookOut® Mycoplasma PCR detection kit (Sigma-Aldrich). The identities of the cell lines were confirmed using a 16-marker AmpFLSTR® Identifiler® system performed by the TCAG facility at the University of Toronto.

2.2.2 Viruses. All recombinant viruses used in this study were derived from a clonal isolate of VACV strain WR, originally obtained from the American Type Culture Collection (ATCC). To

permit *in vivo* imaging, we used homologous recombination to generate new versions of the ΔF4L and ΔJ2R viruses described in [269] that encode mCherry fluorescent protein under virus early/late promoter control. Plasmid DNA encoding mCherry fluorescent protein under control of a synthetic early/late poxvirus promoter was subcloned from plasmid pE/L-mCherry-Topo2 into either pSC66 (to target the *J2R* locus) or R2-pZippyNeoGusA (to target *F4L*) [269]. The resulting constructs were used to transfect Vero cells (ATCC CCL-81), 1 hr after infection with WT VACV at a multiplicity of infection (MOI) of 2 PFU/cell. Transfections were done using Lipofectamine 2000 (Thermo Fisher) as per manufacturer's instructions. The medium was replaced 2 hr later, the cells cultured for 48 hr, and the virus harvested by freeze-thaw. The mCherry-positive viruses were plaque purified using Vero cells. The virus referred to as ΔJ2R VACV encodes *LacZ* and mCherry genes disrupting *J2R*, and ΔF4L VACV encodes NeoGusA and mCherry replacing *F4L* (See **Figure 2.1**).

A third virus was produced by transfecting the R2-pZippyNeoGusA construct into VERO cells infected with ΔJ2R VACV. This created ΔF4LΔJ2R VACV encoding NeoGusA disrupting *F4L*, and *LacZ* and mCherry genes disrupting *J2R*. The viruses were harvested, and recombinants detected by plating under an agar overlay containing 0.4mg/mL of 5-Bromo-4-chloro-3-indolyl-β-D-glucuronic acid (Clontech). PCR was used to confirm the purity of all the recombinant VACVs using primers 5'-TGACGTAAATGTGTGCGAAAGT-3' and 5'-TCAGCACCCATGA-ATGTCGAT-3' to amplify the *F4L* locus and primers 5'-TATTCAGTTGATAATCGGCCCC-ATGTTT-3' and 5'-GAGTCGATGTAACACTTTCTACACACCG-3' to amplify the *J2R* locus.

2.2.3 Antibodies. The primary antibodies used for western blots included: goat anti-RRM1 (Santa Cruz sc-1733), goat anti-RRM2 (Santa Cruz sc-10846), rabbit anti-p53R2 (Abcam ab8105), rabbit anti-TK1 (Abcam ab76495), rabbit anti-TK1 (Abcam ab59271), rabbit anti-ß-actin (LICOR

926-42210), and rabbit anti-ß-tubulin (CST #2416). The secondary antibodies used for western blots included: 680LT donkey anti-rabbit (LICOR 926- 68023) and 800CW donkey anti-goat (LICOR 926-32214).

2.2.4 In vitro infection experiments. Multistep growth curves were obtained by infecting the indicated cell lines in 60 mm plates with VACV at MOI of 0.03 PFU/cell diluted in PBS. After 1 hr at 37^{o}C fresh culture medium was added. For the 0 hr time point, plates were aspirated and fresh medium was added; VACV inoculum was added and cells were then immediately harvested. Infected cells were scraped into the culture medium at the indicated times, subjected to three rounds of freeze-thaw, then 10x serially diluted and plated in duplicate on BSC-40 cells. Infected BSC-40 cells were cultured in medium containing 1% carboxymethyl cellulose for 2 days, then fixed and stained with crystal violet. Plaque counts were determined from wells containing 30-250 plaques.

2.2.5 Cytotoxicity assays. Cells were seeded in 48-well plates at a density estimated to produce ~50% confluency at the time of infection. After an 8 hr incubation, cells were infected with VACV, cultured for 3 days, and the media replaced with fresh cell culture media containing 44 μM resazurin (Sigma-Aldrich). Plates were incubated 4-6 hr at 37˚C, then fluorescence was read using a FLUOstar plate reader (BMG LabTech) with 560 nm excitation/590 nm emission filters.

2.2.6 Western blot analysis. Protein extracts were prepared from cells lysed on ice in buffer containing 150 mM NaCl, 50 mM Tris·HCl (pH 8.0), 0.5% sodium deoxycholate, 0.1% SDS, 1% NP-40, 0.1 mg/mL phenylmethylsulfonyl fluoride, and Halt protease inhibitor cocktail (Thermo Fisher). Protein extracts were prepared from human or animal tissues by adding 1 mL of the same buffer, but containing twice-concentrated protease inhibitors, per 100 μg of tissue, and then

homogenizing the suspension using a gentleMACS tissue dissociator (Miltenyi Biotec) on the protein lysis program. Lysates were clarified by centrifugation and assayed for protein using a BCA protein assay kit (Thermo Fisher). For western blots, up to 30 μg of protein was fractionated by SDS-PAGE and transferred to Immobilon-FL PVDF membrane (EMD Millipore). The membranes were blocked with Odyssey blocking buffer (Li-COR Biosciences), diluted 1:1 with PBS, for 1 hr at room temperature, and incubated overnight at 4^{o}C with primary antibodies diluted in blocking buffer. Fluorescent-conjugated secondary antibodies were diluted in PBS containing 0.1% Tween and 0.01% SDS, and incubated with the membranes at room temperature for 1 hr. The washed membranes were scanned using an Odyssey scanner (Li-COR Biosciences) and the images analyzed using ImageStudioLite software (Li-COR Biosciences).

2.2.7 siRNA knockdown. 12 well plates were seeded with 100,000 HeLa (CCL-2) cells and 24 hr later were transfected with 20 nM AllStars non-targeting siRNAs (Qiagen Cat#1027280) or RRM2 (hs RRM2 5 cat# S102653441) using Dharmafect 4 (GE Dharmacon) as per manufacturer's instructions.

2.2.8 Microarray datasets. Bladder cancer patient microarray expression data (log2 MAS 5.0 normalized Affymetrix U133A human GeneChip values) were retrieved from Sanchez-Carbayo M., *et al*. [295]. Data was selected for RRM1, RRM2, and TK1 expression analysis: 201477_s_at, 209773_s_at, and 202338_at (respectively). For genes with data available for more than one probe (RRM1), the data from the probe with the highest median expression value was chosen for analysis.

2*.2.9 Cell cycle analysis*. Cells were harvested, pelleted by centrifugation for 5 min at 350 x g, washed once in PBS then re-centrifuged. Next, 70% ice-cold ethanol (2-3 mL) was added drop-wise to the cell pellets with continuous vortex-mixing. Cells were kept at 4°C for 30 min and

then centrifuged at 1000 × g and 4°C for 5 min to remove the ethanol. The cell pellets were washed twice with PBS and resuspended in 0.5 mL of 0.50 μg/mL Propidium iodide (PI) (Thermo Fisher) plus 10 μg/mL RNaseA (Thermo Fisher) and incubated at 37°C for 30 min. Cell suspensions were analyzed on LSR-Fortessa X20 flow cytometer (BD Biosciences) using the FACS DiVa software (BD Biosciences). Cell populations were gated using FSC-A and SSC-A and a single cell population was gated by using FSC-H and FSC-A. PI signal was detected on the PE-Texas Red channel using a 488-nm laser. FlowJo (Version 10.2) was used to perform cell cycle analysis.

2.2.10 Animal care and housing. All studies reported were conducted with the approval of the University of Alberta Health Sciences Animal Care and Use Committee in accordance with guidelines from the Canadian Council for Animal Care. Animals were housed with access to food and water *ad libitum* in ventilated cages (1-5 mice per cage) in a biosafety level 2 containment suite at the University of Alberta Health Sciences Laboratory Animal Services Facility.

2.2.11 In vivo RT112-luc and UM-UC3-luc tumor models. For all xenograft models, female Balb/c nude mice (Charles River Laboratories) were 8 weeks old and at least 16 g in weight at the time of tumor implantation. To establish orthotopic RT112-luc tumors, mice were anesthetized with 2% isoflurane and a 24G angiocatheter (BD Biosciences), with the needle removed, was lubricated with sterile Lubrifax and inserted into the bladder *via* the urethra. The bladder was infused for 15 sec with 50 μL of 0.1 M HCl, neutralized with 50 μL of 0.1 M KOH for 15 sec, then washed three times with phosphate buffered saline (PBS). Next, a 50 μL suspension of Hank's balanced salt solution (HBSS) containing $2x10^6$ RT112-luc cells was instilled into the bladder using the catheter and left in-dwelling for 1 hr while the mice remained under anesthesia. To produce RT112-luc or UM-UC3-luc flank tumors, Balb/c nude mice were anesthetized with

isoflurane then injected subcutaneously with 0.1 mL of $2x10^6$ tumor cells in PBS containing 50% Matrigel (Corning). Flank tumor volumes were determined weekly by caliper measurements.

For intravesical virus treatments, the bladders of anesthetized mice were emptied by catheterization and then 50 µL of PBS, containing $1x10^6$ PFU of virus, was instilled into each mouse on day 10 post-implantation. Instillations were repeated on days 13 and 16. The virus was left in-dwelling for 1 hr while the mice remained under anesthesia. For intratumoral virus treatments, 50 µL of PBS, containing $1x10^6$ PFU of virus was injected into the tumor following the same schedule as intravesical treatments.

2.2.13 Bioluminescence and fluorescence imaging. For bioluminescence imaging, mice bearing RT112-luc tumors were anesthetized then given an intraperitoneal injection of a solution containing 0.15 mL of 15 mg/mL D-Luciferin (Gold Biotechnology) in PBS. 12-15 min later, mice were imaged under anesthesia using an IVIS Spectrum imager (Caliper Life Sciences). White-light photographs and bioluminescence images were superimposed using Living Image software (Caliper Life Sciences, v 4.2). An average radiance was determined by manually selecting the tumor center with the Auto1 "region of interest" tool and using a threshold of 5%.

Fluorescence images were taken using the IVIS Spectrum imager (Caliper Life Sciences). All imaging utilized the built-in Image Wizard feature of Living Image software (Caliper Life Sciences, v4.2). Images were acquired using the mCherry Spectral Unmixing spectrum (Excitation: 570 nM and Emission: 620, 640, 660, 680, 700, and 720 nm). A 500 nm excitation wavelength was also used for auto-fluorescence correction. All bioluminescence and fluorescence images are presented on the same intensity scale.

2.2.14 Statistics. Data were analyzed using two-tailed Student's *t* test when comparing the means of two groups. Multiple *t* test was used to determine significance of VACV growth after

siRNA knockdown. Analysis of variance (ANOVA) was used when comparing multiple groups followed by Tukey's multiple comparison test. Microarray data were analyzed in the RStudio programming environment (v0.98.501), with significance analysis performed by means of a one-way ANOVA followed by Tukey's honest significant difference (HSD). Data for animal survival curves were analyzed by log-rank (Mantel-Cox) test. The numbers of animals per group for each figure are indicated at the end of each legend. P-values are indicated within each figure.

2.3 RESULTS

2.3.1 Growth of VACV ΔF4L and ΔJ2R mutants in vitro. To determine whether bladder cancer could be a potential target for oncolytic VACVs, we first tested a panel of bladder cancer cell lines for sensitivity to WT VACV or VACV mutants lacking *F4L, J2R,* or both (a schematic of the viruses is shown in **Figure 2.1)**. Thirteen out of fourteen bladder cancer cell lines grown under normal serum conditions (10%) supported robust WT VACV replication, an exception being UM-UC3-luc cells where there was only a 10-fold increase in virus yield (**Figure 2.2A and E**). ΔF4L and ΔF4LΔJ2R VACVs replicated to within a log of WT in 12 of the 14 cell lines. There was a more significant reduction in replication in T24 and UM-UC9 cell lines, especially with the ΔF4L VACV. In order to mimic *in vivo* conditions, we cultured cells under low serum (0.1%) conditions. We found that both normal N60 and NKC cells grown in 0.1% FBS showed a low proportion of cells in S-phase whereas the proportion of RT112-luc cells in S-phase remained high (**Figure 2.3**), suggesting that proliferation status under our low serum growth conditions may mimic the proliferation status of normal and tumor tissues *in vivo*. Under low serum conditions (0.1%), the WT and ΔJ2R VACV grew nearly as well as was seen in 10% serum. Viruses lacking

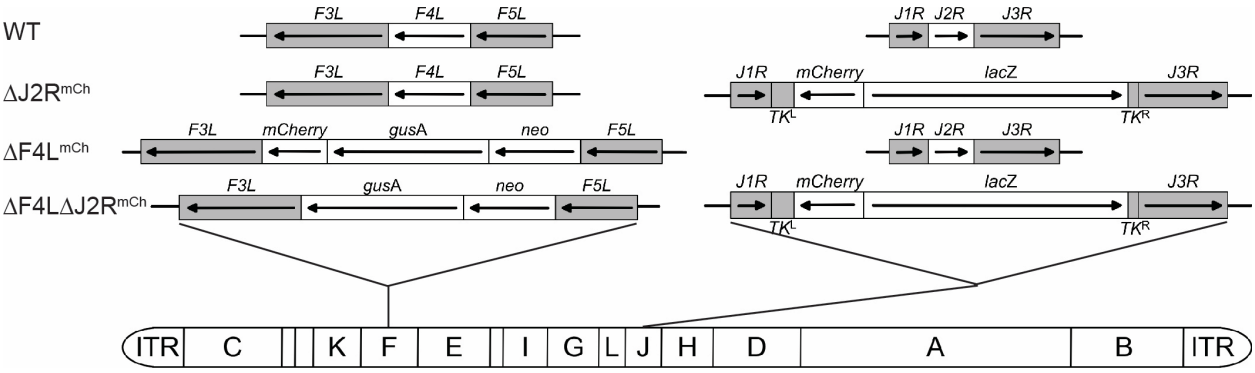

Figure 2.1: Genomic map of VACV constructs. Viruses were generated from the VACV Western Reserve strain. Viral thymidine kinase is encoded by the J2R gene. Subunit 2 of viral ribonucleotide reductase is encoded by the F4L gene. neo, neomycin resistance gene; gusA, β-glucuronidase gene; lacZ, β-galactosidase gene; ITR, inverted terminal repeat; TK_L, viral thymidine kinase gene left homology; TK_R, viral thymidine kinase gene right homology; and WT, wild-type. Letters A-L (M, N, and O not shown) indicate *Hind*III restriction fragments of the viral genome in order of largest to smallest.

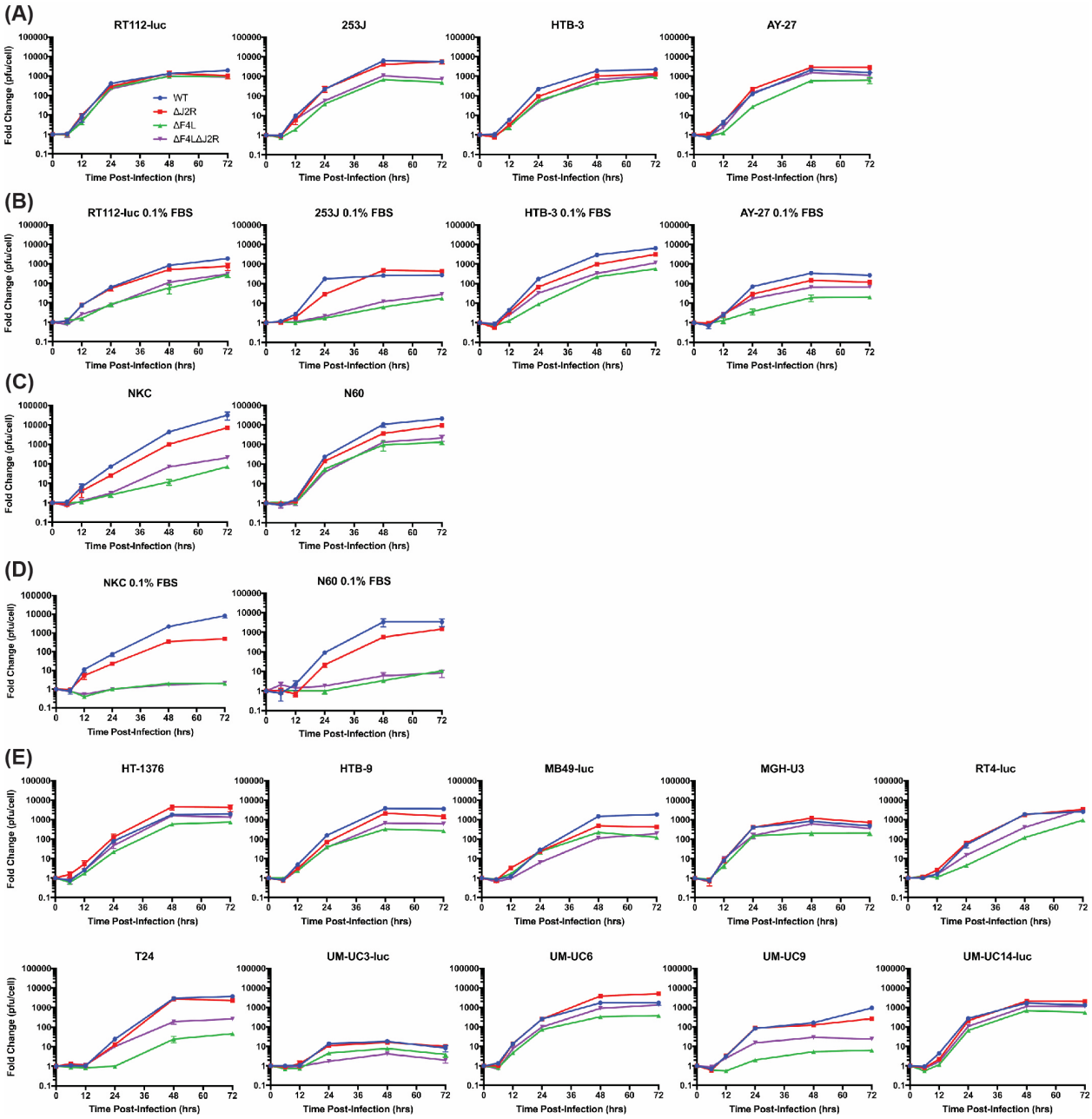
(A)
RT112-luc
253J
HTB-3
AY-27
WT
ΔJ2R
ΔF4L
ΔF4LΔJ2R
(B)
RT112-luc 0.1% FBS
253J 0.1% FBS
HTB-3 0.1% FBS
AY-27 0.1% FBS
(C)
NKC
N60
(D)
NKC 0.1% FBS
N60 0.1% FBS
(E)
HT-1376
HTB-9
MB49-luc
MGH-U3
RT4-luc
T24
UM-UC3-luc
UM-UC6
UM-UC9
UM-UC14-luc
Fold Change (pfu/cell)
Time Post-Infection (hrs)

Figure 2.2: ΔF4LΔJ2R VACV retains much of the replication proficiency of WT VACV in bladder cancer cells. Growth curves are shown for the indicated VACV strains in sub-confluent human bladder cancer cell lines, rat bladder cancer cell line AY-27, murine bladder cancer cell line MB49-luc, normal human kidney epithelial cell line NKC, and normal human skin fibroblast line N60. The cells were infected with 0.03 PFU/cell and cultures were harvested at the indicated times and titered on BSC-40 cells. **(A)** Panel of cancer cells grown under normal (10%) serum conditions. **(B)** Panel of cancer cells grown under low (0.1%) serum conditions. **(C)** Panel of normal cells grown under normal serum conditions. **(D)** Panel of normal cells grown under low serum conditions. **(E)** Additional cancer cells grown under normal serum conditions.

Data Information: Mean ± SEM is shown. Data represent titer of lysates from at least 2 independent lysates, each titered in duplicate.

F4L replicated in the cancer cell lines under low serum conditions, however there was approximately a 10-fold reduction in virus yield at 72 hrs relative to WT (**Figure 2.2B**). Most importantly, compared to WT, growth of ΔF4LΔJ2R and ΔF4L VACVs in low serum was reduced >4000-fold in the NKC (normal epithelial kidney) line and >250-fold in N60 (normal fibroblast) cell line. Whereas the growth of ΔJ2R VACV was only marginally reduced compared to WT in the NKC and N60 cells under the same low serum conditions (**Figure 2.2A and B**). These results highlight the superior tumor cell selectivity of *F4L*-deleted VACVs.

The effect of VACV on cell survival was determined using a resazurin-based viability assay. Similar to growth of virus under normal serum conditions, no dramatic difference in the efficiency of virus-mediated cell killing was seen among the different viruses under normal serum conditions (**Figure 2.4A and E**). However, under low serum conditions, both N60 normal skin fibroblasts and NKC epithelial kidney cells were relatively resistant to ΔF4L and ΔF4LΔJ2R VACV killing (**Figure 2.4C and D**). Interestingly, in low serum conditions, 253J and AY-27 cancer cells were highly susceptible to killing by ΔF4LΔJ2R VACV (**Figure 2.4B**), even though virus replication was attenuated. This was a specific property of the ΔF4LΔJ2R virus; 253J and AY-27 cells were not as easily killed by the ΔF4L VACV. These data indicate that the mutant VACVs, in particular ΔF4LΔJ2R VACV, retained much of the cytotoxic capabilities and replication proficiency of WT virus in bladder cancer cells but did not replicate in non-dividing cells.

2.3.2 Nucleotide biosynthetic proteins are elevated in bladder cancer cells. One might expect that ΔF4L and/or ΔJ2R strains would depend upon complementation from cellular RRM2 and TK1 respectively, to provide the dNTPs required for virus replication. Some limited data suggested that ΔF4L VACVs do grow better in cells expressing higher levels of RRM2 [269].

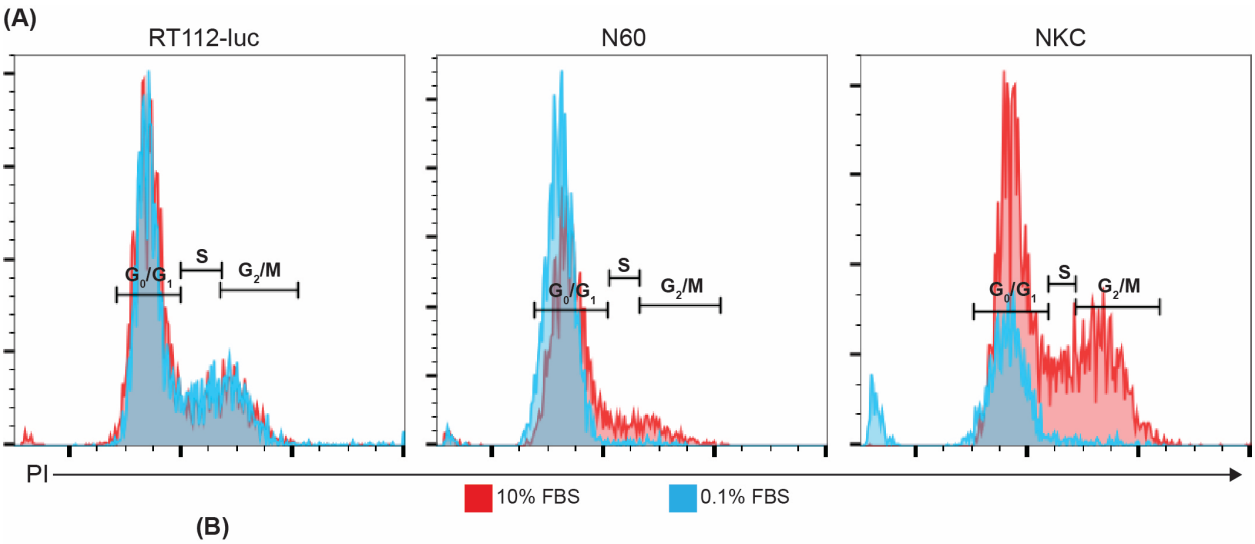

(B)

Cell Line	G_0/G_1	S	G_2/M
RT112-luc 10% FBS	67.1%	15.3%	16.7%
RT112-luc 0.1 % FBS	70.2%	12.1%	16.0%
N60 10% FBS	80.7%	6.9%	9.2%
N60 0.1% FBS	93.4%	1.0%	1.5%
NKC 10% FBS	58.8%	10.6%	28.9%
NKC 0.1% FBS	79.4%	2.8%	3.6%

Figure 2.3: Non-tumorigenic cells have reduced S-phase population when grown under lower serum conditions. (A) Indicated cell lines were grown in media supplemented with either 10% FBS or 0.1% FBS for 48 hrs and then cell cycle distribution was monitored by flow cytometry after PI staining. Red traces indicate cells grown in 10% FBS and blue traces indicate cells grown in 0.1% FBS. **(B)** Analysis of cell cycle phase distribution.

Data Information: Representative flow cytometry traces are shown.

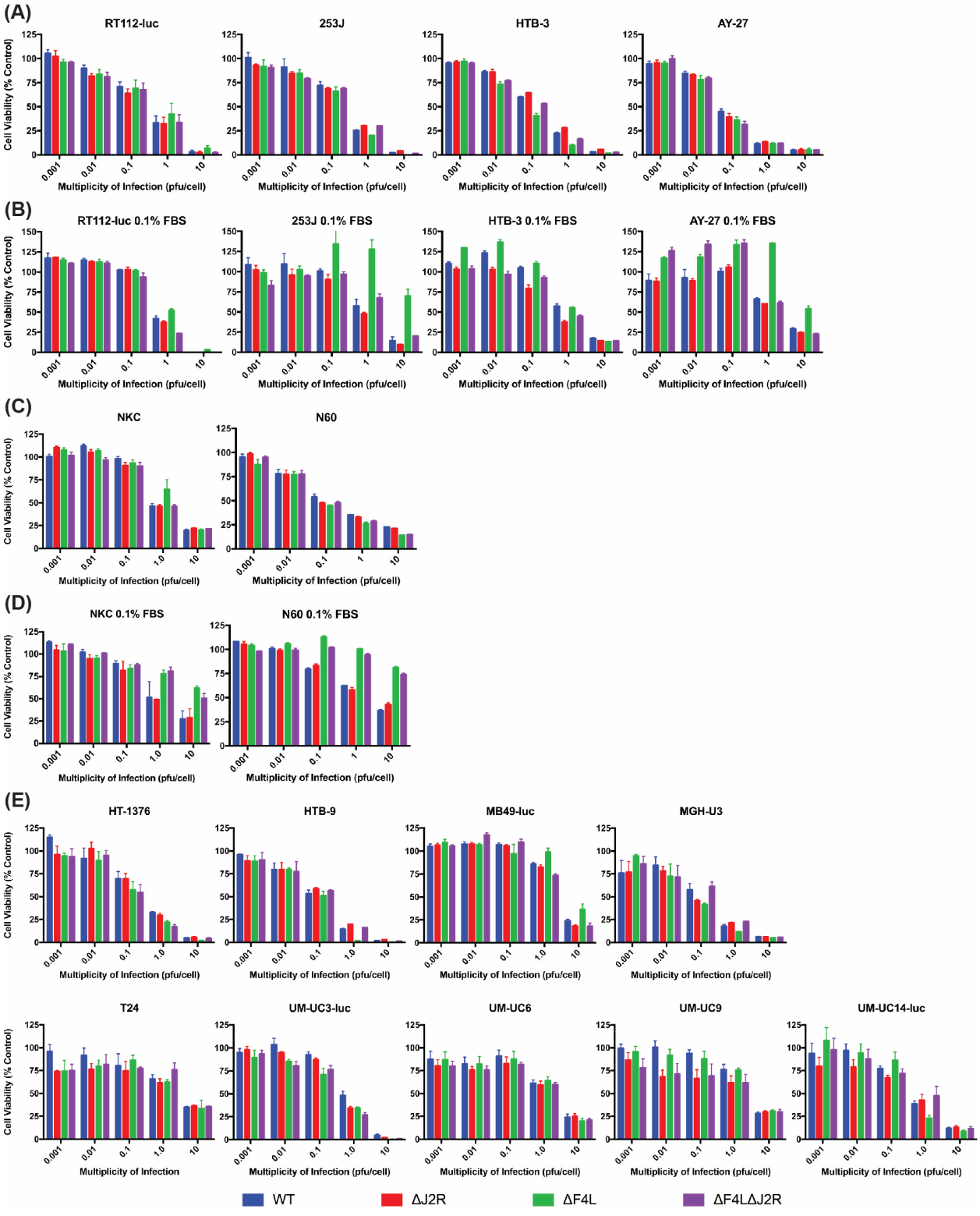
(A)
RT112-luc
253J
HTB-3
AY-27
(B)
RT112-luc 0.1% FBS
253J 0.1% FBS
HTB-3 0.1% FBS
AY-27 0.1% FBS
(C)
NKC
N60
(D)
NKC 0.1% FBS
N60 0.1% FBS
(E)
HT-1376
HTB-9
MB49-luc
MGH-U3
T24
UM-UC3-luc
UM-UC6
UM-UC9
UM-UC14-luc
Cell Viability (% Control)
Multiplicity of Infection (pfu/cell)
WT
ΔJ2R
ΔF4L
ΔF4LΔJ2R

Figure 2.4: ΔF4LΔJ2R VACV kills bladder cancer cells to the same level as WT VACV. Survival of cell lines infected *in vitro* with the indicated VACV strains is shown. Sub-confluent cells were infected at the indicated multiplicities of infection (in PFU/cell). Uninfected cells were used as control. The cells were incubated with resazurin3 days post-infection to assess viability relative to uninfected control cells. **(A)** Panel of cancer cells grown under normal (10%) serum conditions. **(B)** Panel of cancer cells grown under low (0.1%) serum conditions. **(C)** Panel of normal cells grown under normal serum conditions. **(D)** Panel of normal cells grown under low serum conditions. **(E)** Additional cancer cells grown under normal serum conditions.

Data Information: Mean ± SEM is shown. Data represent n≥3 independent experiments, each performed in triplicate.

To examine this matter in more detail, the levels of proteins catalyzing nucleotide biosynthesis were quantified in a panel of human bladder cancer cell lines and in normal N60 fibroblasts under 10% and 0.1% serum conditions (**Figure 2.5A**). Western blots showed a general elevation in the levels of cellular RRM1, RRM2 and TK1 in cancer cell lines compared to normal cells (**Figure 2.6**). The abundance of the DNA damage inducible form of RRM2, p53R2, did not significantly differ between the cancer cell lines and normal skin fibroblasts.

To demonstrate *F4L*-deleted VACVs' dependence on cellular RRM2, we tested whether knockdown of RRM2 in HeLa cells would prevent VACV replication. Efficient knockdown was achieved following transfection with *RRM2*-specific siRNAs, as confirmed by Western blot analysis (**Figure 2.5B**). The cells were then infected with the different VACVs and virus yield measured by plaque assay (**Figure 2.5C**). There was a significant reduction in ΔF4L and ΔF4LΔJ2R VACV replication in cells with RRM2 knockdown, while WT or ΔJ2R VACV replication was unaffected.

We also examined expression of nucleotide metabolism proteins in samples isolated from primary human bladder tumors and from normal bladder urothelium. Western blot analysis showed elevated expression of both RRM1 and RRM2 in the tumor tissues relative to the normal urothelium (**Figure 2.5D**). Additionally, TK1 was only detectable in the tumor lysates, with two of these showing high expression levels, and only minimal expression in the remaining lysates. As in cultured cells, p53R2 expression was not specifically associated with tumors. These observations were generally corroborated by gene expression data obtained from primary tumor samples previously analyzed by Sanchez-Carbayo *et al*. [295]. Reanalysis of these data showed that *RRM2* and *TK1* expression were significantly increased in both NMIBC and MIBC when compared to the normal urothelium (**Figure 2.5E**).

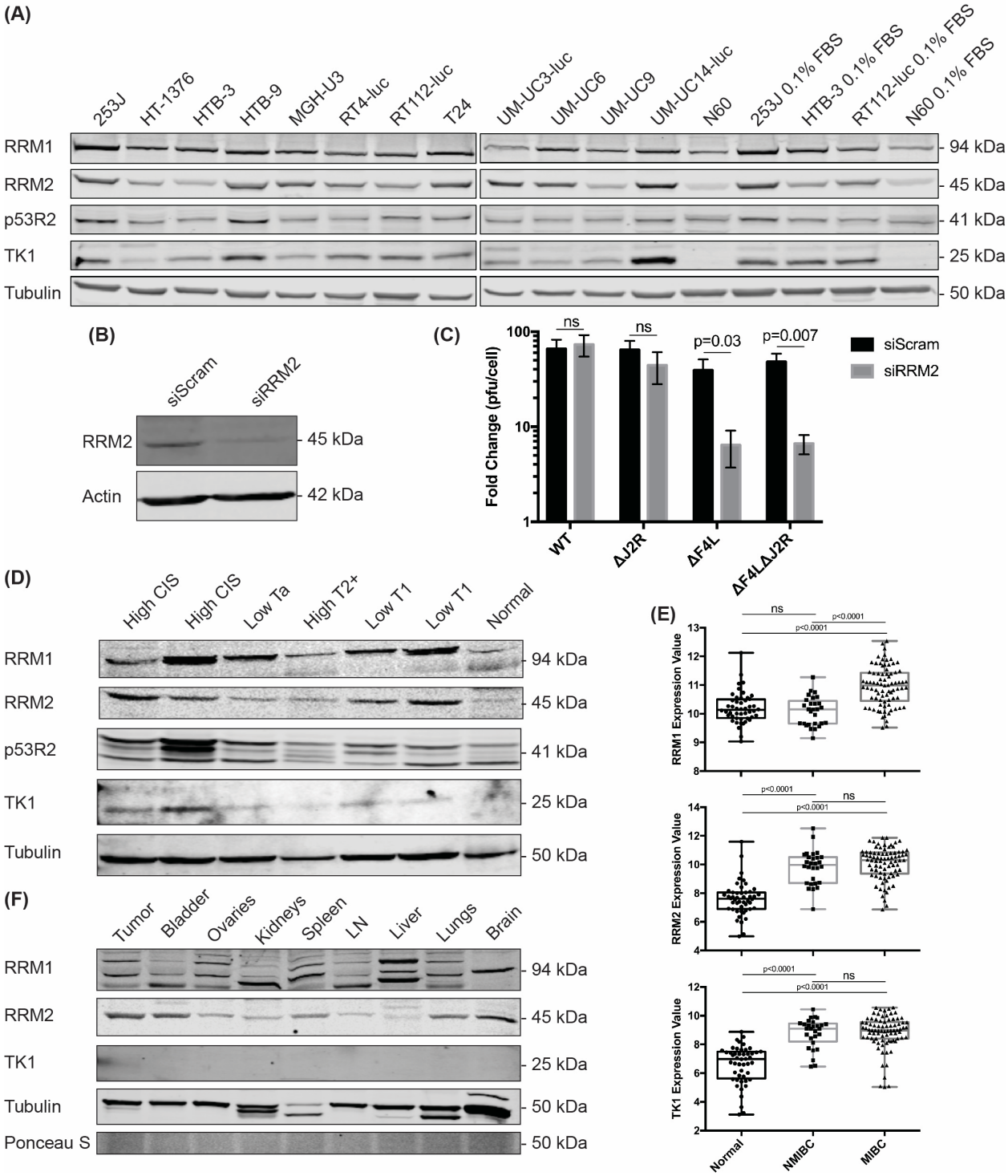
(A)
253J
HT-1376
HTB-3
HTB-9
MGH-U3
RT4-luc
RT112-luc
T24
UM-UC3-luc
UM-UC6
UM-UC9
UM-UC14-luc
N60
253J 0.1% FBS
HTB-3 0.1% FBS
RT112-luc 0.1% FBS
N60 0.1% FBS
RRM1
RRM2
p53R2
TK1
Tubulin
94 kDa
45 kDa
41 kDa
25 kDa
50 kDa
(B)
siScram
siRRM2
RRM2
Actin
45 kDa
42 kDa
(C)
Fold Change (pfu/cell)
ns
ns
p=0.03
p=0.007
siScram
siRRM2
WT
ΔJ2R
ΔF4L
ΔF4LΔJ2R
(D)
High CIS
High CIS
Low Ta
High T2+
Low T1
Low T1
Normal
RRM1
RRM2
p53R2
TK1
Tubulin
94 kDa
45 kDa
41 kDa
25 kDa
50 kDa
(E)
RRM1 Expression Value
RRM2 Expression Value
TK1 Expression Value
ns
p<0.0001
p<0.0001
Normal
NMIBC
MIBC
(F)
Tumor
Bladder
Ovaries
Kidneys
Spleen
LN
Liver
Lungs
Brain
RRM1
RRM2
TK1
Tubulin
Ponceau S
94 kDa
45 kDa
25 kDa
50 kDa
50 kDa

Figure 2.5: Elevated levels of proteins catalyzing nucleotide biosynthesis in bladder cancer cell lines and primary human tumor lysates. (A) Western blot showing RRM1, RRM2, p53R2, and TK1 expression in human bladder cancer cell lines and N60 normal human fibroblasts. β-tubulin is shown as a loading control. **(B)** siRNA depletion of RRM2 in HeLa cells 3 days post-transfection as determined by western blot analysis. **(C)** Growth of the indicated VACV strains in sub-confluent HeLa cells. The cells were treated for 24 hr with a scrambled control siRNA ("Scram") or an *RRM2*-targeted siRNA, then infected with the indicated viruses at 0.03 PFU/cell. The cultures were harvested 2 days later and titered on BSC-40 cells. **(D)** Western blot showing RRM1, RRM2, p53R2, and TK1 expression levels in human primary tumor tissues and adjacent normal urothelium. β-tubulin is shown as a loading control. **(E)** Analysis of *RRM1*, *RRM2*, and *TK1* expression levels from publicly available bladder cancer patient microarray data (NMIBC: non-muscle-invasive bladder cancer; MIBC: muscle-invasive bladder cancer). Data points denote $\log_2$ transformed MAS5.0 normalized values. **(F)** Western blot showing RRM1, RRM2, and TK1 expression in rat AY-27 orthotopic bladder tumor tissue and the indicated normal tissues. β-tubulin and Ponceau S staining are shown as loading controls. In all Western blots, equal amounts of total protein (30 μg) were assayed.

Data Information: Mean ± SEM is shown. Western blots are representative of at least 2 or 3 independent experiments. For (C) n=4 and significance was determined by Multiple *t* test. Microarray data were analyzed using RStudio (v0.98.501) and significance analysis was performed using a one-way ANOVA followed by Tukey's HSD.

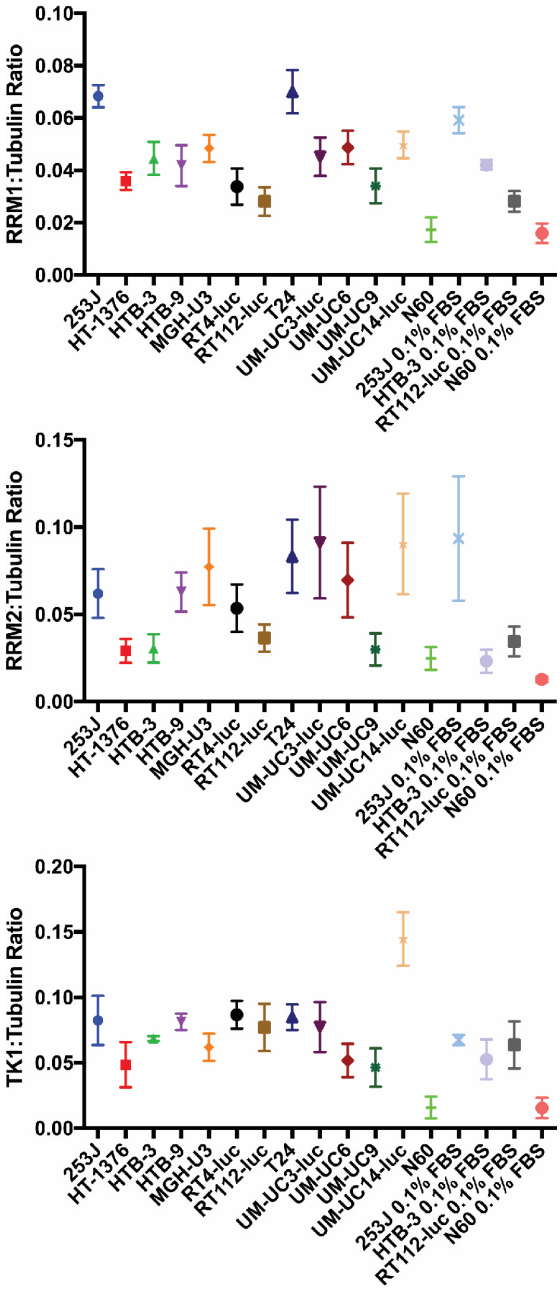

Figure 2.6: Quantification of levels of nucleotide metabolism proteins in bladder cancer cell lines. Quantification of RRM1, RRM2, p53R2, and TK1 expression relative to beta- tubulin (from Figure 2.5A). The images were scanned using the LI-COR Odyssey scanner and quantified using Image Studio software (LI-COR Biosciences).

Data Information: Data are expressed as ratios relative to total beta-tubulin (mean ± SEM) of three independent experiments.

In contrast, *RRM1* was only significantly over-expressed in MIBC.

The expression level of these same proteins was also measured in different tissues recovered from an orthotopic rat AY-27 bladder cancer model (**Figure 2.5F**). We detected high RRM2 expression in tumor tissue as well as from non-tumor bearing bladder tissue. RRM1 did not appear elevated in tumors compared to normal tissues, and very little TK1 expression was detected in any of the tissues.

2.3.3 VACVs encoding F4L and J2R mutations safely clear human bladder tumor xenografts. The safety and oncolytic activity of the mutant VACVs was tested in xenograft models of human bladder cancer. These models were established by subcutaneous or orthotopic implantation of luciferase-expressing human RT112 cells (RT112-luc) in Balb/c immune-deficient mice. In the first study, we injected three doses of virus, each comprising 10^6 PFU of ΔJ2R, ΔF4L, ΔF4LΔJ2, or UV-inactivated VACV as a control, directly into subcutaneous RT112-luc tumors (**Figure 2.7A**). An mCherry signal, indicative of virus replication, was detected in all mice before the third live virus injection (**Figure 2.8**) and all animals treated with live virus showed significantly prolonged survival compared to those treated with UV-inactivated VACV (**Figure 2.7B**). Tumor growth was controlled in all animals treated with live viruses as determined by caliper measurements (**Figure 2.7C**), and by luciferase detection (**Figure 2.7F, G, and 2.9**).

The ΔJ2R virus showed strong anti-tumor activity, but this was only achieved with significant toxicity in Balb/c immune-deficient mice. Seven of ten ΔJ2R VACV-treated mice were euthanized due to excessive weight loss (**Figure 2.7D**). Weight loss in mice euthanized prior to day 50 was due to significant viremia (**Figure 2.7E**) whereas weight loss in mice euthanized at later time points was due to acquired systemic *Staphylococcus aureus* infections (See Appendix Figure 3). These, as well as other ΔJ2R VACV-treated mice, exhibited transient and

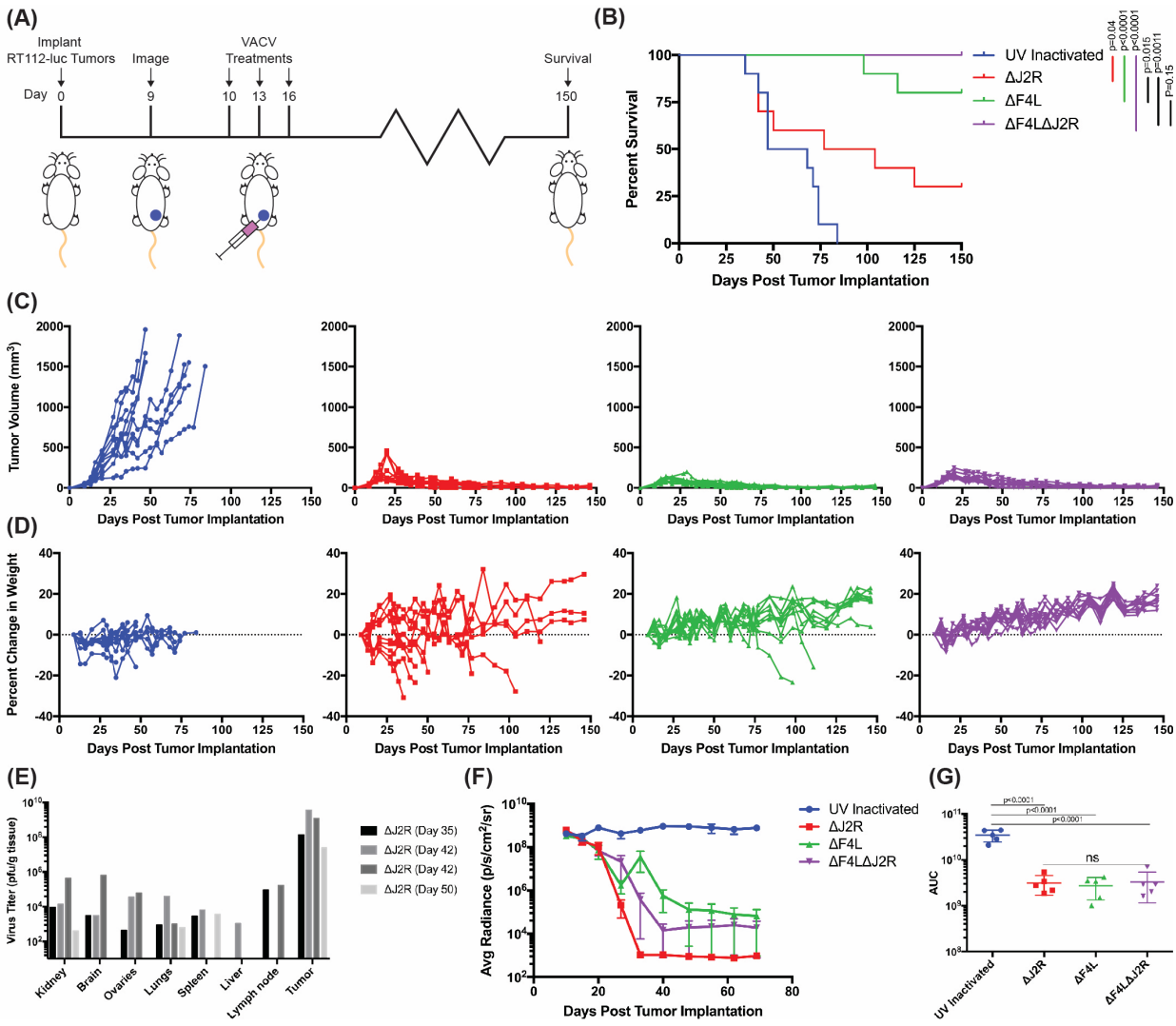
(A)
Implant
RT112-luc Tumors
Image
VACV
Treatments
Survival
Day 0
9
10
13
16
150
(B)
Percent Survival
Days Post Tumor Implantation
UV Inactivated
ΔJ2R
ΔF4L
ΔF4LΔJ2R
p=0.04
p<0.0001
p<0.0001
p=0.015
p=0.0011
P=0.15
(C)
Tumor Volume (mm3)
Days Post Tumor Implantation
(D)
Percent Change in Weight
Days Post Tumor Implantation
(E)
Virus Titer (pfu/g tissue)
ΔJ2R (Day 35)
ΔJ2R (Day 42)
ΔJ2R (Day 42)
ΔJ2R (Day 50)
Kidney
Brain
Ovaries
Lungs
Spleen
Liver
Lymph node
Tumor
(F)
Avg Radiance (p/s/cm2/sr)
Days Post Tumor Implantation
UV Inactivated
ΔJ2R
ΔF4L
ΔF4LΔJ2R
(G)
AUC
p<0.0001
p<0.0001
p<0.0001
ns
UV Inactivated
ΔJ2R
ΔF4L
ΔF4LΔJ2R

Figure 2.7. ΔF4LΔJ2R VACV safely and effectively clears subcutaneous human RT112-luc xenografted tumors. (A) Experimental scheme**.** Balb/c nude mice were injected with $2x10^6$ RT112-luc cells in the left flank at day zero. Then 10^6 PFU of UV-inactivated, ΔJ2R, ΔF4L, or ΔF4LΔJ2R VACV were injected into the tumors on days 10, 13, and 16 post-implantation. **(B)** Overall survival of immunocompromised mice bearing RT112-luc flank tumors following treatment with the indicated viruses (n=10 mice per group). **(C)** Growth of individual virus-treated RT112-luc tumors. Legend as in (B). **(D)** Analysis of individual animal body weights plotted as mean change in body weight relative to day 10. Legend as in (B). **(E)** VACV titers in tissues taken from animals euthanized due to toxicity (note: only mice that had detectable virus (4/10) as determined by plaque assay are shown). **(F)** Quantification of average luminescence (an indication of live tumor cells) from bladder tumors corresponding representative animals in (B) with 5 mice per group. **(G)** Area under the curve (AUC) calculation from the data in (F).

Data Information: Animal survival was analyzed by log-rank (Mantel-Cox) test. One-way ANOVA followed by Tukey's multiple comparison test was used in (G). For luciferase quantification n=5 representative animals per group. Mean ± SEM is shown for F and G.

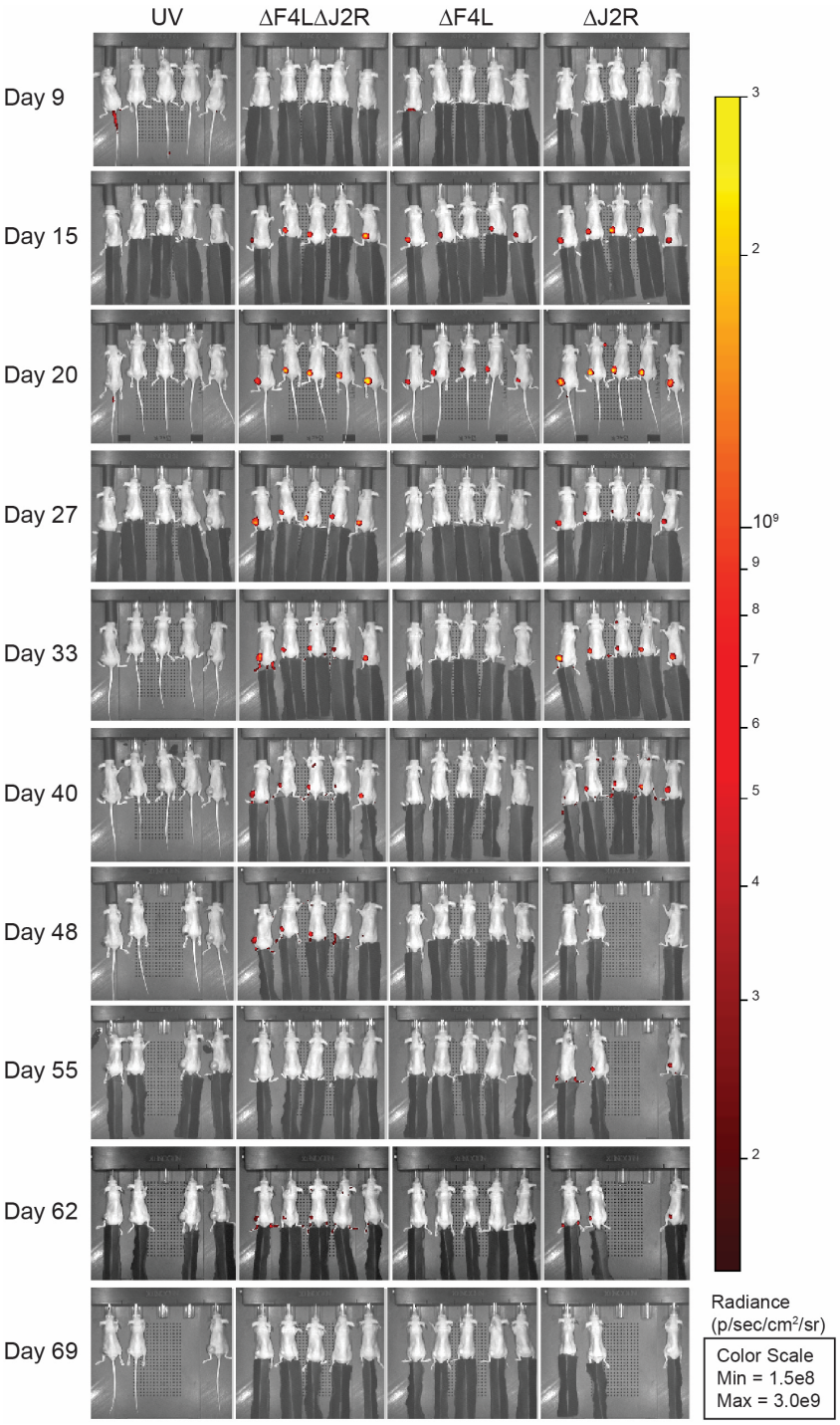

Figure 2.8: mCherry signal is detectable in RT112-luc subcutaneous xenografts after intratumoral injection of VACVs. RT112-luc-tumor-bearing mice (representative animals from Figure 2.7) were imaged for virally encoded mCherry signal on the indicated days. All mCherry images are shown on the same scale.

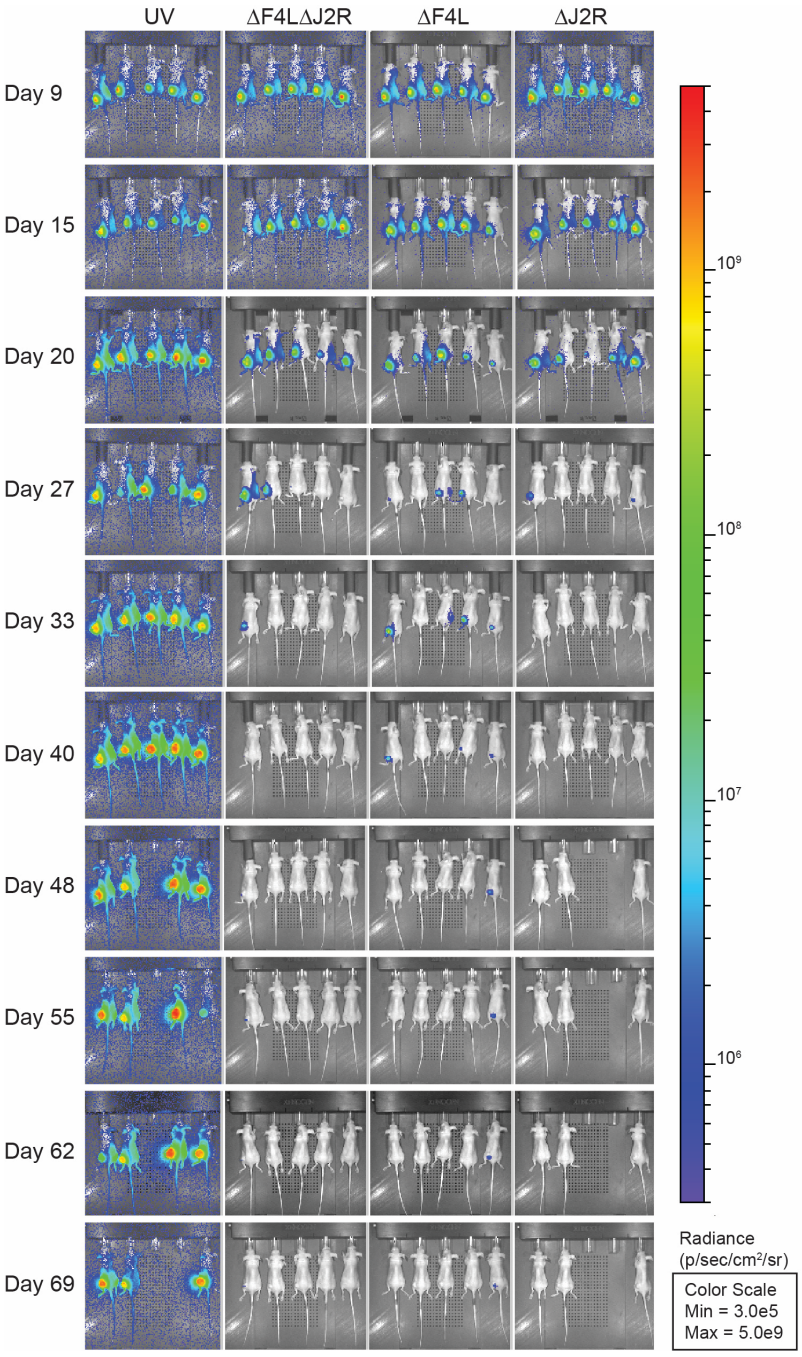

Figure 2.9: Intratumoral ΔF4LΔJ2R VACV effectively clears human RT112-luc subcutaneous xenograft tumors as indicated by luciferase signal. RT112-luc-tumor-bearing mice (from one of the experiment with 5 mice per group shown in Figure 2.7) were imaged for luciferase expression following luciferin injection on the indicated days. All luciferase images are shown on the same scale.

spontaneously-resolving dermal pox lesions at sites distant to the tumor injection site, which may have provided a route for the bacterial infection. In contrast, all mice treated with ΔF4LΔJ2R VACV were completely cured of their RT112-luc tumors and continued to gain weight throughout the experiment (**Figure 2.7D**). We saw no signs of toxicity or virus lesions in this treatment group. Consequently, both ΔF4L and ΔF4LΔJ2R VACV significantly increased survival compared to animals treated with the ΔJ2R strain ($p=0.015$ and $p=0.001$, respectively). A pilot experiment using a subcutaneous UM-UC3-luc xenograft model also suggested strong oncolytic activity from ΔF4LΔJ2R VACV (**Figure 2.10**) even though UM-UC3-luc cells supported only limited VACV growth *in vitro* (**Figure 2.2**).

We next developed a new orthotopic RT112-luc xenograft model to replace the KU7 model that was recently shown to have been contaminated with HeLa cells [296]. The treatment scheme is shown in **Figure 2.11A**. Bioluminescence images show a continuous increase in luciferase signal from tumors treated with UV-inactivated virus, and a decline in signal from all live-VACV-treated animals, with most tumors eventually being cleared (**Figure 2.11B-D**). To measure virus distribution after intravesical treatment, we euthanized mice three days after the last virus instillation and measured virus titers in tumors and other organs. We detected little or no spread of the ΔF4L or ΔF4LΔJ2R virus to other organs (**Figure 2.11F**). In one animal, significant levels of ΔF4LΔJ2R VACV were detected in the kidney, but this coincided with a luciferase signal indicating tumor spread to this site, demonstrating the tumor-selectivity of this virus. In contrast, ΔJ2R VACV was detected in several organs in treated mice (**Figure 2.11F**). Delivering the virus directly into the bladder caused no toxicity as judged by animal weights (**Figure 2.11E**). However, as was seen in the RT112-luc subcutaneous model, most of the ΔJ2R-treated mice developed pox lesions on their backs (**Figure 2.11G**).

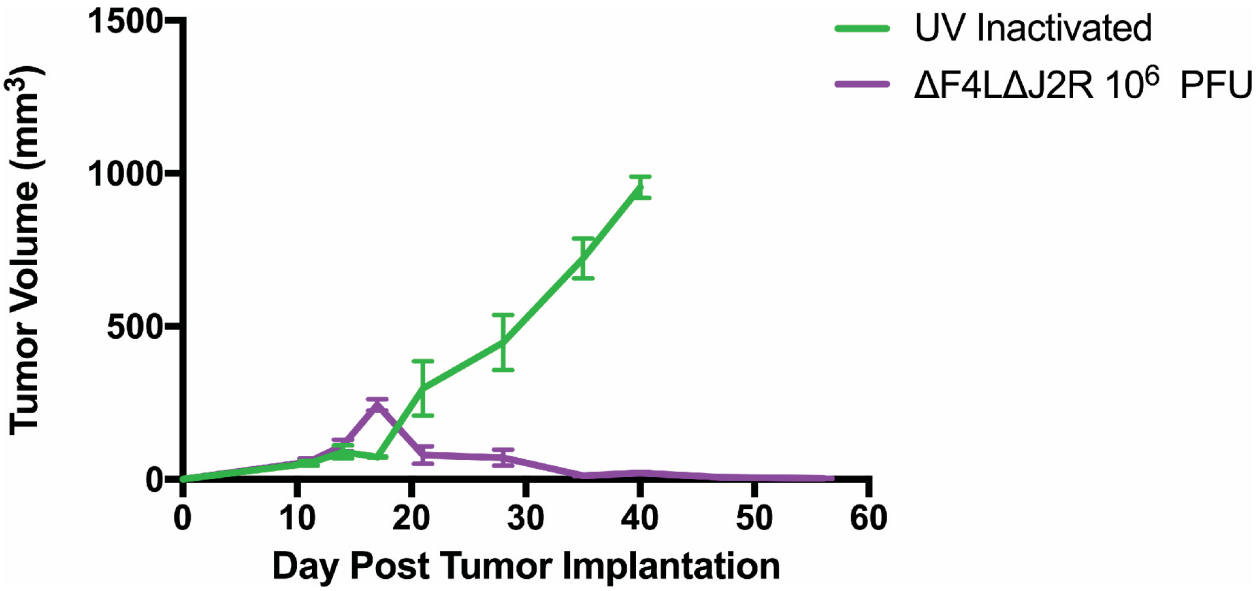

Figure 2.10: Intratumoral ΔF4LΔJ2R VACV safely and effectively clears human UM-UC3-luc subcutaneous xenograft tumors. Balb/c nude mice were injected with $2x10^6$ UM- UC3-luc cells in the left flank (day 0). UV-inactivated or ΔF4LΔJ2R VACVs were injected intratumorally on days 10, 13, and 16 ($1x10^6$ PFU per injection). Average growth of VACV-treated UM-UC3-luc tumors are shown.

Data Information: Data obtained using n=3 mice per group and mean ± SEM is shown.

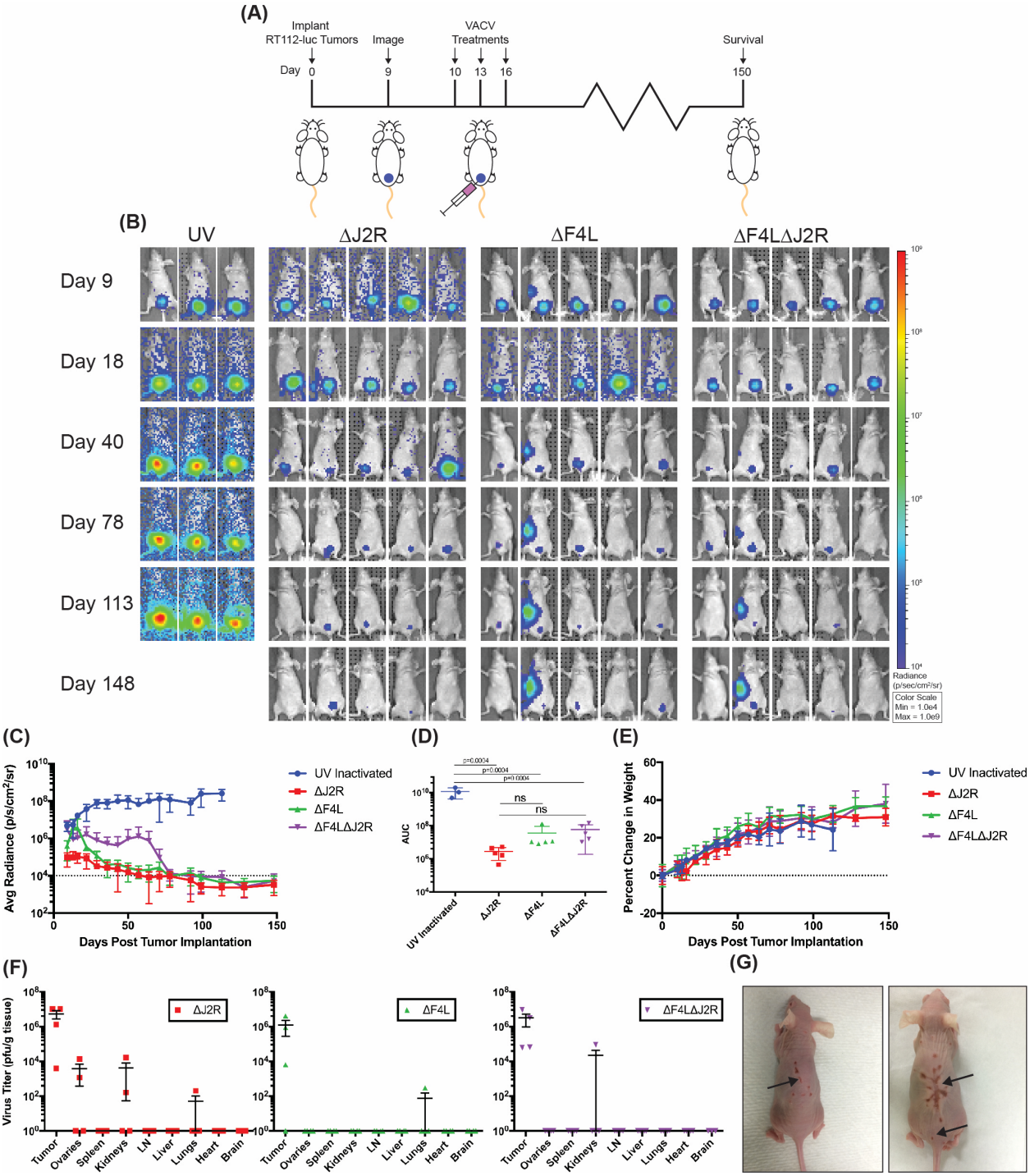
(A)
Implant RT112-luc Tumors
Image
VACV Treatments
Survival
Day 0
9
10
13
16
150
(B)
UV
ΔJ2R
ΔF4L
ΔF4LΔJ2R
Day 9
Day 18
Day 40
Day 78
Day 113
Day 148
Radiance (p/sec/cm²/sr)
Color Scale
Min = 1.0e4
Max = 1.0e9
(C)
Avg Radiance (p/s/cm²/sr)
Days Post Tumor Implantation
UV Inactivated
ΔJ2R
ΔF4L
ΔF4LΔJ2R
(D)
AUC
p=0.0004
p=0.0004
p=0.0004
ns
ns
(E)
Percent Change in Weight
Days Post Tumor Implantation
(F)
Virus Titer (pfu/g tissue)
Tumor
Ovaries
Spleen
Kidneys
LN
Liver
Lungs
Heart
Brain
(G)

Figure 2.11. ΔF4LΔJ2R VACV safely and effectively clears orthotopic human RT112-luc xenografted tumors. (A) Experimental scheme. Balb/c nude mice were instilled with $2x10^6$ RT112-luc cells on day zero. Mice were imaged for luciferase following luciferin injection on day 9 to verify tumor implantation. On each of days 10, 13, and 16 post tumor implantations, 10^6 PFU of UV-inactivated, ΔJ2R, ΔF4L, or ΔF4LΔJ2R VACV was instilled into the bladder and left in-dwelling for 1 hr. n=5 per group. **(B)** Representative luminescence images from animals bearing orthotopic RT112-luc tumors and treated with VACVs. **(C)** Quantification of average luminescence, the dashed line indicates limit of detection. **(D)** Area under the curve calculation from the data in (C). **(E)** Analysis of individual animal body weights plotted as mean change in body weight. **(F)** Virus titers in tissues on day 19. Organs were harvested, homogenized, and the virus titered on BSC-40 cells with n=4 mice per group. **(G)** Representative images of lesions on two mice taken approximately 125 days post-tumor implantation. Arrows indicate lesions.

Data Information: Mean ± SEM is shown. One-way ANOVA followed by Tukey's multiple comparison test was used in (D).

Finally, we tested efficacy and toxicity when virus was administered by intravenous injection in a subcutaneous RT112-luc xenograft tumor model. Although ΔJ2R VACV decreased tumor volume and replication was detectable at the tumor site by day 20, ΔJ2R VACV provided no significant survival benefit over UV-inactivated virus by log-rank test (**Figure 2.12A, B, and 2.13**). The ΔJ2R virus caused significant toxicity in mice as evident by weight loss and virus detection in multiple normal organs (**Figure 2.12C and D**). In contrast, there was a significant increase in the survival of mice treated with the ΔF4L (P=0.0015) and ΔF4LΔJ2R (p=0.013) viruses (**Figure 2.12A**). The ΔF4LΔJ2R group exhibited virus-encoded mCherry fluorescence at the tumor site by day 27 (**Figure 2.13**), while this signal was not seen until day 40 (24 days after the last virus injection) in the ΔF4L group.

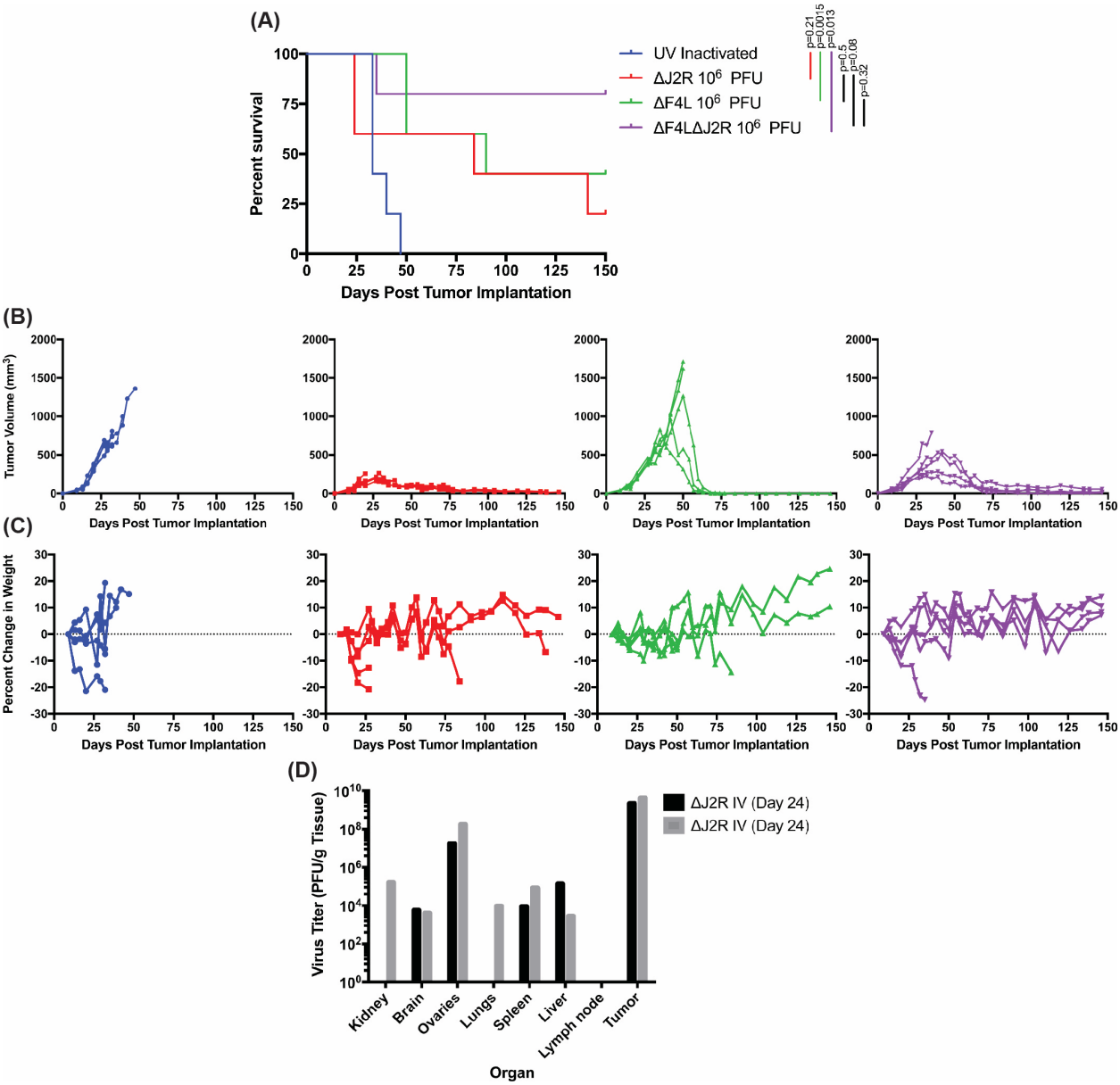
(A)
Percent survival
Days Post Tumor Implantation
UV Inactivated
ΔJ2R 10^6 PFU
ΔF4L 10^6 PFU
ΔF4LΔJ2R 10^6 PFU
p=0.21
p=0.0015
p=0.013
p=0.5
p=0.08
p=0.32
(B)
Tumor Volume (mm^3)
Days Post Tumor Implantation
(C)
Percent Change in Weight
Days Post Tumor Implantation
(D)
Virus Titer (PFU/g Tissue)
ΔJ2R IV (Day 24)
ΔJ2R IV (Day 24)
Kidney
Brain
Ovaries
Lungs
Spleen
Liver
Lymph node
Tumor
Organ

Figure 2.12: Intravenously injected ΔF4LΔJ2R VACV safely and effectively clears human RT112-luc xenografted tumors. Balb/c nude mice were injected with $2x10^6$ RT112-luc cells in the left flank (day 0). $1x10^6$ PFU of UV-inactivated, ΔJ2R, ΔF4L, and ΔF4LΔJ2R VACVs were injected I.V. (via tail vein) on each of days 10, 13, and 16. **(A)** Overall survival of immunocompromised mice bearing RT112-luc flank tumors. **(B)** Growth of individual VACV-treated RT112-luc tumors. **(C)** Analysis of individual animals' body weight plotted as mean change in body weight. **(D)** VACV titers in tissues from euthanized animals (note: only mice that had detectable virus (2/4) as determined by plaque assay are shown). Organs were harvested and homogenized in HBSS using Miltenyi gentleMACS, then homogenates were titered on BSC40 cells.

Data Information: Data for (A) to (C) represent n=5 mice per group. Animal survival was analyzed by log-rank (Mantel-Cox) test.

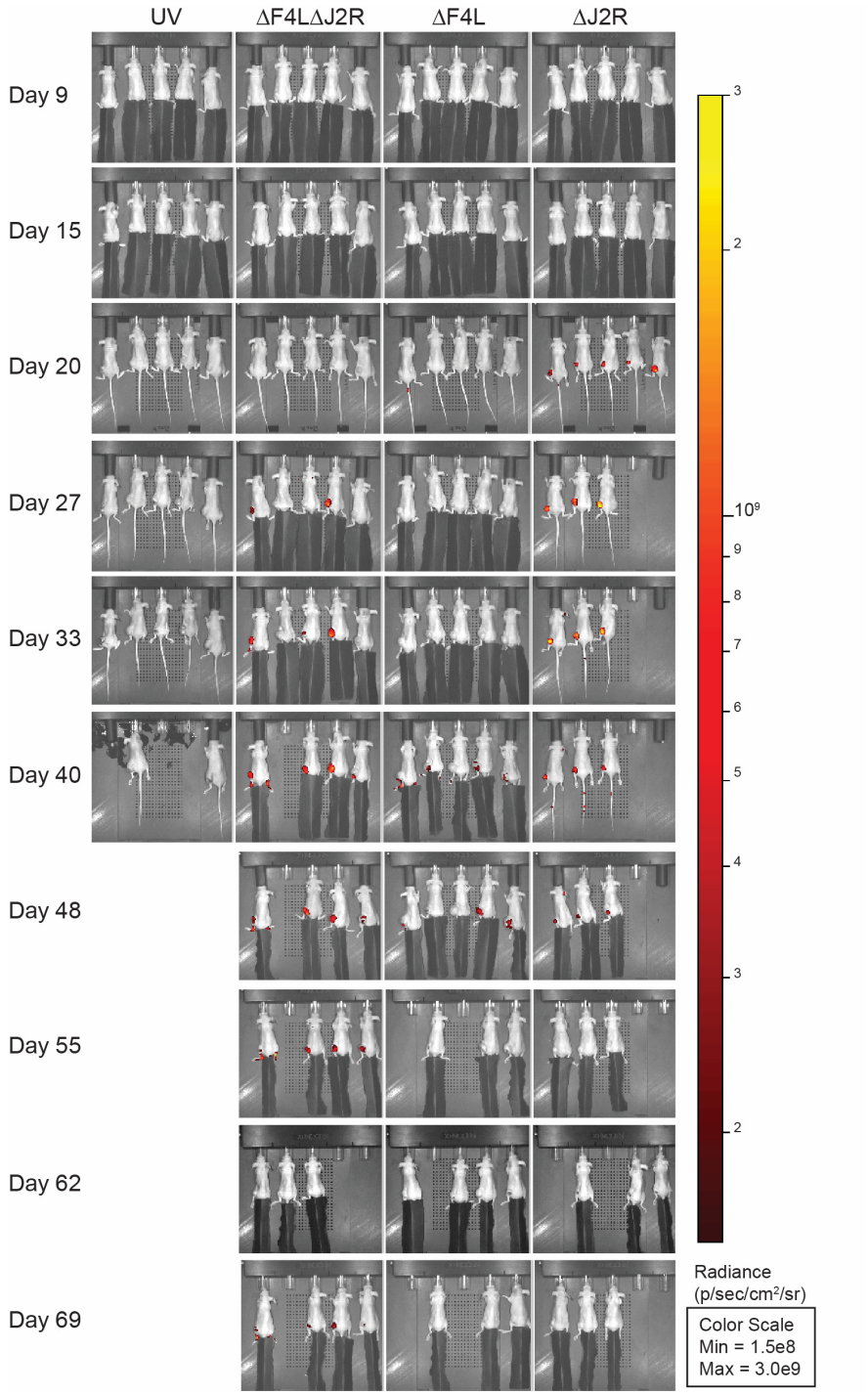

Figure 2.13: mCherry signal is detectable in RT112-luc xenografts after IV injection of VACVs. RT112-luc-tumor-bearing mice (representative animals from Figure 2.12) were imaged for virally encoded mCherry signal on the indicated days. All mCherry images are shown on the same scale.

2.4 DISCUSSION

Most oncolytic VACVs reported to date bear mutations that inactivate *J2R*. *J2R* encodes the viral TK, a critical enzyme in the salvage pathway for nucleotide biosynthesis [297,298]. Deleting the *J2R* gene has been shown to reduce virulence while allowing VACV replication in dividing cells [232]. We have shown here that all our bladder cancer cell lines supported replication of ΔJ2R VACV to nearly the same level seen in cells infected with WT VACV. Surprisingly, we could not detect cellular TK1 in the normal N60 cell line even though it supports robust ΔJ2R VACV growth. This could be explained by the fact that dTTP can also be produced from dUMP by thymidylate synthase and TMK [297,298] and VACV encodes the latter enzyme.

To produce a safer and more tumor-selective oncolytic VACV, we investigated deletion of *F4L*, a homolog of the *RRM2* gene encoding the small subunit of RNR. We used a panel of bladder cancer cell lines and primary tissues to confirm reports that RRM2 is elevated in bladder cancer [285]. Cancer cells often undergo metabolic reprogramming because of aberrant oncogenic-signaling, adopting a state of anabolic metabolism to generate the needed macromolecules and dNTPs for division [200]. Additionally, cancer cells generally have an increased S-phase fraction compared to normal cells [291]. These characteristics of bladder tumor cells may partly explain the complementation of the viral RRM2 deletion, even under low serum conditions. This is consistent with our observations of robust replication of both ΔF4L VACV and ΔF4LΔJ2R VACV in most bladder cancer cell lines. However, unlike a *J2R*-deleted mutant, replication of the *F4L*-deleted viruses was attenuated in non-proliferating (partially serum-deprived) normal cells.

For our initial *in vivo* experiments, we used both subcutaneous and orthotopic RT112-luc tumors as models for NMIBC. This provides a replacement for HeLa-contaminated KU7 or KU7-luc cells [296] and permits bioluminescence monitoring of orthotopic tumor progression. RT112

cells have been used previously to model MIBC cancer by injecting cells into the bladder wall [299]. However, MIBC is not treated by intravesical therapies. Our cell instillation technique produces a model for NMIBC, for which intravesical therapies are appropriate. These orthotopic RT112-luc tumors responded dramatically to intravesical administration of the three mutant VACVs. In addition, intratumoral and intravenous injection of each of the three VACVs in the subcutaneous xenograft model produced tumor control in a manner that corresponded roughly to the degree of virus replication in the tumor. It is interesting to note that ΔF4LΔJ2R VACV consistently produced better anti-tumor activity than ΔF4L VACV in our animal models, and often *in vitro* as well. This seems counterintuitive, and the reason(s) why are unclear, but the mechanism is being investigated.

The VACV WR strain was originally adapted for growth in mice and exhibits virulence in this model. However, we saw no signs of toxicity in any of the immune-compromised mice treated with ΔF4L or ΔF4LΔJ2R VACV, while significant toxicity was observed in animals treated with ΔJ2R VACV. In addition, ΔJ2R VACV was recovered from multiple normal organs after intratumoral or systemic treatments. These data show that the *J2R* mutation does not suffice to prevent VACV replication in normal tissues of immune-compromised mice. Although a number of oncolytic *J2R*-deleted VACV strains have been used safely in many clinical trials, including one based on the VACV strain WR [300], a further improvement might be obtained by incorporating *F4L* mutations.

Accumulating clinical data has shown that OVs have the potential to be a standard in cancer therapy. As with any new treatment, safety is of the utmost importance in the eventual clinical application. Here we describe a unique VACV mutant that shows enhanced safety without a loss

of efficacy over the commonly used ΔJ2R mutation. Results presented here suggest that NMIBC could be a highly suitable target for oncolytic treatment with a WR-based ΔF4LΔJ2R VACV.

CHAPTER 3 – PRE-CLINICAL EVALUATION OF RIBONUCLEOTIDE REDUCTASE MUTANT VACCINIA VIRUS IN IMMUNE COMPETENT AND PATIENT DERIVED MODELS OF BLADDER CANCER

PREFACE

A portion of this chapter has been published in the manuscript: **Potts, K. G**., Irwin, C. R., Favis, N. A., Pink, D. B., Vincent, K. M., Lewis, J. D., Moore, R. B., Hitt, M. M.* and Evans, D. H.* (2017), Deletion of *F4L* (ribonucleotide reductase) in vaccinia virus produces a selective oncolytic virus and promotes anti-tumor immunity with superior safety in bladder cancer models. EMBO Mol Med, e201607296. (* These authors contributed equally). EMBO Molecular Medicine states: "This is an open access article under the terms of the Creative Commons Attribution 4.0 License, which permits use, distribution and reproduction in any medium, provided the original work is properly cited."

Contributions:

I designed and performed experiments, analyzed the data, and prepared the manuscript. Dr. Chad Irwin designed and constructed the viruses used in these studies. Nicole Favis assisted in all animal experiments. Dr. Desmond Pink and Dr. John Lewis helped perform the *ex vivo* tumor imaging experiments and analyzed resulting data. Dr. David Evans, Dr. Mary Hitt, and Dr. Ronald Moore provided guidance in experimental design, data interpretation, and manuscript preparation.

3.1 INTRODUCTION

There has been very little improvement in the treatment of high-grade NMIBC in the last 20 years and recurrence after BCG therapy is still one of the most significant problems in the management of bladder cancer [102]. Additionally, because of the high rates of recurrence and need for lifelong surveillance, bladder cancer is one of the most expensive cancer to treat, imposing a high economic burden [301,302]. Elimination of the transformed cells may allow reduced surveillance and the need for ongoing cystoscopy. The potential high degree of safety and efficacy highlighted in Chapter 2 for oncolytic VACV therapy of bladder cancer warrants immediate further investigation in more clinically relevant preclinical models.

Patient-derived xenografts (PDXs) provide *in vivo* models that closely resemble human tumors by maintaining the cellular and histological features of the original tumor (reviewed in [303]). Additionally, it has been shown that the tumors conserve their genetic and gene expression profiles [304]. These characteristics make PDX models more predictive in determining treatment response. However, these models are developed in severely immune-compromised mice and therefore provide little insight into the role of the immune system. Syngeneic models are established by implanting tumors into immunocompetent animals, allowing the study of both the tumor and immune response (reviewed in [305]. The AY-27 syngeneic rat bladder cancer model closely resembles human disease [297]. This cell line was derived from carcinogen induced bladder tumors in Fischer 344 rats. Both models have advantages and disadvantages but taken together they provide significant insight into the safety and efficacy of a therapy.

Here we describe pre-clinical studies showing that VACV can be used safely as an intravesical treatment for NMIBC. We find that *F4L*-deleted VACVs safely and effectively clear bladder tumors in an immunocompetent animal model as well as induce a durable and protective

anti-tumor immunity that was evidenced by tumor rejection upon challenge, as well as by *ex vivo* cytotoxic T-lymphocyte assays. Finally, ΔF4LΔJ2R VACV replicated in fresh cultures of primary human bladder tumors and safely and effectively clear bladder tumor (PDX) model. These findings highlight the significant potential of using a ΔF4LΔJ2R VACV in the treatment of NMIBC.

3.2 MATERIALS AND METHODS

3.2.1 Cell lines. Cell culture in this chapter was performed as described in Chapter 2.2.1 Materials and Methods.

3.2.2 Viruses. Viruses used in this chapter were generated as described in Chapter 2.2.2 Materials and Methods.

3.2.3 Antibodies. The primary antibodies used for flow cytometry against rat proteins included: mouse anti-CD4 FITC (eBiosciences 11-0040), mouse anti-CD8 APC (eBiosciences 17-0084), and mouse anti-CD107a (Abcam ab2S630). The secondary antibody used for flow cytometry was donkey anti-mouse PE (Abcam ab7003).

3.2.4 Primary cell culture. Primary cancer and adjacent normal tissues were obtained from consenting patients undergoing surgery with the approval of the University of Alberta Health Research Ethics Board. Samples were received in saline and processed within 2 hr of surgery. Sub-mucosal and necrotic tissues were stripped from the tumor tissue and the remaining tumor was processed in 4 mL of "spleen dissociation medium" (STEMCELL Technologies) using a GentleMACS dissociator (Miltenyi Biotec). After rocking at 37^{o}C for 30 min, the suspension was reprocessed on the dissociator, then EDTA was added to 10 mM, and the cells incubated at room temperature for 10 min. The cells were centrifuged for 5 min at 350 x g, washed, and plated in 100 mm tissue culture plates with EpiLife medium (Thermo Fisher Scientific) supplemented with 25 μg/mL bovine pituitary extract (Thermo Fisher Scientific), 0.5 ng/mL epidermal growth factor

(Thermo Fisher Scientific), 3 mM glycine (Sigma-Aldrich), 0.1 mM MEM non-essential amino acids (Gibco), 1% ITS (Gibco) [10 μg/mL insulin, 5.5 μg/mL transferrin, 6.7 ng/mL selenium], 2% FBS, 2 mM L-glutamine, 100 U/mL penicillin, 100 U/mL streptomycin, and 0.25 μg/mL Fungizone® (Gibco). Twelve to 16 hrs after plating the cells were washed twice with PBS and the medium was replaced. Adherent cells were sub-cultured using standard tissue culture techniques.

3.2.5 Animal care and housing. All studies reported were conducted with the approval of the University of Alberta Health Sciences Animal Care and Use Committee in accordance with guidelines from the Canadian Council for Animal Care. Animals were housed with access to food and water *ad libitum* in ventilated cages (1-2 rats per cage) in a biosafety level 2 containment suite at the University of Alberta Health Sciences Laboratory Animal Services Facility.

3.2.6 In vivo AY-27 tumor model. Ten week old Fisher F344 immune-competent female rats (Charles River Laboratories), weighing at least 150 g, were used for orthotopic AY-27 tumor implantation as previously described [297]. Briefly, 0.3 mL 0.1 M HCl was instilled into the bladder of rats anesthetized with isoflurane, left in-dwelling for 15 sec, neutralized with 0.3 mL of 0.1 M KOH for 15 sec, then the bladder washed 3 times with PBS. The catheter was then used to deliver 0.3 mL of saline containing $3x10^6$ AY-27 cells, the cells left in-dwelling for 1 hr, and the rats returned to their cages. Five days later tumor take was confirmed by cystoscopy [306]. For virus treatments, the rats were anesthetized, catheterized, the bladders emptied by suprapubic pressure, and then $3x10^8$ PFU of virus in 0.3 mL PBS was instilled into each bladder on days 6, 9, and 12 and left in-dwelling for 1 hr.

Rats that were determined to be tumor-free by cystoscopy at day 125 post-tumor implantation were challenged with $3x10^6$ AY-27 cells back in the bladder (as described above) or the flank. Cells were resuspended in HBSS and mixed with an equal volume of Matrigel (Corning).

A total of 200 μL was injected per rat. Age matched Fisher F344 immune-competent female rats were used as controls.

3.2.7 In vivo patient-derived xenograft (PDX) model. Primary bladder cancer tissues were obtained from consenting patients undergoing surgery with the approval of the University of Alberta Health Research Ethics Board. Samples were received in saline and processed within 2 h of surgery. Submucosal and necrotic tissues were stripped from the tumor tissue and the remaining tumor was cut into ~3x3x3 mm pieces and placed in HBSS containing 100 U/ml penicillin, 100 U/ml streptomycin, and 0.25 μg/ml Fungizone® (Gibco).

Male NOD SCID gamma (NSG) [NOD.Cg-Prkdc^{scid} Il2rg^{tm1Wjl}/SzJ] mice were 6-12 weeks old and at least 20 g in weight at the time of tumor implantation. To establish subcutaneous PDX tumors, mice were anesthetized with 2% isoflurane and site of implantation was sterilized with 70% isopropanol. A small incision (3-4 mm in length) was made in the right flank of the mice and the connecting tissue was separated via blunt dissection. Tumor tissue from patients, or from mice when performing passages, was then placed into the incision and the tissue was closed with Vetbond™ Tissue Adhesive (3M). Initial implanted tumors were grown to ~500 mm^3 and then were processed as described above for primary patient tissue and implanted into additional NSG mice. This process was performed again to have enough tumor bearing mice for experimentation (These PDX tumors were referred to as Passage 3).

When passage 3 tumor volumes reached approximately 150 mm^3, mice were randomized, and then intratumorally injected with 1x10^6 PFU of UV-inactivated VACV, ΔF4LΔJ2R VACV, or PBS on each of days 1, 4, and 7. Flank tumor volumes were determined weekly by caliper measurements.

3.2.8 Isolation of CD3+cells. Spleens were harvested from euthanized rats and placed in HBSS on ice. Next, they were cut into small pieces, resuspended in 4 mL of spleen dissociation medium, and broken up using a GentleMACS dissociator, followed by rocking at 37^{o}C for 30 min. The dissociation program was run again, EDTA was added to 10 mM, and the cells incubated at room temperature for another 10 min. Cells were then filtered through a 70 μm MACS SmartStrainer (Miltenyi Biotec), centrifuged for 5 min at 350 x g, and washed with HBSS. Red blood cells were lysed with Red Blood Cell Lysis Buffer (eBioscience), then the remaining cells recovered by centrifugation, then resuspended in PBS and counted. $CD3^{+}$ cells were isolated from this preparation using a MagCellect^{TM} Rat $CD3^{+}$ T-cell isolation kit following the manufacturer's protocol (R&D Systems).

3.2.9 Preparation of tumor cells lysates. Cells were washed with PBS and then removed from the tissue culture plate using cell lifters (Thermo Fisher). Cells were the subject to five freeze (liquid nitrogen) and thaw (37^{o}C water bath) cycles. To remove large particles, the lysate was centrifuged (2000 x g for 10 min at 4 ^{o}C). Protein concentration was then determined using a bicinchoninic acid (BCA) protein assay kit (Thermo Fisher).

3.2.10 Bone marrow derived dendritic cell (BMDC) culture and lysate loading. Method is highlighted in **figure 3.1**. The femurs were removed from euthanized naïve Fischer F344 female rats, cleaned of attached tissue, soaked in 70% isopropanol for 2 min, and rinsed in HBSS. Femur ends were removed and the marrow flushed with HBSS. Red blood cells were lysed, and $3x10^{6}$ of the remaining bone marrow cells were plated on 100 mm untreated petri dishes in 8 mL RPMI 1640 medium supplemented with 10% FBS, 50 μM 2-mercaptoethanol, 2 mM L-glutamine, 100 U/mL penicillin, 100 U/mL streptomycin, 0.25 μg/mL Fungizone® (Gibco), 500 U/mL rat GM-CSF (Peprotech), and 20 ng/mL rat IL-4 (Peprotech). The cells were cultured at 37^{o}C and the

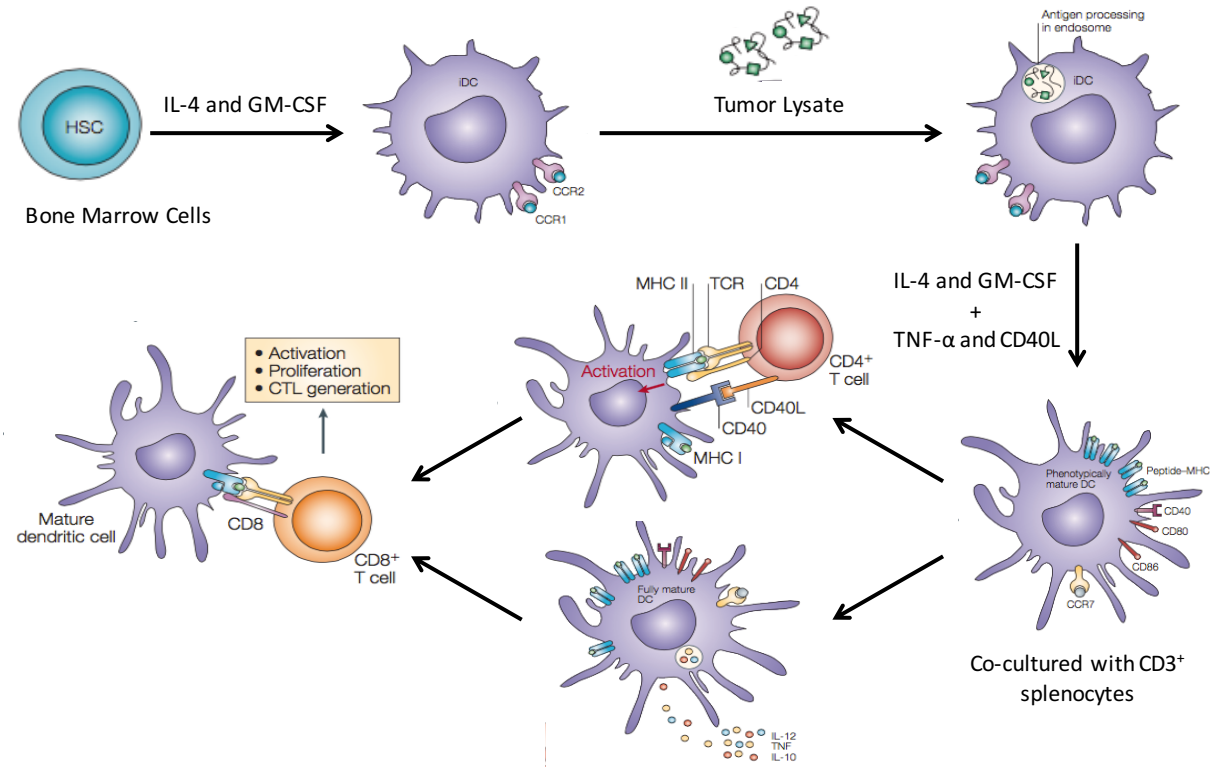

Figure 3.1: Generation of Bone marrow derived dendritic cells (BMDC) and lysate loading. Bone marrow cells were plated on 100 mm untreated petri dishes in medium supplemented 500 U/mL rat GM-CSF and 20 ng/mL rat IL-4. On day 5 the medium was replaced and 100 µg/mL of AY-27 tumor lysate was added to selected dishes. Twelve hours later, the cultures were matured by adding 20 U/mL TNF-α and 0.5 µg/mL CD40L. Two days after adding the tumor cell lysates the cells were washed with PBS, harvested, and co-cultured with $CD3^+$ cells. Figures adapted from [307,308] with permission.

medium, still containing GM-CSF and IL-4, replaced on day 3. On day 5 the medium was replaced again, and 100 μg/mL of AY-27 tumor lysate was added to selected dishes. 12 hours later, the cultures were matured by adding 20 U/mL TNF-α (Peprotech) and 0.5 μg/mL CD40L (AdipoGen) [309,310]. Two days after adding the tumor cell lysates, the cultures were resuspended at $1x10^6$ cells/mL in fresh medium.

3.2.11 T lymphocyte assays. Proliferation assays were performed in 96-well U-bottom plates (Greiner Bio-One). BMDCs (pulsed with or without lysates) were co-cultured with 10^5 $CD3^+$ cells at different ratios (1:1, 10:1, and 100:1 CD3:BMDC) in RPMI 1640 medium as described above. The $CD3^+$ cells were previously labeled with CellTrace Violet per the manufacturer's directions (Thermo Fisher Scientific). After 6 days of co-culture, flow cytometry was used to measure $CD3^+$ T-cells proliferation. Supernatants were collected from cells co-cultured for 24 hr, and assayed by ELISA for interferon-γ (Legend Max, BioLegend™).

Cytotoxicity assays were performed using 10^5 rat splenic $CD3^+$ cells co-cultured in 96-well U-bottom plates with 10^4 BMDCs in RPMI 1640, supplemented with GM-CSF and IL-4 as described above. On day 7, the $CD3^+$ cells were collected, counted, and incubated for 18 hr in flat bottom 96-well plates, along with target cells, at effector-to-target ratios ranging from 20:1 to 0.625:1. The plates were assayed for lysis by LDH assay (Thermo Scientific Pierce).

CD107a expression was measured as described by Betts *et al*. [311] and summarized in **figure 3.2**. Here 10^5 rat splenic $CD3^+$ cells co-cultured in 96-well U-bottom plates with 10^4 BMDCs in RPMI 1640, supplemented with GM-CSF and IL-4 as described above. Cells were co-cultured for 1 hr in the presence of 5 μg/mL CD107a antibody, and incubated for another 5 hr in the presence of 2 μM monensin and 5 μg/mL brefeldin A (BioLegend). The cells were fixed with Fixation Buffer (BioLegend) in the dark for 20 min at room temperature. Cells were stained with

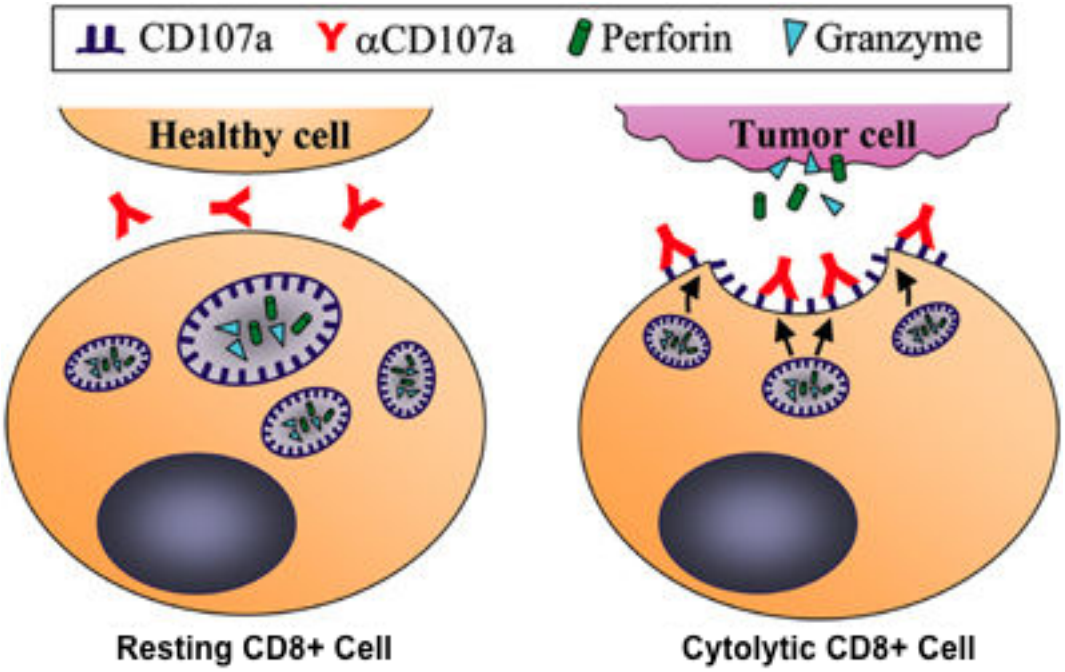

Figure 3.2: CD107a mobilization assay. CD107a glycoproteins line the luminal surface of the outer membrane of lytic granules but are not detectable on the cell surface of resting $CD8^+$ cells (left panel). Upon cell activation, for example, by a tumor cell, lytic granules move to the site of interaction with the target cell and merge with the plasma membrane (right panel). In the course of this process, the lytic content of granules is exocytosed and the CD107a molecules temporarily appear on the cell surface. At this stage, degranulating cells are detected by flow cytometry analysis using CD107a-specific antibodies. Figure and text adapted from [312] with permission.

2.5 µg/mL anti- CD4 and 0.6 µg/mL anti-CD8 for 20 min at 4^{o}C. Cells were washed twice with at least 2 mL of Cell Staining Buffer (BioLegend) with centrifugation at 350 x g for 5 minutes. Next, 5 µg/mL CD107a secondary (Anti-mouse IgG) was added for 20 min at 4^{o}C and cells were then washed as above. Cells were analyzed by flow cytometry.

3.2.12 Flow cytometry. Cell suspensions were analyzed on LSR-Fortessa X20 flow cytometer (BD Biosciences) using the FACS DiVa software (BD Biosciences). In all experiments an eBioscience Fixable Viability Dye was used to determine allow for gating on viable cells. Viability staining was done as per manufactures instructions. Lymphocyte population was gated using forward-scattered light-area (FSC-A) and side-scattered light-area (SSC-A) and a single cell population was gated by using forward-scattered light-height (FSC-H) and FSC-A. Fluorescence-minus-one (FMO) controls [313] were used in all experiments to define cells that have fluorescence above back-ground levels. CellTrace Violet was detected on the DAPI channel using a 405-nm laser. FITC, PE, and APC antibodies were detected on the FITC, PE, and APC-Cy7 channels. FITC and PE were excited using a 488-nm laser and APC was excited with a 561-nm laser. FlowJo (Version 10.2) was used to perform analysis.

3.2.13 Quantitation of VACV neutralizing antibodies. Sera were serially diluted in PBS and incubated with 500 PFU of VACV for 1 hr at 37^{o}C. Next, the viruses were used to infect BSC-40 cells in 60 mm plates, then 48 hr later, cultures were stained with crystal violet and plaques counted.

3.2.14 Ex vivo infection of tumor explants. Primary bladder tumor tissue (~3x3x3 mm) was infected in a 96-well plate with 10^6 PFU of indicated VACVs in PBS at 37^{o}C. After 1 hr at 37^{o}C fresh culture medium was added. Virus-infected tumor tissues were imaged ~24 hr post-infection using a Zeiss Lumar stereomicroscope equipped with a Hamamatsu digital camera and

controlled with Volocity image acquisition software (PerkinElmerTM). The same exposure and contrast settings were used for all tissues. Volocity image analysis software was used to quantify the mCherry signal and mock-infected tissue was used to establish a background.

3.2.15 Statistics. Data were analyzed using two-tailed Student's t-test when comparing the means of two groups. ANOVA was used when comparing multiple groups followed by Tukey's multiple comparison test. Data for animal survival curves were analyzed by log-rank (Mantel–Cox) test. The numbers of animals included in each figure are indicated at the end of each legend. P-values are indicated within each figure.

3.3 RESULTS

3.3.1 VACV mutants clear syngeneic orthotopic rat bladder tumors. The modified VACVs were tested for anti-tumor activity in an orthotopic immune-competent AY-27 rat bladder cancer model. AY-27 tumors resemble high-grade urothelial cell carcinoma in both morphology and tumor biology, providing an excellent model of human bladder cancer [297]. Animals were treated by 3 sequential intravesical instillations with $3x10^8$ PFU of live ΔJ2R, ΔF4L, or ΔF4LΔJ2R VACV, or UV-inactivated virus (**Figure 3.3A**). By day 35, there was a significant reduction in the growth rate of all tumors treated with live virus (**Figure 3.3B**). Following ΔF4LΔJ2R VACV treatment, representative cystoscopic images of the rat bladders revealed tumor necrosis and tumor elimination with little or no inflammation in normal urothelium (**Figure 3.4**). On day 15 after tumor implantation (3 days after final virus instillation), ΔF4L and ΔF4LΔJ2R VACVs could only be detected in the tumor, whereas ΔJ2R VACV was found in the tumor and in the ovaries, kidneys, and lungs (**Figure 3.5**). Of particular concern was the apparent development of cysts on the ovaries of some rats treated with J2R VACV (**Figure 3.6**). However, none of the animals treated with any virus showed signs of overt toxicity. The most important result of this study is that all live VACV

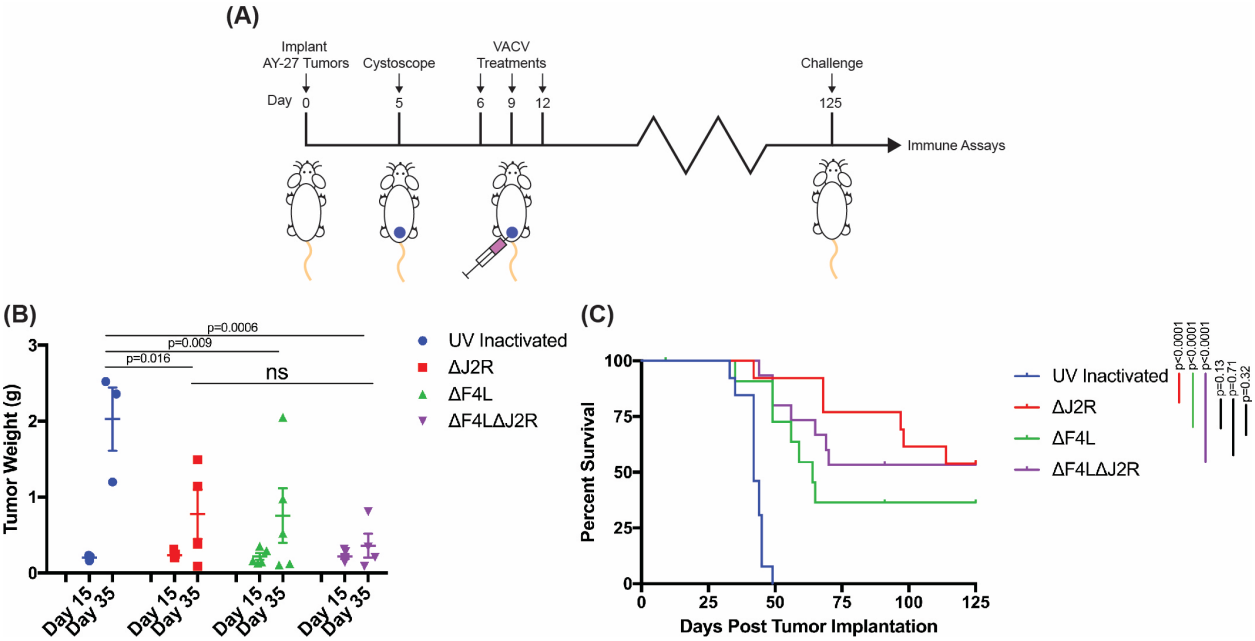

Figure 3.3: ΔF4LΔJ2R VACV safely clears rat orthotopic AY-27 syngeneic tumors. **(A)** Experimental scheme. Rats were instilled in the bladder with $3x10^6$ AY-27 cells on day zero and cystoscoped on day 5 to verify tumor engraftment. Then, $3x10^8$ PFU of UV-inactivated, ΔJ2R, ΔF4L, or ΔF4LΔJ2R VACV were instilled into the bladder of each rat on each of days 6, 9, and 12. **(B)** Tumor weight from animals euthanized on days 15 and 35. **(C)** Overall survival of immunocompetent rats bearing AY-27 bladder tumors following treatment with the indicated VACVs. Data represent combined survival of two independent experiments.

Data Information: Mean ± SEM is shown. Two-way ANOVA followed by Tukey's multiple comparison test was used in (B). Animal survival was analyzed by log-rank (Mantel-Cox) test. n=5 rats per group for each day in (B) and n= 12 to 15 rats per group for (C).

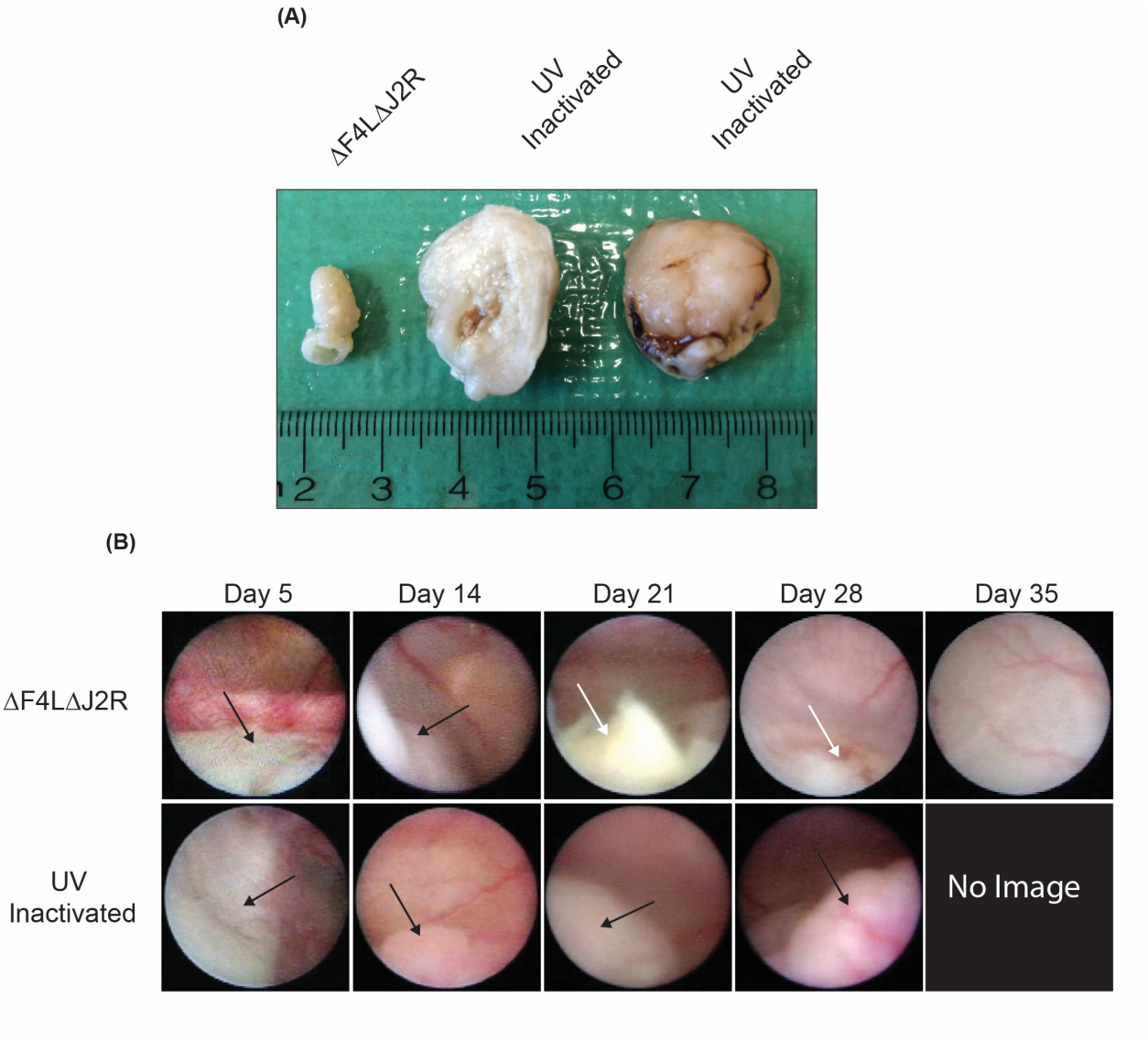

Figure 3.4: Tumor and cystoscope images show tumor control in VACV-treated AY-27 tumor models. (A) Images of rat bladders treated with ΔF4LΔJ2R VACV [left image] or UV-inactivated VACV [center and right images] on days 6, 9 and 12, and then excised on day 35. The bladder tumor treated with UV-inactivated virus has been cut in half. The center sample shows the tumor interior; the right sample shows the exterior. **(B)** Representative cystoscope images of the bladders of a ΔF4LΔJ2R virus-treated rat and a UV-inactivated virus-treated rat on days 5, 14, 21, 28, and 35. Black arrow indicates tumor and white arrow indicates necrotic tumor tissues.

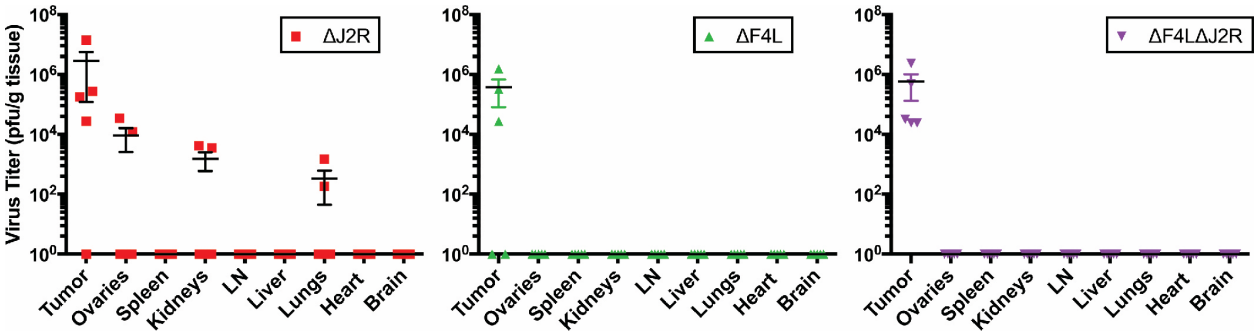

Figure 3.5: *F4L*-deleted VACVs selectively replicate in AY-27 tumors. Virus titers in tissues taken from animals euthanized on day 15 post-implantations. Organs were harvested and homogenized and then lysates were titered on BSC-40 cells.

Data Information Data for each organ represent n=5 rats per group.

Figure 3.6: ΔJ2R VACV treated rats developed ovarian cysts. Ovaries from rats euthanized 15 days post-tumor implantation and 3 days following final treatment with ΔJ2R VACV (left) or ΔF4LΔJ2R VACV (right).

treatments significantly increased survival ($p<0.001$) when compared to the UV-inactivated control (**Figure 3.3C**). It is noteworthy that, although nine of the ΔJ2R VACV-treated animals appeared to be tumor-free by day 75, three of these rats later developed rapidly growing recurrent tumors. This was not seen with either ΔF4L or ΔF4LΔJ2R VACV as far out as 125 days into the study. Interestingly, we also observed significantly higher levels of anti-VACV antibodies in animals treated with ΔJ2R VACV relative to the *F4L*-deleted VACVs (**Figure 3.8**).

3.3.2 Cured animals develop protective anti-tumor immunity. To test whether animals with complete tumor responses had developed anti-tumor immunity, we implanted fresh AY-27 cells in the bladders of eleven surviving VACV-treated animals that were tumor free 125 days post tumor-implantation and all cured animals rejected tumor implantation (**Figure 3.9A**). Systemic anti-tumor immunity was also tested by implanting fresh AY-27 tumor cells subcutaneously in the flanks of six cured ΔF4LΔJ2R-treated animals that were tumor free 125 days post tumor-implantation. Again, all cured rats were protected from tumor development whereas significant tumor growth ($p<0.001$) was seen in the age-matched controls (**Figure 3.9B**).

The cellular anti-tumor immune response was examined in cured animals that were resistant to tumor challenge. One hundred days after subcutaneous challenge with AY-27 cells, cured ΔF4LΔJ2R-treated rats were euthanized, the spleens were removed and $CD3^+$ cells were isolated. The $CD3^+$ cells were stimulated with bone-marrow-derived dendritic cells (BMDCs) previously pulsed with AY-27 tumor lysate to enable antigen presentation [309]. Both splenic $CD3^+CD4^+$ and $CD3^+CD8^+$ cells proliferated when stimulated by lysate-pulsed BMDCs (**Figure 3.9A-C**). To confirm activation of the $CD8^+$ cells, the $CD3^+CD8^+$ population was examined for expression of the CD107a marker [311]. There were significantly more $CD8^+CD107a^+$ cells

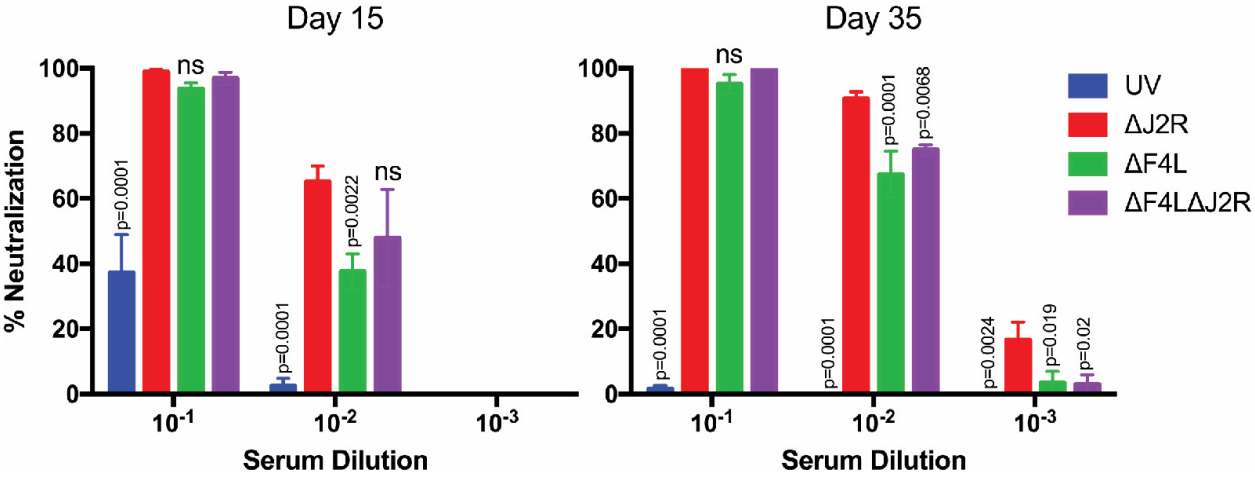

Figure 3.7: VACV treatment generates neutralizing antibodies. VACV neutralizing antibodies in virus-treated rats 15 and 35 days after implantation were measured as described in section 3.2. **Data Information**: Mean ± SEM is shown. Two-way ANOVA followed by Tukey's multiple comparison test was used relative to the ΔJ2R group. n=4-5 rats per group.

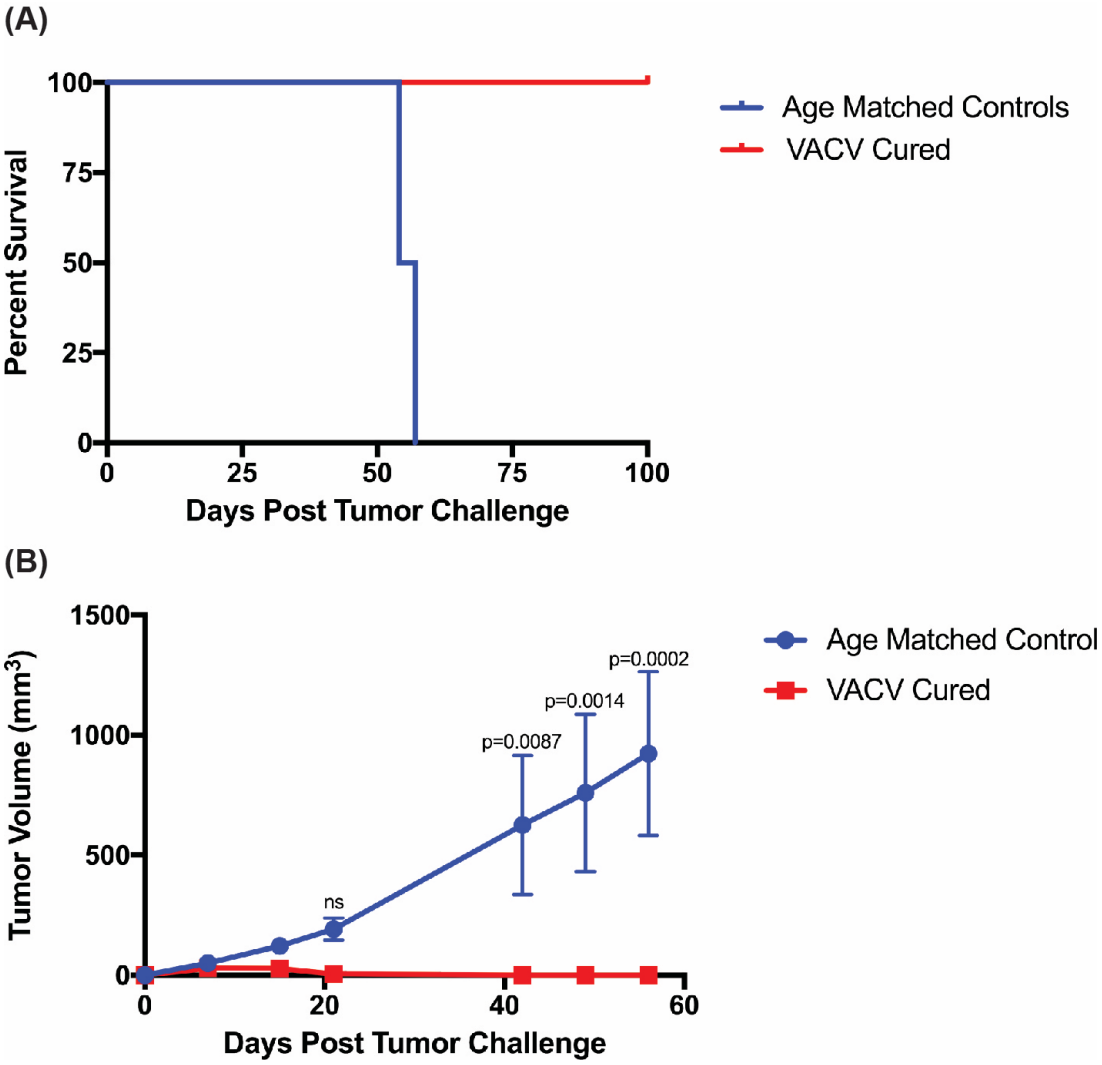

Figure 3.8: ΔF4LΔJ2R VACV generates protective local and systemic antitumor immunity. **(A)** AY-27 cells were implanted in the bladders of cured (n=11) and naïve (n=4) age- matched control rats. Cured animals consisted of 4 ΔJ2R, 2 ΔF4L, and 5 ΔF4LΔJ2R treated animals. **(B)** Protection from subcutaneous tumor challenge after virus-induced tumor clearance. AY-27 cells were implanted in the flanks of ΔF4LΔJ2R cured rats (n=6) and naïve age-matched control rats (n=4).

Data Information: Mean ± SEM is shown. Two-way ANOVA followed by Tukey's multiple comparison test was used in (B).

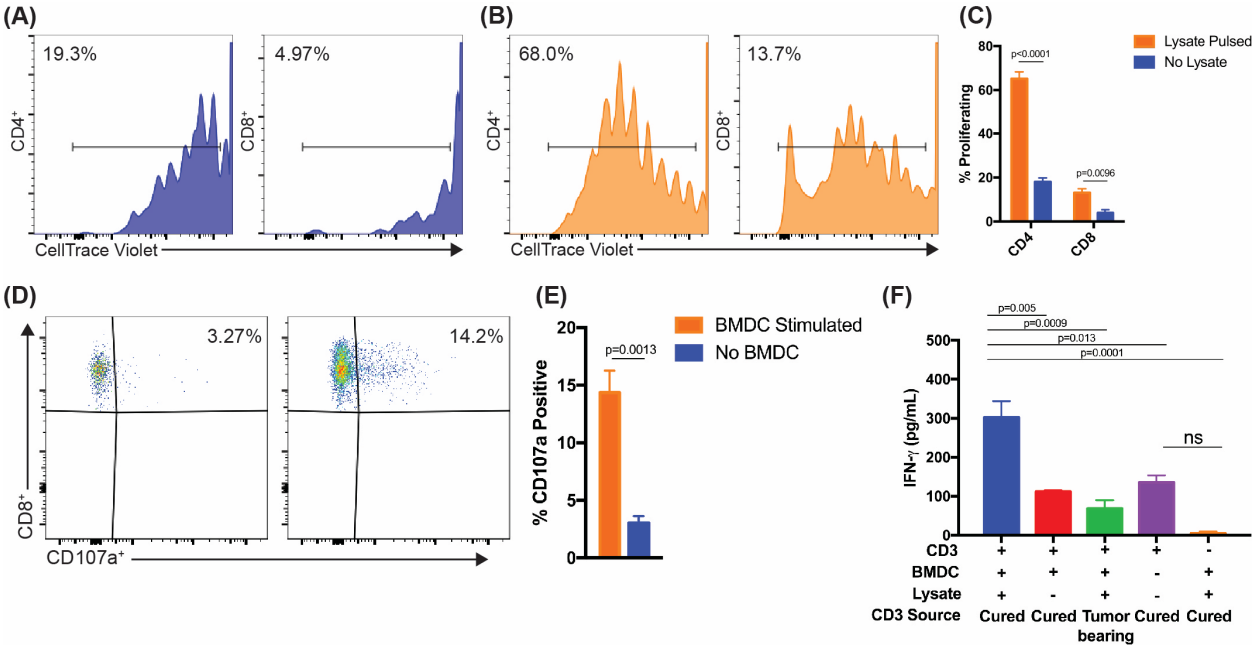

Figure 3.9: ΔF4LΔJ2R activates immune responses in rats bearing AY-27 bladder tumors. **(A-C)** T-cell proliferation after co-culturing with bone marrow derived dendritic cells (BMDC). $CD4^+$ and $CD8^+$ cells, isolated from controls or cured and protected rats (post-challenge), were co-cultured with BMDCs and proliferation assayed with CellTrace Violet. The representative plots show $CD4^+$ and $CD8^+$ T-cell proliferation after co-culture with either mock-pulsed (**A**) or with tumor-lysate-pulsed BMDCs (**B**). Panel (**C**) shows the percentage of $CD4^+$ and $CD8^+$ T-cell that proliferated in response to BMDC stimulation (n=2-3 independent animals). **(D and E)** *Ex vivo* upregulation of CD107a by $CD8^+$ T-cells from challenged rats. (**D**) $CD3^+$ cells were incubated +/- BMDCs for 1 hr in the presence of anti-CD107a antibody, incubated for 5 hr with monensin and brefeldin A, and then stained with anti-CD4 and anti-CD8 antibodies. Events were gated for viable $CD8^+$ T-cells. Panel (**E**) shows the percentage of $CD107a^+$ $CD8^+$ T-cells +/- BMDC stimulation (n=4 independent animals). **(F)** IFN-γ released after 24 hr co-culture of $CD3^+$ cells with BMDCs. **Data Information**: Mean ± SEM is shown. Two-tailed Student's t-test was used in (C) and (E). Two-way ANOVA followed by Tukey's multiple comparison test was used in (F).

following stimulation with lysate-pulsed BMDCs (**Figure 3.9D and E**). These stimulated $CD3^+$ cells also exhibited elevated secretion of IFN-γ (**Figure 3.9F**) and killed AY-27 tumor cells, but not normal RK3E (F344 Fischer rat kidney) or N60 fibroblast cells (**Figure 3.10**). Significantly, $CD3^+$ cells from AY-27-tumor-bearing rats that had never been exposed to VACV could not kill AY-27 cells. Collectively these data show that VACV treatment generated a durable tumor-antigen-specific cytotoxic T-cell response in the AY-27 rat model.

3.3.3 VACV can replicate in primary tumor cell cultures and in tumor explants ex vivo. We also examined whether ΔF4L and/or ΔF4LΔJ2R VACV could replicate in human bladder cancers in either primary cell cultures or tumor explants. Explanted tissues from a low-grade T1 tumor (UCKP-6), a high grade T2+ tumor (UCKP-4), and normal urothelium, were infected with 10^6 PFU of each VACV, and replication detected using a virus-encoded mCherry reporter (**Figure 3.11**). In the low-grade tumor, the ΔF4LΔJ2R and ΔJ2R VACVs produced nearly identical mCherry signals, while ΔF4L VACV produced a much lower signal (**Figure 3.11A and B**). In high-grade tissues, all viruses produced nearly identical mCherry signals (**Figure 3.11C and D**). All viruses had minimal fluorescence in normal urothelium (**Figure 3.11A and B**). We used the same low- and high-grade tumor samples to establish monolayer cell cultures (**Figure 3.11E**). The ΔF4LΔJ2R VACV grew to the same level as ΔJ2R VACV in both low- and high-grade primary tumor cells, whereas the ΔF4L VACV grew more poorly in the low-grade UCKP-6 culture, just as was seen in the tissue explants (**Figure 3.12**). Collectively, these data support the hypothesis that the ΔF4LΔJ2R VACV could be used to treat both high- and low-grade bladder cancer.

3.3.4 ΔF4LΔJ2R VACV clear patient-derived xenografted (PDX) bladder tumors. The ΔF4LΔJ2R VACV was further examined in a PDX model of bladder cancer in NSG mice. The PDX tumor was derived from a primary high-grade T3b urothelial cell carcinoma. Animals were

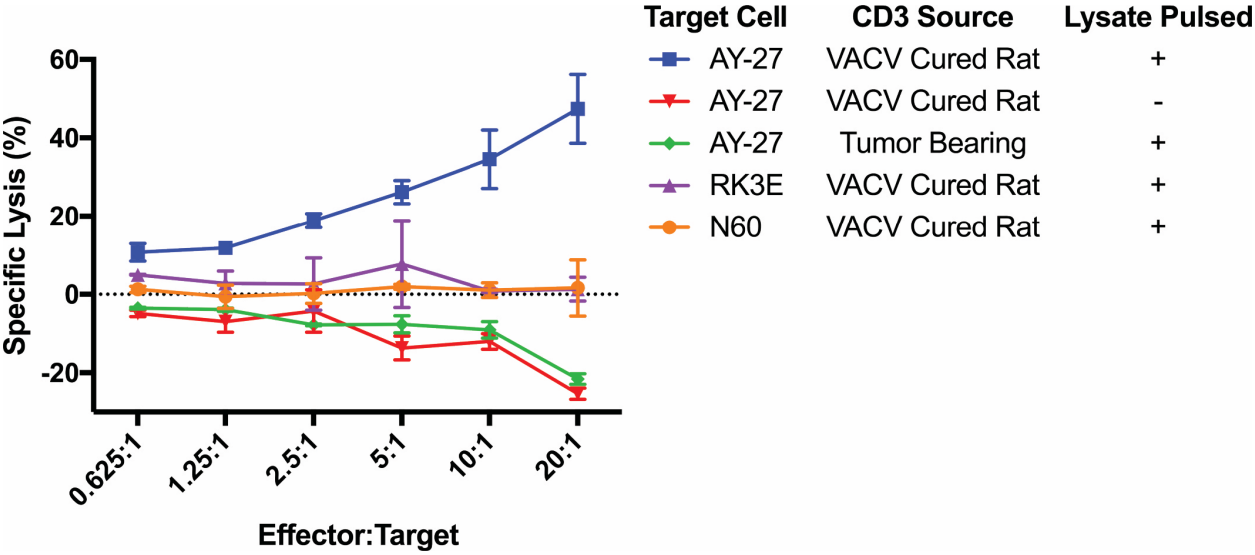

Figure 3.10: Tumor specific cytotoxic T-cells are generated after ΔF4LΔJ2R VACV treatment. CD3+ T-cells were activated *ex vivo* by 6 days of co-culture with tumor-lysate-pulsed BMDCs. The ^{T} cells were then incubated for 18 hr with 10,000 target cells and at different effector to target ratios. Lysis was determined by LDH assay.

Data Information: Mean ± SEM is shown. Data represent n=2-3 independent experiments, each performed in duplicate.

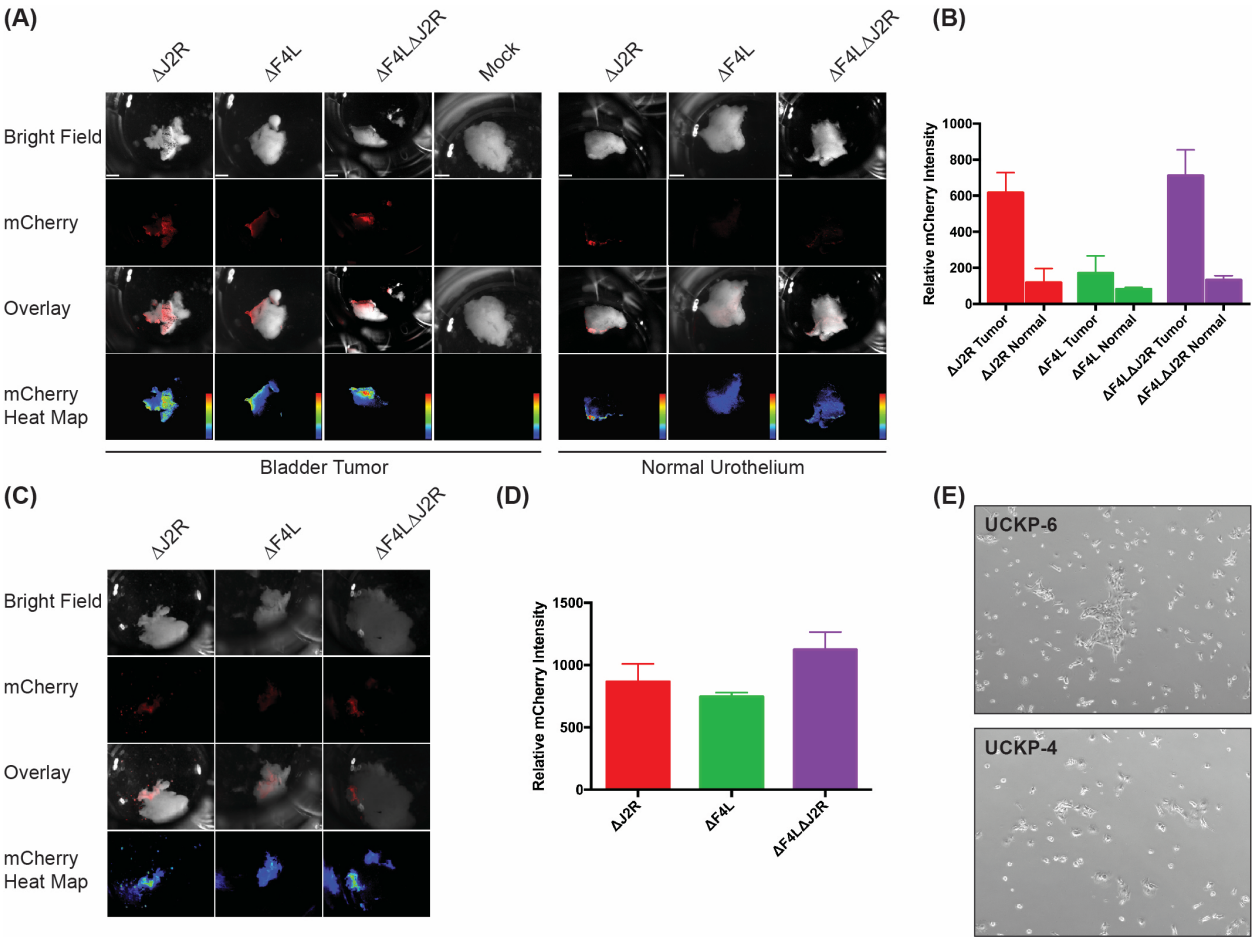
(A)
ΔJ2R
ΔF4L
ΔF4LΔJ2R
Mock
ΔJ2R
ΔF4L
ΔF4LΔJ2R
Bright Field
mCherry
Overlay
mCherry Heat Map
Bladder Tumor
Normal Urothelium
(B)
Relative mCherry Intensity
1000
800
600
400
200
0
ΔJ2R Tumor
ΔJ2R Normal
ΔF4L Tumor
ΔF4L Normal
ΔF4LΔJ2R Tumor
ΔF4LΔJ2R Normal
(C)
ΔJ2R
ΔF4L
ΔF4LΔJ2R
Bright Field
mCherry
Overlay
mCherry Heat Map
(D)
Relative mCherry Intensity
1500
1000
500
0
ΔJ2R
ΔF4L
ΔF4LΔJ2R
(E)
UCKP-6
UCKP-4

Figure 3.11: VACV infects and selectively replicates in primary bladder tumor tissue. (A) Viruses encoding mCherry fluorescent protein were used to infect primary low grade T1 (UCKP-6) and normal urothelial tissue samples from patients undergoing transurethral resection of bladder tumors. Tissues were infected with 10^6 PFU of the indicated viruses using buffered saline as a negative control (mock). The images from top to bottom represent a white light tissue image, mCherry signal, an overlay, and a heat map image showing mCherry expression, respectively (scale bar = 1 mm). **(B)** Quantification of the mCherry expression in panel (A) at 24 hr post-infection. Mock-infected cells were used as background correction. **(C)** *Ex vivo* infection of high grade T2 (UCKP-4) bladder tumor as in (A). **(D)** Quantification of the mCherry expression in panel (C) at 24 hr post-infection. **(E)** Representative (4x) microscope pictures of the uninfected UCKP-4 and UCKP-6 primary cell cultures used in (F).

Data information: Quantification in (B) and (D) shows the mean mCherry signal intensity (value per pixel) over the area of a given tumor sample. Data are shown as the mean ± SEM of these intensities over the tumor area.

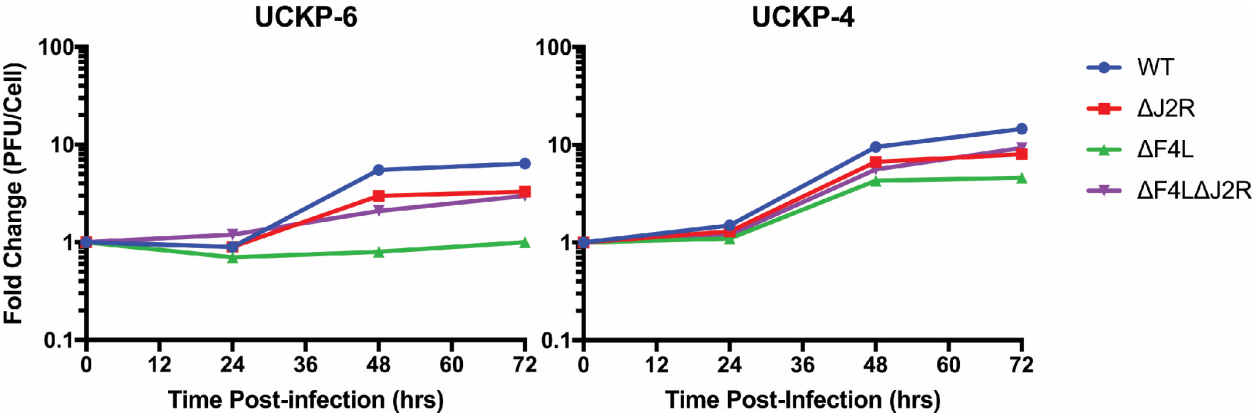

Figure 3.12: ΔF4LΔJ2R VACV maintains replication properties in primary bladder tumor cultures. Growth of the indicated VACV strains in UCKP-4 primary human bladder cancer cultures. The cells were infected at 0.03 PFU/cell, harvested at the indicated times, and titered on BSC-40 cells.

Data Information: Data represents single lysates titered in duplicate.

treated by intratumoral injection with 3 doses of $1x10^6$ PFU of live ΔF4LΔJ2R VACV, UV-inactivated virus, or PBS. ΔF4LΔJ2R VACV treatments significantly increased survival when compared to the UV-inactivated and PBS controls (**Figure 3.13A**). Importantly, all mice treated with ΔF4LΔJ2R VACV were completely cured of their tumors as determined by caliper measurements (**Figure 3.13B**) and continued to gain weight throughout the experiment (**Figure 3.13C**).

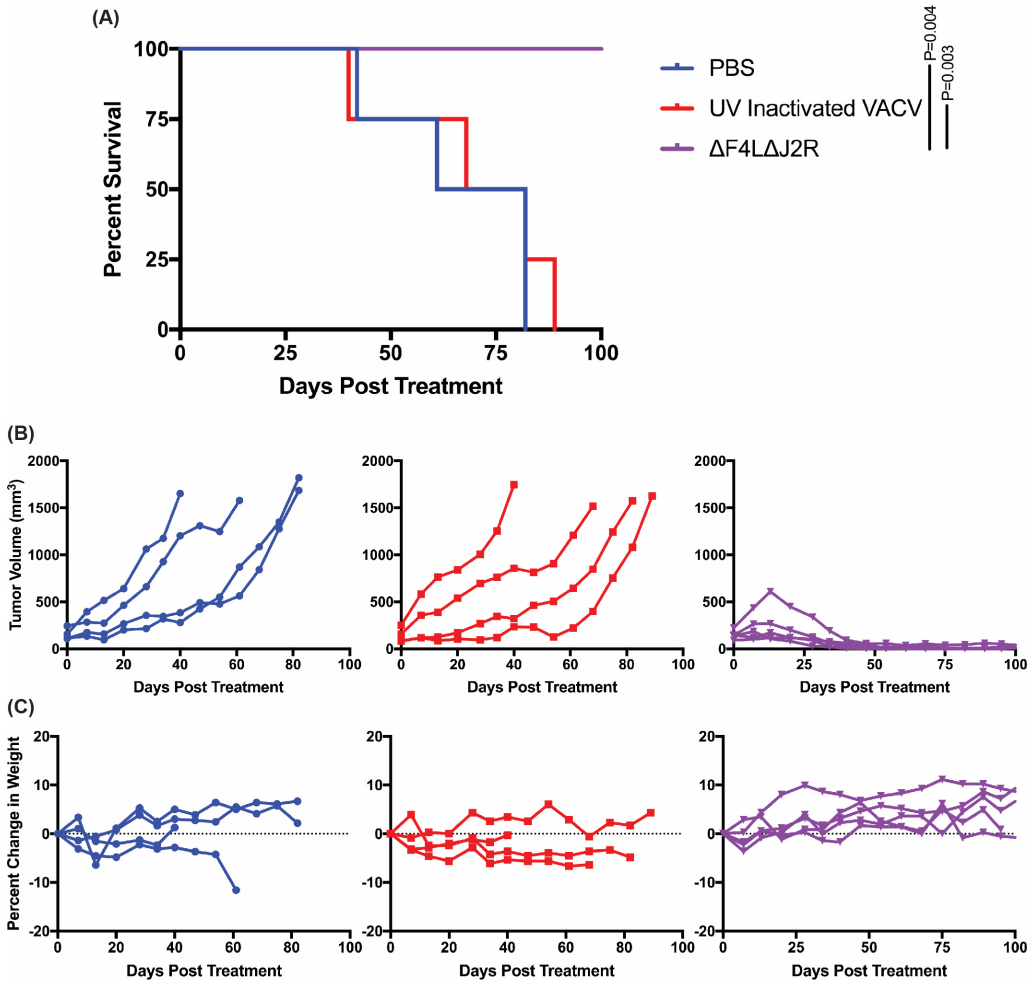

Figure 3.13: ΔF4LΔJ2R VACV safely and effectively clears human patient-derived xenografts (PDX) in immunocompromised mice. Primary bladder cancer tumors (stage T3b) we implanted, then subsequently passaged twice, in NSG mice. When tumor volumes reached approximately 150 mm^3, mice were randomized, and then intratumorally injected with $1x10^6$ PFU of UV inactivated or ΔF4LΔJ2R VACV, or PBS on days 1, 4, and 7. **(A)** Overall survival of NSG mice bearing flank tumors following treatment with the indicated viruses (n=4-5 mice per group). **(B)** Growth of individual virus-treated PDX tumors following virus treatment. **(C)** Analysis of individual animal body weights plotted as mean change in body weight relative to day 1.

Data Information: Animal survival was analyzed by log-rank (Mantel–Cox) test in (A).

3.4 DISCUSSION

Bladder cancer has not received much attention as a target for clinical trials of oncolytic virotherapy [reviewed in [134,178]]. Currently the most advanced clinical trial is one using CG0070, a conditionally replicating Ad. CG0070 has completed a phase I trial [221] and is presently being evaluated in patients with high-risk NMIBC who have failed BCG and refuse a cystectomy. However, the efficacy of this treatment is yet to be determined. It is interesting to note that in 2001, four patients with MIBC were treated with smallpox vaccine (Dryvax) intravesically before cystectomy. Three out of the four patients remained disease-free after 4 years, which highlights the potential of VACV as a durable treatment for bladder cancer [286]. It is difficult to judge whether one could perform such a study today using the WT Dryvax virus, but these intriguing results suggest that a VACV modified to enhance tumor specificity and reduce virulence might offer a superior therapy for bladder cancer.

Our VACVs were evaluated in the AY-27 immune-competent orthotopic rat model of bladder cancer. AY-27 tumors resemble high-grade human urothelial cell carcinoma [297,298]. Oncolytic reovirus was previously tested in this model, where it proved more effective and less toxic than BCG [232]. In the current study, we saw that all rats treated with live VACV showed a reduction in tumor size, with complete tumor clearance in the majority of animals, and a significant increase in survival relative to the controls. One caveat with the AY-27 model is that up to 30% of the tumors have been reported to invade the muscle by day 6 [297,298]. While all three live VACV treatments produced statistically similar outcomes, it is interesting to note that regular monitoring of tumors by cystoscope showed that some of the rats treated with ΔJ2R VACV had relapsed and this was not seen in rats treated with the *F4L*-deleted VACVs. The ΔJ2R VACV-treated animals

had significantly higher levels of neutralizing antibodies suggestive of a more robust anti-viral, and thus possibly a more oncolysis-limiting, response.

Outside of the previously cited studies, there has been little other pre-clinical work with OVs in immune-competent bladder cancer models. Fodor *et al*. studied a p53-expressing *J2R*-deleted VACV in an orthotopic MB49 immune-competent mouse model and obtained three long term survivors out of 9 treated animals [285]. OncoVEX$^{GALV/CD}$, a HSV-1 engineered to express cytosine deaminase and a fusogenic glycoprotein, was tested in the AY-27 rat bladder cancer model [200] and caused a significant reduction in tumor volume. Unfortunately, in neither study was there any further investigation to establish whether treatment generated an anti-tumor immune response.

As in the xenograft studies, the two *F4L*-deleted VACVs proved highly tumor-selective in the rat AY-27 model. In contrast, ΔJ2R VACV was detected in the lungs, kidneys, and ovaries in a subset of animals, although spread was not associated with overt toxicity. The ovaries consistently had the second highest levels of ΔJ2R VACV after the tumor and we also saw what appeared to be ovarian cysts in multiple mice and rats. Other *J2R*-deleted VACVs are reported to replicate in normal mouse tissues, including the ovaries where they can cause pathology and sterility [314-316].

All rats that remained tumor-free through day 125 (as determined by cystoscopy) exhibited anti-tumor immunity as shown by tumor rejection upon challenge. *In vitro* assays performed 100 days after challenge confirmed the presence of long lasting tumor-specific $CD8^+$ T cells in all cured ΔF4LΔJ2R-treated rats (other cured animals were not tested for CD8+ T-cells). It is notable that these tumor-specific cytotoxic T-lymphocytes were only detected in animals that had also been exposed to live virus. Surprisingly, we know of no clear evidence that BCG can induce a

protective anti-tumor immune response [92,317]. If BCG treatment is not also generating anti-tumor immunity, it could explain the high recurrence rate in BCG-treated patients.

As an additional experiment, we showed that primary human bladder cancer tissues, in the form of either monolayers or as tumor fragments, could support the replication of both ΔJ2R and ΔF4LΔJ2R VACV *ex vivo* to a much greater degree than was seen in normal urothelium. This effect is similar to what has been reported for Pexa-Vec (JX-594) using rectal, endometrial, and colon cancer fragments along with adjacent normal tissues [290]. The fact that ΔF4LΔJ2R VACV also grew selectively in primary explanted human bladder cancer tissues provides some promise that these pre-clinical results might also be seen in patients treated with oncolytic VACV.

Finally, we developed a PDX model of high-grade T3b urothelial cell carcinoma. PDX models have been show to maintain characteristics of the original tumor in both genetics and morphology [318,319]. ΔF4LΔJ2R VACV cleared 5/5 PDX tumors while UV-inactivated and PBS treated tumors continued to grow. Interestingly, Pan *et al.* [304] recently characterized several bladder cancer PDX models and subsequently treated animals with gemcitabine, cisplatin, or a combination of the two. Although they could delay tumor growth in many of their models, they were unable to completely clear tumors from the mice. Our results, although only in a single model, provide encouraging evidence for clinical evaluation of a ΔF4LΔJ2R VACV.

In conclusion, these results suggest that NMIBC could be a highly suitable target for oncolytic treatment with a WR-based ΔF4LΔJ2R VACV. From a practical perspective, intravesical bladder delivery offers a way of delivering high doses of virus directly to the tumor while also helping to limit systemic spread. ΔF4LΔJ2R VACV showed an impressive safety profile, selectively infecting both established cell lines, primary cell cultures, and primary human bladder cancer tissues. ΔF4LΔJ2R VACV treatment of AY-27 immune-competent rat model induced an

anti-tumor immunity. Although patients with immune deficiencies and BCG-refractory cancers would be ideal candidates for this therapy, in the longer-term oncolytic ΔF4LΔJ2R VACV might offer a more attractive replacement for BCG and potentially reduce the need for surgical management.

CHAPTER 4 - ΔF4LΔJ2R-DELETED VACV AS A TREATMENT FOR BCG REFRACTORY BLADDER CANCER

PREFACE

This chapter is an original work by Kyle Potts. No part of this thesis has been previously published.

Contributions:

I designed and performed experiments, analyzed the data, and prepared the figures for this chapter. Dr. Chad Irwin designed and constructed the viruses used in these studies. Megan Desaulniers assisted in animal experiments. Brianna Kurtz (undergraduate project student) performed the experiments shown in Figure 4.5 and 4.6 as well as some of the replicates in Figure 4.2. Kalutota Samarasinghe (undergraduate summer and project student) performed most of the replicate experiments shown in Figure 4.12. I performed flow cytometry at the University of Alberta, Faculty of Medicine and Dentistry Flow Cytometry Facility, with assistance in experimental design and analysis from Dr. Aja Rieger. Dr. David Evans, Dr. Mary Hitt, and Dr. Ronald Moore provided guidance in experimental design, data interpretation, and manuscript preparation.

4.1 INTRODUCTION

One of the most significant challenges in the treatment of bladder cancer is management of BCG failure. Up to 40% of patients initially fail or stop responding to BCG therapy [320]. There is an increased risk of disease progression in patients that fail frontline BCG therapy. These patients have very few effective treatment options and cystectomy remains their standard of care [104]. This chapter examines whether VACV can be used to treat NMIBC and in particular, bladder cancer that is refractory to BCG therapy.

Recently, Redelman-Sidi *et al.*[80] found that the ability of bladder cancer cells to take up BCG is determined by macropinocytosis activity. It was also shown by them and others that uptake is a result of oncogenic activation of the Rac1-Cdc42-Pak1 signaling pathway [80,82] downstream of Ras which is commonly activated in bladder cancer cells. Unlike many other viruses, VACV can utilize multiple modes of entry, including fusion with the cellular plasma membrane [248] via a low-pH-dependent endosomal route [249] or through macropinocytosis [250].

Previous reports have shown that knockout of Pak1 from mouse embryonic fibroblasts had a negative impact on VACV replication and spread [321], here we show that Pak1 knockdown sufficient to decrease BCG uptake has little to no effect on VACV production in bladder cancer cells. We wish to further investigate the effect of reduced Pak1 activity on VACV production. Our objective is to test whether ΔF4LΔJ2R oncolytic VACV can be effective in treating bladder cancer that is resistant to BCG due to poor BCG uptake through macropinocytosis. We suggest that blocking macropinocytosis should have little impact on VACV uptake since VACV can use alternative fusion pathways to infect tumor cells.

Here we describe results showing that an oncolytic VACV is effective at replicating in and killing bladder cancer cells with induced BCG resistance. We also find that treatment with

ΔF4LΔJ2R VACV is superior to BCG in a rat model of bladder cancer. These findings highlight the prospects for using the ΔF4LΔJ2R VACV in treating bladder cancer that has become resistant to BCG treatment.

4.2 MATERIALS AND METHODS

4.2.1 VAC viruses. Viruses were generated as described in Chapter 2.2.2 Materials and Methods.

4.2.2 Lenti and retroviruses. Both the scrambled shRNA lentivirus and retrovirus targeted the same sequence. The scrambled shRNA retrovirus plasmid was purchased from OriGene (see below). The lentivirus scrambled shRNA plasmid was generated as follows. The shRNA oligo 5'-CCGGGCACTACCAGAGCTAACTCAGATAGTACTCTCGAGTACTATCTGAGTTAGCTC TGGTAGTGCTTTTTG -3' was annealed with the reverse oligo: 5'- AATTCAAAAAAGAGCT GCTACAGCATCAATTCCTCGAGGAATTGATGCTGTAGCAGCTCCCGG -'3.

Next the plasmid pLKO.1 (Addgene #10878) was digested with *Age*I and *Eco*RI (Thermo Fisher) restriction enzymes. The resulting 7 kbp band was purified using the Qiaquick gel extraction kit (Qiagen). The "shRNA" duplex and the digested pLKO.1 vector were ligated with NEB T4 DNA ligase and used to transform chemically competent Stbl3 cells (Thermo Fisher). Ampicillin-resistant colonies were grown overnight and purified using HiSpeed Plasmid Midi Kit (Qiagen). Correct recombinants were identified by digestion with EcoRI and NcoI (Thermo Fisher) restriction enzyme. This plasmid, as well as other plasmids used to construct shRNA vectors, was purified with HiSpeed Plasmid Midi Kit (Qiagen).

The lentivirus plasmid targeting human Pak1 (TRCN0000197010, from The RNAi Consortium at the Broad Institute, gift of Dr. Maya Shmulevitz), had the sequence 5'-

CCGGGAGCTGCTACAGCATCAATTCCTCGAGGAATTGATGCTGTAGCAGCTCTTTTT TG -3'.

All lentiviruses targeting human Pak1 sequences (or a scrambled control sequence) were generated as described by Campeau *et al.* [322]. Briefly, 293T cells were plated in 100 mm dishes to be 50-60% confluent at the time of transfection. 15 μg of shRNA lentiviral vector plasmid, 15 μg pMDLg/pRRE (Addgene #12251), 6 μg pRSV-REV (Addgene #12253), and 3 μg pMD2.G (Addgene #12259) were mixed with OPTI-MEM (Thermo Fisher) to a final volume of 1.5 mL. 1.5 mL of a 1:50 dilution of Lipofectamine 2000 (Thermo Fisher) in OPTI-MEM was added to the plasmid mixture. The mixture was incubated at room temperature for 25 min, then added to cells plated in 7 ml of OPTI-MEM. After incubating at 37^{o}C for ~6 hrs the medium was replaced with 7 mL of DMEM medium supplemented with 10% fetal bovine serum (FBS), 2 mM L-glutamine, 100 U/mL penicillin, 100 U/mL streptomycin, and 0.25 μg/mL Fungizone® (Gibco). Viral supernatant was collected 48 hr and 72 hr post-transfection (7 mL medium was added back after collecting at 48 hrs). Supernatants were filter through a low protein binding PVDF 0.44 μM filter (Millipore) and this crude vector stock was stored at -80C.

Retrovirus shRNA expression plasmids (pRS-based with MMLV LTRs) were obtained from OriGene (#TR710002). The shRNA targeting sequences were: rat Pak1 shRNA sequence B, 5'- TTGGATGGCACCTGAAGTTGTGACACGCA -3', rat Pak1 shRNA sequence D, 5'-GATTGGACAAGGTGCTTCAGGCACAGTGT -3', scrambled shRNA sequence, 5'-GCACTACCAGAGCTAACTCAGATAGTACT -3'. To produce retroviruses, the same procedure as above was used to co-transfect 6 μg of shRNA vector plasmid, 6 μg pUMVC (Addgene #8449), and 1 μg pCMV-VSV-G (Addgene #8454). Crude vector stock was prepared as described above.

4.2.3 BCG. GFP-expressing BCG (BCG-GFP) was a generous gift of Drs. Gil Redelman-Sidi and Michael Glickman (MSKCC) and has been previously described (Redelman-Sidi *et al.*, 2013) [80]. BCG-GFP was grown in polystyrene roller bottles (Corning) at 37^{o}C in Middlebrook 7H9 medium (Sigma-Aldrich) supplemented with 0.5%bovine serum albumin (Sigma-Aldrich), 0.2% dextrose (Sigma-Aldrich), 0.085% NaCl, 0.5% glycerol (Thermo Fisher), 0.05% Tween 80 (Thermo Fisher), and 20 μg/mL kanamycin (Sigma-Aldrich). BCG-GFP was pelleted, washed in PBS, and then suspended in PBS with 25% glycerol, then frozen at -80^{o}C. BCG-GFP titers were determined by spectrophotometric absorbance at 600 nm with 1 OD600 = 5x10^{8} colony forming units (CFU)/mL [80].

4.2.4 Cell lines. Cell culture methods were performed as described in Chapter 2.2.1 Materials and Methods.

4.2.5 Construction of Pak1 knockdown cell lines. For lenti- and retrovirus transduction, target cells were infected with 1 mL crude undiluted vector stock (from *4.2.2*) containing 6 mg/mL of polybrene (Thermo Fisher) is added per well of 6-well plate. Transduction efficiency was determined in a parallel infection with a GFP-expressing vector. In some cases, infected plates were centrifuged at 20^{o}C for 20 min and 1000 x g to increase efficiency of infection. Infected cultures were incubated at 37^{o}C. Approximately 18 hrs after infection, the infection medium was aspirated, cells were rinsed twice with PBS, and fresh medium was added. Selection with puromycin (Thermo Fisher) at 1-3 μg/ml was started 72 hr post-infection. After 5 days of drug selection, the cells were single-cell-sorted into wells of a 96-well plate by FACS. Six to eight clones were expanded and assayed for BCG internalization.

4.2.6 IPA-3 treatment. IPA-3 [323,324] (Tocris) was dissolved in DMSO at 10 mg/mL and stored at -20^{o}C. Cells were pretreated with IPA-3 for 1 hr in the indicated medium, and drug was

kept in the medium for the duration of the experiment. Treatment with DMSO alone was used as a control.

4.2.7 In vitro VACV infection. VACV infections were performed as described in Chapter 2.2.4 Materials and Methods.

4.2.8 In vitro BCG infection. BCG infections were performed as described by Redelman-Sidi *et al*. [80]. Briefly, bladder cancer cells were washed and held in serum- and antibiotic-free medium for 1 hr prior to infection. A GFP-tagged Pasteur strain of BCG (gift of Drs. Redelman-Sidi and Glickman) was added at a MOI of 10 CFU/cell, then the cells and bacteria were incubated at 37^{o}C for 24 hrs. The plates were washed three times with PBS, three times with medium containing serum and antibiotics, and once with PBS. Next, the cells were detached with trypsin and the trypsin was inactivated with medium containing 10% FBS. Cells were centrifuged at 5^{o}C for 5 min and 300 x g then resuspended in FACS buffer (BioLegend) for analysis by flow cytometry.

4.2.9 Viability assay. The resazurin metabolic assay was performed as described in Chapter 2.2.5 Materials and Methods, and used to determine cytotoxicity in response to treatments.

4.2.10 Western blot analysis. Western blotting was performed as described in Chapter 2.2 Materials and Methods. The primary antibodies used for western blots included: Rabbit anti-Pak1 (Cell Signaling Technologies #2602) and rabbit anti-β-tubulin (Cell Signaling Technologies #2416). The secondary antibodies used for western blots included: 680LT donkey anti-rabbit (LICOR 926- 68023) and 800CW donkey anti-rabbit (LICOR 926-32214).

4.2.11 Flow cytometry. Cell suspensions were analyzed on LSR-Fortessa X20 flow cytometer (BD Biosciences) using the FACS DiVa software (BD Biosciences). Cell populations were gated on FSC-A and SSC-A and a single cell population was gated by using FSC-H and FSC-

A. GFP was detected on the FITC channel using a 488-nm laser. APC antibody was detected on the APC-Cy7 channel and excited with a 561-nm laser. To accurately gate around the population of interest, an empty channel (DAPI) was used. For BCG internalization assays, cells were either fixed with Fixation Buffer (BioLegend) in the dark for 20 min at room temperature, or fixed as above then permeabilized with Permeabilization Buffer (BioLegend) in the dark for 20 min at room temperature. Cells were then stained with a 1:100 dilution of rabbit anti-*mycobacterium tuberculosis* primary antibody (Abcam ab905) and 0.1 μg/10^6 cells goat anti-rabbit APC secondary (Abcam ab130805) antibody for 20 min at 4^{o}C. Cells were wash twice with at least 2 mL of Cell Staining Buffer (BioLegend) with centrifugation at 350 x g for 5 minutes. Cells were analyzed by flow cytometry. FlowJo (Version 10.2) was used to perform analysis.

4.2.12 Animal care and housing. All studies reported were conducted with the approval of the University of Alberta Health Sciences Animal Care and Use Committee in accordance with guidelines from the Canadian Council for Animal Care. Animals were housed with access to food and water *ad libitum* in ventilated cages (1-2 rats per cage) in a biosafety level 2 containment suite at the University of Alberta Health Sciences Laboratory Animal Services Facility.

4.2.13 In vivo AY-27 tumor model and treatments. Orthotopic AY-27 tumor implantation was previously described in Xiao *et al.* [297] as well as in Chapter 3 Materials and Methods. For VACV treatments, 3x10^8 PFU of UV-inactivated or live ΔF4LΔJ2R VACV were instilled into the bladder on each of days 6, 9, and 12 as described in Chapter 3.3.6. For BCG treatments, 3x10^6 CFU of UV-inactivated BCG-GFP, or live BCG-GFP were instilled into the bladder of on each of days 6, 9, 12, 15, 18, and 21 and left to in-dwelling for 1 hr. Rats were weighed weekly and tumor growth monitored by palpation.

4.2.14 Statistics. Data were analyzed using two-tailed Student's *t* test when comparing the means of two groups. ANOVA) was used when comparing multiple groups followed by Tukey's multiple comparison test. Significance analysis was performed by means of a one-way ANOVA followed by Tukey's HSD. Data for animal survival curves were analyzed by log-rank (Mantel-Cox) test. The numbers of animals in each experiment are indicated at the end of each figure legend. P-values are indicated within each figure.

4.3 RESULTS

4.3.1 Determining the number of GFP+ cells by flow cytometry is a valid method to measure internalization of BCG-GFP into bladder cancer cells. Our flow cytometry protocol was carried out with trypsinized cells, so much of the extracellularly bound BCG would likely be removed by trypsin prior to flow cytometric analysis. However, we wished to verify that the flow cytometry protocol used here accurately measures BCG internalization and not merely extracellular binding. Following our standard protocol for quantifying BCG uptake, bladder cancer cells were infected with BCG (Pasteur strain) expressing green fluorescent protein (BCG-GFP), and after 24 hr, the number of GFP+ cells were determined by flow cytometry (**Figure 4.1A and B**). To test whether BCG was bound to the cell surface or internalized, we used an anti-*Mycobacterium tuberculosis* antibody to specifically detect BCG in infected cells with and without cell permeabilization prior to antibody treatment. Following permeabilization, we detected internalized BCG (**Figure 4.1C and D**) at levels similar to that seen with GFP detection. In contrast, we did not see any indication of BCG surface binding (**Figure 4.1E and F**). Therefore, we conclude that it is valid to use GFP detection by flow cytometry as an indicator of BCG-GFP uptake.

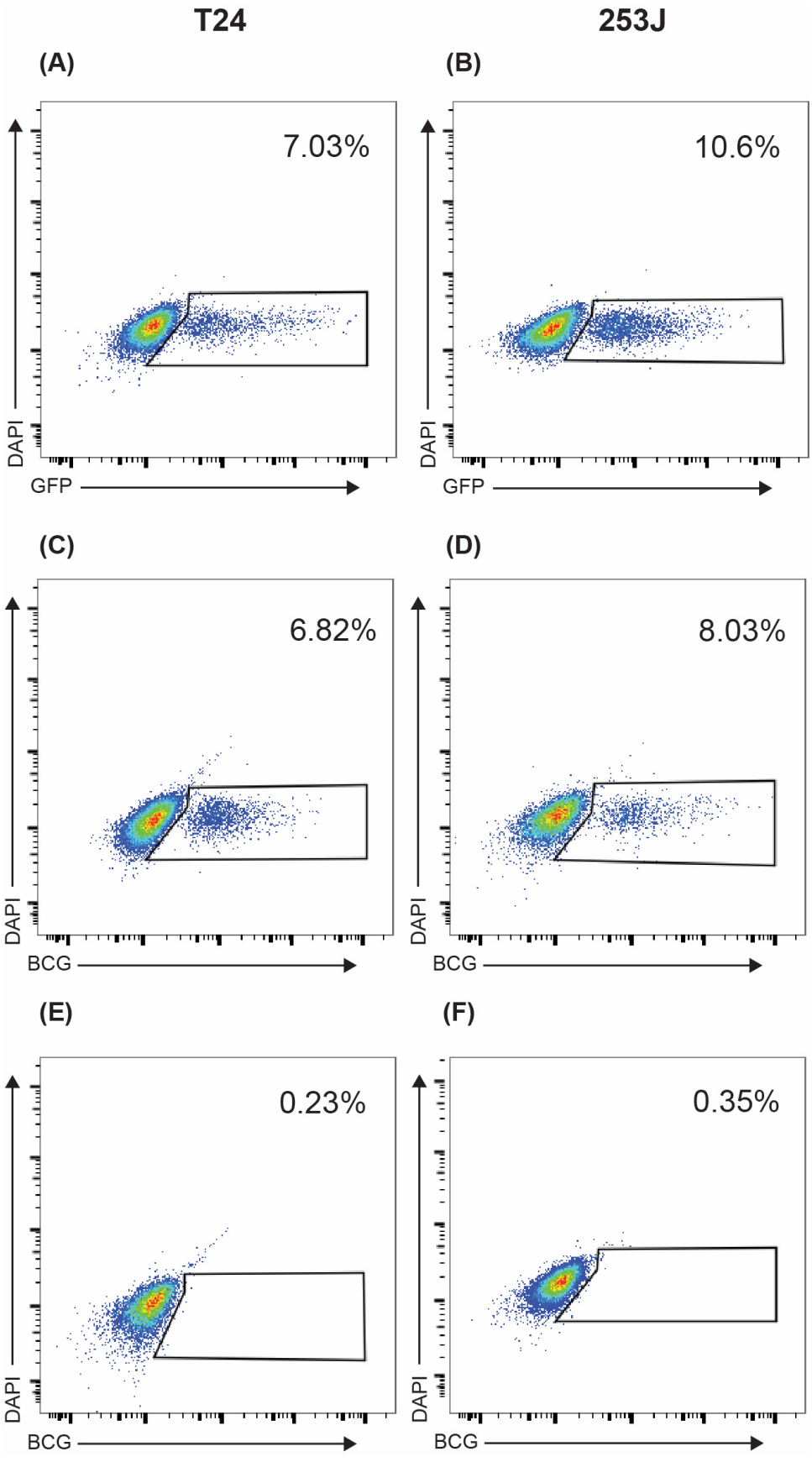
T24
253J
(A)
(B)
7.03%
10.6%
DAPI
GFP
(C)
(D)
6.82%
8.03%
DAPI
BCG
(E)
(F)
0.23%
0.35%
DAPI
BCG

Figure 4.1: BCG is internalized by bladder cancer cells. GFP-tagged Pasteur strain of BCG was added to subconfluent T24 or 253J human bladder cancer cells at an MOI of 10 CFU/cell, then the cells and bacteria were incubated in serum- and antibiotic-free medium for 24 hrs. The plates were washed three times with PBS, three times with medium containing serum and antibiotics, and once with PBS. Cells were detached from plates using trypsin, then analyzed by flow cytometry. **(A and B)** BCG binding/uptake by human bladder cancer cell lines, using GFP as a marker. The numbers show the percentage of GFP-positive events out of total events. **(C and D)** BCG uptake by human bladder cancer cells following permeabilization and treatment with BCG-specific anti-*Mycobacterium tuberculosis* antibody. **(E and F)** BCG binding to the surface of human bladder cancer cell lines following treatment with BCG-specific antibody without permeabilization. In all cases the DAPI channel was used as an empty channel and the gates were set based on uninfected cells.

4.3.2 Bladder cancer cells have different abilities to take up BCG and these do not correlate with VACV sensitivity. To stratify our panel of bladder cancer cell lines based on their ability to internalize BCG, we exposed the cells in culture to BCG-GFP, and measured uptake by flow cytometry (**Figure 4.2**). These studies showed that T24, 253J, HTB-3, and AY-27 cells supported BCG uptake while the RT112-luc and MB49 cells were resistant to BCG uptake (**Figure 4.2**). Nevertheless, as we have shown previously, our VACVs replicated in cell lines from both BCG-sensitive and resistant subtypes (**Figure 2.2**).

4.3.3 ΔF4LΔJ2R VACV effectively kills primary bladder tumor cultures that do not take up BCG. We next examined BCG uptake in primary cultures prepared from NMIBC low-grade Ta (UCKP-16) and low-grade T1 (UCKP-17) bladder tumors. Although both primary cultures were resistant to BCG (**Figure 4.3A**), they still were killed by VACV and for the most part supported virus replication (**Figure 4.3B and C**). Cytotoxicity of primary cultures was similar to that seen in established cell lines (**Figure 2.3**) despite the lower levels of virus replication, especially notable in UCKP-16. Interestingly, while both *F4L*-deleted VACVs replicated to lower levels than WT and ΔJ2R viruses (**Figure 4.3B**), ΔF4LΔJ2R was just as effective at killing these two primary bladder cancer samples as WT and ΔJ2R VACV were. Overall, these results highlight the potential for using oncolytic ΔF4LΔJ2R VACV, to treat BCG-refractory bladder cancer.

*4.3.4 IPA-3 inhibits Pak1 autophosphorylation***.** IPA-3 has been shown to be a highly selective, non-ATP-competitive allosteric inhibitor of Pak1 [323,324]. It was shown that IPA-3 prevents Cdc42-induced Pak1 autophosphorylation at amino acid residue T423 which results in inhibition Pak1 activity. Redelman-Sidi *et al.* have shown that IPA-3 inhibits BCG uptake. In order to confirm that IPA-3 is indeed inhibiting Pak1 we performed western blot analysis of total Pak1 as well as phospho-Pak1 (T423).

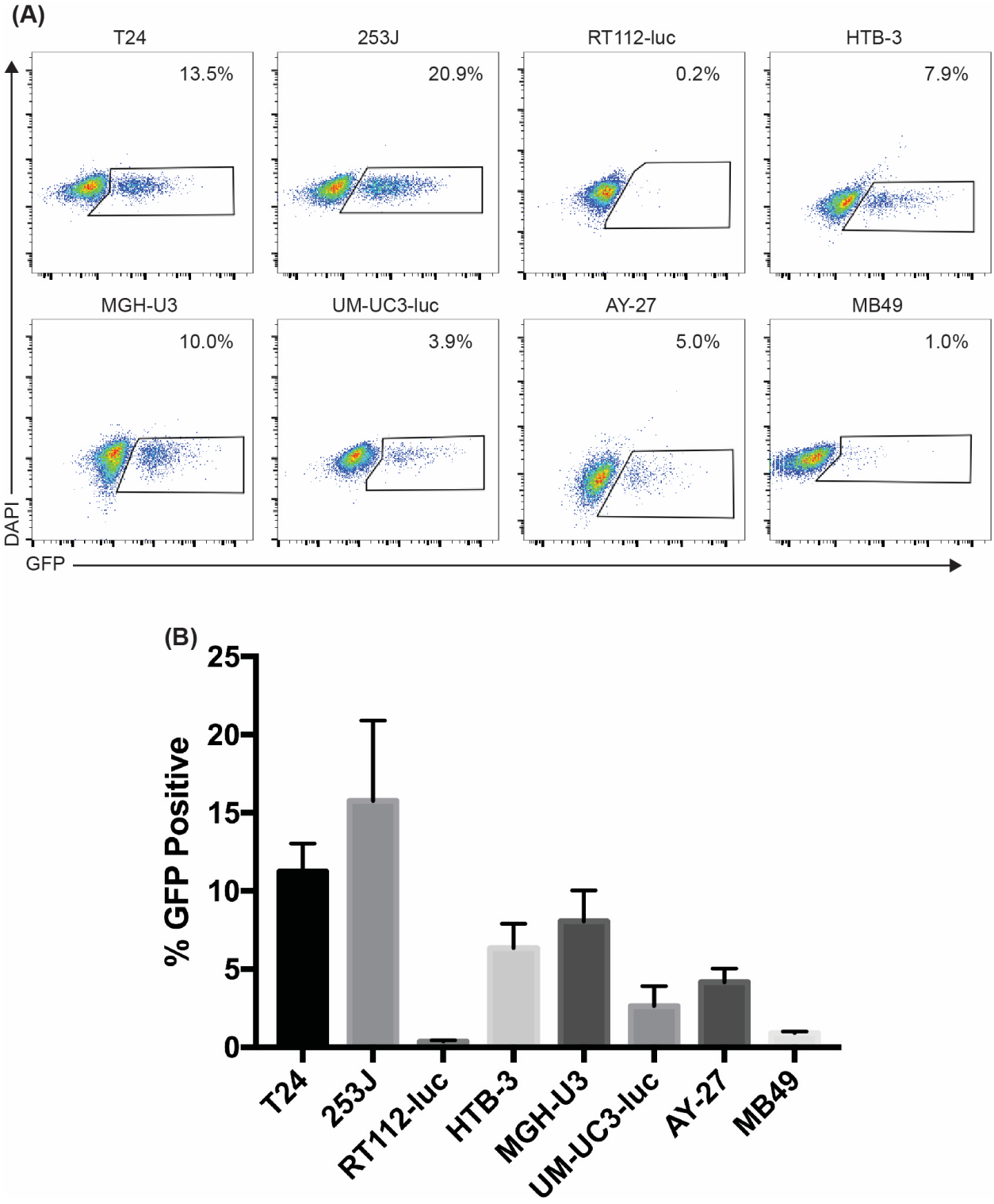
(A)
T24
253J
RT112-luc
HTB-3
13.5%
20.9%
0.2%
7.9%
MGH-U3
UM-UC3-luc
AY-27
MB49
10.0%
3.9%
5.0%
1.0%
DAPI
GFP
(B)
% GFP Positive
25
20
15
10
5
0
T24
253J
RT112-luc
HTB-3
MGH-U3
UM-UC3-luc
AY-27
MB49

Figure 4.2: Bladder cancer cells have different abilities to take up BCG. BCG uptake was measured in sub-confluent human bladder cancer cell lines, the rat bladder cancer cell line AY-27 and the murine bladder cancer cell line MB49-luc. **(A)** Cells were incubated with BCG-GFP in serum- and antibiotic-free medium for 24 hours then BCG uptake was measured by flow cytometry. The numbers show the percentage of GFP-positive events out of total events. DAPI was used as an empty channel and the gates were set based on uninfected cells. **(B)** Quantification of BCG-GFP uptake from (A).

Data Information: Mean ± SEM is shown. Data in (B) represent at least 2 independent experiments.

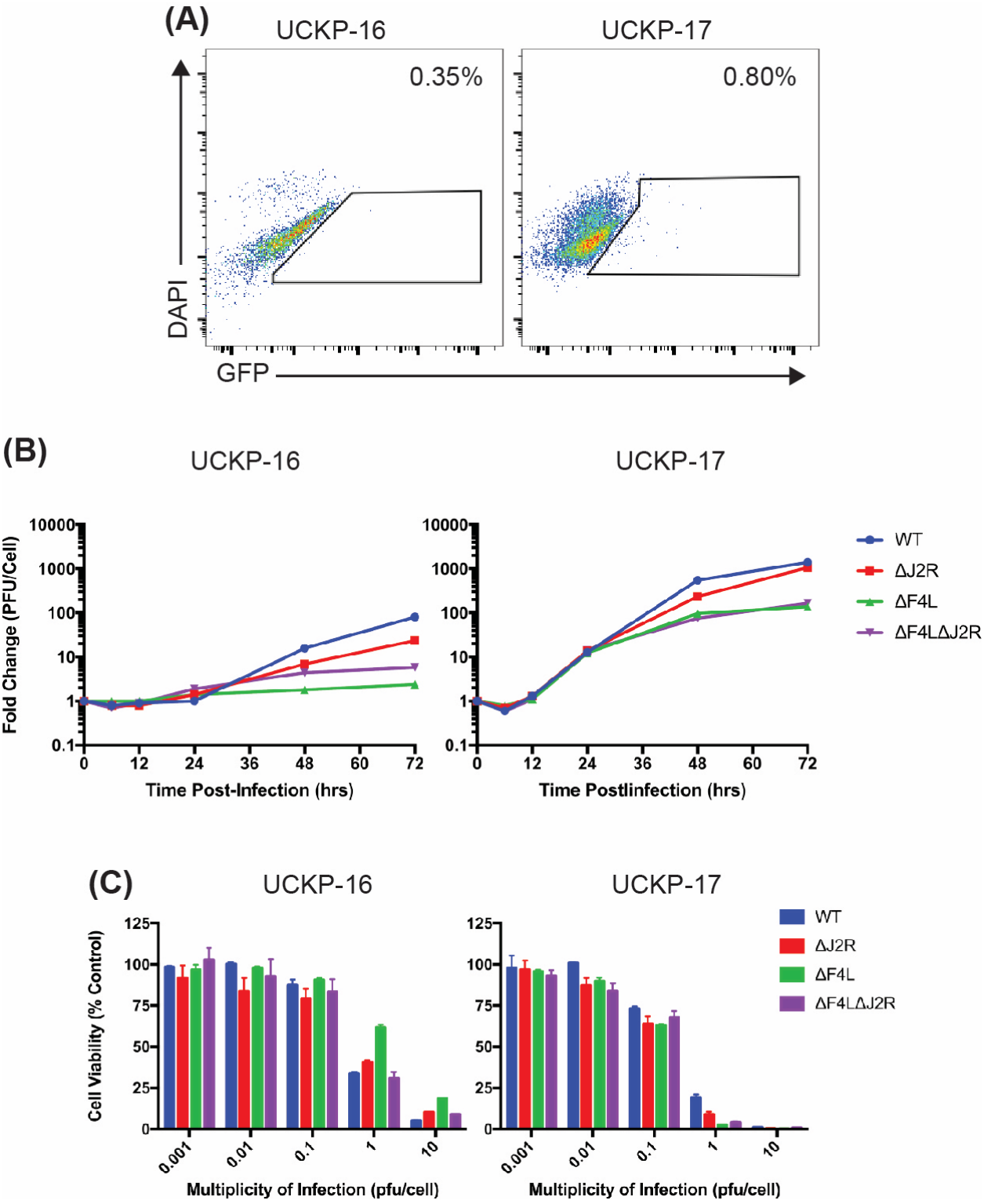
(A)
UCKP-16
UCKP-17
0.35%
0.80%
DAPI
GFP
(B)
UCKP-16
UCKP-17
Fold Change (PFU/Cell)
Time Post-Infection (hrs)
Time Postlinfection (hrs)
WT
ΔJ2R
ΔF4L
ΔF4LΔJ2R
(C)
UCKP-16
UCKP-17
Cell Viability (% Control)
Multiplicity of Infection (pfu/cell)
Multiplicity of Infection (pfu/cell)
WT
ΔJ2R
ΔF4L
ΔF4LΔJ2R

Figure 4.3: ΔF4LΔJ2R VACV effectively kills primary NMIBC cultures that do not take up BCG. **(A)** BCG uptake by primary bladder tumor cultures. UCKP-16 was derived from a low-grade Ta tumor and UCKP-17 was derived from a low grade T1 tumor. Cells were incubated with BCG-GFP for 24 hours then BCG uptake was measured by flow cytometry. The numbers show the percentage of GFP-positive events out of total events. DAPI was used as an empty channel and the gates were set based on uninfected cells. **(B)** Growth of the indicated VACV strains in sub-confluent primary human bladder tumor cultures *in vitro*. Cells were infected at an MOI of 0.03 PFU/cell, harvested at the indicated times, and titered on BSC-40 cells. **(C)** VACV killing of UCKP-16 and UCKP-17 cells. Sub-confluent cells were infected at the indicated MOIs (PFU/cell), cultured for 3 days, and assayed for viability with resazurin dye. Uninfected cells were used as control.

We found that 10 uM IPA-3 treatment decreased phospho-Pak1 (T423) levels at 24 hrs (**Figure 4.4**).

4.3.5 Pak1 inhibitor (IPA-3) decreases BCG uptake in bladder cancer cells and has little effect on VACV infectivity or replication. We first examined Pak1-dependent BCG uptake using a small molecule Pak1 inhibitor, IPA-3 [323,324]. T24 cells were pre-treated for 1 hr with DMSO or 10 μM IPA-3 in serum- and antibiotic-free medium. Cells were then incubated with BCG-GFP (in the presence of DMSO or IPA-3) then 24 hours later, BCG uptake was measured by flow cytometry. Treatment with Pak1 inhibitor resulted in a significant reduction in the uptake of BCG (**Figure 4.5A and B).** To determine whether Pak1 inhibition could alter VACV infection, cells were pre-treated with IPA-3 as above, then infected with 0.3 PFU/cell of ΔF4LΔJ2R VACV and cultured for 24 hours in the presence of drug. Control infections were carried out in parallel, treating with DMSO instead of IPA-3. The number of cells expressing virally encoded mCherry, a marker for infection, was then measured by flow cytometry (**Figure 4.6A and B**). Virus infection was significantly decreased in the IPA-3 treated cells compared to DMSO treated, although infectivity was still high (78% vs. 95%, respectively; p=0.0023). Interestingly, titers of WT and ΔF4LΔJ2R VACV after 24 hrs growth in sub-confluent T24 cells treated with 10 μM IPA-3 were not significantly different from those observed when infected cells were cultured in DMSO (p=0.075 and 0.14, respectively) (**Figure 4.6C**).

4.3.6 Pak1 knockdown reduces BCG uptake in bladder cancer cells. To further investigate the role of Pak1 we depleted Pak1 protein in T24 and 253J cells by lentiviral delivery of short hairpin RNA (shRNA) targeting Pak1. Control lines were generated using a scrambled shRNA vector. Knockdown was verified by western blotting (**Figure 4.7A and C**). Knockdown of Pak1, much like treatment with the inhibitor IPA-3, caused a dramatic reduction in BCG uptake

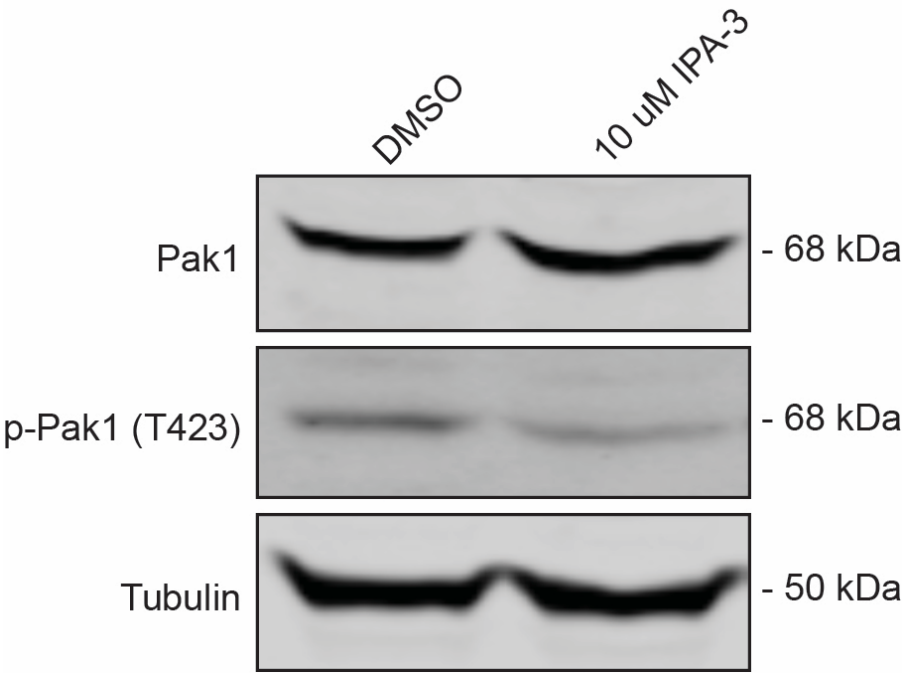

Figure 4.4: IPA-3 inhibits Pak1 autophosphorylation. Pak1 and T423-phospho-Pak1 expression in human T24 bladder cancer cells treated with IPA-3 or DMSO were examined by western blot analysis. β-tubulin is shown as a loading control. Equal amounts of total protein (30 μg) were assayed. The images were scanned using the LI-COR Odyssey scanner (LI-COR Biosciences).

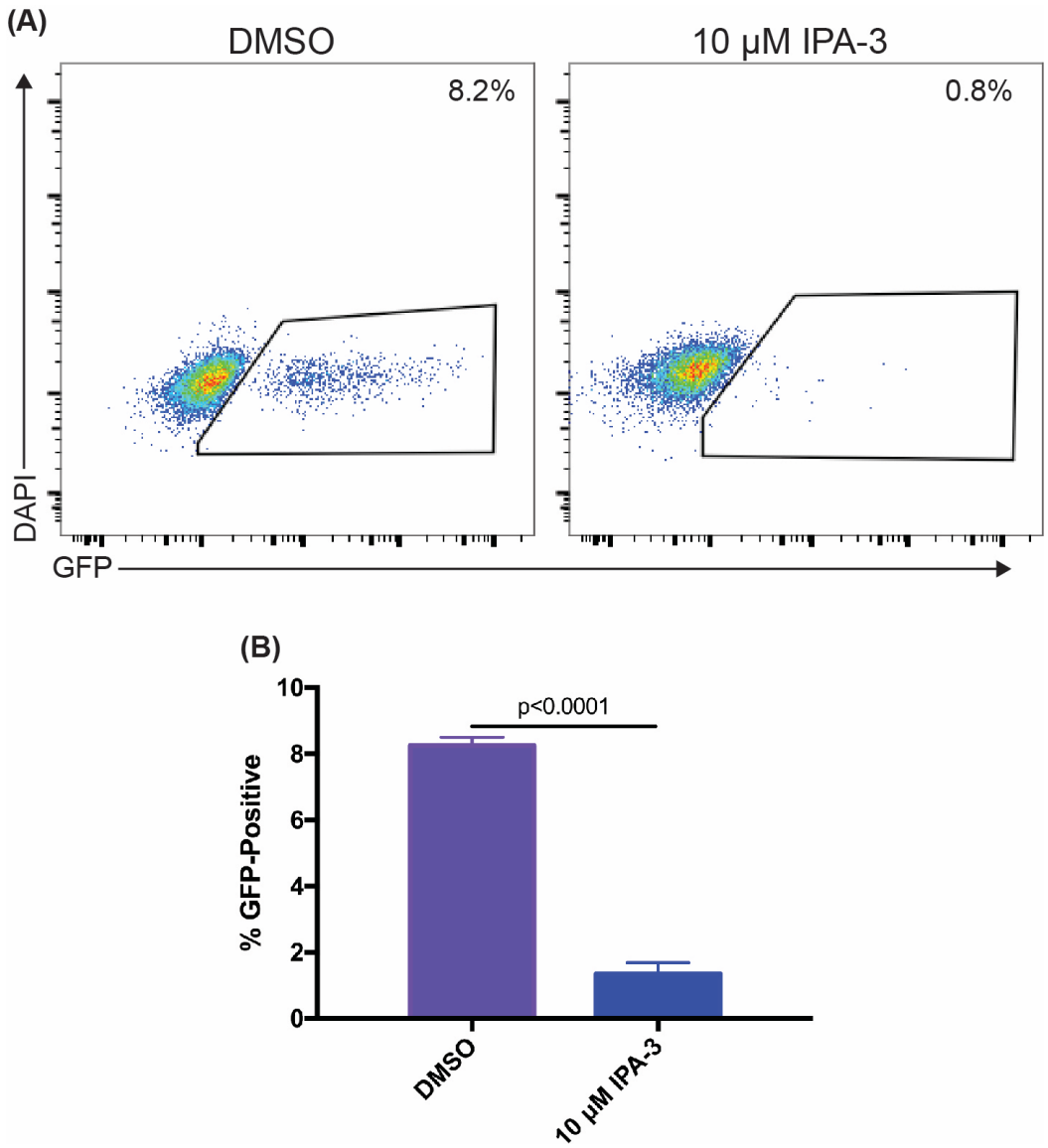

Figure 4.5: Pak1 inhibitor (IPA-3) decreases BCG uptake in T24 bladder cancer cell line. (A) T24 cells were pre-treated for 1 hr with DMSO or 10 μM IPA-3 in serum- and antibiotic-free medium. Cells were then incubated with BCG-GFP (in the presence of DMSO or IPA-3) for 24 hours then BCG uptake was measured by flow cytometry. The numbers show the percentage of GFP-positive events out of total events. DAPI was used as an empty channel and the gates were set based on uninfected cells. **(B)** Quantification of BCG-GFP uptake from (A).

Data Information: Mean ± SEM is shown. For (B) n=3 independent infections.

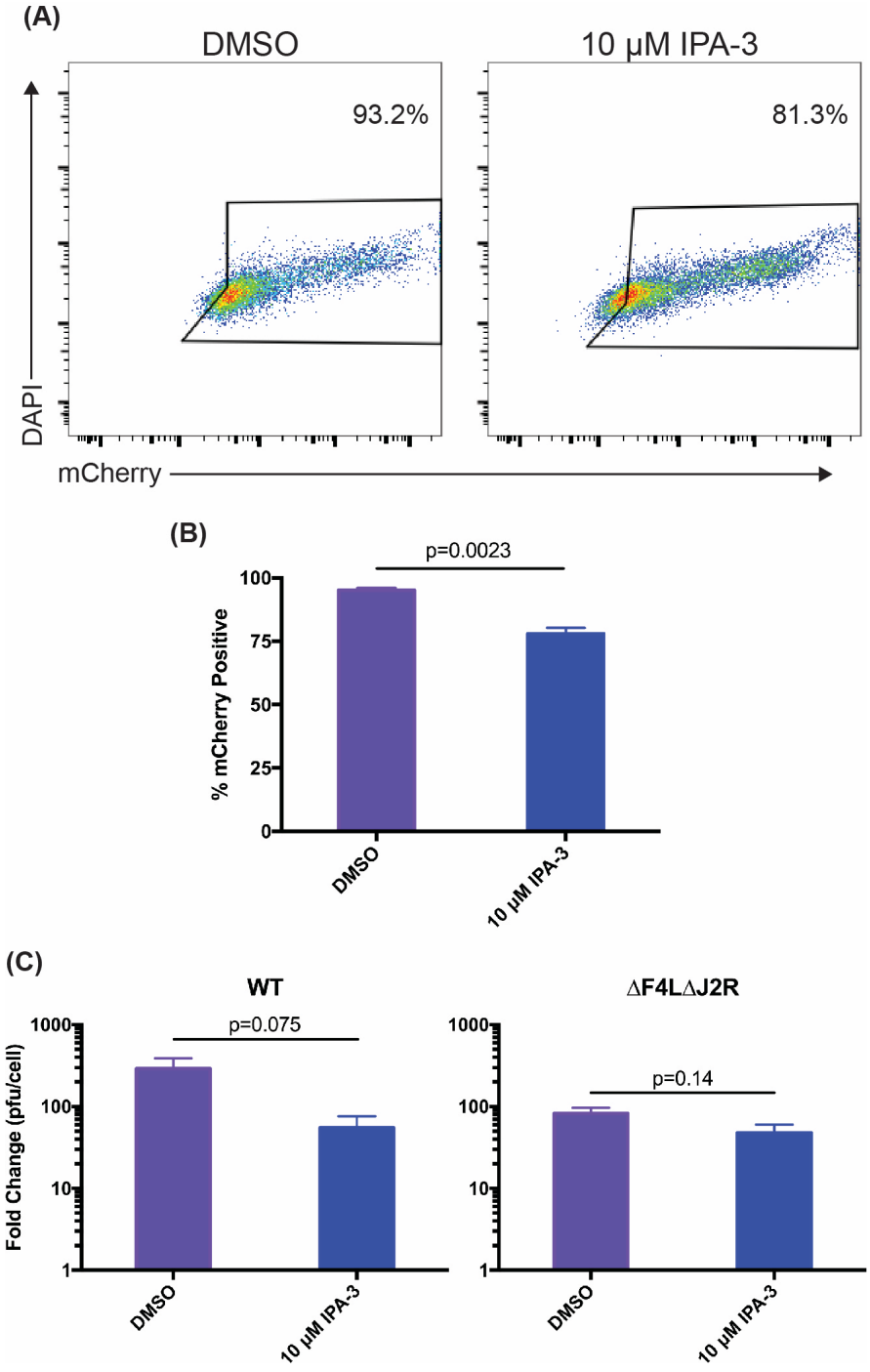
(A)
DMSO
10 μM IPA-3
93.2%
81.3%
DAPI
mCherry
(B)
p=0.0023
% mCherry Positive
100
75
50
25
0
DMSO
10 μM IPA-3
(C)
WT
ΔF4LΔJ2R
p=0.075
p=0.14
Fold Change (pfu/cell)
1000
100
10
1
DMSO
10 μM IPA-3

Figure 4.6: IPA-3 treatment has little effect on VACV infectivity or replication. (A) T24 cells were pre-treated for 1 hr with DMSO or 10 μM IPA-3 in serum- and antibiotic-free medium. Cells were then infected with 0.3 PFU/cell of ΔF4LΔJ2R VACV. mCherry expression, as an indicator of virus infection was measured by flow cytometry 24 hours later. The numbers show the percentage of mCherry-positive events (each indicating a VACV-infected cell) out of total events. DAPI was used as an empty channel and the gates were set based on uninfected cells. **(B)** Quantification of ΔF4LΔJ2R VACV infected cells from (A). **(C)** Growth curves for WT or ΔF4LΔJ2R VACV in sub-confluent T24 cells. Cells were pre-treated for 1 hr with DMSO or 10 μM IPA-3 in serum- and antibiotic-free medium. Cells were then infected with 0.3 PFU/cell. Cultures were harvested after 24 hrs and titered on BSC-40 cells.

Data Information: Mean ± SEM is shown. For (B) n=3. For (C) data represents n=3 independent infections, each titered in duplicate.

(**Figure 4.7B, D, E, and F**). These data highlight the significance of Pak1 in the uptake of BCG in bladder cancer cell lines.

4.3.7 ΔF4LΔJ2R VACV replicates in and kills human bladder cancer cells with induced BCG resistance. Multi-step virus growth curve analysis was carried out to evaluate the replication of ΔF4LΔJ2R VACV in BCG-resistant bladder cancer. T24 and 253J cell lines with and without Pak1 knockdown were infected with virus at an MOI of 0.03 PFU/cell. Cultures were then harvested at the indicated times and titered on BSC40 cells. We saw no difference in VACV growth in T24-shPak1 cells when compared to the T24-shScram cell lines (**Figure 4.8**). In contrast, there was a noticeable decrease in VACV replication in the 253J-shPak1 cells compared to the control at both 48 and 72 hrs post-infection (**Figure 4.8**). Next, the effect of VACV on cell survival was determined using a resazurin-based viability assay. Again, there was no difference in VACV killing between T24 and T24-shPak1 cell lines (**Figure 4.9**). There was a slight reduction in 253J-shPak1 cell killing at an MOI of 1.0 PFU/cell, however, this reduced killing was not observed at any other MOIs (**Figure 4.9**). Overall these results show that ΔF4LΔJ2R VACV maintains almost all its replication and cytotoxic properties in a model of induced BCG resistance.

4.3.8 Evaluation of ΔF4LΔJ2R VACV in BCG-resistant AY-27 cell lines. Since BCG uptake by AY-27 cells was low, we sought to optimize culture conditions for BCG uptake *in vitro* (**Figure 4.10**). We typically saw around 5% BCG uptake when using RPMI 1640 medium without antibiotics or serum. BCG uptake increased to 35% after supplementing the medium with 2% fetal bovine serum, although there was no benefit to further increases in serum concentration. We saw a similar 35% uptake when using the medium in which we grow primary bladder cancer cells (Materials and Methods 3.3.4). Based on these results we opted to use RPMI 1640 medium with 2% serum and no antibiotics for the remainder of the experiments.

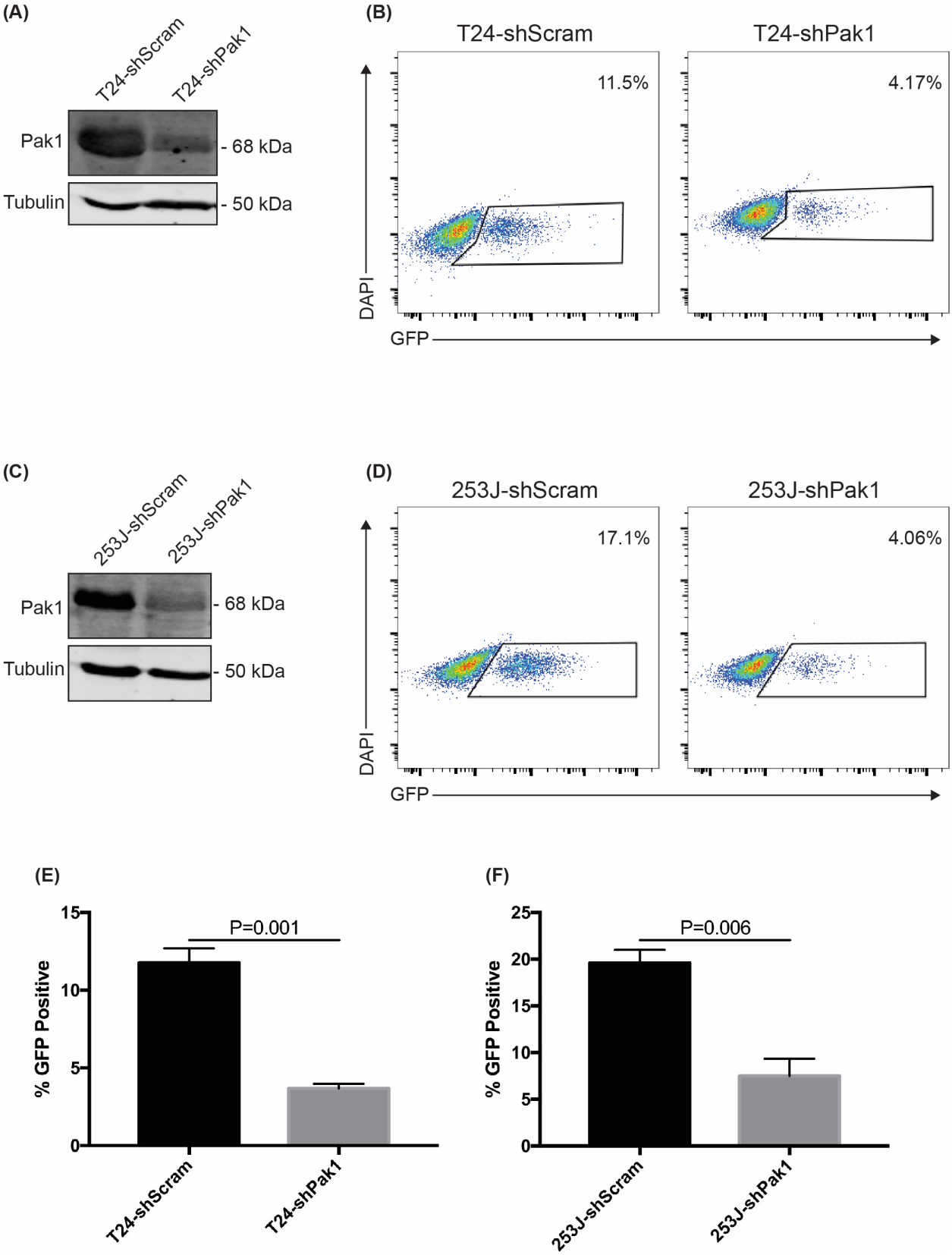
(A)
T24-shScram
T24-shPak1
Pak1
- 68 kDa
Tubulin
- 50 kDa
(B)
T24-shScram
T24-shPak1
11.5%
4.17%
DAPI
GFP
(C)
253J-shScram
253J-shPak1
Pak1
- 68 kDa
Tubulin
- 50 kDa
(D)
253J-shScram
253J-shPak1
17.1%
4.06%
DAPI
GFP
(E)
% GFP Positive
P=0.001
T24-shScram
T24-shPak1
(F)
% GFP Positive
P=0.006
253J-shScram
253J-shPak1

Figure 4.7: Stable Pak1 knockdown reduces BCG uptake in bladder cancer cells. (A and C) Western blot showing Pak1 expression in T24 and 253J human bladder cancer cell lines woth Pak1 or control shRNA expression. β-tubulin was used as loading control. Equal amounts of total protein (30 μg) were assayed in all Western blots. **(B and D)** Cell lines expressing Pak1 shRNA or scrambled shRNA were incubated with BCG-GFP in serum and antibiotic free medium for 24 hours then BCG uptake was measured by flow cytometry. The numbers show the percentage of GFP-positive events out of total events. DAPI was used as an empty channel and the gates were set based on uninfected cells. **(E and F)** Quantification of BCG-GFP uptake from **(B and D)**.

Data Information: Representative flow cytometry traces are shown. For (E) and (F) n=3 independent infections.

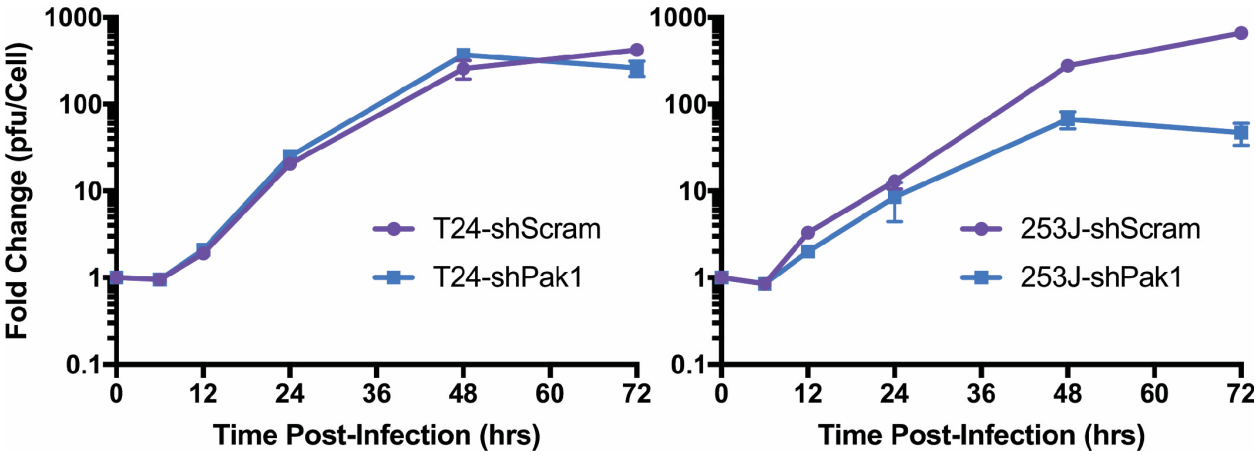

Figure 4.8: ΔF4LΔJ2R VACV effectively replicates in bladder cancer cells with induced BCG-resistance. Growth curves for the ΔF4LΔJ2R VACV in sub-confluent T24 or 253J bladder cancer cell lines with or without Pak1 knockdown. Cells were infected at a multiplicity of infection (MOI) of 0.03 PFU/cell. Cultures were harvested at the indicated times and titered on BSC40 cells. **Data Information:** Mean ± SEM is shown. Data irepresent 2 independent experiments each titered in duplicate.

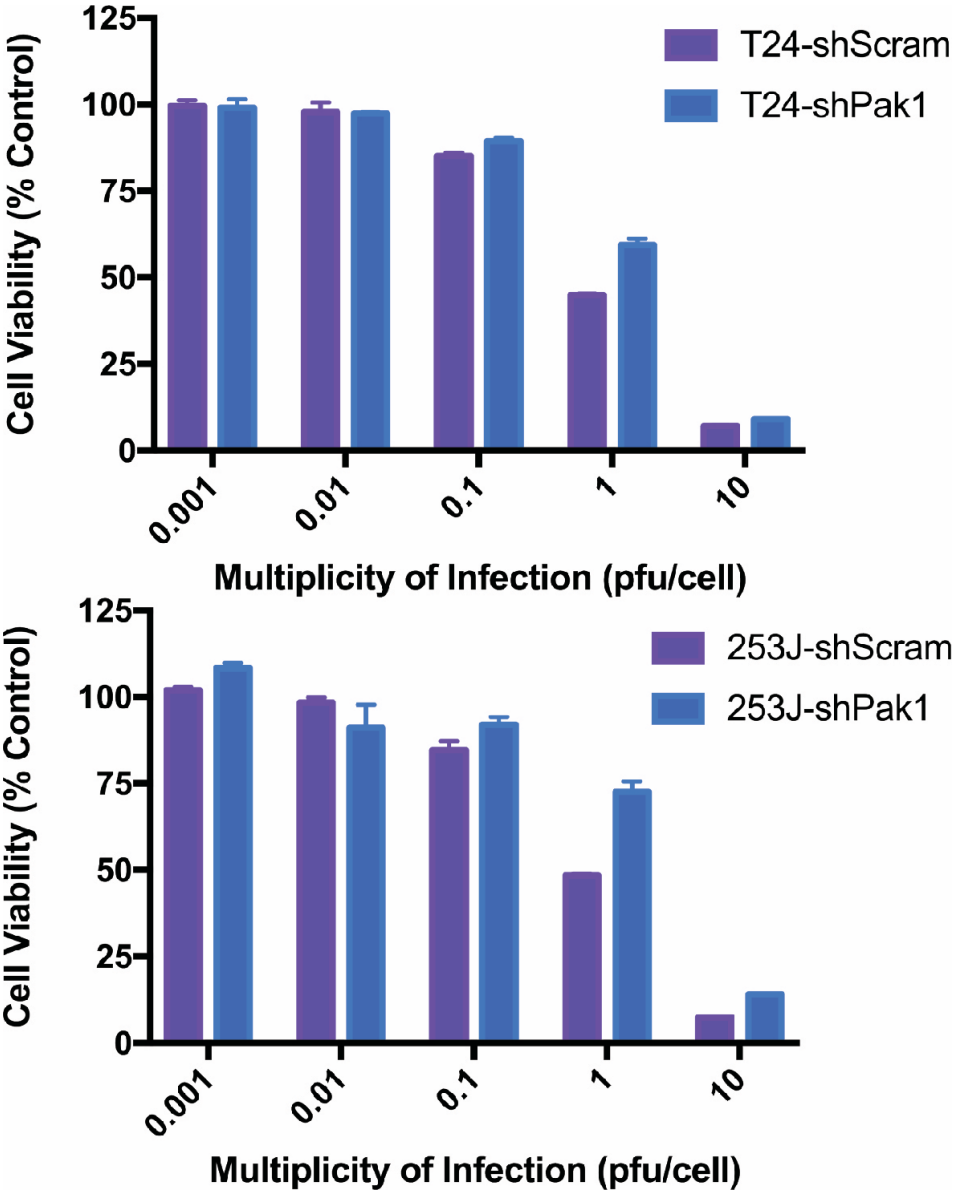

Figure 4.9: ΔF4LΔJ2R VACV effectively kills bladder cancer cells with induced BCG-resistance. Survival of cell lines was analyzed after infection *in vitro* at the indicated MOI with ΔF4LΔJ2R VACV. Cells were incubated with resazurin to assess viability at 72 hr post-infection. Uninfected cells were used as control.

Data Information: Mean ± SEM is shown. Data represent n=3 independent experiments, each performed in triplicate.

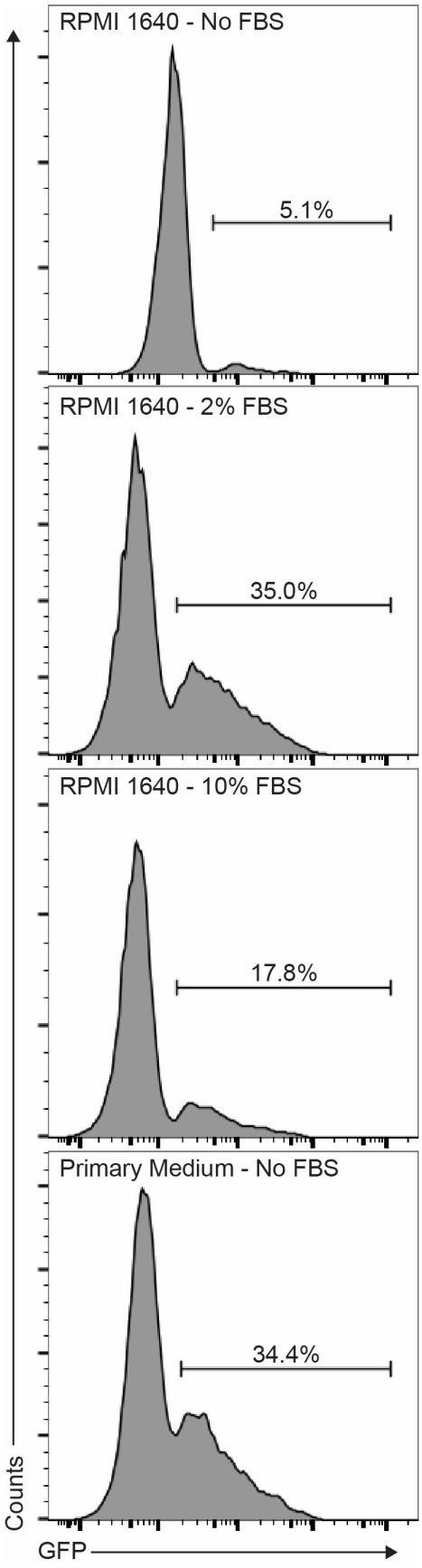
RPMI 1640 - No FBS
5.1%
RPMI 1640 - 2% FBS
35.0%
RPMI 1640 - 10% FBS
17.8%
Primary Medium - No FBS
34.4%
Counts
GFP

Figure 4.10: BCG uptake by AY-27 cells under various culture conditions. Sub-confluent AY-27 cells were incubated with BCG-GFP in the indicated medium without antibiotics for 24 hours, then BCG uptake was measured by flow cytometry. The numbers show the percentage of GFP-positive events out of total events. DAPI was used as an empty channel and the gates were set based on uninfected cells. Primary medium, medium used to culture primary bladder cancer samples (see Section 3.3.4).

Data Information: Representative flow cytometry traces are shown.

Next, we attempted to generate BCG-resistant AY-27 cell lines by depleting Pak1 protein using retrovirus delivery of shRNA targeting Pak1 as described in the Materials and Methods. Control cell line was generated using a scrambled shRNA vector. Knockdown was verified by western blotting (**Figure 4.11A**). Although we only saw a slight decrease in total Pak1 levels there was almost no detectable phosphorylation at T423 of Pak1 following knockdown. Interestingly we saw what looks like a shift in the molecular weight of Pak1. Also, we observed no significant change in the RRM2 protein levels in the Pak1 knockdown cell lines. Knockdown of Pak1 with either of two different shRNA sequences caused a dramatic reduction in BCG uptake (**Figure 4.11B and C**). ΔF4LΔJ2R VACV replication was nearly identical in AY-27-shScram cells and the two AY-27-shPak1 knockdown cell lines (**Figure 4.12**). Next, the effect of VACV infection on cell survival was determined in a resazurin-based viability assay (**Figure 4.13A and B**). EC_{50} values for the AY-27-shScram, AY-27-shPak1-B, and AY-27-shPak1-D were 0.039, 0.079 and 0.078 PFU/cell, respectively. Although there was an apparent increase in EC_{50} values for the shPak1 clones, the difference was not statistically significant. We suggest that tumors established from the AY-27-shPak1 cell line may provide an appropriate immune-competent BCG-refractory bladder cancer model to evaluate oncolytic VACV.

4.3.9 ΔF4LΔJ2R has anti-tumor activity superior to BCG in a bladder cancer model. ΔF4LΔJ2R VACV was also compared to BCG in the orthotopic immune-competent AY-27 rat bladder cancer model. Here, animals were treated by intravesical instillation with $3x10^8$ PFU of live ΔF4LΔJ2R VACV, or UV-inactivated virus on days 6, 9, and 12 post-tumor implantation (**Figure 4.14A**). For BCG treatments animals were instilled with $3x10^6$ CFU of UV-inactivated BCG-GFP (Pasteur strain), or live BCG-GFP on days 6, 9, 12, 15, 18, and 21 after tumor implantation (**Figure 4.14B**). This BCG dose and schedule have previously been used by our group

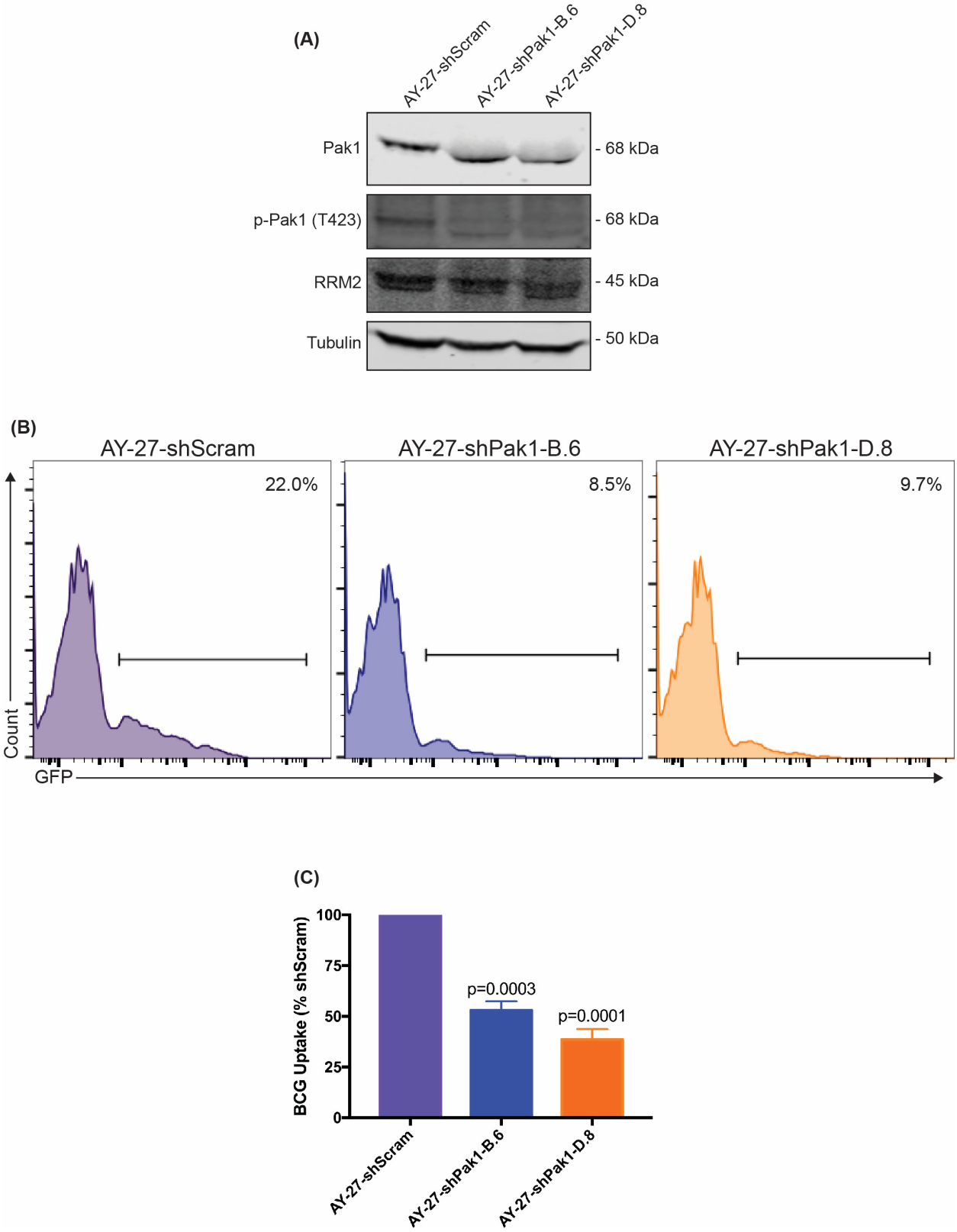
(A)
AY-27-shScram
AY-27-shPak1-B.6
AY-27-shPak1-D.8
Pak1
- 68 kDa
p-Pak1 (T423)
- 68 kDa
RRM2
- 45 kDa
Tubulin
- 50 kDa
(B)
AY-27-shScram
AY-27-shPak1-B.6
AY-27-shPak1-D.8
22.0%
8.5%
9.7%
Count
GFP
(C)
BCG Uptake (% shScram)
100
75
50
25
0
p=0.0003
p=0.0001
AY-27-shScram
AY-27-shPak1-B.6
AY-27-shPak1-D.8

Figure 4.11: Pak1 knockdown reduces BCG uptake in AY-27 rat bladder cancer cells. (**A**) Western blot showing Pak1, phospho-Pak1 (T423), and RRM2 expression in rat AY-27 bladder cancer cell lines. β-tubulin is shown as a loading control. Equal amounts of total protein (30 μg) were assayed. The images were scanned using the LI-COR Odyssey scanner (LI-COR Biosciences). **(B)** Cell lines with or without Pak1 knockdown were incubated with BCG-GFP in antibiotic-free medium supplemented with 2% serum for 24 hours then BCG uptake was measured by flow cytometry. The numbers show the percentage of GFP-positive events out of total events. DAPI was used as an empty channel and the gates were set based on uninfected cells. **(C)** Quantification of BCG-GFP uptake from (A).

Data Information: Mean ± SEM is shown. Data in (B) represent n=3 independent experiments.

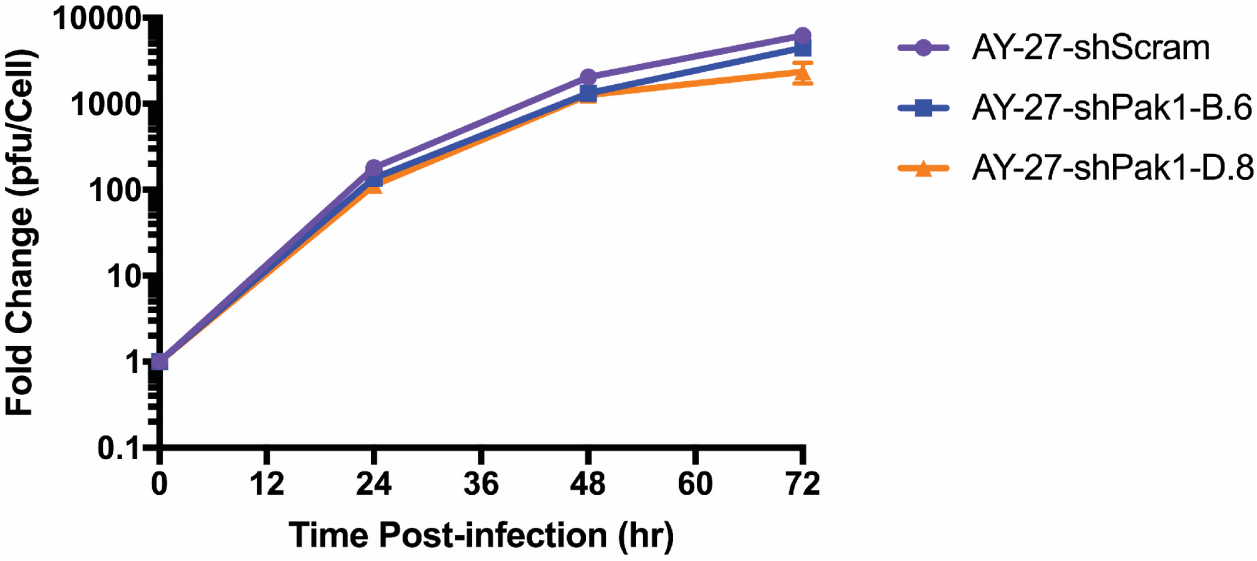

Figure 4.12: ΔF4LΔJ2R VACV maintains replicating capabilities in AY-27-shPak1 cells. Growth ofr ΔF4LΔJ2R VACV was determined in sub-confluent AY-27 rat bladder cancer cell lines cultured in medium with 2% serum. Cells were infected at an MOI of 0.03 PFU/cell. Cultures were harvested at the indicated times and titered on BSC40 cells.

Data Information: Mean ± SEM is shown. Data represent n=3 lysates, each titered in duplicate.

and others [325-327]. ΔF4LΔJ2R VACV treatment significantly increased survival (p=0.003) when compared to the UV-inactivated VACV control, as we have previously seen (**Figure 4.14C**). Additionally, ΔF4LΔJ2R VACV treatment increased survival over live BCG treatment (54% vs. 23%, respectively), however, this was not a statistically significant increase based on our limited sample size. Interestingly, consistent with a previous report [328], approximately 20% (2/11) of animals treated with UV-inactivated BCG cleared their tumors whereas UV-inactivated VACV treated had no apparent anti-tumor activity. These data highlight the potential of ΔF4LΔJ2R VACV to offer a superior therapy for bladder cancer, especially in cases where patients suffer toxicity from BCG or may be ineligible for BGC therapy.

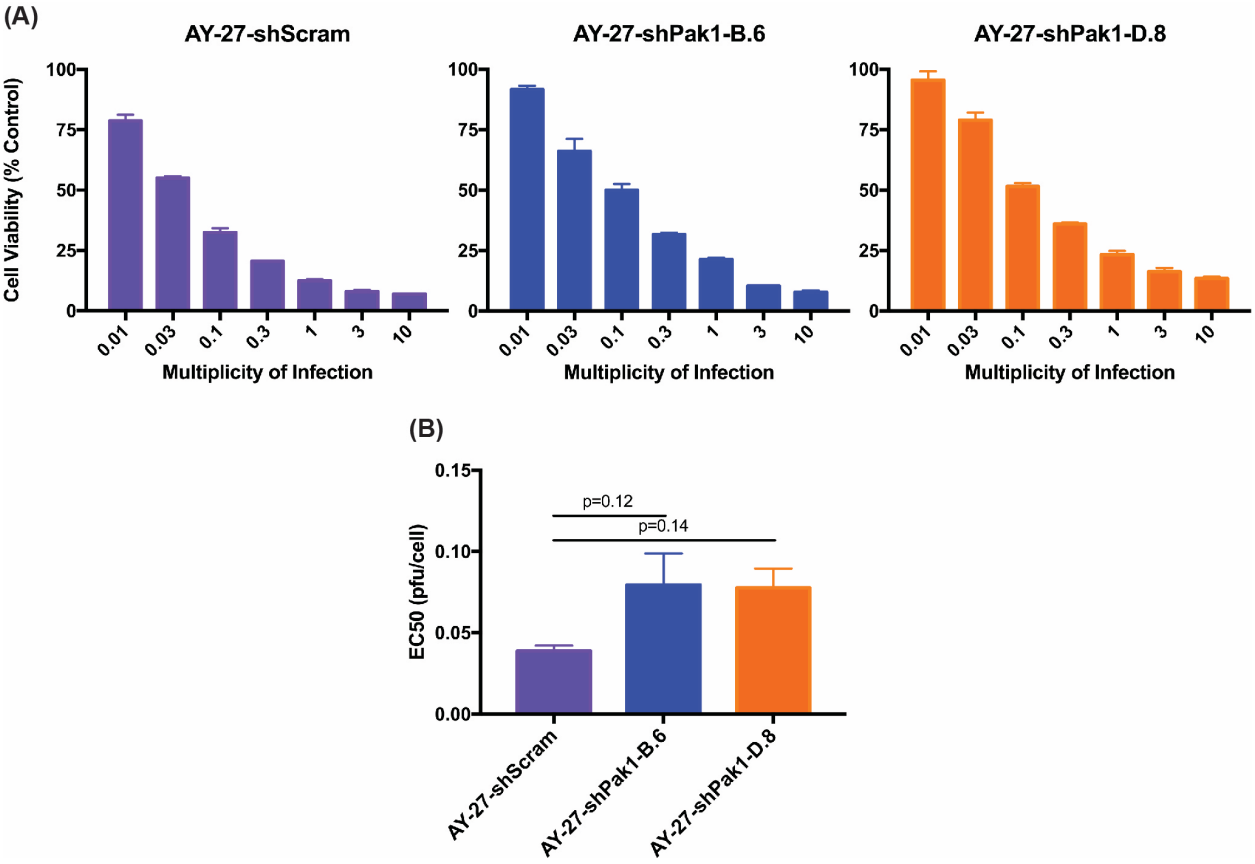

Figure 4.13: ΔF4LΔJ2R VACV effectively kills AY-27-shPak1 cells. (A) Survival of cell lines infected *in vitro* at the indicated MOI (in PFU/cell) with ΔF4LΔJ2R VACV. Cells were incubated with resazurin to assess viability 72 hr post-infection. Uninfected cells were used as control. **(B)** EC_{50} calculation from data in (A).

Data Information: Mean ± SEM is shown. Data in (A) and (B) represent n=3 independent experiments, each performed in triplicate.

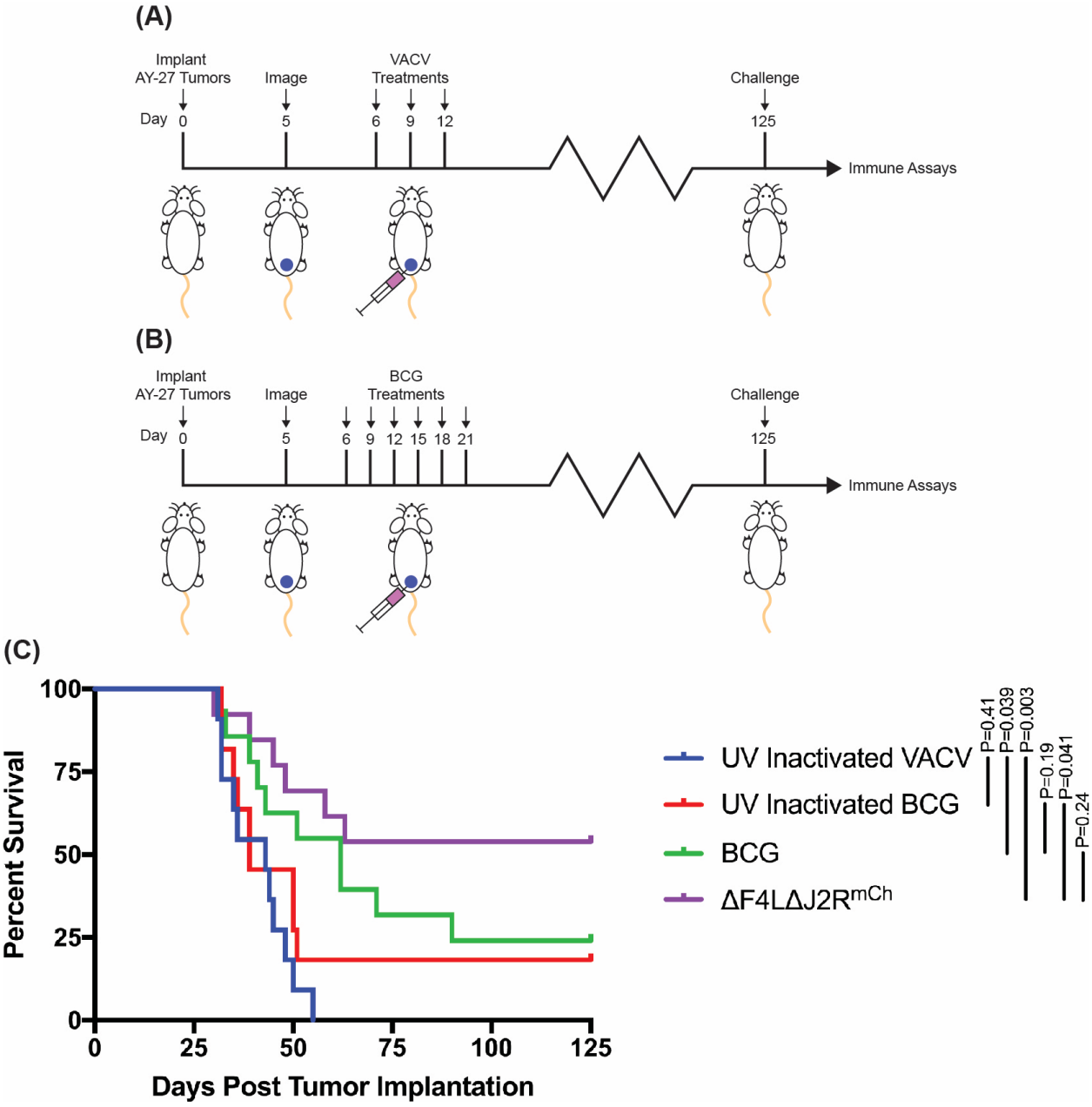
(A)
Implant
AY-27 Tumors
Image
VACV
Treatments
Challenge
Day 0
5
6 9 12
125
Immune Assays
(B)
Implant
AY-27 Tumors
Image
BCG
Treatments
Challenge
Day 0
5
6 9 12 15 18 21
125
Immune Assays
(C)
Percent Survival
100
75
50
25
0
0 25 50 75 100 125
Days Post Tumor Implantation
UV Inactivated VACV
UV Inactivated BCG
BCG
ΔF4LΔJ2R^mCh
P=0.41
P=0.039
P=0.003
P=0.19
P=0.041
P=0.24

Figure 4.14: ΔF4LΔJ2R has anti-tumor activity equal or superior to BCG in the AY-27 bladder cancer model. (A and B) Experimental schemes are shown. Rats were instilled in the bladder with $3x10^6$ AY-27 cells on day zero and cystoscoped on day 5 to verify tumor engraftment. For VACV treatments, $3x10^8$ PFU of UV-inactivated or ΔF4LΔJ2R VACV were instilled into the bladder of each rat on each of days 6, 9, and 12. For BCG treatments, $3x10^6$ CFU of UV-inactivated BCG-GFP, or live BCG-GFP were instilled into the bladder of each rat on each of days 6, 9, 12, 15, 18, and 21. **(C)** Overall survival of immunocompetent rats bearing AY-27 bladder tumors following indicated treatments.

Data Information: Mean ± SEM is shown. Data represent combined survival of two independent experiments. Animal survival was analyzed by log-rank (Mantel-Cox) test; n=8 to 12 rats per group.

4.4 DISCUSSION

Here we investigated the potential of using a novel oncolytic VACV as a safer and potentially more effective treatment for NMIBC, especially for patients who fail BCG. Even though the local immune activation in the bladder after BCG therapy is thought to be primarily responsible for the anti-tumor activities, several lines of investigation indicate that the initial attachment and most importantly, the internalization of BCG by tumor cells are critical first steps in activating the immune response [76,77]. It was previously shown, using confocal microscopy, that BCG is internalized by bladder cancer cells [80]. However, flow cytometry, the standard technique used in this chapter to measure the levels of BCG uptake, does not necessarily distinguish between BCG-GFP binding to the cell surface and BCG-GFP internalization. We found that BCG was indeed internalized and not bound to the cells surface. Using this validated assay, we observed varying degrees of BCG uptake in our panel of bladder cancer cells lines. The human RT112-luc and the murine MB49 cell lines were highly resistant to BCG uptake, while other cell lines showed varying degrees of sensitivity to BCG. It is interesting that the primary human lines UCKP-16 and UCKP-17, established from low grade tumors which are not typically treated with BCG, were resistant to BCG internalization. We have shown that ΔF4LΔJ2R VACV can replicate in, and kill, BCG-resistant cell lines as well as primary bladder cancer cultures. Efficacy of the virus in low grade tumors may also open the possibility of using OVs at early stages in treatment.

To confirm previous reports [80] that inhibition of Pak1 inhibits BCG uptake, we treated cells with the Pak1 inhibitor, IPA-3 [323,324]. Treatment with IPA-3 caused a reduction in autophosphorylation of Pak1 at amino acid residue T423, which is catalyzed by Cdc42, and is normally required for full activation of Pak1. Pretreatment of cells with IPA-3 significantly decreased BCG uptake. We next investigated the effect of IPA-3 treatment on ΔF4LΔJ2R VACV

activities. We saw that IPA-3 treatment caused a small reduction in infection levels, as indicated by the number of mCherry positive cells. However, when we assessed virus yield through plaque assay there was no difference in yield, suggesting that Pak1 inhibition does not strongly affect VACV activity in bladder cancer cells.

We propose that oncolytic VACV has significant activity in human bladder cancer cells that are resistant to BCG due to downregulation of the Pak1 pathway. Toward this end, we successfully generated stable Pak1 shRNA knockdown clones of T24 and 253J human bladder cancer cells. Both Pak1 knockdown clones showed a dramatic decrease in BCG uptake when compared to the parental cells lines. These data confirm reports from , Redelman-Sidi *et al.* [80] who first demonstrated the role of macropinocytosis and Pak1 in BCG uptake. More importantly for our study, just like with IPA-3 treatment, Pak1 knockdown had little effect on ΔF4LΔJ2R VACV replication and cytotoxicity. We did see a minor reduction in 48 and 72 hr virus yields from the 253J-shPak1 cell lines. However, this is likely a result of the slower growth rate of knockdown cells compared to the parental cell line, thus this multi-step virus growth assay would result in reduced virus yields. These data provide promising results to support use of an oncolytic VACV in treating BCG-refractory bladder cancer. The effectiveness of VACV in BCG-resistant cells may be due to the fact VACV utilizes two primary modes of infection: uptake via macropinocytosis [250] and fusion [245] with the cellular membrane, whereas BCG has only been shown to enter through macropinocytosis. Notably, VACV strain WR, which is used in these studies, has been shown to have a higher ability to enter cells via the fusion route than other VACV strains, again enhancing the potential of this treatment [247]. Another important aspect of oncolytic activity is spread of virus to surrounding cells. In order to spread from one cell to another, VACV induces cell motility [329] and the formation of actin projections [330-332] that propel VACV

toward other cells. Pak1 has been shown to be involved in both cell motility and actin tail formation [82,333] and can be directly activated by VACV [250]. This activation of Pak1 could partly explain why ΔF4LΔJ2R VACV maintains most of its replication and cytotoxic properties in BCG resistant cells lines. VACV activation of Pak1 may reverse BCG-resistance allowing for a combination therapy, however further investigation is required.

A key experiment presented is the comparison of ΔF4LΔJ2R VACV and BCG in the AY-27 immune-competent orthotopic rat model of bladder cancer. AY-27 tumors resemble high-grade human urothelial cell carcinoma in both tumor biology and morphology [297,298]. Previously, an oncolytic reovirus in this model demonstrated increased efficacy with less toxicity than BCG [232]. We showed in chapter 3 that ΔF4LΔJ2R VACV increased animal survival with a potential safety advantage. Surprisingly, we know of no clear evidence that BCG can induce a long-term protective anti-tumor immune response [92,317]. Moreover, Biot *et al.* showed that effective tumor clearance by BCG in a mouse model of bladder cancer was determined by an anti-BCG immune response, and that pre-vaccination with BCG enhanced tumor clearance [327]. A lack of BCG-mediated anti-tumor immunity could possibly explain the high recurrence rate in BCG-treated patients.

Finally, we have initiated the development of a BCG-resistant rat model of bladder cancer. We successfully cloned AY-27-shPak1 cell lines that displayed reduced BCG uptake; yet supported ΔF4LΔJ2R VACV replication and cytotoxicity. These cells showed a slight decrease in total Pak1 levels and an even more significant decrease in phospo-Pak1 (T423). One strange observation was the apparent shift down of the Pak1 band. Although the exact explanation for this is unclear there are a few possibilities. One explanation could be that both shRNA sequences map to exon 9 and a variant lacking all or part of exon 9 is over-expressed and translated to a smaller

protein. Alternatively, there could be increased Pak2 expression, which is slightly smaller, to compensate for the decreased Pak1. In future experiments, these cells will be used to establish a model of BCG resistance where we can determine the role of Pak1 in BCG therapy and the efficacy of ΔF4LΔJ2R VACV.

Surgery, BCG, and chemotherapy dramatically slow the progress of bladder cancer but do not totally eradicate the disease in a significant portion of patients. Patients with NMIBC that fail BCG therapy are in urgent need of other bladder-sparing treatment options. Our results highlight the potential of an oncolytic VACV as a treatment option in BCG resistant bladder cancer. The high degree of safety and efficacy seen here with OV therapy warrants immediate further investigation at both the preclinical and clinical levels.

CHAPTER 5 – DISCUSSION AND FUTURE DIRECTIONS

5.1 Summary and key findings

This thesis examines whether the poxvirus, VACV, can be used to kill bladder cancer cells safely and selectively, and therefore would be especially suitable for patients that have failed or even in place of conventional therapies. Tumor development requires multiple genetic mutations and epigenetic alterations that cause continued growth, immune system evasion, and metastasis [161]. This has several consequences that can be exploited in the development of OVs. Rapidly dividing cancer cells have a high level of DNA precursors that are required for the replication of the cell's DNA. One enzyme that plays a critical role is RNR, which catalyzes the formation of deoxyribonucleotides from ribonucleotides. Recent data from the our group suggests that VACV replication can be supported by the combined activities of both host cell and virus RNRs [269]. Disruption of the viral *F4L* gene (encoding the RRM2 protein of the RNR complex) results in virus growth that becomes dependent upon cellular RRM2. This mutation also dramatically reduces the virulence of ΔF4L viruses in infected animals, likely because most cells are not replicating and naturally express too little RRM2 to support efficient virus growth. We have developed VACVs tagged with the gene encoding mCherry and with deletions in *F4L*, *J2R* or both and examined their oncolytic properties in models of bladder cancer.

Using these viruses as a starting point, this thesis reports a number of significant contributions to preclinical studies to improve the treatment of bladder cancer. We show that ΔF4LΔJ2R VACV has superior safety while maintaining efficacy in models of bladder cancer. We have reported the first use of the RT112-luc orthotopic xenograft bladder cancer model that allows for *in vivo* tumor imaging. We have also developed a series of primary bladder tumor cultures, a unique PDX model of high-grade bladder cancer, and a platform for generating additional bladder cancer PDX models. Of most significance, we provide preliminary evidence that ΔF4LΔJ2R

VACV has superior safety over a single *J2R*-deleted VACV and may induce stronger anti-tumor immunity. Our ΔF4LΔJ2R VACV also increases survival in rodent models over BCG and is effective in killing BCG-resistant cells *in vitro*. Collectively, we have contributed both new models and reagents to the field as well as advanced the safety threshold and efficacy of oncolytic VACVs.

5.2 Immunotherapy in bladder cancer

One of the most exciting and promising developments in recent decades in cancer immunotherapy. Cancer immunotherapy is a form of treatment that boosts your body's own immune system to help fight cancer (reviewed in [334-336]). Although this strategy has been studied for over a century [337] it is only in the last few years that phase III clinical trials have shown consistent and significant improvements in the survival of patients with a variety of cancer. Three main types of immunotherapy have been examined in bladder cancer; immune checkpoint inhibitors, cancer vaccines, and OVs. Although these are not the only forms of cancer immunotherapy, they will be the focus of this discussion. The power of genome sequencing has identified many of the genetic alterations that lead to the development and progression of bladder cancer [44]. Lawrence *et al.* showed that bladder cancer has one of the highest rates of somatic mutations of any cancer [338]. This high mutational burden can provide tumor antigens that can be recognized by the immune system. All three forms of immunotherapy take advantage of such mutations to generate an anti-tumor immune response.

5.2.1 Immune checkpoint blockade. Of all the cancer immunotherapies, immune checkpoint inhibitors are leading the way in the clinic for a variety of cancers (reviewed in [339]). There are multiple inhibitory checkpoints that regulate the immune system. Cytotoxic T-cells are activated following interaction with APCs that allow engagement of the T-cell receptor (TCR) with MHC complexed to tumor antigen-derived peptides [340]. These activated T-cells can then

seek out cells displaying the target antigen and kill them. Under normal conditions, immune checkpoints are essential in self-tolerance, preventing states of autoimmunity [341]. However, tumor cells can be selected for and express checkpoint-activating ligands on their surface which ultimately shut down the immune response, preventing tumor clearance. Immune checkpoint blockade therapies are designed to prevent this interaction, allowing maintenance and amplification of antigen-specific T-cell responses. There are two main checkpoint pathways that have been targeted for cancer immunotherapy (reviewed in [342,343]). CTLA-4 is an immune checkpoint protein that antagonizes the stimulatory interaction between CD28 on T-cells and B7-1/B7-2 (CD80/CD86) on APCs. The other pathway is mediated by the programmed death 1 (PD-1) receptor, found mainly on T cells, and its ligand PD-L1 (B7-H1), which is expressed by a number of normal cell types and can be overexpressed on cancer cells. Engagement of PD-L1 with its receptor, PD-1, on T cells results in a signal that inhibits TCR-mediated activation of T-cell proliferation.

Ipilimumab is an anti-CTLA-4 monoclonal antibody that generated significant survival improvements in a phase III clinical trial in patients previously treated for metastatic melanoma [344]. However, grade 3 or 4 toxicities were reported in 10-15% of patients in the trial. In 2011, the FDA approved ipilimumab for the treatment of metastatic melanoma, due to the impressive increase in survival of patients with this difficult to treat cancer. This drug has recently been tested for the treatment of bladder cancer. Liakou *et al.* conducted a pre-surgical clinical trial with ipilimumab in six patients with bladder cancer who were candidates for radical cystectomy [345]. Treatment resulted in an increase in effector T-cells and production of IFN-γ. Ipilimumab was also tested in a phase I trial with 12 NMIBC patients [346]. Treatment was well tolerated, demonstrating only grade 1 and 2 toxicities. Following treatment, all 12 patients had increased

presence of $CD4^{+}ICOS^{hi}$ T-cells [347] which is pharmacodynamic biomarker of successful anti-CTLA-4 treatment. These are encouraging results but further clinical trials are needed to determine if anti-CTLA-4 therapy is superior to current therapies.

Atezolizumab is an anti-PD-L1 monoclonal antibody that has been tested in numerous clinical trials of bladder cancer. In a phase I clinical trial, metastatic bladder cancer patients were treated regardless of PD-L1 status to determine whether PD-L1-negative tumors could be cleared [348]. The authors report that 57% of patients developed treatment-related toxicity, 4% of which were grade 3. The study found that response rate correlated with PD-L1 expression on the tumor. Atezolizumab was next tested in a phase II clinical trial (IMvigor210) of untreated patients with locally advanced or metastatic bladder cancer who were cisplatin-ineligible [349]. The objective response rate was 23%, while complete response rate was 9%. The study also determined that response rate correlated with mutational burden of the tumor. Based on these results, in May 2016 the FDA granted an accelerated approval of atezolizumab as a frontline treatment for cisplatin-ineligible patients with locally advanced or metastatic bladder cancer. Recently, Roche had a press release on their phase III clinical trial (IMvigor211) testing atezolizumab in patients with locally advanced or metastatic bladder cancer whose disease progressed during or after platinum-based chemotherapy. IMvigor211 did not meet its primary endpoint of increasing overall survival compared to chemotherapy alone. Based on these results numerous clinical trials are being planned. However, so far only a fraction of patients are seeing dramatic responses and toxicities are significant, so it is clear that there is still significant room for improvement.

5.2.2 Cancer vaccines. The goal of a cancer vaccine is to expose the host to expressed tumor associated antigens and increase the number of tumor-specific T-cells as well as to reactivate T-cells. In general, this is achieved by stimulating APCs such as DCs with a known tumor antigen.

T-cells can then be activated by interacting with these APCs, allowing antigen presentation and engagement with the TCR. Although not as encouraging as the clinical results of immune checkpoint inhibitor treatment, there are currently several cancer vaccines in clinical trials of bladder cancer. One example is DN24-02, which consists of APCs that have been pulsed with BA7072, a recombinant HER2-derived antigen linked to GM-CSF. DN24-02 is currently being examined in a phase II study of patients with high-risk $HER2^{+}$ bladder cancer. Although no response rates have been reported, interim data showed that DN24-02 activated APCs, increase HER2-specific antibody responses, and increase expression of T-cell cytokines [350,351].

Another cancer vaccine that is of interest to this thesis is PANVAC. A poxvirus-based cancer vaccine that consists of a priming dose with VACV (Wyeth strain) and subsequent boosting doses with fowlpox virus [352]. Both viruses encode the tumor-associated antigens epithelial mucin 1 (MUC1) and carcinoembryonic antigen (CEA). They also express T-cell costimulatory proteins, B7.1, intracellular adhesion molecule-1 (ICAM-1) and leukocyte function-associated antigen-3 (LFA-3), to help enhance the immune response. PANVAC has been tested for activity in multiple cancer types. A clinical trial in metastatic breast cancer showed PANVAC to be well tolerated and saw a trend in improved progression-free survival [353]. In another phase I trial of advanced pancreatic cancer, PANVAC was shown to be capable of generating an antigen-specific immune response [354]. Bladder cancer is also a potential target for PANVAC therapy. MUC1 has been shown to be significantly increased on the surface of bladder cancer cells, and expression levels directly correlate with stage and grade [355,356]. However, CEA levels are not significantly elevated in NMIBC, although they are in MIBC [357]. A phase II clinical trial is currently underway testing PANVAC with BCG therapy versus BCG alone in high-grade NMIBC patients who failed prior BCG therapy (NCT02015104). Cancer vaccines have had limited success in the

clinic as single agents, but the identification of tumor antigens and the ability to present them support the investigation of multiple strategies for cancer immune therapy. Introduction of tumor antigens and immune activating molecules into OVs could enhance their efficacy.

5.3 Oncolytic viruses

Although there has recently been an increased interest in developing new therapies for bladder cancer, it can be seen by the discussion above that many of these treatments have either shown little efficacy or are still under investigation in very early clinical settings. Some of the most promising cancer therapies in recent years have been biological agents, namely immune checkpoint inhibitors. The clinical results with immune checkpoint inhibitors are encouraging but these have primarily been investigated in MIBC or metastatic disease. Additionally, a significant proportion of patients do not respond to these therapies and some have been associated with fairly severe toxicities. There is a dire need for more safe and effective therapies for both MIBC and NMIBC.

This thesis focuses on the development of a highly safe and selective oncolytic VACV for the treatment of NMIBC. Not only is there a strong rationale for using OVs in bladder cancer but the data presented here demonstrates pre-clinical support for a clinical investigation. As introduced in chapter 1, OVs are engineered to selectively replicate in and destroy cancer cells while leaving normal cells unharmed. OVs are unique in that they pose multiple modes of action. Firstly, they directly lyse cancer cells which not only kills the cells, but also releases tumor antigens. Secondly, local virus infection stimulates the immune system, increasing immune cell infiltration, and cytokine production. This can be a critical step in immune system recognition of tumor antigens and generation of an anti-tumor immune response. Finally, since OVs replicate, they self-amplify allowing for spread and additional rounds of infection and lysis. OVs may have added benefit over

immune checkpoint inhibitors that are excellent at reactivating a preexisting immune response, but are unable to generate new anti-tumor T-cells. Additionally, cancers with low mutational burden typically do not respond to checkpoint blockade, but may be responsive to OVs. For these reasons, there is significant interest in investigating OVs as a treatment option bladder cancer.

5.4 *F4L*-deleted VACV as a treatment for bladder cancer

WT VACV encodes many of the proteins required for robust replication in normal cells. Many of these proteins are involved in the synthesis of dNTPs for viral genome replication (**Figure 1.5**). These proteins include TK (*J2R* gene product) and both large (RRM1; *I4L* gene product) and small (RRM2; *F4L* gene product) subunits of the heterodimeric RNR complex. The cellular homologs of these viral proteins are overexpressed in rapidly dividing cancer cells that require a high rate of dNTP production [358]. Since VACV can utilize cellular TK1, and virus-encoded components of RNR can complex with each other or with cellular homologs [269], one can employ a complementation-based strategy to design a cancer-selective OV.

The most common strategy used to generate oncolytic VACVs has been to introduce mutations that inactivate *J2R*. Cellular TK1 is a critical enzyme in the salvage pathway for nucleotide biosynthesis. TK1 catalyzes the reaction of dTh and ATP to generate deoxythymidine monophosphate (dTMP). TK1 is cell cycle regulated, being synthesized during S-phase and subsequently degraded [359]. Many cancers show elevated levels of TK1 and we and others show that TK1 is overexpressed in both NMIBC and MIBC [360]. Interestingly, we have shown here that all our bladder cancer cell lines supported replication of ΔJ2R VACV to nearly the same level as that seen in cells infected with WT VACV. All the bladder cancer cell lines showed high levels of TK1 protein expression but we could not detect cellular TK1 in the normal N60 cell line even though it supported robust ΔJ2R VACV growth. This could be explained by the fact that dTTP

can also be produced *de novo* from dUMP by thymidylate synthase and TMK [297,298] and VACV encodes a homolog of the latter enzyme. It has also been reported that thymidylate synthase is cell cycle regulated much like cellular TK1. It would be of interest to this project to examine thymidylate synthase expression in the N60 cell line to see if its upregulation could explain why we see ΔJ2R VACV replication in the absence of TK1. Additionally, we could perform knockdown studies of TK1 to determine the TK1-dependence of ΔJ2R VACV replication.

Pexa-Vec is the most clinically advanced oncolytic VACV, having completed at least 7 phase I and 6 phase II clinical trials [132]. Pexa-Vec has a deletion of *J2R* and encodes GM-CSF to enhance the host anti-tumor immune response. Although Pexa-Vec has been examined in many clinical trials with minimal toxicity there have been reports that it produced pox lesions in some patients [361-363]. Recently, a phase I clinical trial of another oncolytic VACV, vvDD, was reported [364]. vvDD is based on backbone strain WR, as are viruses we have used in our studies, and contains deletions in the vaccinia growth factor gene and *J2R*. They found evidence of replicating virus in a healing wound and as well as in the oral cavity. They suggest that the attenuating mutations introduced into VACV were unable to prevent virus replication in healing or inflamed tissue. The added safety of our *F4L*-deleted VACVs may provide a benefit when moving to the clinic, especially in patients with compromised immune systems.

RNR is a heterodimeric complex that catalyzes the formation of dNTPs from ribonucleotides (reviewed in [184]). Since RNR is responsible for the *de novo* synthesis of dNTPs, it is essential for cell proliferation. Both subunits (RRM1 and RRM2) have been shown to be overexpressed in cancer cells [291]. We found RRM1 protein levels in all bladder cancer cell lines as well as normal N60 cells. mRNA analysis of patient samples showed that RRM1 was only overexpressed in MIBC. In contrast, we found elevated RRM2 expression in bladder cancer cells

lines, and mRNA expression in patient samples was elevated in both NMIBC and MIBC. RRM1 is constitutively expressed and remains constant throughout the cell cycle [365]. In normal cells, cellular RRM2 is cell-cycle-regulated with levels increasing through S/G2-phase and undetectable for the rest of the cell cycle. Cellular RRM2 (as well as TK1 [366]) has a KEN box sequence in its N-terminal domain, that is targeted by the anaphase promoting complex (APC)-Cdh1 complex for degradation during G0/G1 and mitosis [264]. Because of this, RRM2 has a half-life of approximately 3 hrs and is the rate limiting step in dNTP synthesis [367]. Interestingly, the VACV F4 protein lacks the N-terminal KEN box sequence required for degradation, allowing expression outside of S-phase.

In our *in vitro* experiments we found a link between RRM2 levels and VACV replication. However, rather than a linear correlation between the RRM2 protein level and *F4L*-deleted VACV replication, there seems to be a 'threshold' level of RRM2 required to support robust virus replication. In relation to the work presented here, Fend *et al.* have described an oncolytic WR strain of VACV bearing deletions in *J2R* and in *I4L* (encoding the RRM1 protein of the RNR complex) [292]. While this virus showed promise as a therapeutic agent, in our experience virus replication is regulated more stringently by *F4L* than by *I4L* since cellular RRM2 expression is cell cycle regulated whereas RRM1 is not. Further safety and efficacy studies would need to be performed to determine if *I4L*-deleted VACVs have an advantage over single *J2R*-deleted VACVs.

One interesting observation we made during our *in vitro* characterization of the *F4L*-deleted VACVs was that ΔF4LΔJ2R VACV routinely outperformed ΔF4L VACV in both replication and killing in bladder cancer cells. Additionally, we saw that ΔF4LΔJ2R VACV was superior in our xenograft model after IV injection. This observation was opposite to our initial hypothesis, where we proposed that the multiple mutations in ΔF4LΔJ2R VACV would cause it

to be more attenuated. The reason for these observations is unclear but one possibility is that the presence of *J2R* in ΔF4L VACV causes an over-production of dTTP, which can skew the dNTP pool and thus increase the error rate during DNA replication. This may result in a decreased ratio of infectious to defective virus particles. Additionally, the altered dNTP pool may initiate innate immune signaling pathways. Further work is required to fully understand our observations.

The most advanced OV in bladder cancer is CG0070 which has undergone multiple phase I and II clinical trials. CG0070 conditionally replicating serotype 5 Ad in which the essential E1a viral genes are driven by the human E2F-1 promoter, restricting virus replication to Rb-defective tumor cells. *In vitro* CG0070 shows comparable replication and killing of bladder cancer cells while having lesser effect in normal cells, similar to what we have found with ΔF4LΔJ2R VACV. CG0070 showed tumor killing in orthotopic and subcutaneous human xenograft bladder tumor models, with complete tumor regression in half of the treated animals (5 of 10) after five high dose intratumoral injections. Human GM-CSF encoded by this virus is species-specific and their model was immune compromised; therefore, the antitumor effects seen were likely a result of only the oncolytic activity of CG0070. Although we used different xenograft models (s.c. RT112-luc and PDX models), we saw 100% tumor clearance. In immune competent recipients, GM-CSF expression might enhance the anticancer effect of CG0070 because uninfected local tumor and potentially distant tumor metastases may be targeted by the induced immune response. It would be of interest to directly compare our ΔF4LΔJ2R VACV to CG0070 in a pre-clinical model, however the choice of model is not straightforward, since adenoviruses have limited replication proficiency in rodents. It would be interesting to determine if tumors that were resistant to ΔF4LΔJ2R VACV or CG0070 would be sensitive to the other virus, since it is unlikely that all tumors will be equally susceptible to both viruses.

The most concerning observation made in our immune competent model studies was the apparent development of cysts on the ovaries of some rats treated with ΔJ2R VACV. Other *J2R*-deleted VACVs are reported to replicate in normal mouse tissues, including the ovaries where they can cause pathology and sterility [314-316]. This is of particular concern if *J2R*-deleted VACVs are under consideration for treatment of premenopausal women. These observations provide additional evidence of the increased safety of *F4L*-deleted VACVs.

One of the more interesting observations was that the *F4L*-deleted VACVs induced lower levels of virus-neutralizing antibodies than ΔJ2R VACV in rats bearing AY-27 tumors. While nine of thirteen ΔJ2R VACV-treated animals appeared to be tumor-free by day 75, three of these rats later developed rapidly growing recurrent tumors. This makes us wonder if the animals developed more of an anti-viral as opposed to an anti-tumor immune response. In the future, it would be interesting to conduct another experiment where we euthanize rats on day 35, not only to look for neutralizing antibodies, but to examine the different abilities of the viruses to induce anti-tumor T-cell responses. If in fact ΔF4LΔJ2R VACV does induce superior anti-tumor immunity, this would be another reason to adopt this mutation in a clinical setting.

5.5 Oncolytic VACV in treatment of BCG resistant bladder cancer

Intravesical BCG is the standard of care for high-risk NMIBC which includes CIS, high-grade papillary tumors (stage Ta), and lamina-propria-invasive tumors (stage T1) [368]. Multiple clinical trials have shown BCG to be the most effective treatment available for preventing tumor recurrence. However, despite this strong clinical record, 30% to 40% of patients do not respond to this therapy and up to 50% of BCG-treated patients will develop recurrence within 5 years of treatment [104]. Recurrence after BCG therapy is still one of the most significant problems in the management of bladder cancer since there are no reliable treatment options.

The immune response generated after BCG treatment is dependent on contact between BCG and bladder cancer cells [369]. Recent evidence has shown that the internalization of BCG by bladder cancer cells may also be a critical step in initiating the anti-tumor activities [80]. Redelman-Sidi *et al.* showed that activation of the Cdc42-Rac1-Pak1 signaling pathway by oncogenic activation of PTEN/PI3K and/or Ras determines a cell's ability to internalize BCG through macropinocytosis. Macropinocytosis is a clathrin-independent endocytic process that facilitates the non-selective uptake of molecules, nutrients, and antigens (reviewed in [370]). It is an actin-dependent process resulting in cytoskeleton rearrangement at the plasma membrane leading to formation of endocytic vacuoles called macropinosomes. Pak1 phosphorylates LIM kinase-1 (LIMK1) [371] which goes on to phosphorylate cofilin, consequently rendering it inactive [372]. When cofilin is inactive, Arp2/3 complex activity increases which promotes actin nucleation, creating filaments that grow to form macropinosomes [373]. Finally, Pak1 phosphorylates the C-terminal-binding protein-1/Brefeldin A-ADP-ribosylated substrate (CtBP1/BARS) which is involved in the final fission of macropinosomes [374].

Upwards of 80% of NMIBC can have mutations that lead to activation of the PTEN/PI3K and/or Ras pathways. This may explain why BCG treatment is successful in the majority of situations. The fact that BCG uses macropinocytosis to enter bladder cancer cells is of significant interest to this project. There are numerous viruses, including VACV, that use macropinocytosis as an entry mechanism [250,375]. There is a concern that an oncolytic VACV would have limited efficacy in the same cases as BCG. To investigate this concern, it was necessary to set up a model of induced BCG resistance. We found ΔF4LΔJ2R VACV could effectively replicate in and kill BCG-resistant cell lines and primary cell cultures.

It has previously been shown that Pak1 plays a role in VACV entry via macropinocytosis and cell-to-cell spread [250,321]. Andrade *et al*. showed that the deletion of Pak1 causes a delay in entry and impaired virus spread but it does not play a role in production of progeny virus and lysis of cells [321]. Although these results are informative they may not have a direct relationship to our question since they were using fibroblasts cells deleted in Pak1. This is important since another study by Mercer and Helenius showed that when VACV was added to cells there was an increase in phosphorylation of residue T423 in Pak1, a marker of Pak1 activation [250]. Increased T423 phosphorylation after VACV infection may in part explain why VACV is still effective in BCG-resistant cells. It would be important to examine phospho-Pak1 after VACV infection of BCG-resistant cells to see if it is increased. When we analyzed VACV infection in IPA-3 treated cells we saw decreased infectivity, however there was no significant difference from DMSO-treated cells in terms of virus yield. Therefore, there may just be a delay in virus entry in cells with low phospho-Pak1.

Although our preliminary data on using VACV as a treatment for BCG-resistant bladder cancer is promising, we still have a number of questions that need to be answered. We would like to determine the rate of virus spread in tumors that are resistant to BCG. For this we will utilize tumors grown *in vivo* on the chorioallantoic membrane of the chick embryo model, a site that provides stromal support resembling the mammalian tumor microenvironment [376-379]. We also want to determine if our AY-27shPak1 cells lines are resistant to BCG, when used *in vivo* in our rat model of bladder cancer. Using this BCG-resistant model, we want to evaluate efficacy of ΔF4LΔJ2R VACV. Finally, we would like to correlate Pak1 expression with response rates to BCG in the clinic to determine if Pak1 is a suitable marker for BCG failure.

5.6 Oncolytic virus combination therapies

Although OVs have shown some promising results in both pre-clinical and clinical settings, it is unlikely that they will be curative agents on their own and would benefited from additional biological modifiers. With the ultimate goal of generating a durable anti-tumor immune response, it is becoming obvious that the current single-modality immunotherapies will likely not achieve this goal. It is likely that the most successful therapeutic regime will combine multiple therapies, each with different modes of action. OVs with low toxicity and broad application could play a central role in these combination therapies. The challenge ahead will be how to accurately determine the right combination for each patient. There have been several studies combining OVs with both conventional chemotherapies as well as other immunotherapies.

Recently, Liu *et al.* showed that an oncolytic VACV was synergistic with PD-L1 blockade in pre-clinical models [380]. Treatment with VACV alone attracted effector T-cells to the tumor site and caused an increase in PD-L1 expression. Combination treatment with VACV and anti-PD-L1 reduced the number of PD-L1 positive cells and increased the infiltration of both $CD4^+$ and $CD8^+$ T-cells while also causing a decrease in Tregs. These encouraging pre-clinical results warrant further investigation of combining OVs with immune checkpoint inhibitors.

Another intriguing combination is OVs and gemcitabine. Pre-clinical studies with myxoma virus [381] and HSV [382] as well as a phase I study with revovirus [234] have all shown enhanced responses when combined with gemcitabine. One of the most potent suppressors of various T-cell and NK cell functions are myeloid-derived suppressor cells (MDSCs) [374,375] (Reviewed in [376]). It has been shown that gemcitabine treatment causes depletion of MDSCs in the spleen, which results in a re-establishment of CD4+ and CD8+ T-cell proliferation [383]. Importantly, gemcitabine treatment does not severely harm activated immune cells, particularly CD8+ T-cells

and NK cells in the spleen, and they are able to elicit their tumor killing effects [384]. We also have some data indicating that our oncolytic VACV has enhanced cell killing after pre-treatment with gemcitabine (see Appendix Figure 1). Since gemcitabine is often used in recurrent bladder cancer this could be a rational combination in the clinic.

Additionally, radiotherapy and VACV have been combined in pre-clinical models of melanoma [385] and pancreatic cancer [386]. This combination showed synergistic cytotoxicity *in vitro* and significantly delayed tumor growth and enhanced survival of tumor-bearing animals compared to either single agent. The combination of chemo and radiotherapy with OVs may be of interest in bladder-sparing treatments.

5.7 Improving oncolytic virus therapy

Although we and others have shown oncolytic VACVs to have significant anti-tumor activity, there is still room for improvement. In our hands, we can clear most if not all xenografted tumors however, in immune competent models we achieve around a 50% cure rate. The reason why some animals fail to respond is not fully known, but there are a few possible explanations. Firstly, there may not be sufficient infection of the tumor cells after virus instillation. Secondly, the virus may simply be cleared too rapidly by the host immune response to have a significant lytic effect. Or the virus may simply not stimulate the anti-tumor immunity required for long term tumor control. To enhance the anti-tumor activities of OVs, several strategies could be applied. Immune-stimulating transgenes inserted into the viral genome might help activate the immune system in generating tumor-specific cytotoxic T-cells. OVs have been engineered to express T-cell-activating cytokines that include IL-2, -12, -15 and -18 as well as APC-activating IFNs, TNF-α and GM-CSF (reviewed in [387]). However, the ideal transgene choice is unclear and it may vary significantly between each tumor type and mutational landscape.

Immune evasion strategies have been implemented to increase virus delivery to the tumor site. Rojas *et al.* [388] showed that deglycosylation of VACV particles decreased Toll-like receptor 2 (TLR2) signaling which resulted in decreased anti-viral neutralizing antibodies. Additionally, Rojas' virus expressed the TIR-domain-containing adapter-inducing interferon-β (TRIF)-activating transgene to enhance the cytotoxic T-lymphocyte (CTL) response. TRIF expression pushes the immune response from Th2 to a primarily Th1 response increasing the anti-tumor CTL response. The oncolytic activity was improved over the parental virus and treatment was further improved with repeated treatment. In another study by the same group, they found that MDSCs are key mediators of immunotherapy resistance [389]. It is known that prostaglandin E2 (PGE2), can induce the differentiation of MDSCs from bone marrow cells [390]. To counteract MDSCs, they expressed hydroxy-prostaglandin dehydrogenase 15-(NAD) (HPGD), an enzyme responsible for the metabolism of PGE2, from their oncolytic VACV. HPGD treatment with this modified virus resulted in depletion of MDSC in the tumor, and enhanced antitumor immune responses in both VACV sensitive and resistant tumor models. Another way to limit the consequences of virus neutralization is with a prime-boost strategy. Here two immunologically different viruses are used sequentially to express tumor antigens. This strategy allows for maximal expression of the tumor antigen over time. An adeno-/vaccinia virus combination has been successful in slowing the generation of anti-viral immune responses resulting in better anti-tumor therapy [391].

A variety of antibody therapies have shown excellent results in clinical trials. However, long half-life and poor tumor penetration increase the chances of adverse side effects and decreased efficacy. Local antibody production from a OV could help modify the tumor microenvironment while minimizing the side effects [392]. Recently, oncolytic VACVs that expresses murine programmed cell death-1 (mPD-1) whole antibody (mAb), fragment antigen-binding (Fab), or

single-chain variable fragment (scFv) have been developed [393]. Both mAb and scFv VACVs resulted in tumor growth and survival similar to unarmed VACV combined with systemically administered anti-PD-1, and both treatments were superior to virus alone. Oncolytic measles viruses engineered with transgenes encoding anti-CTLA-4 or anti-PD-L1 antibodies have also been shown to increase survival and improve tumor regression in mouse models [394]. Virally encoded antibodies could be expanded to targets beyond PD-1/PD-L1 or CTLA-4 [395]. Another interesting development are bispecific T-cell engagers (BiTEs) which consist of two linked scFvs specific for the TCR and a tumor-specific surface antigen [396]. Linking of a tumor cells and T-cell by the BiTE causes T-cell activation and tumor cell killing. Yu *et al.* described an oncolytic VACV expressing a BiTE against the tumor cell surface antigen EphA2 which activated human PBMCs and enhanced anti-tumor activity in preclinical models [172]. These antibody expression strategies may be a way to maximize the benefits of them while at the same time minimizing toxicity.

In recent years, it has become clear that generation of a robust and long-lasting anti-tumor immune response is key in the management of cancer. A number if strategies to enhance the anti-tumor activities of OVs have been described here. The challenge moving forward will be to determine which strategy will benefit a particular patient and even which OV is the ideal choice. These optimized OVs can be even further enhanced by combination with conventional cancer therapies.

5.8 Conclusions

OVs have continually shown excellent safety profiles with encouraging pre-clinical and clinical efficacy. However, moving OVs into the clinic requires further investigation into appropriate tumor targets, delivery methods, combination therapies, and evaluation of biosafety

concerns. In this thesis, we show that NMIBC may be an ideal target to treat with OVs. We found *F4L*-deleted VACVs to have improved safety compared to viruses deleted only in the *J2R* gene. Specifically, ΔF4LΔJ2R VACV showed enhanced tumor selectivity while maintaining efficacy both *in vitro* and *in vivo*. This VACV selectively replicated in the orthotopic AY-27 immunocompetent rat model, RT112-luc xenograft model, and a patient derived xenograft model, causing significant tumor regression with no toxicity. Furthermore, rats cured of AY-27 tumors by VACV treatment developed long lasting anti-tumor immunity. Bladder cancer cell lines with inherent or induced BCG resistance were highly susceptible to VACV-mediated killing. Finally, comparison of ΔF4LΔJ2R VACV to BCG in the orthotopic AY-27 immunocompetent rat model found the virus to achieve superior tumor clearance and long term survival. Future studies will further investigate the mechanism of BCG failure and determine if a ΔF4LΔJ2R VACV could provide an improved treatment for this group of patients. Additionally, combining OVs with immune checkpoint inhibitors, chemotherapeutics, or arming the virus with immune-modulatory cytokines or tumor antigens, may help improve the development of a durable anti-tumor immunity.

REFERENCES

1. van der Heijden, A.; Witjes, J. Recurrence, progression, and follow-up in non–muscle-invasive bladder cancer. *European Urology Supplements* **2009**, *8*, 556–562.

2. *Canadian Cancer Society's Advisory Committee on Cancer Statistics*; Canadian Cancer Statistics: Toronto, 2016.

3. Burger, M.; Catto, J. W. F.; Dalbagni, G.; Grossman, H. B.; Herr, H.; Karakiewicz, P.; Kassouf, W.; Kiemeney, L. A.; La Vecchia, C.; Shariat, S.; Lotan, Y. Epidemiology and risk factors of urothelial bladder cancer. *Eur. Urol.* **2013**, *63*, 234–241.

4. Slaughter, D. P.; Southwick, H. W.; Smejkal, W. "Field cancerization" in oral stratified squamous epithelium. Clinical implications of multicentric origin. *Cancer* **1953**, *6*, 963–968.

5. Lochhead, P.; Chan, A. T.; Nishihara, R.; Fuchs, C. S.; Beck, A. H.; Giovannucci, E.; Ogino, S. Etiologic field effect: reappraisal of the field effect concept in cancer predisposition and progression. *Mod. Pathol.* **2015**, *28*, 14–29.

6. Sanli, O.; Dobruch, J.; Knowles, M. A.; Burger, M.; Alemozaffar, M.; Nielsen, M. E.; Lotan, Y. Bladder cancer. *Nat. Rev. Dis. Primers* **2017**, *3*, 17022.

7. Johansson, S. L.; Cohen, S. M. Epidemiology and etiology of bladder cancer. *Seminars in Surgical Oncology* **1997**, *13*, 291–298.

8. Knowles, M. A.; Hurst, C. D. Molecular biology of bladder cancer: new insights into pathogenesis and clinical diversity. *Nat. Rev. Cancer* **2015**, *15*, 25–41.

9. Pasin, E.; Josephson, D. Y.; Mitra, A. P.; Cote, R. J.; Stein, J. P. Superficial bladder cancer: an update on etiology, molecular development, classification, and natural history. *Rev Urol* **2008**, *10*, 31–43.

10. Anastasiadis, A.; de Reijke, T. Best practice in the treatment of nonmuscle invasive bladder cancer. *Ther Adv Urol* **2012**, *4*, 13–32.

11. Ro, J. Y.; Staerkel, G. A.; Ayala, A. G. Cytologic and histologic features of superficial bladder cancer. *Urol. Clin. North Am.* **1992**, *19*, 435–453.

12. Sylvester, R.; van der Meijden, A.; Witjes, J.; Jakse, G.; Nonomura, N.; Cheng, C.; Torres, A.; Watson, R.; Kurth, K. H. High-grade Ta urothelial carcinoma and carcinoma in situ of the bladder. *Urology* **2005**, *66*, 90–107.

13. Kobayashi, H.; Kikuchi, E.; Mikami, S.; Maeda, T.; Tanaka, N.; Miyajima, A.; Nakagawa, K.; Oya, M. Long term follow-up in patients with initially diagnosed low grade Ta non-muscle invasive bladder tumors: tumor recurrence and worsening progression. *BMC Urol* **2014**, *14*.

14. Nepple, K. G.; O'Donnell, M. The optimal management of T1 high-grade bladder cancer.

CUAJ **2009**, *3*, S188–92.

15. Cookson, M. S.; Herr, H. W.; Zhang, Z. F.; Soloway, S.; Sogani, P. C.; Fair, W. R. The treated natural history of high risk superficial bladder cancer: 15-year outcome. *J. Urol.* **1997**, *158*, 62–67.

16. Jakse, G.; Loidl, W.; Seeber, G.; Hofstädter, F. Stage T1, grade 3 transitional cell carcinoma of the bladder: an unfavorable tumor? *J. Urol.* **1987**, *137*, 39–43.

17. M'liss, A. H.; Herr, H. W. Carcinoma in situ of the bladder. *J. Urol.* **1995**.

18. Althausen, A. F.; Prout, G. R.; Daly, J. J. Non-invasive papillary carcinoma of the bladder associated with carcinoma in situ. *J. Urol.* **1976**, *116*, 575–580.

19. Daly, J. J. Carcinoma-in-situ of the urothelium. *Urol. Clin. North Am.* **1976**, *3*, 87–105.

20. Shariat, S. F.; Karakiewicz, P. I.; Palapattu, G. S.; Lotan, Y.; Rogers, C. G.; Amiel, G. E.; Vazina, A.; Gupta, A.; Bastian, P. J.; Sagalowsky, A. I.; Schoenberg, M. P.; Lerner, S. P. Outcomes of Radical Cystectomy for Transitional Cell Carcinoma of the Bladder: A Contemporary Series From the Bladder Cancer Research Consortium. *J. Urol.* **2006**, *176*, 2414–2422.

21. Madersbacher, S.; Hochreiter, W.; Burkhard, F.; Thalmann, G. N.; Danuser, H.; Markwalder, R.; Studer, U. E. Radical cystectomy for bladder cancer today - A homogeneous series without neoadjuvant therapy. *J. Clin. Oncol.* **2003**, *21*, 690–696.

22. Freedman, N. D. Association Between Smoking and Risk of Bladder Cancer Among Men and Women. *JAMA* **2011**, *306*, 737–745.

23. Moolgavkar, S. H.; Stevens, R. G. Smoking and Cancers of Bladder and Pancreas - Risks and Temporal Trends. *J. Natl. Cancer Inst.* **1981**, *67*, 15–23.

24. Hashim, D.; Boffetta, P. Occupational and Environmental Exposures and Cancers in Developing Countries. *Ann Glob Health* **2014**, *80*, 393–411.

25. Castano-Vinyals, G.; Cantor, K. P.; Malats, N.; Tardon, A.; Garcia-Closas, R.; Serra, C.; Carrato, A.; Rothman, N.; Vermeulen, R.; Silverman, D.; Dosemeci, M.; Kogevinas, M. Air pollution and risk of urinary bladder cancer in a case-control study in Spain. *Occup Environ Med* **2008**, *65*, 56–60.

26. Boffetta, P.; Silverman, D. T. A meta-analysis of bladder cancer and diesel exhaust exposure. *Epidemiology* **2001**, *12*, 125–130.

27. Boffetta, P.; Jourenkova, N.; Gustavsson, P. Cancer risk from occupational and environmental exposure to polycyclic aromatic hydrocarbons. *Cancer Causes Control* **1997**, *8*, 444–472.

28. Golka, K.; Wiese, A.; Assennato, G.; Bolt, H. M. Occupational exposure and urological cancer. *World J Urol* **2004**, *21*, 382–391.

29. Ma, O. W.; Lin, G. F.; Oin, Y. Q.; Lu, D.; Golka, K.; Geller, F.; Chen, J.; Shen, J. H. GSTP1 A(1578)G (Ile(105)Val) polymorphism in benzidine-exposed workers: an association with cytological grading of exfoliated urothelial cells. *Pharmacogenetics* **2003**, *13*, 409–415.

30. Letasiova, S.; Medved'ova, A.; Sovcikova, A.; Dusinska, M.; Volkovova, K.; Mosoiu, C.; Bartonova, A. Bladder cancer, a review of the environmental risk factors. *Environ Health* **2012**, *11*.

31. Marcus, P. M.; Vineis, P.; Rothman, N. NAT2 slow acetylation and bladder cancer risk: a meta-analysis of 22 case-control studies conducted in the general population. *Pharmacogenetics* **2000**, *10*, 115–122.

32. An, Y.; Li, H.; Wang, K. J.; Liu, X. H.; Qiu, M. X.; Liao, Y.; Huang, J. L.; Wang, X. S. Meta-analysis of the relationship between slow acetylation of N-acetyl transferase 2 and the risk of bladder cancer. *Genet. Mol. Res.* **2015**, *14*, 16896–16904.

33. Lindgren, D.; Liedberg, F.; Andersson, A.; Chebil, G.; Gudjonsson, S.; Borg, A.; Mansson, W.; Fioretos, T.; Hoglund, M. Molecular characterization of early-stage bladder carcinomas by expression profiles, FGFR3 mutation status, and loss of 9q. *Oncogene* **2006**, *25*, 2685–2696.

34. Simoneau, M.; LaRue, H.; Aboulkassim, T. O.; Meyer, F.; Moore, L.; Fradet, Y. Chromosome 9 deletions and recurrence of superficial bladder cancer: identification of four regions of prognostic interest. *Oncogene* **2000**, *19*, 6317–6323.

35. Sharpless, N. E.; Sherr, C. J. Forging a signature of in vivo senescence. *Nat. Rev. Cancer* **2015**, *15*, 397–408.

36. Serrano, M.; Hannon, G. J.; Beach, D. A New Regulatory Motif in Cell-Cycle Control Causing Specific-Inhibition of Cyclin-D/Cdk4. *Nature* **1993**, *366*, 704–707.

37. Stone, S.; Jiang, P.; Dayananth, P.; Tavtigian, S. V.; Katcher, H.; Parry, D.; Peters, G.; Kamb, A. Complex Structure and Regulation of the P16 (Mts1) Locus. *Cancer Res.* **1995**, *55*, 2988–2994.

38. Quelle, D. E.; Zindy, F.; Ashmun, R. A.; Sherr, C. J. Alternative reading frames of the INK4a tumor suppressor gene encode two unrelated proteins capable of inducing cell cycle arrest. *Cell* **1995**, *83*, 993–1000.

39. Cappellen, D.; De Oliveira, C.; Ricol, D.; de Medina, S.; Bourdin, J.; Sastre-Garau, X.; Chopin, D.; Thiery, J. P.; Radvanyi, F. Frequent activating mutations of FGFR3 in human bladder and cervix carcinomas. *Nat. Genet.* **1999**, *23*, 18–20.

40. Hernandez, S.; Lopez-Knowles, E.; Lloreta, J.; Kogevinas, M.; Amoros, A.; Tardon, A.; Carrato, A.; Serra, C.; Malats, N.; Real, F. X. Prospective study of FGFR3 mutations as a prognostic factor in nonmuscle invasive urothelial bladder carcinomas. *J. Clin. Oncol.* **2006**, *24*, 3664–3671.

41. Tomlinson, D. C.; Baldo, O.; Hamden, P.; Knowles, M. A. FGFR3 protein expression and its relationship to mutation status and prognostic variables in bladder cancer. *J. Pathol.* **2007**, *213*,

91–98.

42. Jebar, A. H.; Hurst, C. D.; Tomlinson, D. C.; Johnston, C.; Taylor, C. F.; Knowles, M. A. FGFR3 and Ras gene mutations are mutually exclusive genetic events in urothelial cell carcinoma. *Oncogene* **2005**, *24*, 5218–5225.

43. Kompier, L. C.; van der Aa, M. N. M.; Lurkin, I.; Vermeij, M.; Kirkels, W. J.; Bangma, C. H.; van der Kwast, T. H.; Zwarthoff, E. C. The development of multiple bladder tumour recurrences in relation to the FGFR3 mutation status of the primary tumour. *J. Pathol.* **2009**, *218*, 104–112.

44. The Cancer Genome Atlas Research Network Comprehensive molecular characterization of urothelial bladder carcinoma. *Nature* **2014**, *507*, 315–322.

45. Borkowska, E.; Binka-Kowalska, A.; Constantinou, M.; Nawrocka, A.; Matych, J.; Kałuzewski, B. P53 mutations in urinary bladder cancer patients from Central Poland. *J. Appl. Genet.* **2007**, *48*, 177–183.

46. Cordes, I.; Kluth, M.; Zygis, D.; Rink, M.; Chun, F.; Eichelberg, C.; Dahlem, R.; Fisch, M.; Höppner, W.; Wagner, W.; Doh, O.; Terracciano, L.; Simon, R.; Wilczak, W.; Sauter, G.; Minner, S. PTEN deletions are related to disease progression and unfavourable prognosis in early bladder cancer. *Histopathology* **2013**, *63*, 670–677.

47. Aveyard, J. S.; Skilleter, A.; Habuchi, T.; Knowles, M. A. Somatic mutation of PTEN in bladder carcinoma. *Br. J. Cancer* **1999**, *80*, 904–908.

48. Kimura, T.; Suzuki, H.; Ohashi, T.; Asano, K.; Kiyota, H.; Eto, Y. The incidence of thanatophoric dysplasia mutations inFGFR3 gene is higher in low-grade or superficial bladder carcinomas. *Cancer* **2001**, *92*, 2555–2561.

49. Bruyninckx, R.; Buntinx, F.; Aertgeerts, B.; Van Casteren, V. The diagnostic value of macroscopic haematuria for the diagnosis of urological cancer in general practice. *Br J Gen Pract* **2003**, *53*, 31–35.

50. Cohen, R. A.; Brown, R. S. Clinical practice. Microscopic hematuria. *N. Engl. J. Med.* **2003**, *348*, 2330–2338.

51. Sharma, S.; Ksheersagar, P.; Sharma, P. Diagnosis and treatment of bladder cancer. *Am Fam Physician* **2009**, *80*, 716–723.

52. Metts, M. C.; Metts, J. C.; Milito, S. J.; Thomas, C. R. Bladder cancer: A review of diagnosis and management. *J Natl Med Assoc* **2000**, *92*, 285–294.

53. Planz, B.; Jochims, E.; Deix, T.; Caspers, H. P.; Jakse, G.; Boecking, A. The role of urinary cytology for detection of bladder cancer. *Eur J Surg Oncol* **2005**, *31*, 304–308.

54. Kausch, I.; Sommerauer, M.; Montorsi, F.; Stenzl, A.; Jacqmin, D.; Jichlinski, P.; Jocham, D.; Ziegler, A.; Vonthein, R. Photodynamic Diagnosis in Non-Muscle-Invasive Bladder Cancer: A Systematic Review and Cumulative Analysis of Prospective Studies. *Eur. Urol.* **2010**, *57*, 595–

606.

55. Brausi, M.; Collette, L.; Kurth, K.; van der Meijden, A. P.; Oosterlinck, W.; Witjes, J.; Newling, D.; Bouffioux, C.; Sylvester, R. J.; (null), E. G.-U. T. C. C. G. Variability in the recurrence rate at first follow-up cystoscopy after TUR in stage Ta T1 transitional cell carcinoma of the bladder: A combined analysis of seven EORTC studies. *Eur. Urol.* **2002**, *41*, 523–530.

56. Miladi, M.; Peyromaure, M.; Zerbib, M.; Saighi, D.; Debre, B. The value of a second transurethral resection in evaluating patients with bladder tumours. *Eur. Urol.* **2003**, *43*, 241–245.

57. Kassouf, W.; Traboulsi, S. L.; Kulkarni, G. S.; Breau, R. H.; Zlotta, A.; Fairey, A.; So, A.; Lacombe, L.; Rendon, R.; Aprikian, A. G.; Robert Siemens, D.; Izawa, J. I.; Black, P. Cua guidelines on the management of non-muscle invasive bladder cancer. *Can Urol Assoc J* **2015**, *9*, E690–E704.

58. Herr, H. W. The value of a second transurethral resection in evaluating patients with bladder tumors. *J. Urol.* **1999**, *162*, 74–76.

59. Friedman, D.; Mooppan, U.; Rosen, Y.; Kim, H. The Effect of Intravesical Instillations of Thiotepa, Mitomycin-C, and Adriamycin on Normal Urothelium - an Experimental-Study in Rats. *J. Urol.* **1991**, *145*, 1060–1063.

60. Sylvester, R. J.; Oosterlinck, W.; van der Meijden, A. A single immediate postoperative instillation of chemotherapy decreases the risk of recurrence in patients with stage Ta T1 bladder cancer: A meta-analysis of published results of randomized clinical trials. *J. Urol.* **2004**, *171*, 2186–2190.

61. Addeo, R.; Caraglia, M.; Bellini, S.; Abbruzzese, A.; Vincenzi, B.; Montella, L.; Miragliuolo, A.; Guarrasi, R.; Lanna, M.; Cennamo, G.; Faiola, V.; Del Prete, S. Randomized Phase III Trial on Gemcitabine Versus Mytomicin in Recurrent Superficial Bladder Cancer: Evaluation of Efficacy and Tolerance. *J. Clin. Oncol.* **2010**, *28*, 543–548.

62. Gardmark, T.; Carringer, M.; Beckman, E.; Malmström, P.-U.; Grp, I. G. S. Randomized phase II marker lesion study evaluating effect of scheduling on response to intravesical gemcitabine in recurrent Stage Ta urothelial cell carcinoma of the bladder. *Urology* **2005**, *66*, 527–530.

63. Onishi, T.; Sugino, Y.; Shibahara, T.; Masui, S.; Yabana, T.; Sasaki, T. Randomized controlled study of the efficacy and safety of continuous saline bladder irrigation after transurethral resection for the treatment of non-muscle-invasive bladder cancer. *BJU International* **2017**, *119*, 276–282.

64. Onishi, T.; Sasaki, T.; Hoshina, A.; Yabana, T. Continuous Saline Bladder Irrigation after Transurethral Resection Is a Prophylactic Treatment Choice for Non-muscle Invasive Bladder Tumor. *Anticancer Res.* **2011**, *31*, 1471–1474.

65. Witjes, J.; van der Meijden, A.; Collette, L.; Sylvester, R.; Debruyne, F.; van Aubel, A.; Witjes, W.; Grp, E. G.; Grp, D. S. C. U. Long-term follow-up of an EORTC randomized prospective trial comparing intravesical bacille Calmette-Guerin-RIVM and mitomycin C in superficial bladder cancer. *Urology* **1998**, *52*, 403–410.

66. Aldousari, S.; Kassouf, W. Update on the management of non-muscle invasive bladder cancer. *Can Urol Assoc J* **2010**, *4*, 56–64.

67. Hall, M. C.; Chang, S. S.; Dalbagni, G.; Pruthi, R. S.; Seigne, J. D.; Skinner, E. C.; Wolf, J. S.; Schellhammer, P. F. Guideline for the management of nonmuscle invasive bladder cancer (stages Ta, T1, and Tis): 2007 update. *J. Urol.* **2007**, *178*, 2314–2330.

68. Luca, S.; Mihaescu, T. History of BCG Vaccine. *Maedica (Buchar)* **2013**, *8*, 53–58.

69. Pearl, R. Cancer and Tuberculosis. *American Journal of Hygiene* **1929**.

70. Old, L. J.; Clarke, D. A.; Benacerraf, B. Effect of Bacillus Calmette-Guerin Infection on Transplanted Tumours in the Mouse. *Nature* **1959**, *184*, 291–292.

71. Zbar, B.; Bernstein, I. D.; Rapp, H. J. Suppression of tumor growth at the site of infection with living Bacillus Calmette-Guérin. *J. Natl. Cancer Inst.* **1971**, *46*, 831–839.

72. Morales, A.; Eidinger, D.; Bruce, A. W. Intracavitary Bacillus Calmette-Guerin in the treatment of superficial bladder tumors. *J. Urol.* **1976**, *116*, 180–183.

73. Lamm, D. L.; Thor, D. E.; Harris, S. C.; Reyna, J. A.; Stogdill, V. D.; Radwin, H. M. Bacillus Calmette-Guerin Immunotherapy of Superficial Bladder-Cancer. *J. Urol.* **1980**, *124*, 38–42.

74. Camacho, F.; Pinsky, C.; Kerr, D.; Whitmore, W.; Oettgen, H. Treatment of Superficial Bladder-Cancer with Intravesical Bcg. *Proceedings of the American Association for Cancer Research* **1980**, *21*, 359–359.

75. Redelman-Sidi, G.; Glickman, M.; Bochner, B. The mechanism of action of BCG therapy for bladder cancer--a current perspective. *Nat Rev Urol* **2014**, *11*, 153–162.

76. Ratliff, T.; Palmer, J. O.; McGarr, J. A.; Brown, E. Intravesical Bacillus Calmette-Guérin therapy for murine bladder tumors: initiation of the response by fibronectin-mediated attachment of Bacillus Calmette-Guérin. *Cancer Res.* **1987**, *47*, 1762–1766.

77. Zhao, W.; Schorey, J.; Bong-Mastek, M.; Ritchey, J.; Brown, E.; Ratliff, T. Role of a bacillus Calmette-Guerin fibronectin attachment protein in BCG-induced antitumor activity. *Int. J. Cancer* **2000**, *86*, 83–88.

78. Coplen, D. E.; Brown, E.; McGarr, J.; Ratliff, T. Characterization of Fibronectin Attachment by a Human Transitional Cell-Carcinoma Line, T24. *J. Urol.* **1991**, *145*, 1312–1315.

79. Bevers, R.; de Boer, E. C.; Kurth, K. H.; Schamhart, D. BCG internalization in human bladder cancer cell lines, especially with regard to cell surface-expressed fibronectin. *Aktuelle Urologie* **2000**, *31*, 31–34.

80. Redelman-Sidi, G.; Iyer, G.; Solit, D.; Glickman, M. Oncogenic activation of Pak1-dependent pathway of macropinocytosis determines BCG entry into bladder cancer cells. *Cancer Res.* **2013**, *73*, 1156–1167.

81. Becich, M. J.; Carroll, S.; Ratliff, T. Internalization of Bacille Calmette-Guerin by Bladder-Tumor Cells. *J. Urol.* **1991**, *145*, 1316–1324.

82. Dharmawardhane, S.; Schürmann, A.; Sells, M. A.; Chernoff, J.; Schmid, S. L.; Bokoch, G. M. Regulation of macropinocytosis by p21-activated kinase-1. *Mol. Biol. Cell* **2000**, *11*, 3341–3352.

83. Bevers, R. F.; de Boer, E. C.; Kurth, K. H.; Schamhart, D. H. BCG-induced interleukin-6 upregulation and BCG internalization in well and poorly differentiated human bladder cancer cell lines. *Eur. Cytokine Netw.* **1998**, *9*, 181–186.

84. Zhang, G. J.; Crist, S. A.; McKerrow, A. K.; Xu, Y.; Ladehoff, D. C.; See, W. A. Autocrine IL-6 production by human transitional carcinoma cells upregulates expression of the alpha5beta1 firbonectin receptor. *J. Urol.* **2000**, *163*, 1553–1559.

85. Kaplanski, G.; Marin, V.; Montero-Julian, F.; Mantovani, A.; Farnarier, C. IL-6: a regulator of the transition from neutrophil to monocyte recruitment during inflammation. *Trends Immunol.* **2003**, *24*, 25–29.

86. Simons, M. P.; Nauseef, W. M.; Griffith, T. S. Neutrophils and TRAIL: insights into BCG immunotherapy for bladder cancer. *Immunol. Res.* **2007**, *39*, 79–93.

87. Ikeda, N.; Toida, I.; Iwasaki, A.; Kawai, K.; Akaza, H. Surface antigen expression on bladder tumor cells induced by bacillus Calmette-Guerin (BCG): A role of BCG internalization into tumor cells. *Int. J. Urol.* **2002**, *9*, 29–35.

88. Pook, S.-H.; Rahmat, J.; Esuvaranathan, K.; Mahendran, R. Internalization of Mycobacterium bovis, Bacillus Calmette Guerin, by bladder cancer cells is cytotoxic. *Oncology Reports* **2007**, *18*, 1315–1320.

89. de Boer, E. C.; De Jong, W. H.; van der Meijden, A. P.; Steerenberg, P. A.; Witjes, J.; Vegt, P. D.; Debruyne, F. M.; Ruitenberg, E. J. Presence of activated lymphocytes in the urine of patients with superficial bladder cancer after intravesical immunotherapy with bacillus Calmette-Guérin. *Cancer Immunol. Immunother.* **1991**, *33*, 411–416.

90. McAveney, K. M.; Gomella, L.; Lattime, E. Induction of TH1- and TH2-associated cytokine mRNA in mouse bladder following intravesical growth of the murine bladder tumor MB49 and BCG immunotherapy. *Cancer Immunol. Immunother.* **1994**, *39*, 401–406.

91. Luo, Y.; Chen, X.; O'Donnell, M. Role of Th1 and Th2 cytokines in BCG-induced IFN-γ production: cytokine promotion and simulation of BCG effect. *Cytokine* **2003**, *21*, 17–26.

92. Ratliff, T.; Ritchey, J.; Yuan, J.; Andriole, G.; Catalona, W. T-Cell Subsets Required for Intravesical Bcg Immunotherapy for Bladder-Cancer. *J. Urol.* **1993**, *150*, 1018–1023.

93. Brandau, S.; Riemensberger, J.; Jacobsen, M.; Kemp, D.; Zhao, W.; Zhao, X.; Jocham, D.; Ratliff, T. L.; B hle, A. NK cells are essential for effective BCG immunotherapy. *Int. J. Cancer* **2001**, *92*, 697–702.

94. Böhle, A.; Gerdes, J.; Ulmer, A. J.; Hofstetter, A. G.; Flad, H. D. Effects of local bacillus Calmette-Guerin therapy in patients with bladder carcinoma on immunocompetent cells of the bladder wall. *J. Urol.* **1990**, *144*, 53–58.

95. Yamada, H.; Matsumoto, S.; Matsumoto, T.; Yamada, T.; Yamashita, U. Enhancing effect of an inhibitor of nitric oxide synthesis on bacillus Calmette-Guerin-induced macrophage cytotoxicity against murine bladder cancer cell line MBT-2 in vitro. *Jpn. J. Cancer Res.* **2000**, *91*, 534–542.

96. Melekos, M. D.; Chionis, H.; Pantazakos, A.; Fokaefs, E.; Paranychianakis, G.; Dauaher, H. Intravesical Bacillus Calmette-Guerin Immunoprophylaxis of Superficial Bladder-Cancer - Results of a Controlled Prospective Trial with Modified Treatment Schedule. *J. Urol.* **1993**, *149*, 744–748.

97. Krege, S.; Giani, G.; Meyer, R.; Otto, T.; Rubben, H. A randomized multicenter trial of adjuvant therapy in superficial bladder cancer: transurethral resection only versus transurethral resection plus mitomycin C versus transurethral resection plus bacillus Calmette-Guerin. Participating Clinics. *J. Urol.* **1996**, *156*, 962–966.

98. Huncharek, M.; Kupelnick, B. Impact of intravesical chemotherapy versus BCG immunotherapy on recurrence of superficial transitional cell carcinoma of the bladder: metaanalytic reevaluation. *Am. J. Clin. Oncol.* **2003**, *26*, 402–407.

99. Sylvester, R. J.; van der Meijden, A.; Witjes, J.; Kurth, K. Bacillus Calmette-Guerin versus chemotherapy for the intravesical treatment of patients with carcinoma in situ of the bladder: A meta-analysis of the published results of randomized clinical trials. *J. Urol.* **2005**, *174*, 86–92.

100. Shelley, M. D.; Wilt, T. J.; Court, J.; Coles, B.; Kynaston, H.; Mason, M. D. Intravesical bacillus Calmette-Guerin is superior to mitomycin C in reducing tumour recurrence in high-risk superficial bladder cancer: a meta-analysis of randomized trials. *BJU International* **2004**, *93*, 485–490.

101. Donat, S. M. Evaluation and follow-up strategies for superficial bladder cancer. *Urologic Clinics of North America* **2003**, *30*, 765–776.

102. Downs, T. M.; Lee, D. J.; Scherr, D. S. Management of BCG Recurrent Bladder Cancer. In; Konety, B. R.; Chang, S. S., Eds.; Springer New York, 2015; pp. 245–263.

103. Zlotta, A.; Fleshner, N.; Jewett, M. The management of BCG failure in non-muscle-invasive bladder cancer: an update. *CUAJ* **2013**, *3*, 199–205.

104. Zlotta, A.; Fleshner, N.; Jewett, M. The management of BCG failure in non-muscle-invasive bladder cancer: an update. *Can Urol Assoc J* **2009**, *3*, S199–205.

105. O'Donnell, M.; Boehle, A. Treatment options for BCG failures. *World J Urol* **2006**, *24*, 481–487.

106. Gallagher, B. L.; Joudi, F. N.; Maymí, J. L.; O'Donnell, M. Impact of Previous Bacille

Calmette-Guérin Failure Pattern on Subsequent Response to Bacille Calmette-Guérin Plus Interferon Intravesical Therapy. *Urology* **2008**, *71*, 297–301.

107. Di Lorenzo, G.; Perdonà, S.; Damiano, R.; Faiella, A.; Cantiello, F.; Pignata, S.; Ascierto, P.; Simeone, E.; De Sio, M.; Autorino, R. Gemcitabine versus bacille Calmette-Guérin after initial bacille Calmette-Guérin failure in non-muscle-invasive bladder cancer. *Cancer* **2010**, *116*, 1893–1900.

108. Shelley, M. D.; Jones, G.; Cleves, A.; Wilt, T. J.; Mason, M. D.; Kynaston, H. G. Intravesical gemcitabine therapy for non-muscle invasive bladder cancer (NMIBC): a systematic review. *BJU International* **2012**, *109*, 496–505.

109. Mohanty, N. K.; Nayak, R. L.; Vasudeva, P.; Arora, R. P. Intravesicle gemcitabine in management of BCG refractory superficial TCC of urinary bladder—our experience. *Urol. Oncol.* **2008**, *26*, 616–619.

110. Barlow, L.; McKiernan, J.; Sawczuk, I.; Benson, M. A single-institution experience with induction and maintenance intravesical docetaxel in the management of non-muscle-invasive bladder cancer refractory to bacille Calmette-Guérin therapy. *BJU International* **2009**, *104*, 1098–1102.

111. Lightfoot, A. J.; Rosevear, H. M.; O'Donnell, M. Recognition and Treatment of BCG Failure in Bladder Cancer. *ScientificWorldJournal* **2011**, *11*, 602–613.

112. Huguet, J.; Crego, M.; Sabate, S.; Salvador, J.; Palou, J.; Villavicencio, H. Cystectomy in patients with high risk superficial bladder tumors who fail intravesical BCG therapy: Pre-cystectomy prostate involvement as a prognostic factor. *Eur. Urol.* **2005**, *48*, 53–59.

113. Fairey, A. S.; Jacobsen, N.-E. B.; Chetner, M. P.; Mador, D. R.; Metcalfe, J. B.; Moore, R. B.; Rourke, K. F.; Todd, G. T.; Venner, P. M.; Voaklander, D. C.; Estey, E. P. Associations Between Comorbidity, and Overall Survival and Bladder Cancer Specific Survival After Radical Cystectomy: Results From the Alberta Urology Institute Radical Cystectomy Database. *J. Urol.* **2009**, *182*, 85–93.

114. Lukka, H. In favour of bladder preservation using combined modality treatment. *Can Urol Assoc J* **2009**, *3*, 412–415.

115. Solsona, E.; Iborra, I.; Collado, A.; Rubio-Briones, J.; Casanova, J.; Calatrava, A. Feasibility of Radical Transurethral Resection as Monotherapy for Selected Patients With Muscle Invasive Bladder Cancer. *J. Urol.* **2010**, *184*, 475–480.

116. Kassouf, W.; Swanson, D.; Kamat, A. M.; Leibovici, D.; Siefker-Radtke, A.; Munsell, M. F.; Grossman, H. B.; Dinney, C. P. N. Partial cystectomy for muscle invasive urothelial carcinoma of the bladder: a contemporary review of the M. D. Anderson Cancer Center experience. *J. Urol.* **2006**, *175*, 2058–2062.

117. Knoedler, J. J.; Boorjian, S. A.; Kim, S. P.; Weight, C. J.; Thapa, P.; Tarrell, R. F.; Cheville, J. C.; Frank, I. Does Partial Cystectomy Compromise Oncologic Outcomes for Patients with

Bladder Cancer Compared to Radical Cystectomy? A Matched Case-Control Analysis. *J. Urol.* **2012**, *188*, 1115–1119.

118. Premo, C.; Apolo, A. B.; Agarwal, P. K.; Citrin, D. E. Trimodality Therapy in Bladder Cancer Who, What, and When? *Urol. Clin. North Am.* **2015**, *42*, 169–180.

119. James, N. D.; Hussain, S. A.; Hall, E.; Jenkins, P.; Tremlett, J.; Rawlings, C.; Crundwell, M.; Sizer, B.; Sreenivasan, T.; Hendron, C.; Lewis, R.; Waters, R.; Huddart, R. A.; Investigators, B. Radiotherapy with or without Chemotherapy in Muscle-Invasive Bladder Cancer. *N. Engl. J. Med.* **2012**, *366*, 1477–1488.

120. Ploussard, G.; Daneshmand, S.; Efstathiou, J. A.; Herr, H. W.; James, N. D.; Roedel, C. M.; Shariat, S. F.; Shipley, W. U.; Sternberg, C. N.; Thalmann, G.; Kassouf, W. Critical Analysis of Bladder Sparing with Trimodal Therapy in Muscle-invasive Bladder Cancer: A Systematic Review. *Eur. Urol.* **2014**, *66*, 120–137.

121. Park, J. C.; Hahn, N. M. Bladder cancer: a disease ripe for major advances. *Clin Adv Hematol Oncol* **2014**, *12*, 838–845.

122. Carneiro, B. A.; Meeks, J. J.; Kuzel, T. M.; Scaranti, M.; Abdulkadir, S. A.; Giles, F. J. Emerging therapeutic targets in bladder cancer. *Cancer Treatment Reviews* **2015**, *41*, 170–178.

123. Gozgit, J. M.; Wong, M. J.; Moran, L.; Wardwell, S.; Mohemmad, Q. K.; Narasimhan, N. I.; Shakespeare, W. C.; Wang, F.; Clackson, T.; Rivera, V. M. Ponatinib (AP24534), a Multitargeted Pan-FGFR Inhibitor with Activity in Multiple FGFR-Amplified or Mutated Cancer Models. *Mol. Cancer Ther.* **2012**, *11*, 690–699.

124. Chell, V.; Balmanno, K.; Little, A. S.; Wilson, M.; Andrews, S.; Blockley, L.; Hampson, M.; Gavine, P. R.; Cook, S. J. Tumour cell responses to new fibroblast growth factor receptor tyrosine kinase inhibitors and identification of a gatekeeper mutation in FGFR3 as a mechanism of acquired resistance. *Oncogene* **2013**, *32*, 3059–3070.

125. Tabernero, J.; Bahleda, R.; Dienstmann, R.; Infante, J. R.; Mita, A.; Italiano, A.; Calvo, E.; Moreno, V.; Adamo, B.; Gazzah, A.; Zhong, B.; Platero, S. J.; Smit, J. W.; Stuyckens, K.; Chatterjee-Kishore, M.; Rodon, J.; Peddareddigari, V.; Luo, F. R.; Soria, J.-C. Phase I Dose-Escalation Study of JNJ-42756493, an Oral Pan-Fibroblast Growth Factor Receptor Inhibitor, in Patients With Advanced Solid Tumors. *J. Clin. Oncol.* **2015**, *33*, 3401–.

126. Porta, C.; Paglino, C.; Mosca, A. Targeting PI3K/Akt/mTOR Signaling in Cancer. *Frontiers in Oncology* **2014**, *4*, 64.

127. Wu, D.; Tao, J.; Xu, B.; Qing, W.; Li, P.; Lu, Q.; Zhang, W. Phosphatidylinositol 3-Kinase Inhibitor LY294002 Suppresses Proliferation and Sensitizes Doxorubicin Chemotherapy in Bladder Cancer Cells. *Urol. Int.* **2011**, *86*, 346–354.

128. Moon, D. G.; Lee, S. E.; Oh, M. M.; Lee, S. C.; Jeong, S. J.; Hong, S. K.; Yoon, C. Y.; Byun, S. S.; Park, H. S.; Cheon, J. NVP-BEZ235, a dual PI3K/mTOR inhibitor synergistically potentiates the antitumor effects of cisplatin in bladder cancer cells. *Int. J. Oncol.* **2014**, *45*, 1027–1035.

129. Iqbal, N.; Iqbal, N. Human Epidermal Growth Factor Receptor 2 (HER2) in Cancers: Overexpression and Therapeutic Implications. *Mol Biol Int* **2014**, *2014*, 852748–9.

130. Skagias, L.; Politi, E.; Karameris, A.; Sambaziotis, D.; Archondakis, A.; Vasou, O.; Ntinis, A.; Michalopoulou, F.; Moreas, I.; Koutselini, H.; Patsouris, E. Prognostic impact of HER2/neu protein in urothelial bladder cancer. Survival analysis of 80 cases and an overview of almost 20 years' research. *J BUON* **2009**, *14*, 457–462.

131. Hussain, M. H. A.; MacVicar, G. R.; Petrylak, D. P.; Dunn, R. L.; Vaishampayan, U.; Lara, P. N. J.; Chatta, G. S.; Nanus, D. M.; Glode, L. M.; Trump, D. L.; Chen, H.; Smith, D. C. Trastuzumab, paclitaxel, carboplatin, and gemcitabine in advanced human epidermal growth factor receptor-2/neu-positive urothelial carcinoma: Results of a multicenter phase II National Cancer Institute trial. *J. Clin. Oncol.* **2007**, *25*, 2218–2224.

132. Kaufman, H.; Kohlhapp, F.; Zloza, A. Oncolytic viruses: a new class of immunotherapy drugs. *Nat Rev Drug Discov* **2015**, *14*, 642–662.

133. Russell, S.; Peng, K.-W.; Bell, J. Oncolytic virotherapy. *Nat. Biotechnol.* **2012**, *30*, 658–670.

134. Delwar, Z.; Zhang, K.; Rennie, P.; Jia, W. Oncolytic virotherapy for urological cancers. *Nat Rev Urol* **2016**, *13*, 334–352.

135. Potts, K. G.; Irwin, C. R.; Favis, N. A.; Pink, D. B.; Vincent, K. M.; Lewis, J. D.; Moore, R. B.; Hitt, M. M.; Evans, D. H. Deletion of F4L (ribonucleotide reductase) in vaccinia virus produces a selective oncolytic virus and promotes anti-tumor immunity with superior safety in bladder cancer models. *EMBO Mol Med* **2017**, e201607296.

136. Kelly, E.; Russell, S. History of oncolytic viruses: Genesis to genetic engineering. *Mol. Ther.* **2007**, *15*, 651–659.

137. Dock, G. The influence of complicating diseases upon leukemia. *Am. J. Med. Sci.* **1904**, *127*, 563–592.

138. De Pace, N. Sulla scomparsa di un enorme cancro vegetante del callo dell'utero senza cura chirurgica. *Ginecologia* **1912**, *9*, 82–89.

139. Hoster, H. A.; Zanes, R. P.; Vonhaam, E. Studies in Hodgkin"s syndrome; the association of viral hepatitis and Hodgkin"s disease; a preliminary report. *Cancer Res.* **1949**, *9*, 473–480.

140. Southam, C. M.; Moore, A. E. Clinical Studies of Viruses as Antineoplastic Agents, with Particular Reference to Egypt 101 Virus. *Cancer* **1952**, *5*, 1025–1034.

141. Georgiades, J.; Zielinski, T.; Cicholska, A.; Jordan, E. Research on the oncolytic effect of APC viruses in cancer of the cervix uteri; preliminary report. *Biul Inst Med Morsk Gdansk* **1959**, *10*, 49–57.

142. Asada, T. Treatment of Human Cancer with Mumps Virus. *Cancer* **1974**, *34*, 1907–1928.

143. Sato, M.; Urade, M.; Sakuda, M.; Shirasuna, K.; Yoshida, H.; Maeda, N.; Yanagawa, T.; Morimoto, M.; Yura, Y.; Miyazaki, T.; Okuno, Y.; Takahashi, M. Attenuated Mumps-Virus Therapy of Carcinoma of the Maxillary Sinus. *Int J Oral Surg* **1979**, *8*, 205–211.

144. Okuno, Y.; Asada, T.; Yamanishi, K.; Otsuka, T.; Takahashi, M.; Tanioka, T.; Aoyama, H.; Fukui, O.; Matsumoto, K.; Uemura, F.; Wada, A. Studies on the use of mumps virus for treatment of human cancer. *Biken J* **1978**, *21*, 37–49.

145. Southam, C. M. Present status of oncolytic virus studies. *Transactions of the New York Academy of Sciences* **1960**, *22*, 657–673.

146. Martuza, R. L.; Malick, A.; Markert, J. M.; Ruffner, K. L.; Coen, D. M. Experimental therapy of human glioma by means of a genetically engineered virus mutant. *Science* **1991**, *252*, 854–856.

147. Guo, Z.; Liu, Z.; Bartlett, D. Oncolytic Immunotherapy: Dying the Right Way is a Key to Eliciting Potent Antitumor Immunity. *Frontiers in Oncology* **2014**, *4*, 1–11.

148. Tong, A. W.; Senzer, N.; Cerullo, V.; Templeton, N. S.; Hemminki, A.; Nemunaitis, J. Oncolytic Viruses for Induction of Anti-Tumor Immunity. *Curr Pharm Biotechnol* **2012**, *13*, 1750–1760.

149. Chiocca, E. A.; Rabkin, S. D. Oncolytic Viruses and Their Application to Cancer Immunotherapy. *Cancer Immunol Res* **2014**, *2*, 295–300.

150. Workenhe, S. T.; Mossman, K. L. Rewiring cancer cell death to enhance oncolytic viro-immunotherapy. *Oncoimmunology* **2013**, *2*.

151. Workenhe, S. T.; Mossman, K. L. Oncolytic Virotherapy and Immunogenic Cancer Cell Death: Sharpening the Sword for Improved Cancer Treatment Strategies. *Mol. Ther.* **2014**, *22*, 251–256.

152. Bhat, R.; Rommelaere, J. Emerging role of Natural killer cells in oncolytic virotherapy. *Immunotargets Ther* **2015**, *4*, 65–77.

153. Karre, K.; Ljunggren, H. G.; Piontek, G.; Kiessling, R. Selective Rejection of H-2-Deficient Lymphoma Variants Suggests Alternative Immune Defense Strategy. *Nature* **1986**, *319*, 675–678.

154. Choi, Y.-E.; Yu, H.-N.; Yoon, C.-H.; Bae, Y.-S. Tumor-mediated down-regulation of MHC class II in DC development is attributable to the epigenetic control of the CIITA type I promoter. *Eur. J. Immunol.* **2009**, *39*, 858–868.

155. Grote, D.; Cattaneo, R.; Fielding, A. K. Neutrophils contribute to the measles virus-induced antitumor effect: Enhancement by granulocyte macrophage colony-stimulating factor expression. *Cancer Res.* **2003**, *63*, 6463–6468.

156. Uribe-Querol, E.; Rosales, C. Neutrophils in Cancer: Two Sides of the Same Coin. *J Immunol Res* **2015**, *2015*, –21.

157. Breitbach, C.; Paterson, J. M.; Lemay, C. G.; Falls, T. J.; McGuire, A.; Parato, K. A.; Stojdl, D. F.; Daneshmand, M.; Speth, K.; Kirn, D.; McCart, A.; Atkins, H.; Bell, J. Targeted inflammation during oncolytic virus therapy severely compromises tumor blood flow. *Mol. Ther.* **2007**, *15*, 1686–1693.

158. Breitbach, C.; Arulanandam, R.; De Silva, N.; Thorne, S. H.; Patt, R.; Daneshmand, M.; Moon, A.; Ilkow, C.; Burke, J.; Hwang, T.-H.; Heo, J.; Cho, M.; Chen, H.; Angarita, F. A.; Addison, C.; McCart, A.; Bell, J.; Kirn, D. Oncolytic vaccinia virus disrupts tumor-associated vasculature in humans. *Cancer Res.* **2013**, *73*, 1265–1275.

159. Breitbach, C.; De Silva, N. S.; Falls, T. J.; Aladl, U.; Evgin, L.; Paterson, J.; Sun, Y. Y.; Roy, D. G.; Rintoul, J. L.; Daneshmand, M.; Parato, K.; Stanford, M. M.; Lichty, B. D.; Fenster, A.; Kirn, D.; Atkins, H.; Bell, J. Targeting Tumor Vasculature With an Oncolytic Virus. *Mol. Ther.* **2011**, *19*, 886–894.

160. Michaelis, M.; Driever, P. H.; Cinatl, J.; Hrabeta, J.; Suhan, T.; Doerr, H. W.; Vogel, J. U. Multimutated herpes simplex virus G207 is a potent inhibitor of angiogenesis. *Neoplasia* **2004**, *6*, 725–735.

161. Hanahan, D.; Weinberg, R. A. Hallmarks of Cancer: The Next Generation. *Cell* **2011**, *144*, 646–674.

162. Coffey, M. C.; Strong, J. E.; Forsyth, P. A.; Lee, P. Reovirus therapy of tumors with activated Ras pathway. *Science* **1998**, *282*, 1332–1334.

163. Chan, W. M.; Rahman, M. M.; McFadden, G. Oncolytic myxoma virus: The path to clinic. *Vaccine* **2013**, *31*, 4252–4258.

164. Barber, G. N. Vesicular stomatitis virus as an oncolytic vector. *Viral Immunol.* **2004**, *17*, 516–527.

165. Au, G. G.; Lincz, L. F.; Enno, A.; Shafren, D. R. Oncolytic Coxsackievirus A21 as a novel therapy for multiple myeloma. *Br. J. Haematol.* **2007**, *137*, 133–141.

166. Singh, P. K.; Doley, J.; Kumar, G. R.; Sahoo, A. P.; Tiwari, A. K. Oncolytic viruses & their specific targeting to tumour cells. *Indian Journal of Medical Research* **2012**, *136*, 571–584.

167. Verheije, M. H.; Rottier, P. J. M. Retargeting of viruses to generate oncolytic agents. *Adv Virol* **2012**, *2012*, 798526–15.

168. Murofushi, Y.; Nagano, S.; Kamizono, J.; Takahashi, T.; Fujiwara, H.; Komiya, S.; Matsuishi, T.; Kosai, K.-I. Cell cycle-specific changes in hTERT promoter activity in normal and cancerous cells in adenoviral gene therapy: A promising implication of telomerase-dependent targeted cancer gene therapy. *Int. J. Oncol.* **2006**, *29*, 681–688.

169. Bao, R. D.; Connolly, D. C.; Murphy, M.; Green, J.; Weinstein, J. K.; Pisarcik, D. A.; Hamilton, T. C. Activation of cancer-specific gene expression by the survivin promoter. *J. Natl. Cancer Inst.* **2002**, *94*, 522–528.

170. Gotoh, A.; Ko, S. C.; Shirakawa, T.; Cheon, J.; Kao, C. H.; Miyamoto, T.; Gardner, T. A.; Ho, L. J.; Cleutjens, C.; Trapman, J.; Graham, F. L.; Chung, L. Development of prostate-specific antigen promoter-based gene therapy for androgen-independent human prostate cancer. *J. Urol.* **1998**, *160*, 220–229.

171. Pesonen, S.; Diaconu, I.; Kangasniemi, L.; Ranki, T.; Kanerva, A.; Pesonen, S. K.; Gerdemann, U.; Leen, A. M.; Kairemo, K.; Oksanen, M.; Haavisto, E.; Holm, S.-L.; Karioja-Kallio, A.; Kauppinen, S.; Partanen, K. P. L.; Laasonen, L.; Joensuu, T.; Alanko, T.; Cerullo, V.; Hemminki, A. Oncolytic Immunotherapy of Advanced Solid Tumors with a CD40L-Expressing Replicating Adenovirus: Assessment of Safety and Immunologic Responses in Patients. *Cancer Res.* **2012**, *72*, 1621–1631.

172. Yu, F.; Wang, X.; Guo, Z. S.; Bartlett, D.; Gottschalk, S. M.; Song, X.-T. T-cell Engager-armed Oncolytic Vaccinia Virus Significantly Enhances Antitumor Therapy. *Mol. Ther.* **2014**, *22*, 102–111.

173. Shen, Z.; Shen, T.; Wientjes, M.; O'Donnell, M.; Au, J. Intravesical treatments of bladder cancer: review. *Pharm. Res.* **2008**, *25*, 1500–1510.

174. de Bruijn, E. A.; Sleeboom, H. P.; van Helsdingen, P. J. R. O.; van Oosterom, A. T.; Tjden, U. R.; Maes, R. A. A. Pharmacodynamics and pharmacokinetics of intravesical mitomycin C upon different dwelling times. *Int. J. Cancer* **1992**.

175. Song, D.; Wientjes, M. G.; Au, J. Bladder tissue pharmacokinetics of intravesical taxol. *Cancer Chemother. Pharmacol.* **1997**, *40*, 285–292.

176. Lamm, D. L.; van der Meijden, P. M.; Morales, A.; Brosman, S. A.; Catalona, W.; Herr, H. W.; Soloway, M. S.; Steg, A.; Debruyne, F. M. Incidence and treatment of complications of bacillus Calmette-Guerin intravesical therapy in superficial bladder cancer. *J. Urol.* **1992**, *147*, 596–600.

177. Lamm, D. L. Bacillus Calmette-Guerin Immunotherapy for Bladder-Cancer. *J. Urol.* **1985**, *134*, 40–47.

178. Potts, K. G.; Hitt, M. M.; Moore, R. B. Oncolytic viruses in the treatment of bladder cancer. *Adv. Urol.* **2012**, *2012*, 404581.

179. Whitley, R. J.; Kimberlin, D. W.; Roizman, B. Herpes simplex viruses. *Clin. Infect. Dis.* **1998**, *26*, 541–553.

180. Kieff, E. D.; Bachenheimer, S. L.; Roizman, B. Size, composition, and structure of the deoxyribonucleic acid of herpes simplex virus subtypes 1 and 2. *J. Virol.* **1971**, *8*, 125–132.

181. Whitley, R. J.; Roizman, B. Herpes simplex virus infections. *Lancet* **2001**, *357*, 1513–1518.

182. Mineta, T.; Rabkin, S. D.; Martuza, R. L. Treatment of Malignant Gliomas Using Ganciclovir-Hypersensitive, Ribonucleotide Reductase-Deficient Herpes-Simplex Viral Mutant. *Cancer Res.* **1994**, *54*, 3963–3966.

183. Varghese, S.; Rabkin, S. D. Oncolytic herpes simplex virus vectors for cancer virotherapy. *Cancer Gene Ther.* **2002**, *9*, 967–978.

184. Nordlund, P.; Reichard, P. Ribonucleotide reductases. *Annu. Rev. Biochem.* **2006**, *75*, 681–706.

185. Bolovan, C. A.; Sawtell, N. M.; Thompson, R. L. ICP34.5 Mutants of Herpes-Simplex Virus Type-1 Strain 17syn+ Are Attenuated for Neurovirulence in Mice and for Replication in Confluent Primary Mouse Embryo Cell-Cultures. *J. Virol.* **1994**, *68*, 48–55.

186. Brown, S. M.; MacLean, A. R.; Aitken, J. D.; Harland, J. ICP34.5 influences herpes-simplex virus type-1 maturation and egress from infected cells *in vitro*. *J. Gen. Virol.* **1994**, *75*, 3679–3686.

187. He, B.; Gross, M.; Roizman, B. The gamma(1)34.5 protein of herpes simplex virus I complexes with protein phosphatase 1 alpha to dephosphorylate the alpha subunit of the eukaryotic translation initiation factor 2 and preclude the shutoff of protein synthesis by double-stranded RNA-activated protein kinase. *PNAS* **1997**, *94*, 843–848.

188. Chou, J.; Kern, E. R.; Whitley, R. J.; Roizman, B. Mapping of herpes simplex virus-1 neurovirulence to gamma 134.5, a gene nonessential for growth in culture. *Science* **1990**, *250*, 1262–1266.

189. McKie, E. A.; MacLean, A. R.; Lewis, A. D.; Cruickshank, G.; Rampling, R.; Barnett, S. C.; Kennedy, P.; Brown, S. M. Selective in vitro replication of herpes simplex virus type 1 (HSV-1) ICP34.5 null mutants in primary human CNS tumours - evaluation of a potentially effective clinical therapy. *Br. J. Cancer* **1996**, *74*, 745–752.

190. Sanders, P. G.; Wilkie, N. M.; Davison, A. J. Thymidine Kinase Deletion Mutants of Herpes-Simplex Virus Type-1. *J. Gen. Virol.* **1982**, *63*, 277–295.

191. Wong, R. J.; Patel, S. G.; Kim, S. H.; DeMatteo, R. P.; Malhotra, S.; Bennett, J. J.; St-Louis, M.; Shah, J. P.; Johnson, P. A.; Fong, Y. M. Cytokine gene transfer enhances herpes oncolytic therapy in murine squamous cell carcinoma. *Hum. Gene Ther.* **2001**, *12*, 253–265.

192. Carew, J. F.; Kooby, D. A.; Halterman, M. W.; Kim, S. H.; Federoff, H. J.; Fong, Y. M. A novel approach to cancer therapy using an oncolytic herpes virus to package amplicons containing cytokine genes. *Mol. Ther.* **2001**, *4*, 250–256.

193. Toda, M.; Martuza, R. L.; Kojima, H.; Rabkin, S. D. In situ cancer vaccination: An IL-12 defective vector replication-competent herpes simplex virus combination induces local and systemic antitumor activity. *J. Immunol.* **1998**, *160*, 4457–4464.

194. Todo, T.; Martuza, R. L.; Dallman, M. J.; Rabkin, S. D. In situ expression of soluble B7-1 in the context of oncolytic herpes simplex virus induces potent antitumor immunity. *Cancer Res.* **2001**, *61*, 153–161.

195. Pawlik, T. M.; Nakamura, H.; Yoon, S. S.; Mullen, J. T.; Chandrasekhar, S.; Chiocca, E. A.; Tanabe, K. K. Oncolysis of diffuse hepatocellular carcinoma by intravascular administration of a

replication-competent, genetically engineered herpesvirus. *Cancer Res.* **2000**, *60*, 2790–2795.

196. Yoon, S. S.; Carroll, N. M.; Chiocca, E. A.; Tanabe, K. K. Cancer gene therapy using a replication-competent herpes simplex virus type 1 vector. *Ann. Surg.* **1998**, *228*, 366–372.

197. Cozzi, P. J.; Malhotra, S.; Mcauliffe, P.; Kooby, D. A.; Federoff, H. J.; Huryk, B.; Johnson, P.; Scardino, P. T.; Heston, W.; Fong, Y. Intravesical oncolytic viral therapy using attenuated, replication-competent herpes simplex viruses G207 and Nv1020 is effective in the treatment of bladder cancer in an orthotopic syngeneic model. *FASEB J.* **2001**, *15*, 1306–1308.

198. Mineta, T.; Rabkin, S. D.; Yazaki, T.; Hunter, W. D.; Martuza, R. L. Attenuated Multi-Mutated Herpes-Simplex Virus-1 for the Treatment of Malignant Gliomas. *Nat. Med.* **1995**, *1*, 938–943.

199. Kelly, K.; Wong, J.; Fong, Y. Herpes simplex virus NV1020 as a novel and promising therapy for hepatic malignancy. *Expert Opin Investig Drugs* **2008**, *17*, 1105–1113.

200. Simpson, G.; Horvath, A.; Annels, N.; Pencavel, T.; Metcalf, S.; Seth, R.; Peschard, P.; Price, T.; Coffin, R.; Mostafid, H.; Melcher, A.; Harrington, K.; Pandha, H. Combination of a fusogenic glycoprotein, pro-drug activation and oncolytic HSV as an intravesical therapy for superficial bladder cancer. *Br. J. Cancer* **2012**, *106*, 496–507.

201. Higuchi, H.; Bronk, S. F.; Bateman, A.; Harrington, K.; Vile, R. G.; Gores, G. J. Viral fusogenic membrane glycoprotein expression causes syncytia formation with bioenergetic cell death: implications for gene therapy. *Cancer Res.* **2000**, *60*, 6396–6402.

202. Rehman, H.; Silk, A. W.; Kane, M. P.; Kaufman, H. Into the clinic: Talimogene laherparepvec (T-VEC), a first-in-class intratumoral oncolytic viral therapy. *J Immunother Cancer* **2016**, *4*, 53.

203. Hu, J. C. C.; Coffin, R.; Davis, C. J.; Graham, N. J.; Groves, N.; Guest, P. J.; Harrington, K. J.; James, N. D.; Love, C. A.; McNeish, I.; Medley, L. C.; Michael, A.; Nutting, C. M.; Pandha, H. S.; Shorrock, C. A.; Simpson, J.; Steiner, J.; Steven, N. M.; Wright, D.; Coombes, R. C. A phase I study of OncoVEXGM-CSF, a second-generation oncolytic herpes simplex virus expressing granulocyte macrophage colony-stimulating factor. *Clin. Cancer Res.* **2006**, *12*, 6737–6747.

204. Senzer, N. N.; Kaufman, H.; Amatruda, T.; Nemunaitis, M.; Reid, T.; Daniels, G.; Gonzalez, R.; Glaspy, J.; Whitman, E.; Harrington, K.; Goldsweig, H.; Marshall, T.; Love, C.; Coffin, R.; Nemunaitis, J. Phase II clinical trial of a granulocyte-macrophage colony-stimulating factor-encoding, second-generation oncolytic herpesvirus in patients with unresectable metastatic melanoma. *J. Clin. Oncol.* **2009**, *27*, 5763–5771.

205. Andtbacka, R.; Kaufman, H.; Collichio, F.; Amatruda, T.; Senzer, N.; Chesney, J.; Delman, K.; Spitler, L.; Puzanov, I.; Agarwala, S.; Milhem, M.; Cranmer, L.; Curti, B.; Lewis, K.; Ross, M.; Guthrie, T.; Linette, G.; Daniels, G.; Harrington, K.; Middleton, M.; Miller, W.; Zager, J.; Ye, Y.; Yao, B.; Li, A.; Doleman, S.; VanderWalde, A.; Gansert, J.; Coffin, R. Talimogene Laherparepvec Improves Durable Response Rate in Patients With Advanced Melanoma. *J. Clin. Oncol.* **2015**, *33*, 2780–2788.

206. Martuza, R. L. Conditionally replicating herpes vectors for cancer therapy. *J. Clin. Invest.* **2000**, *105*, 841–846.

207. Früh, K.; Ahn, K.; Djaballah, H.; Sempé, P.; van Endert, P. M.; Tampé, R.; Peterson, P. A.; Yang, Y. A viral inhibitor of peptide transporters for antigen presentation. *Nature* **1995**, *375*, 415–418.

208. Kaufman, H.; Bines, S. D. OPTIM trial: a Phase III trial of an oncolytic herpes virus encoding GM-CSF for unresectable stage III or IV melanoma. *Future Oncol* **2010**, *6*, 941–949.

209. Ghebremedhin, B. Human adenovirus: Viral pathogen with increasing importance. *Eur J Microbiol Immunol (Bp)* **2014**, *4*, 26–33.

210. Habib, N.; Salama, H.; Abd El Latif Abu Median, A.; Isac Anis, I.; Abd Al Aziz, R. A.; Sarraf, C.; Mitry, R.; Havlik, R.; Seth, P.; Hartwigsen, J.; Bhushan, R.; Nicholls, J.; Jensen, S. Clinical trial of E1B-deleted adenovirus (dl1520) gene therapy for hepatocellular carcinoma. *Cancer Gene Ther.* **2002**, *9*, 254–259.

211. Lu, W. Intra-tumor injection of H101, a recombinant adenovirus, in combination with chemotherapy in patients with advanced cancers: A pilot phase II clinical trial. *World Journal of Gastroenterology* **2004**, *10*, 3634.

212. Garber, K. China approves world's first oncolytic virus therapy for cancer treatment. *J. Natl. Cancer Inst.* **2006**, *98*, 298–300.

213. Fueyo, J.; Gomez-Manzano, C.; Alemany, R.; Lee, P. S.; McDonnell, T. J.; Mitlianga, P.; Shi, Y.-X.; Levin, V. A.; Yung, W. K. A.; Kyritsis, A. P. A mutant oncolytic adenovirus targeting the Rb pathway produces anti-glioma effect in vivo. *Oncogene* **2000**, *19*, 2–12.

214. Heise, C.; Ganly, I.; Kim, Y. T.; Sampson-Johannes, A.; Brown, R.; Kirn, D. Efficacy of a replication-selective adenovirus against ovarian carcinomatosis is dependent on tumor burden, viral replication and p53 status. *Gene Therapy* **2000**, *7*, 1925–1929.

215. Edwards, S. J.; Dix, B. R.; Myers, C. J.; Dobson-Le, D.; Huschtscha, L.; Hibma, M.; Royds, J.; Braithwaite, A. W. Evidence that Replication of the Antitumor Adenovirus ONYX-015 Is Not Controlled by the p53 and p14ARF Tumor Suppressor Genes. *J. Virol.* **2002**, *76*, 12483–12490.

216. Sadeghi, H.; Hitt, M. Transcriptionally Targeted Adenovirus Vectors. *Current Gene Therapy* **2005**, *5*, 411–427.

217. Rodriguez, R.; Schuur, E. R.; Lim, H. Y.; Henderson, G. A.; Simons, J. W.; Henderson, D. R. Prostate attenuated replication competent adenovirus (ARCA) CN706: A selective cytotoxic for prostate-specific antigen-positive prostate cancer cells. *Cancer Res.* **1997**, *57*, 2559–2563.

218. van Beusechem, V. W.; Mastenbroek, D. C. J.; van den Doel, P. B.; Lamfers, M. L. M.; Grill, J.; Wurdinger, T.; Haisma, H. J.; Pinedo, H. M.; Gerritsen, W. R. Conditionally replicative adenovirus expressing a targeting adapter molecule exhibits enhanced oncolytic potency on CAR-deficient tumors. *Gene Therapy* **2003**, *10*, 1982–1991.

219. Yang, Y.; Xu, H.; Shen, J.; Wu, S.; Xiao, J.; Xu, Y.; Liu, X.-Y.; Chu, L. RGD-modifided oncolytic adenovirus exhibited potent cytotoxic effect on CAR-negative bladder cancer-initiating cells. *Cell Death Dis* **2015**, *6*, e1760.

220. Toth, K.; Dhar, D.; Wold, W. S. M. Oncolytic (replication-competent) adenoviruses as anticancer agents. *Expert Opin Biol Ther* **2010**, *10*, 353–368.

221. Burke, J.; Lamm, D.; Meng, M.; Nemunaitis, J.; Stephenson, J.; Arseneau, J.; Aimi, J.; Lerner, S.; Yeung, A.; Kazarian, T.; Maslyar, D.; McKiernan, J. A first in human phase 1 study of CG0070, a GM-CSF expressing oncolytic adenovirus, for the treatment of nonmuscle invasive bladder cancer. *J. Urol.* **2012**, *188*, 2391–2397.

222. Ramesh, N.; Ge, Y.; Ennist, D.; Zhu, M.; Mina, M.; Ganesh, S.; Reddy, P.; Yu, D.-C. CG0070, a conditionally replicating granulocyte macrophage colony-stimulating factor-armed oncolytic adenovirus for the treatment of bladder cancer. *Clin. Cancer Res.* **2006**, *12*, 305–313.

223. Neuman, E.; Flemington, E. K.; Sellers, W. R.; Kaelin, W. G. Transcription of the E2F-1 gene is rendered cell cycle dependent by E2F DNA-binding sites within its promoter. *Mol. Cell. Biol.* **1994**, *14*, 6607–6615.

224. Miyamoto, H.; Shuin, T.; Torigoe, S.; Iwasaki, Y.; Kubota, Y. Retinoblastoma Gene-Mutations in Primary Human Bladder-Cancer. *Br. J. Cancer* **1995**, *71*, 831–835.

225. Nemunaitis, J. A comparative review of colony-stimulating factors. *Drugs* **1997**, *54*, 709–729.

226. Friedlander, T. W.; Weinberg, V. K.; Yeung, A.; Burke, J.; Lamm, D.; McKiernan, J.; Nemunaitis, J.; Stephenson, J.; Small, E. J.; Fong, L.; Meng, M. Activity of intravesical CG0070 in Rb-inactive superficial bladder cancer after BCG failure: Updated results of a phase I/II trial. *J. Clin. Oncol.* **2012**, *30*.

227. Danthi, P.; Guglielmi, K. M.; Kirchner, E.; Mainou, B.; Stehle, T.; Dermody, T. S. From touchdown to transcription: the reovirus cell entry pathway. *Curr. Top. Microbiol. Immunol.* **2010**, *343*, 91–119.

228. Hashiro, G.; Loh, P. C.; Yau, J. T. The preferential cytotoxicity of reovirus for certain transformed cell lines. *Arch. Virol.* **1977**, *54*, 307–315.

229. Bos, J. L. Ras Oncogenes in Human Cancer - a Review. *Cancer Res.* **1989**, *49*, 4682–4689.

230. Oxford, G.; Theodorsecu, D. Review Article: The Role of Ras Superfamily Proteins in Bladder Cancer Progression. *J. Urol.* **2003**, *170*, 1987–1993.

231. Gong, J.; Sachdev, E.; Mita, A. C.; Mita, M. M. Clinical development of reovirus for cancer therapy: An oncolytic virus with immune-mediated antitumor activity. *World J Methodol* **2016**, *6*, 25–42.

232. Hanel, E.; Xiao, Z. W.; Wong, K.; Lee, P.; Britten, R.; Moore, R. A novel intravesical therapy

for superficial bladder cancer in an orthotopic model: Oncolytic reovirus therapy. *J. Urol.* **2004**, *172*, 2018–2022.

233. Thirukkumaran, C.; Morris, D. G. Oncolytic Viral Therapy Using Reovirus. *Methods Mol. Biol.* **2015**, *1317*, 187–223.

234. Vidal, L.; Pandha, H. S.; Yap, T. A.; White, C. L.; Twigger, K.; Vile, R. G.; Melcher, A.; Coffey, M.; Harrington, K. J.; DeBono, J. S. A phase I study of intravenous oncolytic reovirus type 3 Dearing in patients with advanced cancer. *Clin. Cancer Res.* **2008**, *14*, 7127–7137.

235. Riedel, S. Edward Jenner and the history of smallpox and vaccination. *Proc (Bayl Univ Med Cent)* **2005**, *18*, 21–25.

236. Qin, L.; Favis, N.; Famulski, J.; Evans, D. H. Evolution of and Evolutionary Relationships between Extant Vaccinia Virus Strains. *J. Virol.* **2015**, *89*, 1809–1824.

237. Baxby, D. The origins of vaccinia virus. *J. Infect. Dis.* **1977**, *136*, 453–455.

238. Sanchez-Sampedro, L.; Perdiguero, B.; Mejias-Perez, E.; Garcia-Arriaza, J.; Di Pilato, M.; Esteban, M. The Evolution of Poxvirus Vaccines. *Viruses* **2015**, *7*, 1726–1803.

239. Jacobs, B. L.; Langland, J. O.; Kibler, K. V.; Denzier, K. L.; White, S. D.; Holechek, S. A.; Wong, S.; Huynh, T.; Baskin, C. R. Vaccinia virus vaccines: Past, present and future. *Antiviral Res.* **2009**, *84*, 1–13.

240. Qin, L.; Upton, C.; Hazes, B.; Evans, D. H. Genomic Analysis of the Vaccinia Virus Strain Variants Found in Dryvax Vaccine. *J. Virol.* **2011**, *85*, 13049–13060.

241. McFadden, G. Poxvirus tropism. *Nat Rev Micro* **2005**, *3*, 201–213.

242. Beaud, G. Vaccinia virus DNA replication: a short review. *Biochimie* **1995**, *77*, 774–779.

243. Seet, B. T.; Johnston, J. B.; Brunetti, C. R.; Barrett, J. W.; Everett, H.; Cameron, C.; Sypula, J.; Nazarian, S. H.; Lucas, A.; McFadden, G. Poxviruses and immune evasion. *Annu. Rev. Immunol.* **2003**, *21*, 377–423.

244. Condit, R. C.; Moussatche, N.; Traktman, P. In a nutshell: structure and assembly of the vaccinia virion. *Adv. Virus Res.* **2006**, *66*, 31–124.

245. Moss, B. Poxvirus entry and membrane fusion. *Virology* **2006**, *344*, 48–54.

246. Smith, G.; Vanderplasschen, A. Extracellular enveloped vaccinia virus - Entry, egress, and evasion. *Adv. Exp. Med. Biol.* **1998**, *440*, 395–414.

247. Bengali, Z.; Townsley, A. C.; Moss, B. Vaccinia virus strain differences in cell attachment and entry. *Virology* **2009**, *389*, 132–140.

248. Laliberte, J. P.; Weisberg, A. S.; Moss, B. The membrane fusion step of vaccinia virus entry is cooperatively mediated by multiple viral proteins and host cell components. *PLoS Pathog.* **2011**,

7, e1002446.

249. Townsley, A.; Weisberg, A.; Wagenaar, T.; Moss, B. Vaccinia virus entry into cells via a low-pH-dependent endosomal pathway. *J. Virol.* **2006**, *80*, 8899–8908.

250. Mercer, J.; Helenius, A. Vaccinia virus uses macropinocytosis and apoptotic mimicry to enter host cells. *Science* **2008**, *320*, 531–535.

251. Broyles, S. S. Vaccinia virus transcription. *J. Gen. Virol.* **2003**, *84*, 2293–2303.

252. Roberts, K. L.; Smith, G. L. Vaccinia virus morphogenesis and dissemination. *Trends Microbiol.* **2008**, *16*, 472–479.

253. Schramm, B.; Locker, J. K. Cytoplasmic organization of POXvirus DNA replication. *Traffic* **2005**, *6*, 839–846.

254. Assarsson, E.; Greenbaum, J. A.; Sundstrom, M.; Schaffer, L.; Hammond, J. A.; Pasquetto, V.; Oseroff, C.; Hendrickson, R. C.; Lefkowitz, E. J.; Tscharke, D. C.; Sidney, J.; Grey, H. M.; Head, S. R.; Peters, B.; Sette, A. Kinetic analysis of a complete poxvirus transcriptome reveals an immediate-early class of genes. *PNAS* **2008**, *105*, 2140–2145.

255. Baldick, C. J.; Moss, B. Characterization and temporal regulation of mRNAs encoded by vaccinia virus intermediate-stage genes. *J. Virol.* **1993**, *67*, 3515–3527.

256. Maruri Avidal, L.; Weisberg, A. S.; Moss, B. Vaccinia Virus L2 Protein Associates with the Endoplasmic Reticulum near the Growing Edge of Crescent Precursors of Immature Virions and Stabilizes a Subset of Viral Membrane Proteins. *J. Virol.* **2011**, *85*, 12431–12441.

257. Howell, M. L.; Roseman, N. A.; Slabaugh, M. B.; Mathews, C. Vaccinia Virus Ribonucleotide Reductase - Correlation Between Deoxyribonucleotide Supply-and-Demand. *J. Biol. Chem.* **1993**, *268*, 7155–7162.

258. Jungwirth, C.; Launer, J. Effect of poxvirus infection on host cell deoxyribonucleic acid synthesis. *J. Virol.* **1968**, *2*, 401–408.

259. Lane, A. N.; Fan, T. W. M. Regulation of mammalian nucleotide metabolism and biosynthesis. *Nucleic Acids Res.* **2015**, *43*, 2466–2485.

260. Reichard, P. Interactions Between Deoxyribonucleotide And DNA Synthesis. *Annu. Rev. Biochem.* **1988**, *57*, 349–374.

261. Kolberg, M.; Strand, K. R.; Graff, P.; Andersson, K. K. Structure, function, and mechanism of ribonucleotide reductases. *Biochim. Biophys. Acta* **2004**, *1699*, 1–34.

262. Engström, Y.; Eriksson, S.; Jildevik, I.; Skog, S.; Thelander, L.; Tribukait, B. Cell cycle-dependent expression of mammalian ribonucleotide reductase. Differential regulation of the two subunits. *J. Biol. Chem.* **1985**, *260*, 9114–9116.

263. Chabes, A. L.; Pfleger, C. M.; Kirschner, M. W.; Thelander, L. Mouse ribonucleotide reductase R2 protein: A new target for anaphase-promoting complex-Cdh1-mediated proteolysis. *PNAS* **2003**, *100*, 3925–3929.

264. Pfleger, C. M.; Kirschner, M. W. The KEN box: an APC recognition signal distinct from the D box targeted by Cdh1. *Genes Dev.* **2000**, *14*, 655–665.

265. Tanaka, H.; Arakawa, H.; Yamaguchi, T.; Shiraishi, K.; Fukuda, S.; Matsui, K.; Takei, Y.; Nakamura, Y. A ribonucleotide reductase gene involved in a p53-dependent cell-cycle checkpoint for DNA damage. *Nature* **2000**, *404*, 42–49.

266. Guittet, O.; Hakansson, P.; Voevodskaya, N.; Fridd, S.; Gräslund, A.; Arakawa, H.; Nakamura, Y.; Thelander, L. Mammalian p53R2 protein forms an active ribonucleotide reductase in vitro with the R1 protein, which is expressed both in resting cells in response to DNA damage and in proliferating cells. *J. Biol. Chem.* **2001**, *276*, 40647–40651.

267. Pontarin, G.; Ferraro, P.; Hakansson, P.; Thelander, L.; Reichard, P.; Bianchi, V. p53R2-dependent ribonucleotide reduction provides Deoxyribonucleotides in quiescent human fibroblasts in the absence of induced DNA damage. *J. Biol. Chem.* **2007**, *282*, 16820–16828.

268. Slabaugh, M.; Roseman, N.; Davis, R.; Mathews, C. Vaccinia Virus-Encoded Ribonucleotide Reductase - Sequence Conservation of the Gene for the Small Subunit and Its Amplification in Hydroxyurea-Resistant Mutants. *J. Virol.* **1988**, *62*, 519–527.

269. Gammon, D.; Gowrishankar, B.; Duraffour, S.; Andrei, G.; Upton, C.; Evans, D. H. Vaccinia virus-encoded ribonucleotide reductase subunits are differentially required for replication and pathogenesis. *PLoS Pathog.* **2010**, *6*, e1000984.

270. Yen, Y. Ribonucleotide reductase subunit one as gene therapy target. *Clin. Cancer Res.* **2003**, *9*, 4304–4308.

271. Weir, J. P.; Moss, B. Nucleotide-Sequence of the Vaccinia Virus Thymidine Kinase Gene and the Nature of Spontaneous Frameshift Mutations. *J. Virol.* **1983**, *46*, 530–537.

272. Topalis, D.; Collinet, B.; Gasse, C.; Dugue, L.; Balzarini, J.; Pochet, S.; Deville-Bonne, D. Substrate specificity of vaccinia virus thymidylate kinase. *FEBS J.* **2005**, *272*, 6254–6265.

273. Black, M. E.; Hruby, D. E. A single amino acid substitution abolishes feedback inhibition of vaccinia virus thymidine kinase. *J. Biol. Chem.* **1992**, *267*, 9743–9748.

274. Buller, R.; Smith, G.; Cremer, K.; Notkins, A.; Moss, B. Decreased Virulence of Recombinant Vaccinia Virus Expression Vectors Is Associated with a Thymidine Kinase-Negative Phenotype. *Nature* **1985**, *317*, 813–815.

275. Buller, R.; Chakrabarti, S.; Cooper, J.; Twardzik, D.; Moss, B. Deletion of the Vaccinia Virus Growth-Factor Gene Reduces Virus Virulence. *J. Virol.* **1988**, *62*, 866–874.

276. Hengstschläger, M.; Knöfler, M.; Müllner, E. W.; Ogris, E.; Wintersberger, E.; Wawra, E.

Different regulation of thymidine kinase during the cell cycle of normal versus DNA tumor virus-transformed cells. *J. Biol. Chem.* **1994**, *269*, 13836–13842.

277. Buller, R.; Chakrabarti, S.; Moss, B.; FREDRICKSON, T. Cell Proliferative Response to Vaccinia Virus Is Mediated by Vgf. *Virology* **1988**, *164*, 182–192.

278. Tzahar, E.; Moyer, J. D.; Waterman, H.; Barbacci, E. G.; Bao, J.; Levkowitz, G.; Shelly, M.; Strano, S.; Pinkas-Kramarski, R.; Pierce, J. H.; Andrews, G. C.; Yarden, Y. Pathogenic poxviruses reveal viral strategies to exploit the ErbB signaling network. *EMBO J.* **1998**, *17*, 5948–5963.

279. McCart, J.; Ward, J.; Lee, J.; Hu, Y.; Alexander, H.; Libutti, S.; Moss, B.; Bartlett, D. Systemic cancer therapy with a tumor-selective vaccinia virus mutant lacking thymidine kinase and vaccinia growth factor genes. *Cancer Res.* **2001**, *61*, 8751–8757.

280. Kim, J.; Oh, J.; Park, B.; Lee, D.; Kim, J.; Park, H.; Roh, M.; Je, J.; Yoon, J.; Thorne, S.; Kirn, D.; Hwang, T. Systemic armed oncolytic and immunologic therapy for cancer with JX-594, a targeted poxvirus expressing GM-CSF. *Mol. Ther.* **2006**, *14*, 361–370.

281. Kirn, D.; Wang, Y.; Le Boeuf, F.; Bell, J.; Thorne, S. H. Targeting of interferon-beta to produce a specific, multi-mechanistic oncolytic vaccinia virus. *PLoS Med.* **2007**, *4*, 2001–2012.

282. Scholl, S. M.; Balloul, J. M.; Le Goc, G.; Bizouarne, N.; Schatz, C.; Kieny, M. P.; Mensdorff-Pouilly, von, S.; Vincent-Salomon, A.; Deneux, L.; Tartour, E.; Fridman, W.; Pouillart, P.; Acres, B. Recombinant vaccinia virus encoding human MUC1 and IL2 as immunotherapy in patients with breast cancer. *J. Immunother.* **2000**, *23*, 570–580.

283. Biron, C. A. Role of early cytokines, including alpha and beta interferons (IFN-alpha/beta), in innate and adaptive immune responses to viral infections. *Semin. Immunol.* **1998**, *10*, 383–390.

284. Thorne, S.; Tam, B.; Kirn, D. H.; Contag, C. H.; Kuo, C. J. Selective intratumoral amplification of an antiangiogenic vector by an oncolytic virus produces enhanced antivascular and anti-tumor efficacy. *Mol. Ther.* **2006**, *13*, 938–946.

285. Fodor, I.; Timiryasova, T.; Denes, B.; Yoshida, J.; Ruckle, H.; Lilly, M. Vaccinia virus mediated p53 gene therapy for bladder cancer in an orthotopic murine model. *J. Urol.* **2005**, *173*, 604–609.

286. Gomella, L.; Mastrangelo, M.; McCue, P.; Maguire, H.; Mulholland, S.; Lattime, E. Phase I study of intravesical vaccinia virus as a vector for gene therapy of bladder cancer. *J. Urol.* **2001**, *166*, 1291–1295.

287. Mastrangelo, M.; Maguire, H.; Eisenlohr, L. C.; Laughlin, C. E.; Monken, C. E.; McCue, P.; Kovatich, A. J.; Lattime, E. Intratumoral recombinant GM-CSF-encoding virus as gene therapy in patients with cutaneous melanoma. *Cancer Gene Ther.* **1999**, *6*, 409–422.

288. Park, B.-H.; Hwang, T.; Liu, T.-C.; Sze, D. Y.; Kim, J.-S.; Kwon, H.-C.; Oh, S. Y.; Han, S.-Y.; Yoon, J.-H.; Hong, S.-H.; Moon, A.; Speth, K.; Park, C.; Ahn, Y.-J.; Daneshmand, M.; Rhee, B.-G.; Pinedo, H. M.; Bell, J.; Kirn, D. Use of a targeted oncolytic poxvirus, JX-594, in patients

with refractory primary or metastatic liver cancer: a phase I trial. *Lancet Oncol.* **2008**, *9*, 533–542.

289. Heo, J.; Reid, T.; Ruo, L.; Breitbach, C.; Rose, S.; Bloomston, M.; Cho, M.; Lim, H.; Chung, H. C.; Kim, C. W.; Burke, J.; Lencioni, R.; Hickman, T.; Moon, A.; Lee, Y.-S.; Kim, M. K.; Daneshmand, M.; Dubois, K.; Longpre, L.; Ngo, M.; Rooney, C.; Bell, J.; Rhee, B.-G.; Patt, R.; Hwang, T.-H.; Kirn, D. Randomized dose-finding clinical trial of oncolytic immunotherapeutic vaccinia JX-594 in liver cancer. *Nat. Med.* **2013**, *19*, 329–336.

290. Breitbach, C.; Burke, J.; Jonker, D.; Stephenson, J.; Haas, A.; Chow, L.; Nieva, J.; Hwang, T.-H.; Moon, A.; Patt, R.; Pelusio, A.; Le Boeuf, F.; Burns, J.; Evgin, L.; De Silva, N.; Cvancic, S.; Robertson, T.; Je, J.-E.; Lee, Y.-S.; Parato, K.; Diallo, J.-S.; Fenster, A.; Daneshmand, M.; Bell, J.; Kirn, D. Intravenous delivery of a multi-mechanistic cancer-targeted oncolytic poxvirus in humans. *Nature* **2011**, *477*, 99–102.

291. Aye, Y.; Li, M.; Long, M.; Weiss, R. Ribonucleotide reductase and cancer: biological mechanisms and targeted therapies. *Oncogene* **2015**, *34*, 2011–2021.

292. Fend, L.; Remy-Ziller, C.; Foloppe, J.; Kempf, J.; Cochin, S.; Barraud, L.; Accart, N.; Erbs, P.; Fournel, S.; Préville, X. Oncolytic virotherapy with an armed vaccinia virus in an orthotopic model of renal carcinoma is associated with modification of the tumor microenvironment. *Oncoimmunology* **2016**, *5*, e1080414.

293. Eriksson, S.; Gräslund, A.; Skog, S.; Thelander, L.; Tribukait, B. Cell cycle-dependent regulation of mammalian ribonucleotide reductase. The S phase-correlated increase in subunit M2 is regulated by de novo protein synthesis. *J. Biol. Chem.* **1984**, *259*, 11695–11700.

294. Morikawa, T.; Maeda, D.; Kume, H.; Homma, Y.; Fukayama, M. Ribonucleotide reductase M2 subunit is a novel diagnostic marker and a potential therapeutic target in bladder cancer. *Histopathology* **2010**, *57*, 885–892.

295. Sanchez-Carbayo, M.; Socci, N.; Lozano, J.; Saint, F.; Cordon-Cardo, C. Defining molecular profiles of poor outcome in patients with invasive bladder cancer using oligonucleotide microarrays. *J. Clin. Oncol.* **2006**, *24*, 778–789.

296. Jäger, W.; Horiguchi, Y.; Shah, J.; Hayashi, T.; Awrey, S.; Gust, K.; Hadaschik, B.; Matsui, Y.; Anderson, S.; Bell, R.; Ettinger, S.; So, A.; Gleave, M.; Lee, I.-L.; Dinney, C.; Tachibana, M.; McConkey, D.; Black, P. Hiding in plain view: genetic profiling reveals decades old cross contamination of bladder cancer cell line KU7 with HeLa. *J. Urol.* **2013**, *190*, 1404–1409.

297. Xiao, Z.; McCallum, T.; Brown, K.; Miller, G.; Halls, S.; Parney, I.; Moore, R. Characterization of a novel transplantable orthotopic rat bladder transitional cell tumour model. *Br. J. Cancer* **1999**, *81*, 638–646.

298. Hendricksen, K.; Molkenboer-Kuenen, J.; Oosterwijk, E.; Hulsbergen-van de Kaa, C.; Witjes, J. Evaluation of an orthotopic rat bladder urothelial cell carcinoma model by cystoscopy. *BJU International* **2008**, *101*, 889–893.

299. Gust, K.; McConkey, D.; Awrey, S.; Hegarty, P.; Qing, J.; Bondaruk, J.; Ashkenazi, A.;

Czerniak, B.; Dinney, C.; Black, P. Fibroblast growth factor receptor 3 is a rational therapeutic target in bladder cancer. *Mol. Cancer Ther.* **2013**, *12*, 1245–1254.

300. Zeh, H.; Downs-Canner, S.; McCart, A.; Guo, Z.; Rao, U.; Ramalingam, L.; Thorne, S.; Jones, H.; Kalinski, P.; Wieckowski, E.; O'Malley, M.; Daneshmand, M.; Hu, K.; Bell, J.; Hwang, T.-H.; Moon, A.; Breitbach, C.; Kirn, D.; Bartlett, D. First-in-man study of western reserve strain oncolytic vaccinia virus: safety, systemic spread, and antitumor activity. *Mol. Ther.* **2015**, *23*, 202–214.

301. Avritscher, E. B. C.; Cooksley, C. D.; Grossman, H. B.; Sabichi, A. L.; Hamblin, L.; Dinney, C.; Elting, L. S. Clinical model of lifetime cost of treating bladder cancer and associated complications. *Urology* **2006**, *68*, 549–553.

302. Sievert, K. D.; Amend, B.; Nagele, U.; Schilling, D.; Bedke, J.; Horstmann, M.; Hennenlotter, J.; Kruck, S.; Stenzl, A. Economic aspects of bladder cancer: what are the benefits and costs? *World J Urol* **2009**, *27*, 295–300.

303. Lai, Y.; Wei, X.; Lin, S.; Qin, L.; Cheng, L.; Li, P. Current status and perspectives of patient-derived xenograft models in cancer research. *J Hematol Oncol* **2017**, *10*.

304. Pan, C.-X.; Zhang, H.; Tepper, C. G.; Lin, T.-Y.; Davis, R. R.; Keck, J.; Ghosh, P. M.; Gill, P.; Airhart, S.; Bult, C.; Gandara, D. R.; Liu, E.; White, R. W. de V. Development and Characterization of Bladder Cancer Patient-Derived Xenografts for Molecularly Guided Targeted Therapy. *PLoS ONE* **2015**, *10*.

305. Ding, J.; Xu, D.; Pan, C.; Ye, M.; Kang, J.; Bai, Q.; Qi, J. Current animal models of bladder cancer: Awareness of translatability (Review). *Exp Ther Med* **2014**, *8*, 691–699.

306. Asanuma, H.; Arai, T.; Seguchi, K.; Kawauchi, S.; Satoh, H.; Kikuchi, M.; Murai, M. Successful diagnosis of orthotopic rat superficial bladder tumor model by ultrathin cystoscopy. *J. Urol.* **2003**, *169*, 718–720.

307. Hackstein, H.; Thomson, A. W. Dendritic cells: Emerging pharmacological targets of immunosuppressive drugs. *Nat. Rev. Immunol.* **2004**, *4*, 24–34.

308. Bevan, M. J. Helping the CD8(+) T-cell response. *Nat. Rev. Immunol.* **2004**, *4*, 595–602.

309. Bachleitner-Hofmann, T.; Stift, A.; Friedl, J.; Pfragner, R.; Radelbauer, K.; Dubsky, P.; Schuller, G.; Benko, T.; Niederle, B.; Brostjan, C.; Jakesz, R.; Gnant, M. Stimulation of autologous antitumor T-cell responses against medullary thyroid carcinoma using tumor lysate-pulsed dendritic cells. *J. Clin. Endocrinol. Metab.* **2002**, *87*, 1098–1104.

310. Labeur, M.; Roters, B.; Pers, B.; Mehling, A.; Luger, T.; Schwarz, T.; Grabbe, S. Generation of tumor immunity by bone marrow-derived dendritic cells correlates with dendritic cell maturation stage. *J. Immunol.* **1999**, *162*, 168–175.

311. Betts, M.; Brenchley, J.; Price, D.; De Rosa, S.; Douek, D.; Roederer, M.; Koup, R. Sensitive and viable identification of antigen-specific CD8+T cells by a flow cytometric assay for

degranulation. *J. Immunol. Methods* **2003**, *281*, 65–78.

312. Uhrberg, M. The CD107 mobilization assay: viable isolation and immunotherapeutic potential of tumor-cytolytic NK cells - Commentary. *Leukemia* **2005**, *19*, 707–709.

313. Perfetto, S. P.; Chattopadhyay, P. K.; Roederer, M. Seventeen-colour flow cytometry: unravelling the immune system. *Nat. Rev. Immunol.* **2004**, *4*, 648–655.

314. MacTavish, H.; Diallo, J.-S.; Huang, B.; Stanford, M.; Le Boeuf, F.; De Silva, N.; Cox, J.; Simmons, J.; Guimond, T.; Falls, T.; McCart, A.; Atkins, H.; Breitbach, C.; Kirn, D.; Thorne, S.; Bell, J. Enhancement of vaccinia virus based oncolysis with histone deacetylase inhibitors. *PLoS ONE* **2010**, *5*, e14462.

315. Gentschev, I.; Adelfinger, M.; Josupeit, R.; Rudolph, S.; Ehrig, K.; Donat, U.; Weibel, S.; Chen, N.; Yu, Y.; Zhang, Q.; Heisig, M.; Thamm, D.; Stritzker, J.; MacNeill, A.; Szalay, A. Preclinical evaluation of oncolytic vaccinia virus for therapy of canine soft tissue sarcoma. *PLoS ONE* **2012**, *7*, e37239.

316. Zhao, Y.; Adams, Y. F.; Croft, M. Preferential replication of vaccinia virus in the ovaries is independent of immune regulation through IL-10 and TGF-β. *Viral Immunol.* **2011**, *24*, 387–396.

317. Gan, Y.; Zhang, Y.; Khoo, H.; Esuvaranathan, K. Antitumour immunity of Bacillus Calmette-Guerin and interferon alpha in murine bladder cancer. *Eur. J. Cancer* **1999**, *35*, 1123–1129.

318. Izumchenko, E.; Meir, J.; Bedi, A.; Wysocki, P. T.; Hoque, M. O.; Sidransky, D. Patient-derived xenografts as tools in pharmaceutical development. *Clin. Pharmacol. Ther.* **2016**, *99*, 612–621.

319. Cassidy, J. W.; Caldas, C.; Bruna, A. Maintaining Tumor Heterogeneity in Patient-Derived Tumor Xenografts. *Cancer Res.* **2015**, *75*, 2963–2968.

320. Brooks, N. A.; O'Donnell, M. Treatment options in non-muscle-invasive bladder cancer after BCG failure. *Indian Journal of Urology* **2015**, *31*, 312–319.

321. Andrade, L. G.; Albarnaz, J. D.; Mügge, F. L. B.; David, B. A.; Abrahão, J. S.; da Fonseca, F. G.; Kroon, E. G.; Menezes, G. B.; McFadden, G.; Bonjardim, C. A. Vaccinia virus dissemination requires p21-activated kinase 1. *Arch. Virol.* **2016**, *161*, 2991–3002.

322. Campeau, E.; Ruhl, V. E.; Rodier, F.; Smith, C. L.; Rahmberg, B. L.; Fuss, J. O.; Campisi, J.; Yaswen, P.; Cooper, P. K.; Kaufman, P. D. A versatile viral system for expression and depletion of proteins in mammalian cells. *PLoS ONE* **2009**, *4*, e6529.

323. Deacon, S. W.; Beeser, A.; Fukui, J. A.; Rennefahrt, U. E. E.; Myers, C.; Chernoff, J.; Peterson, J. R. An isoform-selective, small-molecule inhibitor targets the autoregulatory mechanism of p21-activated kinase. *Chem. Biol.* **2008**, *15*, 322–331.

324. Viaud, J.; Peterson, J. R. An allosteric kinase inhibitor binds the p21-activated kinase autoregulatory domain covalently. *Mol. Cancer Ther.* **2009**, *8*, 2559–2565.

325. Xiao, Z.; Hanel, E.; Mak, A.; Moore, R. B. Antitumor Efficacy of Intravesical BCG, Gemcitabine, Interferon-α and Interleukin-2 as Mono- or Combination-Therapy for Bladder Cancer in an Orthotopic Tumor Model. *Clin Med Insights Oncol* **2011**, *5*, 315–323.

326. Günther, J. H.; Jurczok, A.; Wulf, T.; Brandau, S.; Deinert, I.; Jocham, D.; Böhle, A. Optimizing syngeneic orthotopic murine bladder cancer (MB49). *Cancer Res.* **1999**, *59*, 2834–2837.

327. Biot, C.; Rentsch, C.; Gsponer, J.; Birkhaeuser, F.; Jusforgues-Saklani, H.; Lemaitre, F.; Auriau, C.; Bachmann, A.; Bousso, P.; Demangel, C.; Peduto, L.; Thalmann, G.; Albert, M. Preexisting BCG-Specific T Cells Improve Intravesical Immunotherapy for Bladder Cancer. *Sci Transl Med* **2012**, *4*, –137ra72.

328. Kreider, J. W.; Bartlett, G. L.; Purnell, D. M. Immunotherapeutic effectiveness of BCG inactivated by various modalities. *Cancer* **1980**, *46*, 480–487.

329. Sanderson, C. M.; Smith, G. Vaccinia virus induces Ca2+-independent cell-matrix adhesion during the motile phase of infection. *J. Virol.* **1998**, *72*, 9924–9933.

330. Blasco, R.; Cole, N. B.; Moss, B. Sequence analysis, expression, and deletion of a vaccinia virus gene encoding a homolog of profilin, a eukaryotic actin-binding protein. *J. Virol.* **1991**, *65*, 4598–4608.

331. Doceul, V.; Hollinshead, M.; van der Linden, L.; Smith, G. L. Repulsion of superinfecting virions: a mechanism for rapid virus spread. *Science* **2010**, *327*, 873–876.

332. Condit, R. C. Surf and turf: mechanism of enhanced virus spread during poxvirus infection. *Viruses* **2010**, *2*, 1050–1054.

333. Kumar, R.; Gururaj, A. E.; Barnes, C. J. p21-activated kinases in cancer. *Nat. Rev. Cancer* **2006**, *6*, 459–471.

334. Khalil, D. N.; Smith, E. L.; Brentjens, R. J.; Wolchok, J. D. The future of cancer treatment: immunomodulation, CARs and combination immunotherapy. *Nat Rev Clin Oncol* **2016**, *13*, 394–394.

335. Pardoll, D. M. The blockade of immune checkpoints in cancer immunotherapy. *Nat. Rev. Cancer* **2012**, *12*, 252–264.

336. Restifo, N. P.; Dudley, M. E.; Rosenberg, S. A. Adoptive immunotherapy for cancer: harnessing the T cell response. *Nat. Rev. Immunol.* **2012**, *12*, 269–281.

337. Coley, W. B. The Treatment of Inoperable Sarcoma by Bacterial Toxins (the Mixed Toxins of the Streptococcus erysipelas and the Bacillus prodigiosus). *Proc. R. Soc. Med.* **1910**, *3*, 1–48.

338. Lawrence, M. S.; Stojanov, P.; Polak, P.; Kryukov, G. V.; Cibulskis, K.; Sivachenko, A.; Carter, S. L.; Stewart, C.; Mermel, C. H.; Roberts, S. A.; Kiezun, A.; Hammerman, P. S.; McKenna, A.; Drier, Y.; Zou, L.; Ramos, A. H.; Pugh, T. J.; Stransky, N.; Helman, E.; Kim, J.;

Sougnez, C.; Ambrogio, L.; Nickerson, E.; Shefler, E.; Cortes, M. L.; Auclair, D.; Saksena, G.; Voet, D.; Noble, M.; DiCara, D.; Lin, P.; Lichtenstein, L.; Heiman, D. I.; Fennell, T.; Imielinski, M.; Hernandez, B.; Hodis, E.; Baca, S.; Dulak, A. M.; Lohr, J.; Landau, D.-A.; Wu, C. J.; Melendez-Zajgla, J.; Hidalgo-Miranda, A.; Koren, A.; McCarroll, S. A.; Mora, J.; Lee, R. S.; Crompton, B.; Onofrio, R.; Parkin, M.; Winckler, W.; Ardlie, K.; Gabriel, S. B.; Roberts, C. W. M.; Biegel, J. A.; Stegmaier, K.; Bass, A. J.; Garraway, L. A.; Meyerson, M.; Golub, T. R.; Gordenin, D. A.; Sunyaev, S.; Lander, E. S.; Getz, G. Mutational heterogeneity in cancer and the search for new cancer-associated genes. *Nature* **2013**, *499*, 214–218.

339. Postow, M. A.; Callahan, M. K.; Wolchok, J. D. Immune Checkpoint Blockade in Cancer Therapy. *J. Clin. Oncol.* **2015**, *33*, 1974–U161.

340. Smith-Garvin, J. E.; Koretzky, G. A.; Jordan, M. S. T Cell Activation. *Annu. Rev. Immunol.* **2009**, *27*, 591–619.

341. Chikuma, S. Basics of PD-1 in self-tolerance, infection, and cancer immunity. *Int. J. Clin. Oncol.* **2016**, *21*, 448–455.

342. Buchbinder, E. I.; Desai, A. CTLA-4 and PD-1 Pathways Similarities, Differences, and Implications of Their Inhibition. *Am. J. Clin. Oncol.* **2016**, *39*, 98–106.

343. Zou, W.; Chen, L. Inhibitory B7-family molecules in the tumour microenvironment. *Nat. Rev. Immunol.* **2008**, *8*, 467–477.

344. Hodi, F. S.; O'Day, S. J.; McDermott, D. F.; Weber, R. W.; Sosman, J. A.; Haanen, J. B.; Gonzalez, R.; Robert, C.; Schadendorf, D.; Hassel, J. C.; Akerley, W.; van den Eertwegh, A. J. M.; Lutzky, J.; Lorigan, P.; Vaubel, J. M.; Linette, G.; Hogg, D.; Ottensmeier, C. H.; Lebbé, C.; Peschel, C.; Quirt, I.; Clark, J. I.; Wolchok, J. D.; Weber, J. S.; Tian, J.; Yellin, M. J.; Nichol, G. M.; Hoos, A.; Urba, W. J. Improved Survival with Ipilimumab in Patients with Metastatic Melanoma. *N. Engl. J. Med.* **2010**, *363*, 711–723.

345. Liakou, C. I.; Kamat, A.; Tang, D. N.; Chen, H.; Sun, J.; Troncoso, P.; Logothetis, C.; Sharma, P. CTLA-4 blockade increases IFNgamma-producing CD4+ICOShi cells to shift the ratio of effector to regulatory T cells in cancer patients. *Proc. Natl. Acad. Sci. U.S.A.* **2008**, *105*, 14987–14992.

346. Carthon, B. C.; Wolchok, J. D.; Yuan, J.; Kamat, A.; Tang, D. S. N.; Sun, J.; Ku, G.; Troncoso, P.; Logothetis, C. J.; Allison, J. P.; Sharma, P. Preoperative CTLA-4 Blockade: Tolerability and Immune Monitoring in the Setting of a Presurgical Clinical Trial. *Clin. Cancer Res.* **2010**, *16*, 2861–2871.

347. Dong, C.; Juedes, A. E.; Temann, U. A.; Shresta, S.; Allison, J. P.; Ruddle, N. H.; Flavell, R. A. ICOS co-stimulatory receptor is essential for T-cell activation and function. *Nature* **2001**, *409*, 97–101.

348. Powles, T.; Eder, J. P.; Fine, G. D.; Braiteh, F. S.; Loriot, Y.; Cruz, C.; Bellmunt, J.; Burris, H. A.; Petrylak, D. P.; Teng, S.-L.; Shen, X.; Boyd, Z.; Hegde, P. S.; Chen, D. S.; Vogelzang, N. J. MPDL3280A (anti-PD-L1) treatment leads to clinical activity in metastatic bladder cancer.

Nature **2014**, *515*, 558–.

349. Balar, A. V.; Galsky, M. D.; Rosenberg, J. E.; Powles, T.; Petrylak, D. P.; Bellmunt, J.; Loriot, Y.; Necchi, A.; Hoffman-Censits, J.; Perez-Gracia, J. L.; Dawson, N. A.; van der Heijden, M. S.; Dreicer, R.; Srinivas, S.; Retz, M. M.; Joseph, R. W.; Drakaki, A.; Vaishampayan, U. N.; Sridhar, S. S.; Quinn, D. I.; Duran, I.; Shaffer, D. R.; Eigl, B. J.; Grivas, P. D.; Yu, E. Y.; Li, S.; Kadel, E. E. I.; Boyd, Z.; Bourgon, R.; Hegde, P. S.; Mariathasan, S.; Thastrom, A.; Abidoye, O. O.; Fine, G. D.; Bajorin, D. F.; Grp, I. S. Atezolizumab as first-line treatment in cisplatin-ineligible patients with locally advanced and metastatic urothelial carcinoma: a single-arm, multicentre, phase 2 trial. *Lancet* **2017**, *389*, 67–76.

350. Bajorin, D. F.; Sharma, P.; Gomella, L. G.; Plimack, E. R.; O'Donnell, P. H.; Hoffman-Censits, J. H.; Flaig, T. W.; Quinn, D. I.; Sims, R. B.; Locker, M.; Sheikh, N. A.; DeVries, T.; Lerner, S. P. NeuACT, a phase II, randomized, open-label trial of DN24-02: Updated analysis of HER2 expression, immune responses, product parameters, and safety in patients with surgically resected HER2+ urothelial cancer. *J. Clin. Oncol.* **2017**, *32*, 296–296.

351. Bajorin, D. F.; Sharma, P.; Quinn, D. I.; Plimack, E. R.; Hoffman-Censits, J. H.; O'Donnell, P. H.; Siefker-Radtke, A. O.; Sheikh, N. A.; LIll, J. S.; Trager, J. B.; Gomella, L. G. Phase 2 trial results of DN24-02, a HER2-targeted autologous cellular immunotherapy in HER2+ urothelial cancer patients (pts). *J. Clin. Oncol.* **2017**, *34*, 4513–4513.

352. Madan, R. A.; Arlen, P. M.; Gulley, J. L. PANVAC-VF: poxviral-based vaccine therapy targeting CEA and MUC1 in carcinoma. *Expert Opin Biol Ther* **2007**, *7*, 543–554.

353. Heery, C. R.; Ibrahim, N. K.; Arlen, P. M.; Mohebtash, M.; Murray, J. L.; Koenig, K.; Madan, R. A.; McMahon, S.; Marté, J. L.; Steinberg, S. M.; Donahue, R. N.; Grenga, I.; Jochems, C.; Farsaci, B.; Folio, L. R.; Schlom, J.; Gulley, J. L. Docetaxel Alone or in Combination With a Therapeutic Cancer Vaccine (PANVAC) in Patients With Metastatic Breast Cancer: A Randomized Clinical Trial. *JAMA Oncol* **2015**, *1*, 1087–1095.

354. Kaufman, H.; Kim-Schulze, S.; Manson, K.; DeRaffele, G.; Mitcham, J.; Seo, K. S.; Kim, D. W.; Marshall, J. Poxvirus-based vaccine therapy for patients with advanced pancreatic cancer. *J Transl Med* **2007**, *5*, 60.

355. Ahmad, S.; Lam, T. B. L.; N'Dow, J. Significance of MUC1 in bladder cancer. *BJU International* **2015**, *115*, 161–162.

356. Cardillo, M. R.; Castagna, G.; Memeo, L.; De Bernardinis, E.; Di Silverio, F. Epidermal growth factor receptor, MUC-1 and MUC-2 in bladder cancer. *J. Exp. Clin. Cancer Res.* **2000**, *19*, 225–233.

357. Hegele, A.; Mecklenburg, V.; Varga, Z.; Olbert, P.; Hofmann, R.; Barth, P. CA19.9 and CEA in transitional cell carcinoma of the bladder: serological and immunohistochemical findings. *Anticancer Res.* **2010**, *30*, 5195–5200.

358. Mathews, C. K. Deoxyribonucleotide metabolism, mutagenesis and cancer. *Nat. Rev. Cancer* **2015**, *15*, 528–539.

359. Munch-Petersen, B.; Cloos, L.; Jensen, H. K.; Tyrsted, G. Human Thymidine Kinase-1 - Regulation in Normal and Malignant Cells. *Adv. Enzyme Regul.* **1995**, *35*, 69–89.

360. Rausch, S.; Hennenlotter, J.; Teepe, K.; Kuehs, U.; Aufderklamm, S.; Bier, S.; Mischinger, J.; Gakis, G.; Stenzl, A.; Schwentner, C.; Todenhoefer, T. Muscle-invasive bladder cancer is characterized by overexpression of thymidine kinase 1. *Urol. Oncol.* **2015**, *33*, –9.

361. Park, S.; Breitbach, C.; Lee, J.; Park, J. O.; Lim, H.; Kang, W. K.; Moon, A.; Mun, J.-H.; Sommermann, E.; Maruri Avidal, L.; Patt, R.; Pelusio, A.; Burke, J.; Hwang, T.-H.; Kirn, D.; Park, Y. S. Phase 1b Trial of Biweekly Intravenous Pexa-Vec (JX-594), an Oncolytic and Immunotherapeutic Vaccinia Virus in Colorectal Cancer. *Mol. Ther.* **2015**, *23*, 1532–1540.

362. Cripe, T.; Ngo, M.; Geller, J.; Louis, C.; Currier, M.; Racadio, J.; Towbin, A.; Rooney, C.; Pelusio, A.; Moon, A.; Hwang, T.-H.; Burke, J.; Bell, J.; Kirn, D.; Breitbach, C. Phase 1 study of intratumoral Pexa-Vec (JX-594), an oncolytic and immunotherapeutic vaccinia virus, in pediatric cancer patients. *Mol. Ther.* **2015**, *23*, 602–608.

363. Kung, C.-H.; Kuo, S.-C.; Chen, T.-L.; Weng, W.-S. Isolation of vaccinia JX594 from pustules following therapy for hepatocellular carcinoma. *BMC Cancer* **2015**, *15*, 704.

364. Downs-Canner, S.; Guo, Z.; Ravindranathan, R.; Breitbach, C.; O'Malley, M.; Jones, H.; Moon, A.; McCart, J. A.; Shuai, Y.; Zeh, H.; Bartlett, D. Phase 1 Study of Intravenous Oncolytic Poxvirus (vvDD) in Patients With Advanced Solid Cancers. *Mol. Ther.* **2016**, *24*, 1492–1501.

365. Eriksson, S.; Gräslund, A.; Skog, S.; Thelander, L.; Tribukait, B. Cell cycle-dependent regulation of mammalian ribonucleotide reductase. The S phase-correlated increase in subunit M2 is regulated by de novo protein synthesis. *J. Biol. Chem.* **1984**, *259*, 11695–11700.

366. Ke, P. Y.; Chang, Z. F. Mitotic degradation of human thymidine kinase 1 is dependent on the anaphase-promoting complex/cyclosome-Cdh1-mediated pathway. *Mol. Cell. Biol.* **2004**, *24*, 514–526.

367. Chabes, A.; Thelander, L. Controlled protein degradation regulates ribonucleotide reductase activity in proliferating mammalian cells during the normal cell cycle and in response to DNA damage and replication blocks. *J. Biol. Chem.* **2000**, *275*, 17747–17753.

368. Kawai, K.; Miyazaki, J.; Joraku, A.; Nishiyama, H.; Akaza, H. Bacillus Calmette-Guerin (BCG) immunotherapy for bladder cancer: current understanding and perspectives on engineered BCG vaccine. *Cancer Sci.* **2013**, *104*, 22–27.

369. Kavoussi, L. R.; Brown, E.; Ritchey, J.; Ratliff, T. Fibronectin-mediated Calmette-Guerin bacillus attachment to murine bladder mucosa. Requirement for the expression of an antitumor response. *Journal of Clinical Investigation* **1990**, *85*, 62–67.

370. Lim, J. P.; Gleeson, P. A. Macropinocytosis: an endocytic pathway for internalising large gulps. *Immunol. Cell Biol.* **2011**, *89*, 836–843.

371. Edwards, D. C.; Sanders, L. C.; Bokoch, G. M.; Gill, G. N. Activation of LIM-kinase by Pak1

couples Rac/Cdc42 GTPase signalling to actin cytoskeletal dynamics. *Nat. Cell Biol.* **1999**, *1*, 253–259.

372. Yang, N.; Higuchi, O.; Ohashi, K.; Nagata, K.; Wada, A.; Kangawa, K.; Nishida, E.; Mizuno, K. Cofilin phosphorylation by LIM-kinase 1 and its role in Rac-mediated actin reorganization. *Nature* **1998**, *393*, 809–812.

373. Svitkina, T. M.; Borisy, G. G. Arp2/3 complex and actin depolymerizing factor cofilin in dendritic organization and treadmilling of actin filament array in lamellipodia. *J. Cell Biol.* **1999**, *145*, 1009–1026.

374. Liberali, P.; Kakkonen, E.; Turacchio, G.; Valente, C.; Spaar, A.; Perinetti, G.; Böckmann, R. A.; Corda, D.; Colanzi, A.; Marjomaki, V.; Luini, A. The closure of Pak1-dependent macropinosomes requires the phosphorylation of CtBP1/BARS. *EMBO J.* **2008**, *27*, 970–981.

375. Mercer, J.; Knebel, S.; Schmidt, F. I.; Crouse, J.; Burkard, C.; Helenius, A. Vaccinia virus strains use distinct forms of macropinocytosis for host-cell entry. *PNAS* **2010**, *107*, 9346–9351.

376. Kain, K. H.; Miller, J. W. I.; Jones-Paris, C. R.; Thomason, R. T.; Lewis, J. D.; Bader, D. M.; Barnett, J. V.; Zijlstra, A. The chick embryo as an expanding experimental model for cancer and cardiovascular research. *Dev. Dyn.* **2014**, *243*, 216–228.

377. Leong, H. S.; Steinmetz, N. F.; Ablack, A.; Destito, G.; Zijlstra, A.; Stuhlmann, H.; Manchester, M.; Lewis, J. D. Intravital imaging of embryonic and tumor neovasculature using viral nanoparticles. *Nat Protoc* **2010**, *5*, 1406–1417.

378. Pink, D.; Luhrs, K. A.; Zhou, L.; Schulte, W.; Chase, J.; Frosch, C.; Haberl, U.; Nguyen, V.; Roy, A. I.; Lewis, J. D.; Zijlstra, A.; Parseghian, M. H. High efficacy vasopermeability drug candidates identified by screening in an ex ovo chorioallantoic membrane model. *Scientific Reports* **2015**, *5*, 15756.

379. Cho, C.-F.; Ablack, A.; Leong, H. S.; Zijlstra, A.; Lewis, J. Evaluation of nanoparticle uptake in tumors in real time using intravital imaging. *J Vis Exp* **2011**.

380. Liu, Z.; Ravindranathan, R.; Kalinski, P.; Guo, Z. S.; Bartlett, D. Rational combination of oncolytic vaccinia virus and PD-L1 blockade works synergistically to enhance therapeutic efficacy. *Nat Commun* **2017**, *8*, 14754.

381. Wennier, S. T.; Liu, J.; Li, S.; Rahman, M. M.; Mona, M.; McFadden, G. Myxoma virus sensitizes cancer cells to gemcitabine and is an effective oncolytic virotherapeutic in models of disseminated pancreatic cancer. *Mol. Ther.* **2012**, *20*, 759–768.

382. Eisenberg, D. P.; Adusumilli, P. S.; Hendershott, K. J.; Yu, Z.; Mullerad, M.; Chan, M.-K.; Chou, T.-C.; Fong, Y. 5-fluorouracil and gemcitabine potentiate the efficacy of oncolytic herpes viral gene therapy in the treatment of pancreatic cancer. *J. Gastrointest. Surg.* **2005**, *9*, 1068–1079.

383. Suzuki, E.; Jassar, A. S. Gemcitabine has significant immunomodulatory activity in murine tumor models independent of its cytotoxic effects. **2007**, *6*, 880–885.

384. Suzuki, E.; Kapoor, V.; Jassar, A. S.; Kaiser, L. R.; Albelda, S. M. Gemcitabine selectively eliminates splenic Gr-1(+)/CD11b(+) myeloid suppressor cells in tumor-bearing animals and enhances antitumor immune activity. *Clin. Cancer Res.* **2005**, *11*, 6713–6721.

385. Kyula, J. N.; Khan, A. A.; Mansfield, D.; Karapanagiotou, E. M.; McLaughlin, M.; Roulstone, V.; Zaidi, S.; Pencavel, T.; Touchefeu, Y.; Seth, R.; Chen, N. G.; Yu, Y. A.; Zhang, Q.; Melcher, A.; Vile, R. G.; Pandha, H.; Ajaz, M.; Szalay, A. A.; Harrington, K. Synergistic cytotoxicity of radiation and oncolytic Lister strain vaccinia in (V600D/E)BRAF mutant melanoma depends on JNK and TNF-alpha signaling. *Oncogene* **2014**, *33*, 1700–1712.

386. Dai, M. H.; Liu, S. L.; Chen, N. G.; Zhang, T. P.; You, L.; Zhang, F. Q.; Chou, T. C.; Szalay, A. A.; Fong, Y.; Zhao, Y. P. Oncolytic vaccinia virus in combination with radiation shows synergistic antitumor efficacy in pancreatic cancer. *Cancer Lett.* **2014**, *344*, 282–290.

387. de Gruijl, T. D.; Janssen, A. B.; van Beusechem, V. W. Arming oncolytic viruses to leverage antitumor immunity. *Expert Opin Biol Ther* **2015**, *15*, 959–971.

388. Rojas, J. J.; Sampath, P.; Bonilla, B.; Ashley, A.; Hou, W.; Byrd, D.; Thorne, S. H. Manipulating TLR Signaling Increases the Anti-tumor T Cell Response Induced by Viral Cancer Therapies. *Cell Rep* **2016**, *15*, 264–273.

389. Hou, W.; Sampath, P.; Rojas, J. J.; Thorne, S. H. Oncolytic Virus-Mediated Targeting of PGE2 in the Tumor Alters the Immune Status and Sensitizes Established and Resistant Tumors to Immunotherapy. *Cancer Cell* **2016**, *30*, 108–119.

390. Sinha, P.; Clements, V. K.; Fulton, A. M.; Ostrand-Rosenberg, S. Prostaglandin E2 promotes tumor progression by inducing myeloid-derived suppressor cells. *Cancer Res.* **2007**, *67*, 4507–4513.

391. Vähä-Koskela, M.; Tähtinen, S.; Grönberg-Vähä-Koskela, S.; Taipale, K.; Saha, D.; Merisalo-Soikkeli, M.; Ahonen, M.; Rouvinen-Lagerström, N.; Hirvinen, M.; Veckman, V.; Matikainen, S.; Zhao, F.; Pakarinen, P.; Salo, J.; Kanerva, A.; Cerullo, V.; Hemminki, A. Overcoming tumor resistance by heterologous adeno-poxvirus combination therapy. *Mol Ther Oncolytics* **2015**, *1*, 14006.

392. Vile, R. G. How to train your oncolytic virus: the immunological sequel. *Mol. Ther.* **2014**, *22*, 1881–1884.

393. Kleinpeter, P.; Fend, L.; Thioudellet, C.; Geist, M.; Sfrontato, N.; Koerper, V.; Fahrner, C.; Schmitt, D.; Gantzer, M.; Remy-Ziller, C.; Brandely, R.; Villeval, D.; Rittner, K.; Silvestre, N.; Erbs, P.; Zitvogel, L.; Quéméneur, E.; Préville, X.; Marchand, J.-B. Vectorization in an oncolytic vaccinia virus of an antibody, a Fab and a scFv against programmed cell death -1 (PD-1) allows their intratumoral delivery and an improved tumor-growth inhibition. *Oncoimmunology* **2016**, *5*, e1220467.

394. Engeland, C. E.; Grossardt, C.; Veinaide, R.; Bossow, S.; Lutz, D.; Kaufmann, J. K.; Shevchenko, I.; Umansky, V.; Nettelbeck, D. M.; Weichert, W.; Jaeger, D.; Katie, von, C.; Ungerechts, G. CTLA-4 and PD-L1 Checkpoint Blockade Enhances Oncolytic Measles Virus

Therapy. *Mol. Ther.* **2014**, *22*, 1949–1959.

395. Bauzon, M.; Hermiston, T. Armed therapeutic viruses - a disruptive therapy on the horizon of cancer immunotherapy. *Front Immunol* **2014**, *5*, 74.

396. Iwahori, K.; Kakarla, S.; Velasquez, M. P.; Yu, F.; Yi, Z.; Gerken, C.; Song, X.-T.; Gottschalk, S. Engager T cells: a new class of antigen-specific T cells that redirect bystander T cells. *Mol. Ther.* **2015**, *23*, 171–178.

397. Plunkett, W.; Huang, P.; Gandhi, V. Preclinical characteristics of gemcitabine. *Anticancer Drugs* **1995**, *6 Suppl 6*, 7–13.

398. Huang, P.; Chubb, S.; Hertel, L. W.; Grindey, G. B.; Plunkett, W. Action of 2“,2-”difluorodeoxycytidine on DNA synthesis. *Cancer Res.* **1991**, *51*, 6110–6117.

399. Gandhi, V.; Legha, J.; Chen, F.; Hertel, L. W.; Plunkett, W. Excision of 2“,2-”difluorodeoxycytidine (gemcitabine) monophosphate residues from DNA. *Cancer Res.* **1996**, *56*, 4453–4459.

400. Cerqueira, N.; Fernandes, P. A.; Ramos, M. J. Understanding ribonucleotide reductase inactivation by gemcitabine. *Chemistry* **2007**, *13*, 8507–8515.

401. Maréchal, R.; Mackey, J. R.; Lai, R.; Demetter, P.; Peeters, M.; Polus, M.; Cass, C. E.; Young, J.; Salmon, I.; Devière, J.; Van Laethem, J.-L. Human equilibrative nucleoside transporter 1 and human concentrative nucleoside transporter 3 predict survival after adjuvant gemcitabine therapy in resected pancreatic adenocarcinoma. *Clin. Cancer Res.* **2009**, *15*, 2913–2919.

402. García-Manteiga, J.; Molina-Arcas, M.; Casado, F. J.; Mazo, A.; Pastor-Anglada, M. Nucleoside transporter profiles in human pancreatic cancer cells: role of hCNT1 in 2“,2-”difluorodeoxycytidine- induced cytotoxicity. *Clin. Cancer Res.* **2003**, *9*, 5000–5008.

403. Goan, Y. G.; Zhou, B.; Hu, E.; Mi, S.; Yen, Y. Overexpression of ribonucleotide reductase as a mechanism of resistance to 2,2-difluorodeoxycytidine in the human KB cancer cell line. *Cancer Res.* **1999**, *59*, 4204–4207.

404. Ohhashi, S.; Ohuchida, K.; Mizumoto, K.; Fujita, H.; Egami, T.; Yu, J.; Toma, H.; Sadatomi, S.; Nagai, E.; Tanaka, M. Down-regulation of deoxycytidine kinase enhances acquired resistance to gemcitabine in pancreatic cancer. *Anticancer Res.* **2008**, *28*, 2205–2212.

APPENDICES

Appendix 1. VACV in combination with gemcitabine for treatment of bladder cancer cells *in vitro*

Contributions: Data presented here were generated by Katelynn Rowe (undergraduate summer and project student whom I supervised). I assisted in the experimental design, performed some of the replicates and the data analysis.

Gemcitabine (GEM) is an anticancer drug that has shown activity against bladder cancer [108]. A systematic review of clinical studies provides evidence that GEM may as effective as BCG at preventing tumor recurrence and disease progression while at the same time was found to cause fewer side effects [107,108]. Overall, intravesical GEM has shown encouraging results and may be an option in treating patients with NMIBC.

GEM (2,2 difluorodeoxycytidine; dFdC) is a deoxycytidine analog that is used for the treatment of a variety of cancers, including pancreatic, lung, ovarian, and bladder cancer. There are several characteristics of GEM that make it an ideal candidate drug for use in intravesical therapy (reviewed in [397]). These include rapid uptake into cells and high rate of plasma clearance, which ensures any drug that enters the systemic circulation is rapidly cleared. Once inside the cell, GEM is phosphorylated to its monophosphate form by deoxycytidine kinase (DCK). Further phosphorylation to its di-phosphate (dFdCDP) and tri-phosphate (dFdCTP) derivatives generates the active forms of GEM. dFdCTP is incorporated into DNA and inhibits the DNA polymerase consequently causing inhibition of further DNA synthesis [398]. After dFdCTP is introduced into replicating DNA, an additional nucleotide is added by the polymerase, preventing dFdCMP from being excised by proofreading enzymes [399]. In addition, the dFdCDP form can inhibit the RNR complex, depleting the cellular deoxynucleoside triphosphates (dNTP

pools) allowing increased GEM incorporation into DNA [400]. Replication stress caused by GEM can activate the DNA damage and replication stress signaling pathways.

Although GEM is promising as an intravesical therapy for NMIBC [108], there is a significant issue with patients developing resistance to this drug. GEM is transported into cells by the human concentrative nucleoside transporter (hCNT) 1 and equilibrative nucleoside transporter (hENT) 1 [401]. Cells with reduced levels of these transporters are highly resistant to GEM because they are unable take up GEM [402]. Resistance also results from an up-regulation of RNR protein leading to increased RNR activity [403]. Higher activity increases the dNTP pool in the cells which creates a negative feedback loop that decreases DCK activity causing a reduction in GEM phosphorylation and ultimately less activity [404]. Moreover, the increased dNTP pool that results from elevated RNR activity can reduce GEM incorporation into DNA due to competitive inhibition. Due to the increased frequency of clinical use of GEM for bladder cancer, especially after BCG failure, we investigated the combination of VACV and GEM, a likely combination treatment in a clinical trial.

Sensitivity of a subset of bladder cancer cells to short term (4 hr) GEM treatment was initially tested. We chose a short treatment to mimic the intravesical therapy used in the clinic. When viability was assed at 48 hrs post-treatment, we found that some cell lines were highly resistant (**Figure A.1A**). Next, we showed that in the HTB-3 bladder cancer cell line, there was an increase in cellular RRM2 as soon as 4 hr after GEM treatment (**Figure A.1B**) which could allow for enhanced complementation of our ΔF4LΔJ2R VACV. ΔF4LΔJ2R VACV was still able to replicate efficiently after a 4 hr GEM pretreatment, although there was a reduction in replication compared to control cells (**Figure A.1C**). We have preliminary data indicating that treatment of bladder cancer cells with GEM followed by ΔF4LΔJ2R VACV infection enhances cell killing. For

the combination treatments, cells were treated with GEM only, virus only, or GEM followed by virus. We found that using short-term (4 hr) treatment with GEM followed by VACV infection resulted in greater cell killing than either treatment alone, as determined by resazurin assay (**Figure A.1D**).

These data suggest that there is a significant potential for the combination of ΔF4LΔJ2R VACV and GEM in the treatment of bladder cancer and warrant further investigation.

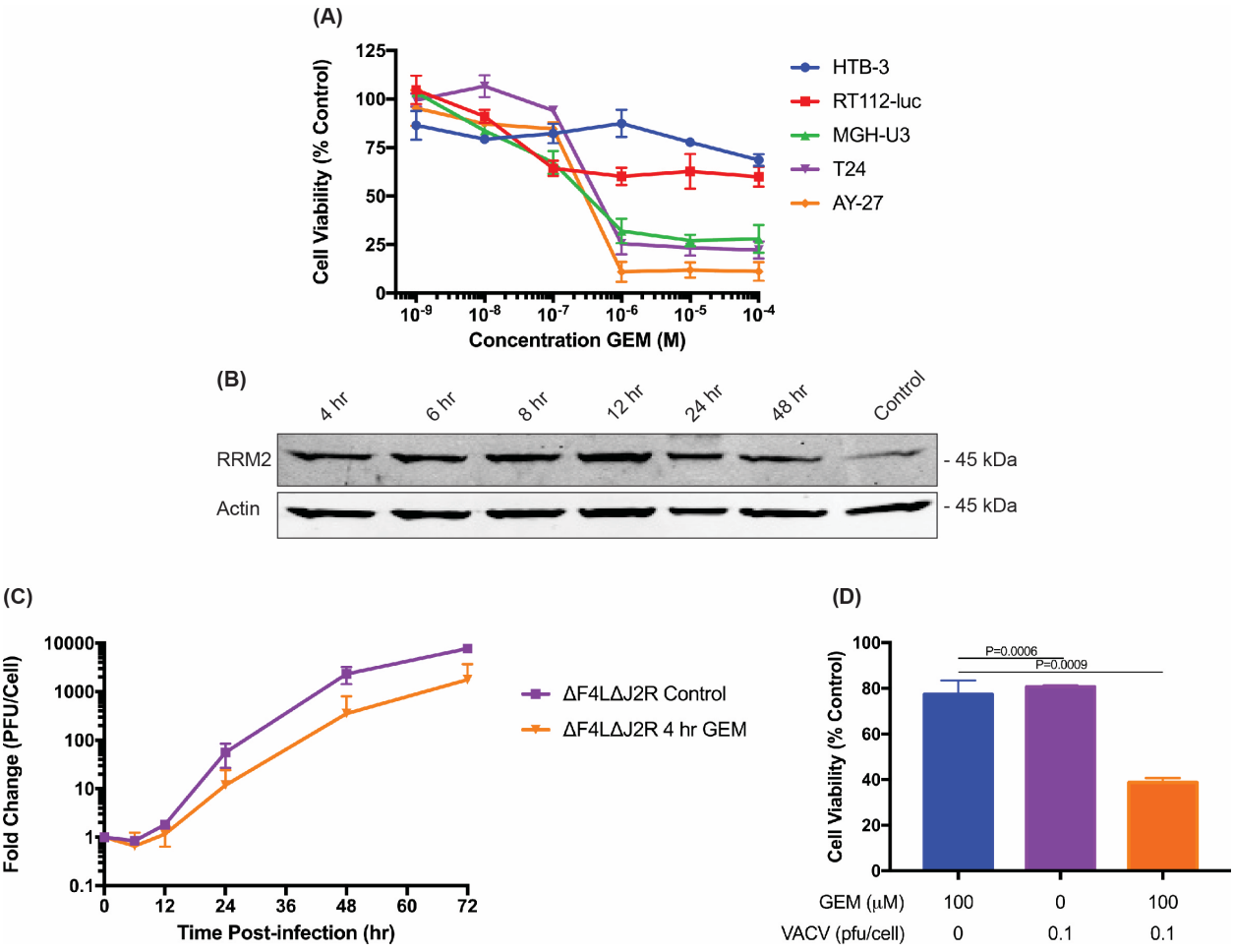
(A)
Cell Viability (% Control)
125
100
75
50
25
0
10-9
10-8
10-7
10-6
10-5
10-4
Concentration GEM (M)
HTB-3
RT112-luc
MGH-U3
T24
AY-27
(B)
4 hr
6 hr
8 hr
12 hr
24 hr
48 hr
Control
RRM2
- 45 kDa
Actin
- 45 kDa
(C)
Fold Change (PFU/Cell)
10000
1000
100
10
1
0.1
0
12
24
36
48
60
72
Time Post-infection (hr)
ΔF4LΔJ2R Control
ΔF4LΔJ2R 4 hr GEM
(D)
Cell Viability (% Control)
100
80
60
40
20
0
P=0.0006
P=0.0009
GEM (μM)
100
0
100
VACV (pfu/cell)
0
0.1
0.1

Figure A.1: Pretreatment with gemcitabine enhances VACV mediated killing. (A) Viability of bladder cancer cells following GEM treatment. To mimic clinical treatment of bladder cancer with GEM, the indicated cell lines were treated with GEM for 4 hr then washed and incubated for 48 hr. Control cultures were treated with PBS instead of GEM. Cell viability was determined by resazurin assay. **(B)** Western blot analysis of cellular RRM2 expression following GEM treatment. HTB-3 cells were untreated, or treated with 100 μM GEM for 4 hr. Cells were then washed and incubated in fresh medium for the indicated time. Control was collected at 24 hr. ß-actin was used as a loading control. **(C)** Multistep growth curve of ΔF4LΔJ2R VACV following 4 hr pretreatment with GEM. HTB-3 cells were treated with PBS or 100 μM GEM for 4 hr, then washed, and incubated for an additional 20 hr. Cells were then infected at an MOI of 0.03 PFU/cell. Cells were incubated for the indicated time before harvesting and titrating on BSC40 cells. **(D)** Sequential GEM + VAC treatment. HTB-3 cells were treated for 4 hours with PBS or 100 μM GEM, then washed, and incubated for an additional 20 hr. Cells were then infected at an MOI of 0.1 PFU/cell, then 48 hr later assayed for cell viability by resazurin assay.

Data Information: Mean ± SEM is shown. Data in (A), (C), and (D) represent n=3 independent experiments.

Appendix 2. Tumor abscess in RT112-luc xenografts

Contributions: I performed the tissue collection and processing. Histological analysis was performed by Dr. Nick Nation.

In chapter 2 we showed that ΔF4L and ΔF4LΔJ2R VACVs safely clear human bladder tumor xenografts. The majority of RT112-luc flank tumors were completely cleared at the end of the experiment. Interestingly, we noticed that a subset of animals retained, at the tumor cell injection site, a palpable mass that produced no luciferase signal. The masses were unusual and had a white color to them (**Figure A.2A**). The presence of the mass was not dependent on which VACV was used to treat the animal. Histological examination (**Figure A.2B-D)** suggested that the mass from the subcutaneous tumor injection site was an abscess. It had a uniform thin but fibrous wall with an inner layer of necrotic inflammatory debris and degenerate neutrophils. It was also determined by a pathologist that there was no evidence of any tumor cells remaining. The cause of the mass is not clear, but it did not seem to be deleterious to the animal's health.

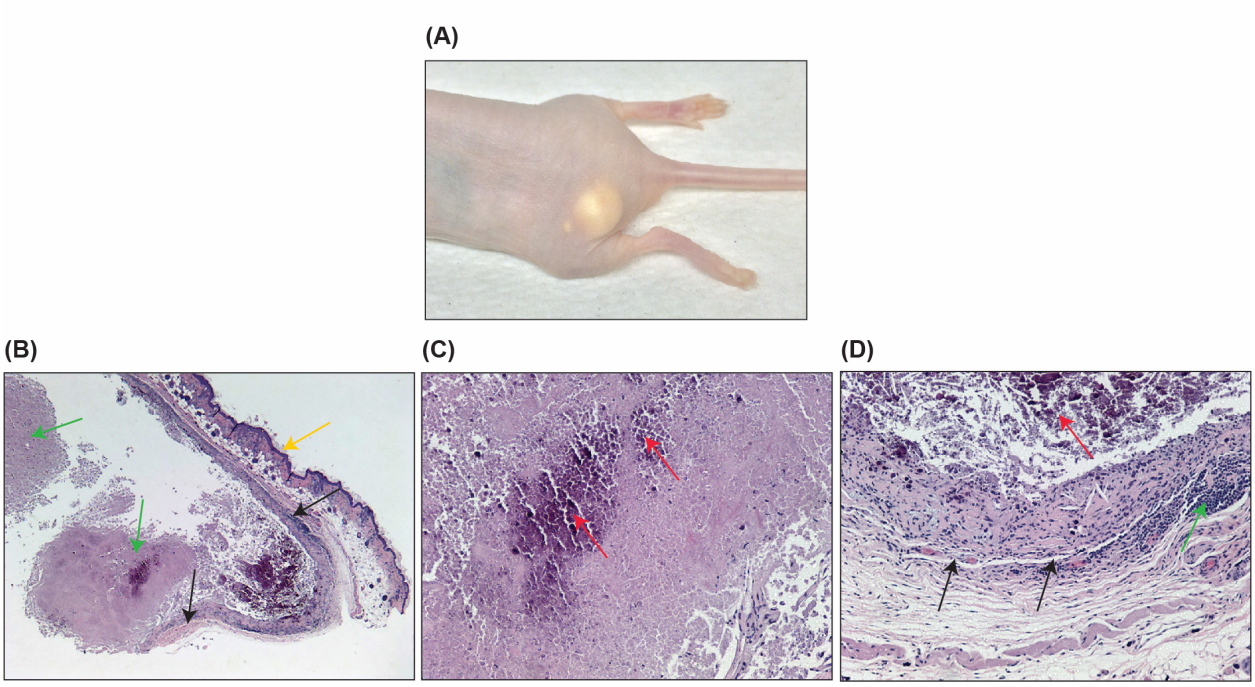
(A)
(B)
(C)
(D)

Figure A.2: Abscess development after VACV treatment. (**A**) Representative photograph of an abscess remaining after the bulk of the tumor is cleared by VACV treatment. (**B-D**) Histological ections of the mass were stained with hematoxylin and eosin (H&E) and analyzed by microscopy. (**B**) 20x magnification image of the entire abscess structure. The green arrows indicate the central mass of the abscess. The fibrous wall of the abscess is indicated by the black arrows while the skin surface is indicated by the orange arrows. (**C**) 100x magnification image of necrotic core. The red arrows show areas of mineralization of the debris in the abscess. (**D**) 100x magnification image of the details of the abscess wall. Red arrows show the necrotic debris in the core of the abscess, black arrows outline the abscess wall, and the green arrow points to a cluster of lymphocytes just outside the abscess wall.

Appendix 3. *Staphylococcus aureus* infections in ΔJ2R-treated mice.

Contributions: I performed the tissue collection and processing. Histological analysis was performed by Dr. Nick Nation.

As show in chapter 2, the ΔJ2R virus had strong anti-tumor activity. However, this was only achieved with significant toxicity in immune-deficient Balb/c nude mice. Mice euthanized prior to day 50 of the experiment were found to have significant viremia and this was determined to be the main factor behind their weight loss (**Figure 2.7**). Surprisingly, mice euthanized after day 50 had no detectable virus in any organs. Instead it was determined that they acquired systemic *Staphylococcus aureus* infections (**Figure A.3**). It was concluded that the infection likely occurred at transient dermal pox lesions characteristic of some of the mice treated with ΔJ2R VACV (**Figure 2.11**). These lesions, while not sufficiently active to cause significant systemic spread of virus, were capable of compromising integrity of the skin barrier, making the animal susceptible to opportunistic *S. aureus* infection which can be lethal in immune compromised animals.

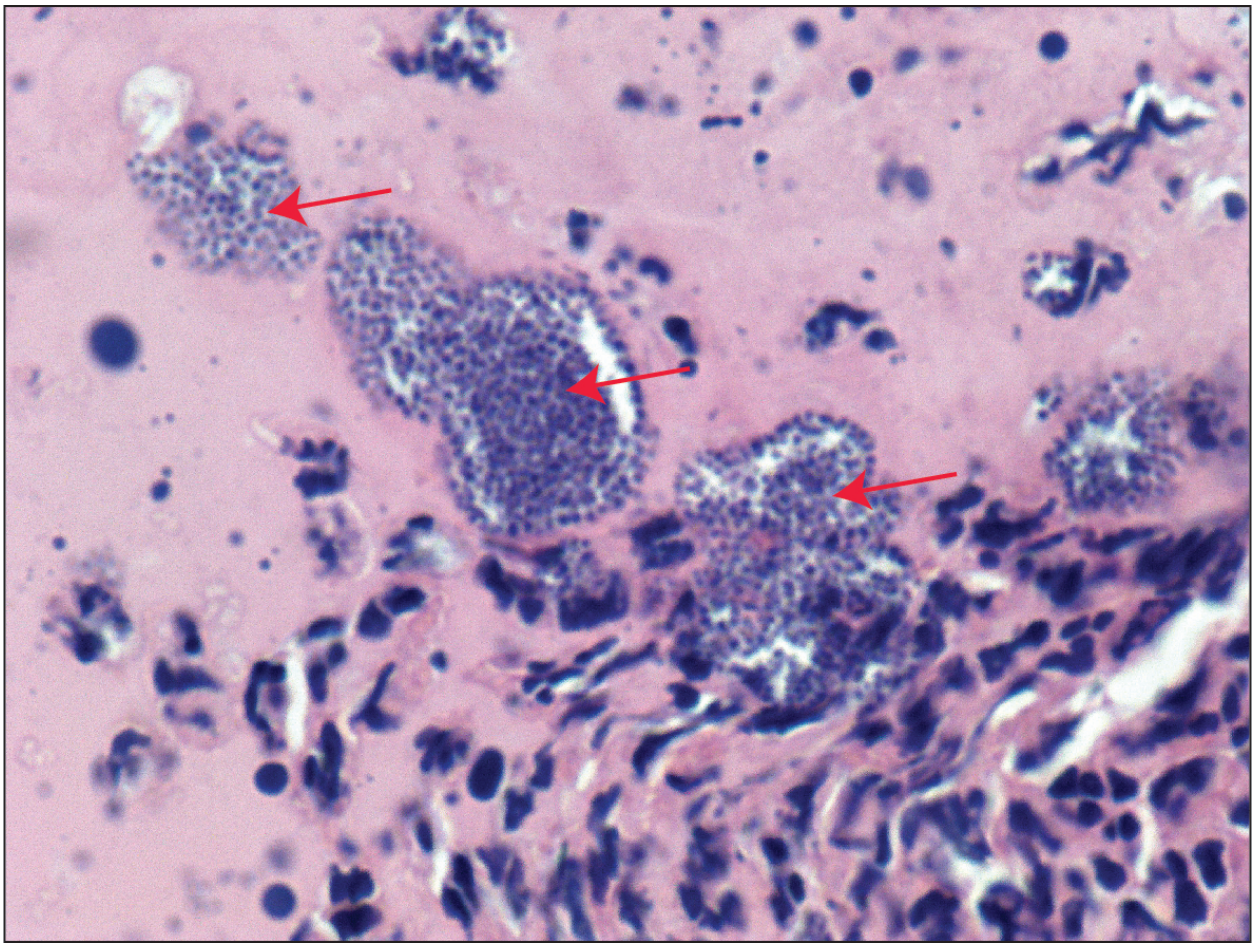

Figure A.3: *Staphylococcus aureus* infections in ΔJ2R treated mice. Representative photograph of skin tissue from mouse with *S. aureus* infection. Section was stained with hematoxylin and eosin (H&E) and analyzed by microscopy. 100x magnification image is shown. The red arrows indicate colonies of *S. aureus*. Tissue collection, processing and analysis was performed by Dr. Nick Nation.